

SPECTROSCOPIC AND THERMOCHEMICAL STUDIES
OF SOME NITROSONIUM AND SQUARE PLANAR MCl_4^- (M = I, Au) SPECIES

T
CDC
Pag
146,508
Jan 79

A thesis submitted by
TERENCE HENRY PAGE
in candidature for
the degree of Doctor of Philosophy
of the University of London

May, 1978

The Bourne Laboratory
Royal Holloway College
University of London
Egham Hill
Egham
Surrey

ProQuest Number: 10097453

All rights reserved

INFORMATION TO ALL USERS

The quality of this reproduction is dependent upon the quality of the copy submitted.

In the unlikely event that the author did not send a complete manuscript and there are missing pages, these will be noted. Also, if material had to be removed, a note will indicate the deletion.



ProQuest 10097453

Published by ProQuest LLC(2016). Copyright of the Dissertation is held by the Author.

All rights reserved.

This work is protected against unauthorized copying under Title 17, United States Code.
Microform Edition © ProQuest LLC.

ProQuest LLC
789 East Eisenhower Parkway
P.O. Box 1346
Ann Arbor, MI 48106-1346

ACKNOWLEDGEMENTS

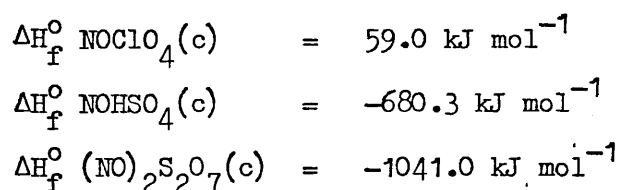
The author would like to express his gratitude to Dr. Arthur Finch and Dr. Peter N. Gates of Royal Holloway College for their advice, help and encouragement throughout this work and to Dr. Keith B. Dillon and Dr. R.J. Lynch of Durham University for measurement of N.Q.R. spectra and many helpful discussions of the results. Additionally, the author would like to thank Mr B. Smethurst and the technical staff at Royal Holloway College for assistance with instrumentation and Dr. D. Steele and Mr J.W. Tindle for invaluable help with the interferometer and Fourier transform programme.

A research studentship from the Science Research Council and a generous loan of gold salts from Johnson-Matthey Chemicals Ltd. are also gratefully acknowledged.

Finally, the author would like to thank Mrs E.I. Kearsey for typing this thesis.

ABSTRACT

The course of the decomposition of the nitrosonium ion by aqueous base has been investigated, and the formation of both nitrite and nitrate ions has been established. Measurements of the enthalpies of decomposition of $\text{NOClO}_4(\text{c})$, $\text{NOHSO}_4(\text{c})$ and $(\text{NO})_2\text{S}_2\text{O}_7(\text{c})$ permit evaluation of the ΔH_f° values:



The limitations of this approach and the marked deviations of these values from previously published data are discussed.

The system NOCl-BCl_3 has been investigated by Raman spectroscopy and two apparent modifications of a volatile 1:1 solid adduct have been characterised as $\text{NO}^+\text{BCl}_4^-$. Measurement of the temperature dependence of the dissociation pressure leads to a value for $\Delta H_f^\circ \text{ NOBCl}_4$ of -391 kJ mol^{-1} . The evaluation of a thermochemical radius for NO^+ is described.

Methods of solid-state vibrational spectroscopic analysis are reviewed and their application to various ICl_4^- and AuCl_4^- compounds with MCl_3^+ ($\text{M} = \text{S, Se, Te}$), $[\text{MeSCl}_2]^+$, $[\phi_n \text{Cl}_{(4-n)}\text{P}]^+$ and NO^+ as cations is presented. Two modifications of the compound $\text{SCl}_3^+\text{ICl}_4^-$ have been characterised, one of which is shown to be identical with the compound previously described as a mixed crystal containing $\text{SCl}_3^+\text{ICl}_2^-$ and SiCl_3 . Secondary bonding interactions as contributions to the low symmetry field created at anion sites in some of these compounds are postulated in order to explain the vibrational and NQR spectra. The combined use of vibrational spectroscopy and NQR in structural chemistry is briefly discussed.

CONTENTS

	<u>Page</u>
CHAPTER 1	
THE NITROSONIUM ION - INTRODUCTION	1
CHAPTER 2	
SOLUTION CALORIMETRY OF NITROSONIUM COMPOUNDS	
2.1 Introduction	10
2.2 Enthalpy of formation data reported for nitrosonium compounds	
(a) Nitrosonium perchlorate	11
(b) Nitrosonium hydrogen sulphate	12
(c) Dinitrosonium disulphate	21
(d) Nitrosonium fluorosulphate	21
2.3 Solution calorimetry of nitrosonium salts in aqueous alkaline sodium hypochlorite solution	22
2.4 Measurement of the difference between ΔH_f° values for two nitrosonium salts by calorimetry in basic solution	24
2.5 Interpretation of the solution calorimetry described in 2.3 and 2.4	31
2.6 Conclusions	40
References.	44
CHAPTER 3	
A THERMODYNAMIC AND SPECTROSCOPIC INVESTIGATION OF NOBCl_4	
3.1 Introduction	45
3.2 NOBCl_4 , preparation and Raman spectroscopy	45
3.3 Interpretation of the Raman spectra for the system NOCl/BCl_3	47
3.4 ΔH_f° NOBCl_4 (c) from the temperature dependence of the dissociation pressure	64
3.5 Investigation of the $\text{NO}_2\text{Cl}/\text{BCl}_3$ Reaction	78
References.	83

CHAPTER 4	<u>Page</u>
VIBRATIONAL SPECTROSCOPY AND CHEMICAL STRUCTURE	
4.1 Introduction	87
4.2 Point group symmetry and vibrational analysis	88
4.3 Site group analysis (S.G.A.)	93
4.4 Factor group analysis (F.G.A.)	96
4.5 The applications of S.G.A. and F.G.A. to solid state vibrational spectra	102
4.6 N.Q.R. spectroscopy	106
References.	111
CHAPTER 5	
A STRUCTURAL INVESTIGATION OF ICl_4^- AND AuCl_4^- COMPOUNDS USING VIBRATIONAL SPECTROSCOPY AND N.Q.R.	
5.1 Jaillard's compound - introduction	113
5.2 The constitution of Jaillard's compound	116
5.3 ICl_4^- salts of $[\text{SMe}_n\text{Cl}_{3-n}]^+$ cations	137
5.4 Trichlorochalcogen cations with AuCl_4^-	140
5.5 ICl_4^- and AuCl_4^- compounds of substituted chlorophosphorus cations	162
5.6 AuCl_4^- and ICl_4^- with nitrogenous bases	166
5.7 NOAuCl_4	178
5.8 Structural information for ICl_4^- and AuCl_4^- salts from vibrational spectroscopy and N.Q.R.	184
References.	189

CHAPTER 6	<u>Page</u>
EXPERIMENTAL	
6.1 Preparative	192
6.2 Elemental analysis	209
6.3 Solution calorimetry	213
6.4 Vibrational spectroscopy	216
6.5 Tensimetry	219
6.6 Differential scanning calorimetry (D.S.C.)	220
6.7 N.Q.R. spectroscopy	220
References.	221
Appendix 1	223
Appendix 2	225

CHAPTER 1

THE NITROSONIUM ION - INTRODUCTION

Nitric oxide is a paramagnetic species and readily loses an electron to form the nitrosonium ion, NO^+ , which is formally isoelectronic with dinitrogen, N_2 . The strong π -acceptor properties of nitric oxide when coordinated to a transition metal may be attributed to the formation of the nitrosonium ion. Raynor²⁴ believes that in all complexes containing a linear NO group, formal oxidation numbers should be chosen such that NO is considered as NO^+ .

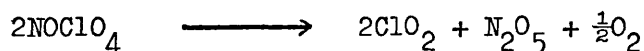
The loss of an electron by NO is not restricted to transition-metal complexes. Ionic salts containing NO^+ ions have also been prepared which resemble in certain respects the corresponding alkali-metal compounds with which they are often isomorphous. Such species have been described as salts of the nitrosyl or nitrosonium cation. However, the latter term only will be used in this thesis, thus avoiding any confusion with the covalently-bonded NO in nitrosyl chloride. Certain higher oxides of nitrogen - N_2O_3 and N_2O_4 , have been considered to behave as though they were the nitrite and nitrate salts respectively^{29,34} of NO^+ . This is purely a formalism, however, since both of these oxides are covalently bonded species containing a long N-N bond.⁸ For N_2O_3 , matrix isolation techniques⁸ have characterised a metastable modification ONONO containing no nitrogen-nitrogen bond. This is the nearest species to nitrosonium nitrite which has so far been isolated.

A wide range of nitrosonium salts have been reported and for the purposes of discussion, it is appropriate to classify these according to anion types as it is the anion which largely determines the physical properties. Care should be taken with more complicated species to

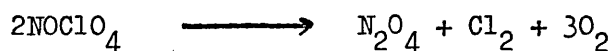
ascertain that NO^+ is indeed the cation and is not coordinated to the anion. Four different categories may be considered:

(a) NITROSONIUM SALTS OF SIMPLE INORGANIC IONS

As in the case of the nitrite and nitrate, the simplest compounds with halides and pseudohalides - Cl^- , Br^- , SCN^- , are covalently bonded species. With the heavier halides, there is considerable dissociation at ambient temperatures into nitric oxide and halogen. This category, therefore, includes the perchlorate, sulphate, selenate and phosphate derivatives. NOClO_4 and NOHSO_4 are by far the most widely investigated nitrosonium salts. NOClO_4 is a potential explosive, which may explode violently on contact with certain organic solvents. The thermal decomposition^{6,26} of NOClO_4 in vacuo has been studied and below 100°C the reaction proceeds thus:



whereas above 100°C , the decomposition proceeds:



NOClO_4 has been considered as a useful precursor in the synthesis of anhydrous metal perchlorates.^{18,27} Thus heating NOClO_4 with ZnO at $190 - 200^\circ\text{C}$ produces $\text{Zn}(\text{ClO}_4)_2$ of 99% purity, the principal impurities being NO_2ClO_4 and ZnO .

Crystalline NOHSO_4 , was found in the reaction chambers of the plants used for manufacturing H_2SO_4 by the Lead Chamber process and hence is more commonly known as 'chamber crystals'. It has been identified as a component in the system $\text{N}_2\text{O}_3/\text{H}_2\text{O}/\text{H}_2\text{SO}_4$ by X-ray diffraction.⁴³ However, additionally various polysulphate species have also been isolated.^{22,45} Those containing two NO^+ cations may be

regarded as adducts of N_2O_3 with $SO_3 - N_2O_3 \cdot nSO_3$. The simplest member $(NO)_2SO_4$ has not apparently been prepared. Salts containing one NO^+ ion and a second (different) cation - e.g. K^+ , H^+ , NO_2^+ , are also known. The NO^+/NO_2^+ salts are effectively adducts of N_2O_4 with $SO_3 - N_2O_4 \cdot nSO_3$, and this is reported^{22,45} to be the usual method of preparation. An analogous series of compounds of N_2O_3 and N_2O_4 with SeO_3 has also been reported.^{7,14} The compounds $(NO)K S_2O_7^{15}$ and $(NO)H S_2O_7^{25}$ have been prepared, respectively, by the action of N_2O_4 on KHS_2O_7 and reaction of $NOHSO_4$ with SO_3 . All these compounds are white crystalline salts which are characterised by a band in the infra-red spectrum in the region $2250-2300 \text{ cm}^{-1}$ due to NO^+ stretching.⁴² A corresponding series of nitrosonium salts of polyphosphate anions has been reported,⁴⁰ but these have not apparently been characterised.

(b) NITROSONIUM COMPOUNDS FORMALLY DERIVED FROM NOF

A wide range of compounds within this category have been prepared. The complex fluoroanions are both metallic^{4,5} e.g. $NOVF_6$, $NONbF_6$, $NOTaF_6$, $(NO)_2SnF_6$, and non-metallic^{4,48} e.g. $NOBF_4$, $(NO)_2SiF_6$, $NOPF_6$, $(NO)_2GeF_6$ in nature. The properties of these compounds are related to the stability of the fluoroanion. The majority are ionic, high-melting involatile compounds - e.g. $NOBF_4$, $NOPF_6$ which resemble $NOClO_4$. However, several compounds e.g. $NOBrF_4$,⁴ and more volatile resembling certain $NOCl$ derivatives described in section c. Salts which are not derivatives of a metal fluoride are rare. $NOSO_3F$ may be formally considered as an example and also $NOPO_2F_2$.² All these compounds are seldom prepared by direct interaction. A more usual procedure is to pass $NOCl$ or N_2O_3 into a solution of the Lewis acid, e.g. BF_3 in HF .

The stable salts may again be characterised by a band in the infra red in the region $2250 - 2300 \text{ cm}^{-1}$ due to NO^+ stretching.⁴²

(c) NITROSONIUM COMPOUNDS FORMALLY DERIVED FROM NOCl

A wide range of compounds within this category have been prepared. As in the previous case, the complex chloroanions are again either metallic^{19,20} e.g. NOAuCl_4 , $(\text{NO})_2\text{SnCl}_6$, NOAlCl_4 , or non-metallic^{19,20} e.g. NOBCl_4 , NOPCl_6 in nature, the latter compounds being relatively volatile at ambient temperatures. Examples in this category showing anion-cation association have been recognised and are fully discussed in chapters 3 and 5. Interaction of NOCl , with Lewis acids is not restricted to metal chlorides. Substituted metal chlorides and non-chlorine-containing Lewis acids also undergo reaction e.g. NOTiOCl_3 ,⁴⁶ $\text{TiCl}_3(\text{RCO}_2)\text{NOCl}$,¹ NO.NbOCl_4 ,¹⁷ NOBF_3Cl ,⁴⁷ NOSbF_5Cl ⁴⁷ and NOSO_3Cl .¹³

(d) NITROSONIUM SALTS OF COMPLEX ANIONS [NOT HALOGENATED]

This category includes all those miscellaneous compounds which may not be classified under (a), (b) and (c). Typical examples include $(\text{NO})_2[\text{Ho}(\text{NO}_3)_5]$,⁴⁴ $(\text{NO})_2[\text{Fe}(\text{CN})_5\text{NO}]$.³⁰ None of these compounds has been extensively studied.

The nitrosonium ion is a reactive species and has been studied in detail by Seel in a series of papers²⁹⁻³⁹ published between 1950 and 1957. The NO^+ ion has been characterised by vibrational spectroscopy,⁴² conductance³¹ measurements and X-ray crystallography.¹³ A single crystal X-ray study of NOSO_3Cl has identified¹³ distinct NO^+ and SO_3Cl^- ions. NO^+ is readily hydrolysed, although the nature of the degradation

by aqueous base is a subject of some controversy. This is fully discussed in chapter 2 in conjunction with the associated errors resulting in various reported solution calorimetric studies. In certain non-aqueous solvents e.g. SO_2 , the nitrosonium ion is reported to be stable and to undergo both oxidation and reduction reactions. Thus the reaction with N_3^- in $\text{SO}_2(1)$ is reported to proceed:^{33,35}

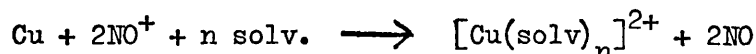


There is limited evidence¹⁶ to suggest that NON_3 exists at low temperatures. The reaction of NO^+ with I^- in $\text{SO}_2(1)$ is reported to proceed:³²



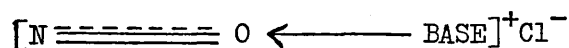
When compared with the complex degradation of NO^+ by aqueous base (see chapter 2), these reactions are comparatively simple. The use of these reactions in solution calorimetry has not been evaluated (in $\text{SO}_2(1)$ or in other less unattractive solvents). The conclusions from the work presented in chapter 2 would suggest that such reactions should be considered, despite the numerous subsidiary experiments required to derive all the necessary ancillary data.

NO^+ has been reported⁹ to undergo reaction with SO_3^{2-} to form the species $[\text{SO}_3.\text{NO}]^-$. This has been termed the Bodeker reaction and is reported for coordinated NO^+ . Thus addition of methanol to an aqueous solution of caesium sulphite and caesium nitroprusside precipitates the coordinated species which has been characterised by infra-red spectroscopy. The reaction of NO^+ with metals and transition-metal complexes has also been studied.^{11,12,41} Thus NOClO_4 or NOBF_4 will react slowly with metallic copper¹¹ in suspension in CH_3CN or EtOAc according to:



Metallic Mn, Fe, Co, Ni and Zn react similarly.¹² The reactions are usually carried out under reduced pressure to avoid contamination with the nitrate salts. With metallic palladium, however, the product⁴¹ is the yellow diamagnetic Pd(1) complex $[\text{Pd}(\text{CH}_3\text{CN})_4]\text{ClO}_4$. NO^+ salts react²³ with the complexes $\text{M}(\text{PPh}_3)_2\text{O}_2$ (M = Pt, Pd) in CH_3CN with formation of $[\text{M}(\text{PPh}_3)_2\text{NO}_3]^+$. In less basic solvents containing traces of water, OH bridged dimers are produced $[\text{M}_2(\text{PPh}_3)_4(\text{OH})_2]^{2+}$. Ni(II) complexes are reported³ to be oxidised to Ni(III) complexes by NOBF_4 in CH_3CN .

Nitrosonium salts in solution, e.g. NOHSO_4 in conc. H_2SO_4 , NOAlCl_4 in $\text{SO}_2(1)$, absorb small amounts of nitric oxide NO at atmospheric pressure to form blue solutions.³⁹ Upon cooling, the colour changes to red. These observations are attributed to the interaction of NO with NO^+ . F. Seel²⁸ has isolated a compound $\text{NOAlCl}_4 \cdot \text{NO}$ by reacting NOAlCl_4 with NO under pressure. The reaction of NO^+ with NOCl forming salts e.g. $\text{NOAlCl}_4 \cdot \text{NOCl}$ has been postulated and is discussed in chapter 3. It has also been reported²¹ that NOCl reacts with nitrogenous bases e.g. pyridine, picoline, quinoline to form NO^+ salts, as identified by i.r. The nitrogen atom of the base is believed to act as a donor to NO^+



There is also limited evidence¹⁰ for the formation of the ion N_2O_3^+ when NO^+ interacts with NO_2 .

REFERENCES

1. J. Amaudrut, C. Devin, C.R. Acad. Sci. Ser. C (1967) 264 2156-9.
2. V.P. Babaeva, V. Ya. Rosolovskii, Russ. J. Inorg. Chem. (1971) 16 471-3.
3. E.K. Barefield, D.H. Busch, JCS D (1970) 522-3.
4. P. Bouy, Ann. Chim [13], (1959) 4 853-90.
5. H.C. Clark, H.J. Emeleus, JCS (1958) 190-5.
6. K. Cruse, G. Huck, H. Moller, Zeit anorg. allgem. chem. (1949) 259 159-72.
7. K. Dostal, A. Ruzicka, P. Rumisek, Zeit. anorg. allgem. Chem. (1965) 336 219-24.
8. W.G. Fateley, H.A. Bent, B. Crawford, J. Chem. Phys. (1959) 31 204-17.
9. A.G. Fogg, A.H. Norbury, W. Moser, J.I.N.C. (1966) 28 2753-5.
10. J.D.S. Goulden, D.J. Millen, JCS (1950) 2620-7.
11. B.J. Hathaway, D.G. Holah, J.D. Postlethwaite, JCS (1961) 3215-8.
12. B.J. Hathaway, D.G. Holah, A.E. Underhill, JCS (1962) 2444-8.
13. T. Hohle, F.C. Mijlhoff, Rec. Trav. Chim (1967) 86 1153-8.
14. G. Kempe, Zeit. anorg. allgem. Chem. (1968) 363 273-81.
15. P. Legrand, M. Wartel, J. Heubel C.R. Acad. Sci. Ser C (1966) 263 1425-8.
16. H.W. Lucien, J.A.C.S. (1958) 80 4458-60.
17. J. MacCordick, Separ. Sci., (1969), 4, 191-6.
18. M.M. Markowitz, J.E. Ricci, R.J. Goldman, P.F. Winternitz J.I.N.C. (1960) 16 159-61.

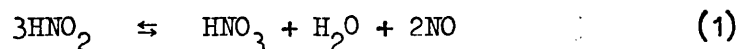
19. J.R. Partington, A.L. Whynes, J.C.S. (1948) 1952-8.
20. J.R. Partington, A.L. Whynes, J.C.S. (1949) 3135-41.
21. R.C. Paul, S.L. Chadha, Ind. J. Chem. (1968) 6, 272-4.
22. R.C. Paul, C.L. Arora, K.C. Malhotra, Ind. J. Chem. (1972) 10 94-6.
23. D.A. Phillips, M. Kubota, J. Thomas, Inorg. Chem. (1976) 15 118-20.
24. J.B. Raynor, Inorg. Chim. Acta. (1972) 6 347-8.
25. G. Ribaldone, A. Nenz, C.A. 67, 116,621r.
26. V. Ya. Rosolovskii, E.S. Rummyantsev. Russ. J. Inorg. Chem. (1963) 8 689-92.
27. V. Ya. Rosolovskii, E.S. Rummyantsev, N.N. Maltseva, Russ. J. Inorg. Chem. (1963) 8 692-5.
28. F. Seel, Zeit. Naturforsch. (1953) 8 607.
29. F. Seel, Zeit. anorg. allgem. Chem. (1950) 261 75-84.
30. F. Seel, N.H. Walassis, Zeit. anorg. allgem. Chem. (1950) 263 85-93.
31. F. Seel, T. Gössl Zeit. anorg. allgem. Chem. (1950) 263 253-60.
32. F. Seel, A.K. Bocz, J. Nogradi, Zeit. anorg. allgem. Chem. (1951) 264 298-310.
33. F. Seel, J. Nogradi, Zeit. anorg. allgem. Chem. (1951) 264 311-20.
34. F. Seel, J. Nogradi, H. Breit, Zeit. anorg. allgem. Chem. (1952) 269 102-16.
35. F. Seel, R. Schwaebel, Zeit. anorg. allgem. Chem. (1953) 274 169-89.
36. F. Seel, H. Meier, Zeit. anorg. allgem. Chem. (1953) 274 190-6.
37. F. Seel, H. Meier, Zeit. anorg. allgem. Chem. (1953) 274 197-222.
38. F. Seel, E. Degener, Zeit. anorg. allgem. Chem. (1956) 284 101-30.

39. F. Seel, H. Sauer, Zeit. anorg. allgem. Chem. (1957) 292 1-19.
40. F. Seel, R. Schmutzler, K. Wasem, Angew. Chem. (1959) 71 340.
41. R.F. Schramm, B.B. Wayland, Chem. Comm. (1968) 898-9.
42. D.W.A. Sharp, J. Thorley, J.C.S. (1963) 3557-60.
43. K. Stopperka, F. Kilz, Zeit. Chem. (1968) 8 435.
44. G.E. Toogood, C. Chieh, Can. J. Chem. (1975) 53 831-5.
45. B. Vandorpe, Rev. Chim. Miner (1967) 4 589-620.
46. B. Viard, J. Amaudrut, C. Devin, C.R. Acad. Sci. Ser. C (1973)
276 1279-82.
47. T.C. Waddington, F. Klanberg, Zeit. anorg. allgem. Chem. (1960)
304 185-90.
48. A.A. Woolf, J.C.S. (1950) 1053-6.

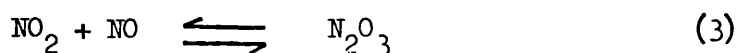
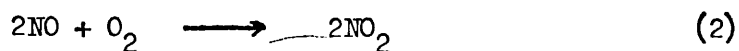
CHAPTER 2 SOLUTION CALORIMETRY OF NITROSONIUM COMPOUNDS

2.1 INTRODUCTION

Thermodynamic data for nitrosonium compounds are not extensively reported in the literature. Several simple nitrosonium salts, NO^+X^- ($\text{X} = \text{ClO}_4^-$, HSO_4^- , $\text{S}_2\text{O}_7^{2-}$, SO_3F^-) have been investigated by solution calorimetry, but several of the postulated calorimetric reactions may be regarded as somewhat speculative because nitrous acid is involved as a reaction intermediate. After decomposing a nitrosonium salt in aqueous base, both nitrite and nitrate ions can be detected, the latter arising from the disproportionation of nitrous acid:¹⁴



In the presence of oxygen, the situation is further complicated by gaseous phase oxidation of nitric oxide to nitrogen dioxide,¹⁴ which can be absorbed into basic solution:



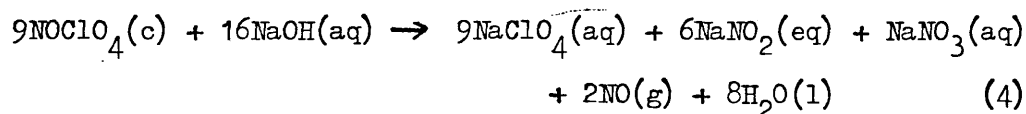
The following critical assessment of enthalpy of formation data for nitrosonium compounds currently available in the literature suggests several errors and reveals a serious discrepancy between the values reported for $\Delta H_f^\circ \text{NOHSO}_4$ by two independent methods.^{6,11}

2.2 ENTHALPY OF FORMATION DATA REPORTED FOR NITROSONIUM COMPOUNDS

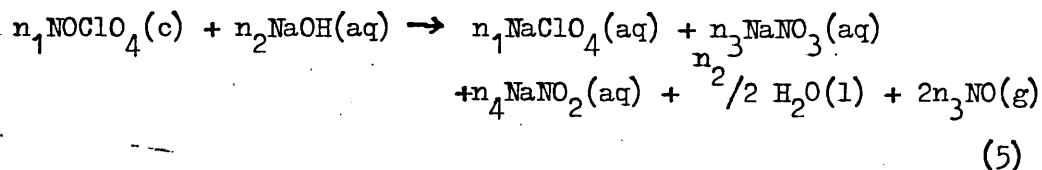
(a) NITROSONIUM PERCHLORATE

$\Delta H_f^\circ \text{NOClO}_4$ has been determined by Cruse et al.³ from measurements of the enthalpy of decomposition of the salt in 0.5M sodium hydroxide solution in a nitrogen atmosphere. This study recognised the formation of both nitrite and nitrate ions in solution and careful post-calorimetric analysis was performed in order to establish the stoichiometry of each calorimetric reaction. Several factors, however, combine to reduce confidence in the reported values. Firstly, an inconsistency between the sign conventions adopted for the measured enthalpy of reaction and the ancillary data, noted by Woolf and Richards,¹¹ leads to a corrected value for $\Delta H_f^\circ \text{NOClO}_4$ of $-9.0 \text{ kcal mol}^{-1}$ (cf. $-39.6 \pm 0.3 \text{ kcal mol}^{-1}$). This value was in good agreement with that predicted from some of their own thermochemical measurements.

However, this recalculation was based on an assumption that the decomposition proceeded according to equation (4):



A very careful study of the analytical data shows that this assumption is incorrect. Cruse et al.³ in fact calculated a value for $\Delta H_f^\circ \text{NOClO}_4$ from each individual calorimetric run by considering the reaction in the form:

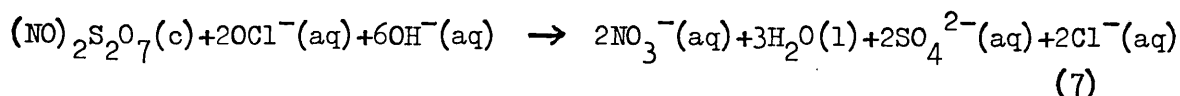
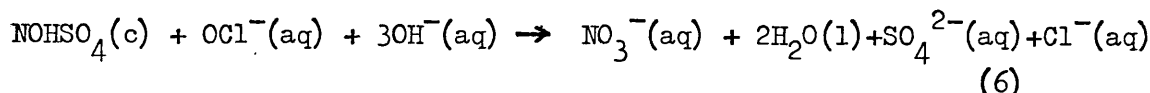


The coefficients were determined experimentally and the analytical data

are reproduced in table 2.1. The calculated coefficients, which are not presented in the original paper, clearly illustrate that the reaction is not reproducible and the inclusion of equation (4) in the original paper is misleading. Recalculation of a value for $\Delta H_f^{\circ} \text{NOClO}_4$ from each individual run in table 2.2, employing updated ancillary data, leads to a mean value of $+15.88 \pm 0.69 \text{ kcal mol}^{-1}$. This positive value is plausible in view of the explosive nature of nitrosonium perchlorate.⁴

(b) NITROSONIUM HYDROGEN SULPHATE

Values of $\Delta H_f^{\circ} \text{NOHSO}_4$ and $\Delta H_f^{\circ} (\text{NO})_2\text{S}_2\text{O}_7$ have been determined by Woolf and Richards¹¹ from measurements of their enthalpies of decomposition in aqueous alkaline sodium hypochlorite solution. Decomposition of the salts was considered to proceed as follows:



However, no analytical data are given to substantiate these reactions and the possible formation of nitrate in solution by disproportionation of nitrous acid, which is undoubtedly involved as an intermediate (see later), was not considered. The value of $\Delta H_f^{\circ} \text{NOHSO}_4 = -182.5 \pm 0.7 \text{ kcal mol}^{-1}$ based upon only three experimental measurements and differing from an earlier determination⁶ ($-160.2 \text{ kcal mol}^{-1}$) by some 20 kcal mol^{-1} is suspect.

Wt NOClO ₄ /g	MOLES OF REACTANT USED OR PRODUCT FORMED AND MOLE RATIO (NO ₃ ⁻ = 1)										-ΔH _R /kcal
	NOClO ₄ /n ₁	OH ⁻ /n ₂	ClO ₄ ⁻ /n ₄	NO ₃ ⁻ /n ₃	NO/2n ₃	H ₂ O/n ₂ /2	NO ₂ ⁻ /n ₄				
1	1.5343	0.01185 7.27	0.02044 12.54	0.01185 7.27	0.00163 1	0.00326 2	0.01022 6.27	0.00695 4.26	0.3130		
2	1.6535	0.01277 6.42	0.02157 10.84	0.01277 6.42	0.00199 1	0.00397 2	0.01079 5.42	0.00680 3.42	0.3403		
3	1.4992	0.01158 6.93	0.01982 11.87	0.01158 6.93	0.00167 1	0.00334 2	0.00991 5.93	0.00656 3.93	0.3087		
4	1.5453	0.01194 7.06	0.02049 12.12	0.01193 7.06	0.00169 1	0.00337 2	0.01025 6.07	0.00686 4.06	0.3121		
5	1.5971	0.01234 8.45	0.02174 14.89	0.01233 8.45	0.00146 1	0.00292 2	0.001087 7.45	0.00793 5.43	0.3156		
6	1.5110	0.01167 6.67	0.01984 11.34	0.01167 6.67	0.00175 1	0.00346 2	0.00981 5.61	0.00644 3.68	0.3151		
7	1.5886	0.01227 7.09	0.02104 12.16	0.01225 7.09	0.00173 1	0.00346 2	0.01052 6.08	0.00706 4.08	0.3189		
8	1.5819	0.01222 7.02	0.02099 12.06	0.01222 7.02	0.00174 1	0.00345 2	0.01050 6.03	0.00701 4.03	0.3161		

TABLE 2.1

	1	2	3	4	5	6	7	8
$n_i \Delta H_f^\circ$								
$\Delta H_f^\circ / \text{kcal mol}^{-1}$								
$\text{ClO}_4^- (\text{aq})$	-30.91	-0.3947	-0.3579	-0.3688	-0.3811	-0.3607	-0.3787	-0.3777
$\text{NO}_3^- (\text{aq})$	-49.519	-0.0985	-0.0827	-0.0837	-0.0723	-0.0867	-0.0857	-0.0862
$\text{NO}_2^- (\text{aq})$	-25.00	-0.1738	-0.1640	-0.1715	-0.1983	-0.1610	-0.1765	-0.1753
$\text{NO}(\text{g})$	+21.561	0.0703	0.0720	0.0727	0.0630	0.0746	0.0746	0.0744
$\text{H}_2\text{O}(\text{l})$	-68.32	-0.7372	-0.6771	-0.7003	-0.7426	-0.6702	-0.7187	-0.7174
$\text{OH}^- (\text{aq})$	-54.97	-1.1236	-1.0895	-1.1263	-1.1951	-1.0906	-1.1566	-1.1538
ΔH_R	-	-0.3130	-0.3087	-0.3121	-0.3156	-0.3151	-0.3189	-0.3161
$n_i \Delta H_f^\circ \text{NOClO}_4(\text{c})$	-	+0.1879	+0.1885	+0.1869	+0.1793	+0.2017	+0.1905	+0.1878
n_1	-	0.01185	0.01277	0.01194	0.01234	0.01167	0.01227	0.01222
$\Delta H_f^\circ \text{NOClO}_4(\text{c})$	-	15.856	16.281	15.651	14.530	17.285	15.528	15.369

$$\Delta H_f^\circ \text{NOClO}_4(\text{c}) = 15.88 \pm 0.69 \text{ kcal mol}^{-1} / \hat{S} = 0.830$$

TABLE 2.2

Kunin⁶ had derived $\Delta H_f^\circ \text{NOHSO}_4$ in 1954 from a consideration of the enthalpy changes associated with the dissolution of the compound in aqueous sulphuric acid solutions of different strengths. This study was apparently very thorough and merits serious consideration. Numerous corrections were applied to account for impurities in the starting material, but the absence of analytical data and omission of essential steps in the working renders the derivation of the final result impossible to check. Moreover, the final result is obtained using some doubtful ancillary data as the following synopsis of the method illustrates:-

(i) THE SAMPLE

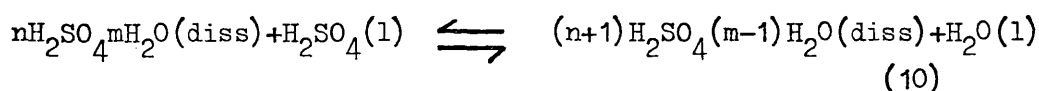
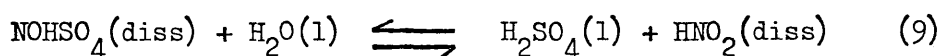
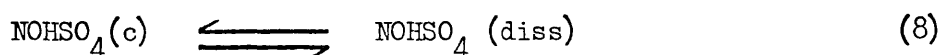
Since Kunin was apparently unable to prepare large quantities of pure crystalline NOHSO_4 , measurements were carried out using a sample contaminated with aqueous sulphuric acid containing some dissolved and some partially hydrolysed compound - the mother liquor. The purity of the NOHSO_4 was established from chemical analyses, not explicitly reported, and the quantity of dissolved product was calculated from some previously published data⁷ (calculation not given). The extent of hydrolysis of the dissolved compound in the mother liquor was calculated as 30% (method not given).

(ii) THE MEASUREMENT OF ENTHALPIES OF SOLUTION

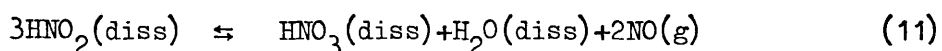
Enthalpies of solution were measured in a non-vented calorimeter vessel and the measurements corrected for the heat of dilution/concentration of the mother liquor in the test solution using literature data (source and calculation not given). The heat of dilution of NOHSO_4 dissolved in the mother liquor was stated to be very small and indeterminate.

(iii) CORRECTION OF THE RESULTS FOR DISPROPORTIONATION OF
NITROUS ACID

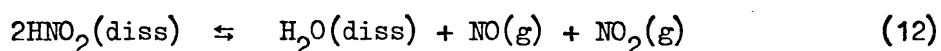
The process of dissolution was considered to involve the following steps:



The measured enthalpies of solution are presented graphically in fig. 2.1 and the inflection at 73% H_2SO_4 concentration is considered to indicate that some disproportionation of the dissolved nitrous acid, and the associated hydration of the solvent by the liberated water, is beginning to occur at that point.



Separate experiments were carried out under identical conditions in order to assess the extent of disproportionation of the dissolved nitrous acid at a given acid concentration by considering the species in the gas phase. The results are presented in fig. 2.2. The method used to measure the $\text{NO}:\text{NO}_2$ concentration in the gas phase is not given, but a knowledge of the equilibrium



must also be involved. Since at acid levels less than 73% H_2SO_4 disproportionation is occurring, then undoubtedly the equilibrium in equation (9) is being displaced to the right. The step in fig. 2.2 at $\approx 58\%$ H_2SO_4 is considered to indicate that below this point all

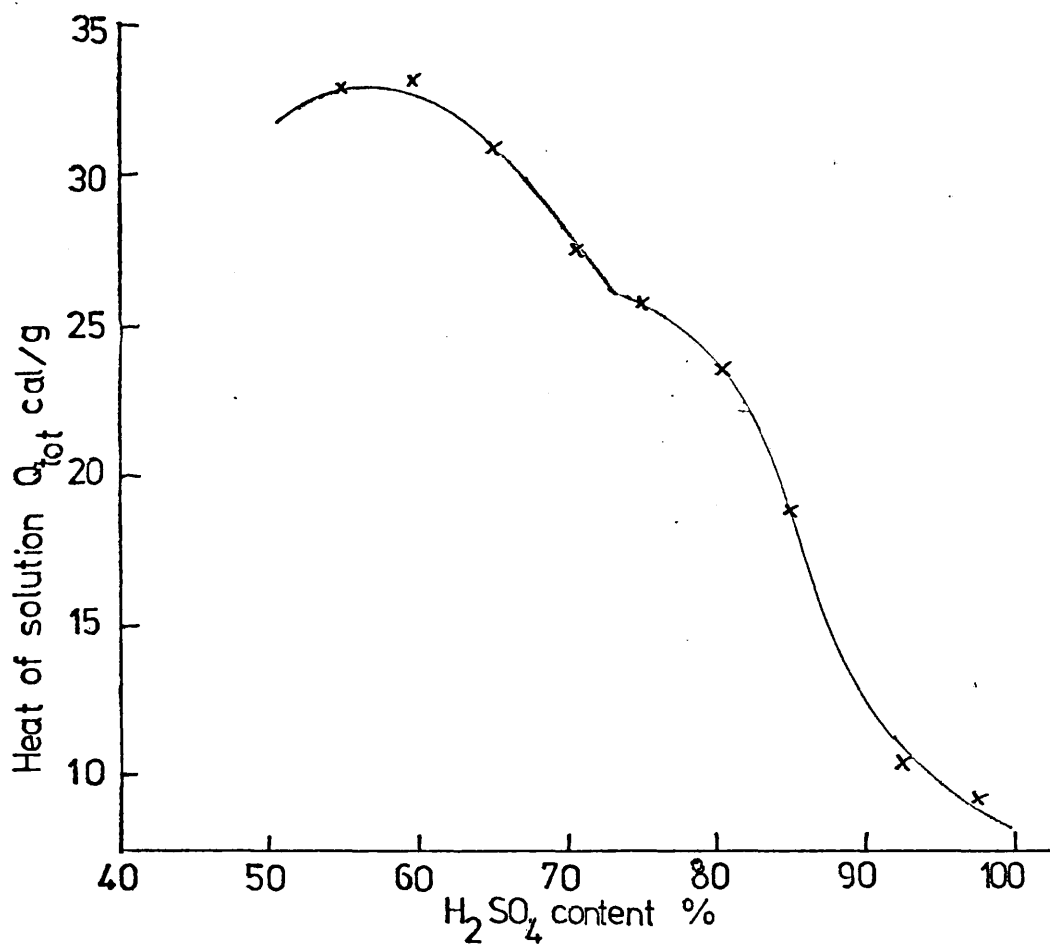


Fig 2-1

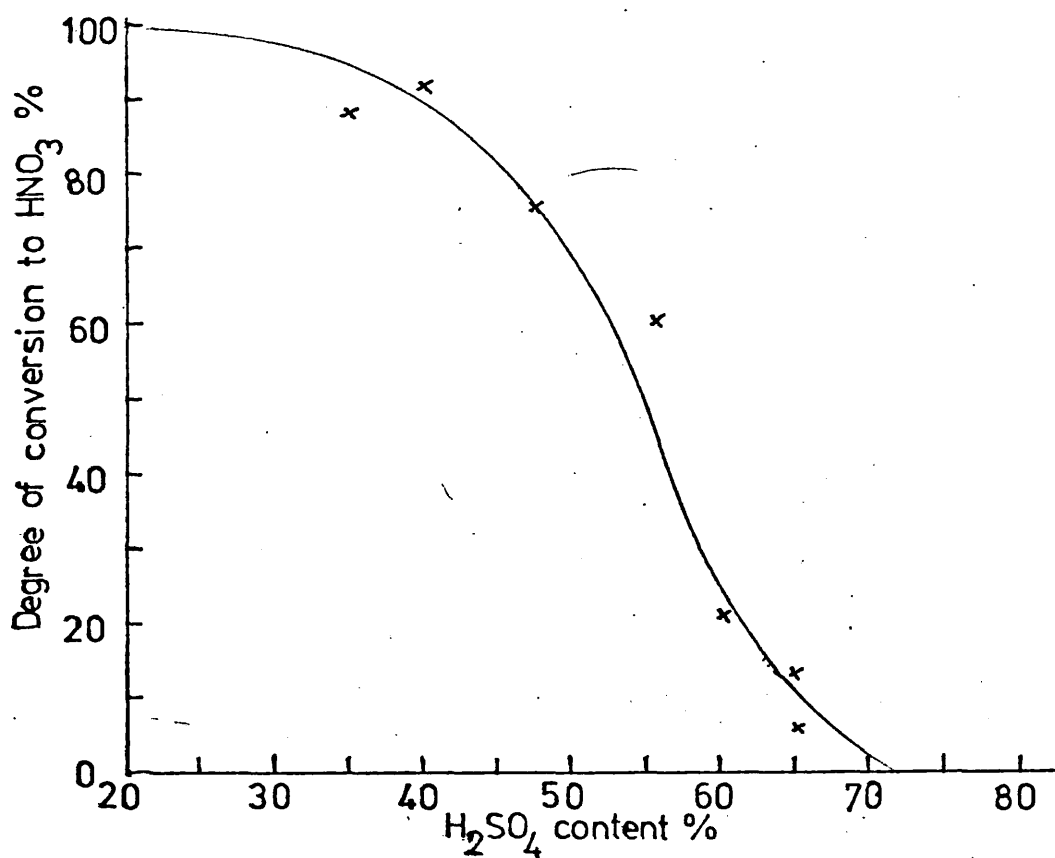


Fig 2-2

NOHSO_4 has hydrolysed. Kunin stated that the observed enthalpies of solution in fig. 2.1 had been corrected in order to account for the disproportionation and hydration processes so that the dissolution could be considered only in terms of equations (8), (9) and (10). The procedure for applying this correction is not at all clear and since no data are given, it is assumed that the values for (i) the extent of disproportionation of dissolved nitrous acid and (ii) the hydrolysis of dissolved NOHSO_4 at a given acid concentration, together with (iii) the literature value for the enthalpy change for process (II) were known.

(iv) CALCULATION OF THE RESULTS

Let q_{TOT} = measured heat of solution corrected for
disproportionation $\text{cal g}^{-1} \text{NOHSO}_4$

q_1 = heat of solution of NOHSO_4 (c) $\text{cal g}^{-1} \text{NOHSO}_4$

q_2 = heat of hydrolysis of NOHSO_4 (diss) $\text{cal g}^{-1} \text{NOHSO}_4$

q_3 = heat of hydration/dehydration of solvent $\text{cal g}^{-1} \text{NOHSO}_4$

a = fraction of NOHSO_4 in sample as crystal

b = fraction of NOHSO_4 in sample dissolved in mother liquor

c = fraction of NOHSO_4 in mother liquor as HNO_2

x_A = degree of hydrolysis at acid concentration A based upon the total amount of NOHSO_4 .

Heat contribution from process (8) = $-q_1 a \text{ cal g}^{-1}$

Total NOHSO_4 present in sample = $(a + b + c)$

At H_2SO_4 concentration A, fraction of NOHSO_4 hydrolysed = $(a+b+c)x_A$

But since fraction c already hydrolysed, heat contribution from process (9) = $-[(a + b + c)x_A - c]q_2 \text{ cal g}^{-1}$

Sulphuric acid liberated by process (10) = $(a + b + c) x_A$

Heat contribution from process (10) = $+(a + b + c)q_3 x_A$

$$\therefore q_{\text{TOT}} = -q_1 a - [(a+b+c)x_A - c]q_2 + (a+b+c)x_A q_3 \quad (13)$$

At A = 100% H_2SO_4 , $x_A = 0$

At A = 58% H_2SO_4 , $x_A = 1$

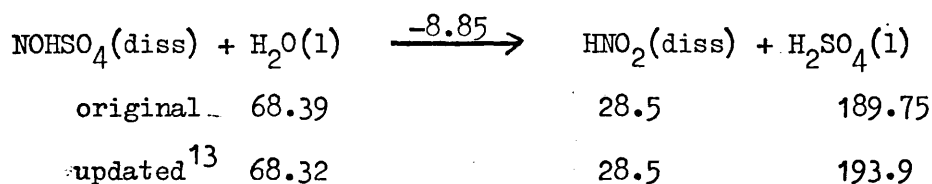
q_3 may be calculated from literature data.

Hence substitution of the above data into (13) generates two simultaneous equations from which q_1 and q_2 may be deduced. The data employed were not given and so the error limits for the numerical solutions cannot be assessed

$$q_1 = -11.35 \text{ cal g}^{-1} \text{NOHSO}_4 = -1.44 \text{ kcal mol}^{-1} \text{NOHSO}_4$$

$$q_2 = -69.7 \text{ cal g}^{-1} \text{NOHSO}_4 = -8.85 \text{ kcal mol}^{-1} \text{NOHSO}_4$$

The physical significance of q_2 and the standard states for the reactants and products in (9), to which q_2 refers, are open to speculation. Kunin's interpretation, which seems reasonable, was that q_2 refers to the process in which one mole of NOHSO_4 dissolved in pure sulphuric acid reacts with one mole of pure water at room temperature to give one mole of nitrous acid dissolved in pure sulphuric acid and one mole of pure sulphuric acid. The substitution of standard thermochemical data into (9) gives a value for $\Delta H_f^\circ \text{NOHSO}_4(\text{diss})$



$$\begin{aligned}
 \text{Hence } \Delta H_f^\circ \text{ NOHSO}_4(\text{diss}) &= 158.71 \text{ kcal mol}^{-1} \text{ (original)} \\
 &= 162.93 \text{ kcal mol}^{-1} \text{ (updated)} \\
 \text{and } \Delta H_f^\circ \text{ NOHSO}_4(\text{c}) &= 160.15 \text{ kcal mol}^{-1} \text{ (original)} \\
 &= 164.37 \text{ kcal mol}^{-1} \text{ (updated)}
 \end{aligned}$$

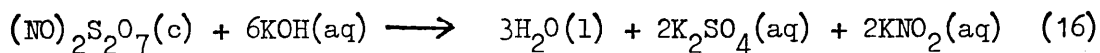
This study is clearly dependent upon the derivation of q_2 , for which it is not possible to check the calculations. If the derivation of q_2 is accepted, the physical significance remains open to discussion. If the interpretation of Kunin is believed, then there remains a problem concerning the value of $\Delta H_f^\circ \text{ HNO}_2(\text{diss}) = 28.5 \text{ kcal mol}^{-1}$, which is numerically identical with the value compiled by NBS¹³ for $\Delta H_f^\circ \text{ HNO}_2$ (undissociated 1M aqueous solution). Since it has been impossible to find any reference to data for $\Delta H_f^\circ \text{ HNO}_2(\text{diss in H}_2\text{SO}_4)$, this coincidence is somewhat disturbing, although the difference between the standard enthalpies of formation of nitrous acid in water and concentrated sulphuric acid solutions may be very small. The gas-liquid equilibrium was not considered.



Although Kunin corrected his heat measurements for the disproportionation of nitrous acid, it is not clear whether corrections were also applied for the dissociation (14) of nitrous acid. These considerations clearly illustrate that there is some need to reinvestigate the thermodynamic data for NOHSO_4 .

(c) DINITROSONIUM DISULPHATE

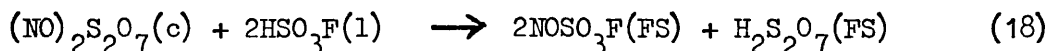
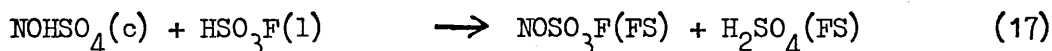
Three independent solution calorimetric studies have been reported for $(\text{NO})_2\text{S}_2\text{O}_7$.^{2,11,12} The two earlier determinations are based on the decomposition of the salt by base in aqueous solution:



The possibility of the disproportionation of nitrous acid was not considered. Vaughan¹² reported a value of $-107.0 \text{ kcal mol}^{-1}$ for the enthalpy of reaction and NBS¹³ have recalculated $\Delta H_f^\circ(\text{NO})_2\text{S}_2\text{O}_7(\text{c})$ from equation (16) as $-253 \text{ kcal mol}^{-1}$ using updated ancillary data. Briner et al² reported the value of $-74 \text{ kcal mol}^{-1}$ for the enthalpy of reaction, but on checking the calculation, the value $-75.2 \text{ kcal mol}^{-1}$ is obtained from which a value for $\Delta H_f^\circ(\text{NO})_2\text{S}_2\text{O}_7 = -284.8 \text{ kcal mol}^{-1}$ is derived from equation (16). The value reported by Woolf and Richards¹¹ by the oxidative degradation of the salt in aqueous alkaline hypochlorite solution under the same conditions described for NOHSO_4 is $-275.4 \pm 0.6 \text{ kcal mol}^{-1}$.

(d) NITROSONIUM FLUOROSULPHATE

$\Delta H_f^\circ\text{NOSO}_3\text{F}(\text{c})$ has been reported by Woolf and Richards¹¹ who measured the enthalpy of solution of NOHSO_4 and $(\text{NO})_2\text{S}_2\text{O}_7$ in fluorosulphonic acid (FS). The dissolution processes were represented by:



The values for $\Delta H_f^\circ\text{NOSO}_3\text{F}(\text{c})$ derived from reactions (17) and (18) were $-180.6 \pm 0.4 \text{ kcal mol}^{-1}$ and $-181.0 \text{ kcal mol}^{-1}$ respectively, which would seem to indicate consistency with their previously reported values for $\Delta H_f^\circ\text{NOHSO}_4(\text{c})$ and $\Delta H_f^\circ(\text{NO})_2\text{S}_2\text{O}_7(\text{c})$.

2.3 SOLUTION CALORIMETRY OF NITROSONIUM SALTS IN AQUEOUS ALKALINE SODIUM HYPOCHLORITE SOLUTION

An investigation of some of the reactions discussed in the previous section for the determination of thermochemical data for nitrosonium salts was made with a view to extending the studies to some other simple compounds. The initial investigations were carried out using aqueous alkaline hypochlorite solution^{5,8} which is not an attractive calorimetric reaction because enthalpies of neutralisation are involved. A series of calorimetric measurements on NOHSO_4 and NOClO_4 were carried out in a non-vented calorimeter from which air had not been displaced. The measured enthalpies of reaction are presented in table 2.3 and the mean value for NOHSO_4 of $-76.22 \pm 2.2 \text{ kcal mol}^{-1}$ is in poor agreement with the value of $-69.4 \pm 0.7 \text{ kcal mol}^{-1}$ determined by Woolf and Richards.¹¹ The air-space in the calorimeter vessel was observed to fill with brown fumes immediately after breaking the ampoule to initiate reaction. The same effect was observed when the reaction was carried out under nitrogen. When the brown fumes had been absorbed by the alkaline solution in the latter case, a current of nitrogen passed through the air space was found to remove nitric oxide gas as indicated by the formation of brown fumes when the emitted gas came into contact with air. These observations clearly indicate that some disproportionation of the transiently-formed nitrous acid occurs under these conditions and that the thermochemical reactions proposed by Woolf [(6) and (7)] have been oversimplified.

The oxidation of nitrite ion by sodium hypochlorite in basic solution was also investigated. It was found impossible to estimate the unreacted sodium hypochlorite iodometrically in strongly basic solution. In a typical experiment, 0.09N sodium nitrite solution

TABLE 2.3

ENTHALPY data for the decomposition of $\text{NOHSO}_4(\text{c})$ by a solution
 0.25M with respect to OCl^- and 0.1M with respect to OH^- (100 cm^3)

NOHSO_4/g	$\text{NOHSO}_4/\text{mol} \times 10^3$	$-\Delta H_{\text{R}}/\text{kcal mol}^{-1}$	$N = \frac{\text{mols of solvent}}{\text{mols of NOHSO}_4}$
0.0937	0.737	74.072	7,506
0.0715	0.563	74.052	9,837
0.0753	0.593	78.032	9,341
0.1053	0.829	77.976	6,679
0.0620	0.488	78.363	11,344
0.0485	0.382	74.817	14,502

$$\begin{aligned} \langle \Delta H_{\text{R}} \rangle &= -76.22 \pm 2.21 \text{ kcal mol}^{-1} \\ &= -318.90 \pm 9.26 \text{ kJ mol}^{-1} \end{aligned}$$

Enthalpy data for the decomposition of $\text{NOClO}_4(\text{c})$ under the same
 conditions

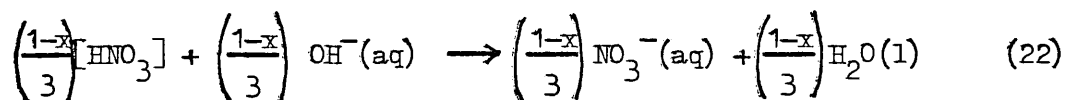
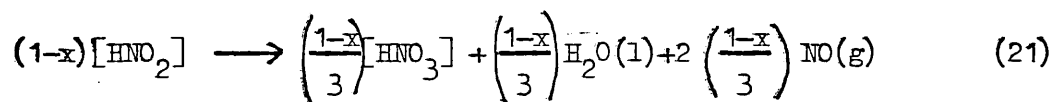
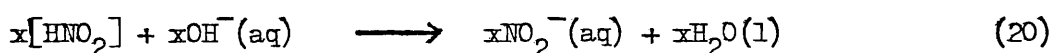
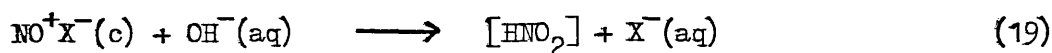
NOClO_4/g	$\text{NOClO}_4/\text{mol} \times 10^3$	$-\Delta H_{\text{R}}/\text{kcal mol}^{-1}$	$N = \frac{\text{mols of solvent}}{\text{mols of NOClO}_4}$
0.0806	0.623	54.873	8,890
0.1025	0.792	56.537	6,990

$$\begin{aligned} \langle \Delta H_{\text{R}} \rangle &= -55.71 \text{ kcal mol}^{-1} \\ &= -233.09 \text{ kJ mol}^{-1} \end{aligned}$$

(20.0 cm³) reacted with 0.11N sodium hypochlorite solution (25.0 cm³) in a medium 0.05N with respect to base, required greater than 25.0 cm³ of 0.1N sodium thiosulphate solution to titrate the liberated iodine after addition of excess of acidulated potassium iodide solution. The analysis was successfully carried out in a bicarbonate medium.¹ It was therefore found impossible to measure the extent of the oxidation in a strongly basic medium and the oxidation of nitrosonium salts by alkaline hypochlorite solution was not considered further.

2.4 MEASUREMENT OF THE DIFFERENCE BETWEEN ΔH_f° VALUES FOR TWO NITROSONIUM SALTS BY CALORIMETRY IN BASIC SOLUTION

In the absence of air, the decomposition of the nitrosonium ion in basic solution can be considered to involve the following steps:



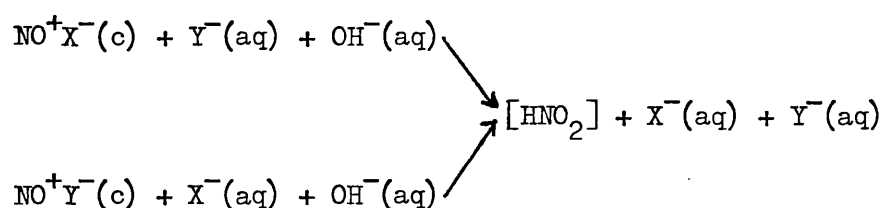
where x = fraction of nitrous acid which does not disproportionate.

The problem could be very much simplified, if the decomposition were carried out under conditions such that $x = 0$ or $x = 1$. Some earlier work¹⁰ concerning the basic hydrolysis of nitrosyl chloride, in which nitrous acid is also involved as an intermediate, has shown that reaction (20) is favoured in strongly basic solution ($\approx 17M$). However, it is not

practicable to carry out calorimetric measurements in very strong base when very thin glass ampoules are involved, and hence conditions leading to identical values for x were considered. The following hypothesis was proposed and a series of experiments were carried out for NOHSO_4 , NOClO_4 and $(\text{NO})_2\text{S}_2\text{O}_7$.

HYPOTHESIS

If two nitrosonium salts NO^+X^- , NO^+Y^- are decomposed in turn by an excess of aqueous alkali in the presence of the anion of the other, then the final state of each solution after decomposition will be identical provided that the conditions of the decomposition are identical



Constancy of the stirring rate is probably most important, since the rate of dissolution of the sample is probably associated with the extent of the disproportionation reaction. The measured enthalpies of reaction for the decomposition of NOClO_4 , NOHSO_4 and $(\text{NO})_2\text{S}_2\text{O}_7$ by 0.1M sodium hydroxide solution under nitrogen are presented in tables 2.4, 2.5 and 2.6 respectively.

An attempt was made to establish the extent of disproportionation by measuring the nitrite level in solution for selected calorimetric runs after having displaced the liberated nitric oxide gas from the air space. Results are presented in table 2.7. Post-calorimetric analyses were made on the solutions from calorimetric runs carried out in 200 cm³ vessels for both nitrite and nitrate after having displaced the nitric oxide gas. Results are presented in table 2.8.

TABLE 2.4

Enthalpy data for the decomposition of NOClO_4 in 0.1M NaOH
(100 cm^3) at 298.2 K

NOClO_4/g	$\text{NOClO}_4/\text{mol} \times 10^3$	$-\Delta H_R/\text{kcal mol}^{-1}$	$N = \frac{\text{mols of solvent}}{\text{mols of NOClO}_4}$
0.1717	1.326	26.48	4173
0.1358	1.049	26.49	5276
0.1240	0.958	26.10	5777
0.1311	1.013	25.94	5464
0.0869	0.671	26.05	8248
0.1494	1.154	26.24	4796
0.1575	1.217	26.19	4548
0.1540	1.190	25.96	4651

$$\langle \Delta H_R \rangle = -26.19 \pm 0.18 \text{ kcal mol}^{-1}$$

$$\langle \Delta H_R \rangle = -109.58 \pm 0.75 \text{ kJ mol}^{-1}$$

TABLE 2.5

Enthalpy data for the decomposition of NOHSO_4 in 0.1M NaOH
(100 cm^3) at 298.2 K

NOHSO_4/g	$\text{NOHSO}_4/\text{mol} \times 10^3$	$-\Delta H_R/\text{kcal mol}^{-1}$	$N = \frac{\text{mols of solvent}}{\text{mols of NOHSO}_4}$
0.1130	0.889	50.115	6224
0.0949	0.747	50.015	7411
0.1208	0.951	49.476	5822
0.1030	0.811	49.587	6829
0.1404	1.105	50.247	5010
0.0927	0.729	50.523	7587
0.0988	0.777	50.276	7119

$$\begin{aligned} \langle \Delta H_R \rangle &= -50.03 \pm 0.35 \text{ kcal mol}^{-1} \\ &= -209.33 \pm 1.46 \text{ kJ mol}^{-1} \end{aligned}$$

TABLE 2.6

Enthalpy data for the decomposition of $(\text{NO})_2\text{S}_2\text{O}_7$ in 0.1MNaOH (100 cm³)
at 298.2 K

$(\text{NO})_2\text{S}_2\text{O}_7/\text{g}$	$(\text{NO})_2\text{S}_2\text{O}_7/\text{mol} \times 10^3$	$-\Delta H_R/\text{kcal mol}^{-1}$	$N = \frac{\text{mols of solvent}}{\text{mols of } (\text{NO})_2\text{S}_2\text{O}_7}$
0.1044	0.442	105.470	12,518
0.0948	0.401	104.990	13,786
0.1040	0.440	106.304	12,566
0.0848	0.359	104.647	15,412
0.1227	0.520	107.390	10,651
0.1366	0.578	105.351	9,567

$$\langle \Delta H_R \rangle = -105.69 \pm 1.05 \text{ kcal mol}^{-1}$$

$$= -442.21 \pm 4.39 \text{ kJ mol}^{-1}$$

TABLE 2.7

NO_2^- Level in solution after decomposition of NO^+ salts

NOClO_4/g	$\text{NOClO}_4/\text{mol} \times 10^3$	$\text{NO}_2^-/\text{mol} \times 10^3$	x
0.1860	1.437	1.084	0.755
0.1313	1.014	0.775	0.764
0.1775	1.371	1.050	0.766
0.2719	2.100	1.559	0.742
0.2220	1.715	1.290	0.752
			$\langle x \rangle = 0.756$

NOHSO_4/g	$\text{NOHSO}_4/\text{mol} \times 10^3$	$\text{NO}_2^-/\text{mol} \times 10^3$	x
0.1219	0.959	0.819	0.854
0.1710	1.346	1.138	0.846
0.2500	1.967	1.631	0.829
[0.1870	1.472	1.177	0.800]
			$\langle x \rangle = 0.84$

$(\text{NO})_2\text{S}_2\text{O}_7/\text{g}$	$(\text{NO})_2\text{S}_2\text{O}_7/\text{mol} \times 10^3$	$\text{NO}_2^-/\text{mol} \times 10^3$	x
0.1040	0.440	0.626	0.712
0.1227	0.520	0.747	0.719
0.1366	0.578	0.818	0.707
			$\langle x \rangle = 0.713$

TABLE 2.8

NO:NO₃⁻ mole ratio following the decomposition of NO⁺ salts by aqueous base.

(i) NOClO₄

	Run 1	Run 2
NOClO ₄ /g	0.2719	0.2220
NOClO ₄ /mol x 10 ³	2.100	1.715
NO ₃ ⁻ + NO ₂ ⁻ /mol x 10 ³	1.760	1.440
NO ₂ ⁻ /mol x 10 ³	1.559	1.290
NO ₃ ⁻ /mol x 10 ³	0.201	0.150
NO/mol x 10 ³	0.340	0.275
-ΔH _R /Kcal mol ⁻¹	26.15	25.99
NO:NO ₃ ⁻ mol ratio	1.70:1	1.83:1

(ii) NOHSO₄

	Run 1	Run 2
NOHSO ₄ /g	0.1870	0.2500
NOHSO ₄ /mol x 10 ³	1.472	1.967
NO ₃ ⁻ + NO ₂ ⁻ /mol x 10 ³	1.340	1.760
NO ₂ ⁻ /mol x 10 ³	1.177	1.631
NO ₃ ⁻ /mol x 10 ³	0.163	0.129
NO/mol x 10 ³	0.132	0.207
-ΔH _R /Kcal mol ⁻¹	49.55	49.95
NO:NO ₃ ⁻ mol ratio	0.81:1	1.60:1

2.5 INTERPRETATION OF SOLUTION CALORIMETRY DESCRIBED IN SECTIONS 2.3 AND 2.4.

The data presented in table 2.7 clearly indicate that the extent of disproportionation of the nitrous acid transiently formed during the degradation in basic solution is variable, although it is possible to reproduce, within experimental error, the same final state for the degradation of any one compound. The data presented in table 2.8 apparently indicate that the mole ratio of $\text{NO}^+:\text{NO}_3^-$ of 2:1 was not obtained, but the low values obtained undoubtedly reflect the limitations of the analytical procedure. Consider the differences between this work and the similar study carried out by Cruse et al.³:

(i) Scale of reaction

The extreme sensitivity of the thermistors used in this calorimeter required that calorimetric reactions were carried out on a scale of 0.2 - 0.3 g NOClO_4 in 0.1M sodium hydroxide (200 cm^3). Cruse et al. using a calibrated Beckmann thermometer to measure temperature changes were able to use 1.5 g samples of NOClO_4 in 50 cm^3 of 0.5M NaOH.

(ii) The calorimeter

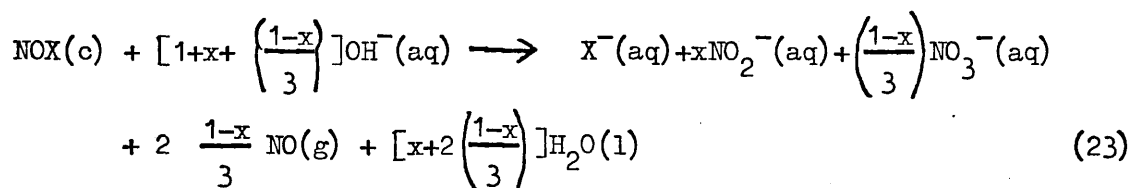
The calorimeter vessel used in this work could not be conveniently adapted to measure small volumes of gas liberated during thermochemical reactions. Hence the quantity of nitric oxide gas liberated during the reaction was determined indirectly. The analytical procedure therefore relied entirely upon the effective removal of nitric oxide from the system, by passing a stream of oxygen-free nitrogen through the solution and air-space for five minutes. Great care had to be taken when solutions were to be analysed after calibrating the system electrically, to ensure that air did not diffuse into the system

during the cooling period between carrying out the reaction and calibration. In these reactions the calorimeter vessel was allowed to cool slowly to equilibrium, the process not being aided by passing a current of nitrogen. The empty calorimeter vessel was frequently tested for leakage by noting the positive pressure retained inside the vessel five minutes after adding one drop of liquid nitrogen.

(iii) The analysis

The principal sources of error undoubtedly arise from the determination of very small quantities of nitrate ion and nitric oxide gas by indirect methods. Small errors arising in the analyses of either nitrite or combined nitrate and nitrite, due to inefficient removal of nitric oxide, although not seriously affecting the value for x , significantly change the value for the ratio $\text{NO}:\text{NO}_3^-$. The analytical calculation for NOClO_4 presented in Appendix (1) clearly illustrates that the apparently anomalous ratio of $\text{NO}:\text{NO}_3^-$ is well within experimental error.

Further, differences in values of standard enthalpies of formation are insensitive to small differences in the value of x . The combination of equations (19), (20), (21) and (22) leads to the following equation for the reaction in terms of x :



By substituting standard thermochemical data from table 2.9 into equation (23), a thermochemical relationship, showing the dependence

TABLE 2.9
Ancillary Thermochemical Data

Compound	$-\Delta H_f^\circ/\text{kcal mol}^{-1}$	$-\Delta H_f^\circ/\text{kJ mol}^{-1}$
NO(g)	-21.56 ± 0.05	-90.21 ± 0.21
NO ₂ ⁻ (aq)	25.00 ± 1.00	104.60 ± 4.18
NO ₃ ⁻ (aq)	49.52 ± 0.11	207.19 ± 0.46
SO ₄ ²⁻ (aq)	217.32 ± 0.00	909.27 ± 0.00
ClO ₄ ⁻ (aq)	30.91 ± 0.10	129.33 ± 0.43
Cl ⁻ (aq)	39.93 ± 0.00	167.08 ± 0.00
OCl ⁻ (aq)	$26.20 \pm ?$	$109.72 \pm ?$
O ₂ (g)	0	0
HNO ₂ (m = 1)	28.50 ± 1.00	119.24 ± 4.18
H ₂ SO ₄ (l)	$193.9 \pm ?$	$811.28 \pm ?$
OH ⁻ (aq)	54.98 ± 0.00	230.02 ± 0.00
H ₂ O(l)	68.32 ± 0.00	285.83 ± 0.00

of the enthalpy of reaction ΔH_R on the fraction x , can be generated. A problem does arise concerning the standard state of nitric oxide, some of which may be dissolved in the calorimetric fluid in the non-vented system, which will be under a slight pressure. The analyses carried out by Cruse et al.³ indicated that all the nitric oxide was in the gaseous state under the conditions of his experiment, and this is assumed here. Since the ultimate consideration of the results will be in terms of differences between the standard enthalpies of formation of two nitrosonium salts, then provided that the nitric oxide is in the same state for each calorimetric experiment, the specification of this state is unnecessary.

Hence substituting ancillary data into (23):

$$\text{for NOClO}_4: \Delta H_R = -5.26 - 9.01x - \Delta H_F^{\circ} \text{NOClO}_4(c) \quad (24)$$

$$\text{for NOHSO}_4: \Delta H_R = -205.06 - 9.01x - \Delta H_F^{\circ} \text{NOHSO}_4(c) \quad (25)$$

$$\text{for (NO)}_2\text{S}_2\text{O}_7: \Delta H_R = -341.72 - 18.00x - \Delta H_F^{\circ} \text{(NO)}_2\text{S}_2\text{O}_7(c) \quad (26)$$

The error limits have been omitted and all values are in kcal mol⁻¹.

The relatively low values of the x coefficient in equations (24), (25) and (26) lend confidence to explain the high precision of the enthalpy data presented in tables 2.4, 2.5 and 2.6. If the experimentally determined enthalpies of reaction are now substituted into equations (24), (25) and (26), the following relationships are obtained:

$$\Delta H_F^{\circ} \text{NOClO}_4(c) = (+20.92 - 9.01x) \text{ kcal mol}^{-1} \quad (27)$$

$$\Delta H_F^{\circ} \text{NOHSO}_4(c) = (-155.03 - 9.01x) \text{ kcal mol}^{-1} \quad (28)$$

$$\Delta H_F^{\circ} \text{(NO)}_2\text{S}_2\text{O}_7(c) = (-236.03 - 18.00x) \text{ kcal mol}^{-1} \quad (29)$$

Thus it is possible to consider quantitatively the differences between the standard enthalpies of formation of two nitrosonium salts since a small variation in x does not seriously affect $\Delta H_f^\circ \text{NOX}(c)$.

Equations (28) and (29) are inconsistent with the data obtained by Woolf and Richards for NOHSO_4 and $(\text{NO})_2\text{S}_2\text{O}_7$. Since $0 \leq x \leq 1$, it follows that $\Delta H_f^\circ \text{NOHSO}_4(c)$ can never assume the value of $-182.5 \text{ kcal mol}^{-1}$ and $\Delta H_f^\circ (\text{NO})_2\text{S}_2\text{O}_7(c)$ can never be $-275.4 \text{ kcal mol}^{-1}$. If the experimentally determined values for x from table 2.7 are now substituted into equations (27), (28) and (29), the standard enthalpy of formation values for the compounds are obtained:

For NOClO_4 : $x = 0.76$

$$\Delta H_f^\circ \text{NOClO}_4(c) = +14.10 \text{ kcal mol}^{-1} (+ 15.58 \text{ kcal mol}^{-1} \text{ Gruse}^3)$$

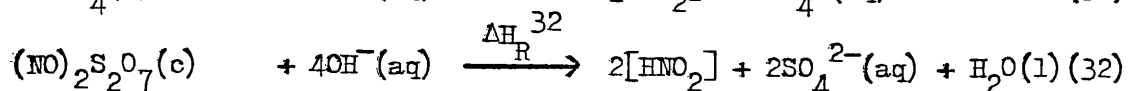
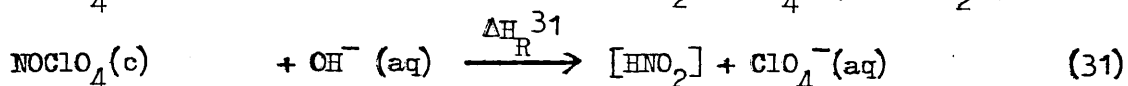
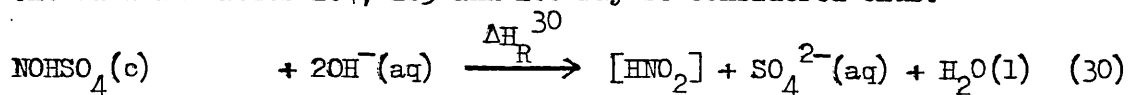
For NOHSO_4 : $x = 0.84$

$$\Delta H_f^\circ \text{NOHSO}_4(c) = -162.59 \text{ kcal mol}^{-1} (-164.37 \text{ kcal mol}^{-1} \text{ Kunin}^6)$$

For $(\text{NO})_2\text{S}_2\text{O}_7$: $x = 0.71$

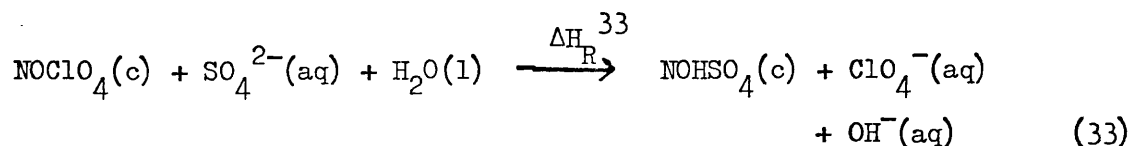
$$\Delta H_f^\circ (\text{NO})_2\text{S}_2\text{O}_7 = -248.81 \text{ kcal mol}^{-1} (-253 \text{ kcal mol}^{-1} \text{ NBS}^{13})$$

The agreement with literature data is of particular interest. If the problem of the standard state for nitric oxide is to be eliminated, the data in tables 2.4, 2.5 and 2.6 may be considered thus:



If x values are taken to be identical in each case, then consider the

reaction obtained by subtracting (30) from (31):



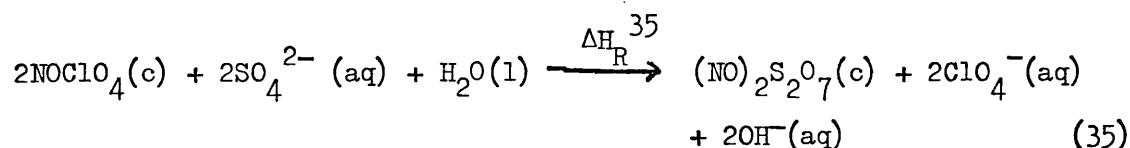
The associated enthalpy change can be expressed:

$$\Delta H_{\text{R}}^{33} = \Delta H_{\text{R}}^{31} - \Delta H_{\text{R}}^{30} \quad (34)$$

and substitution of thermochemical data from table 2.9 into (33) gives that:

$$\begin{aligned} [\Delta H_{\text{f}}^{\circ} \text{NOClO}_4(\text{c}) - \Delta H_{\text{f}}^{\circ} \text{NOHSO}_4(\text{c})] &= +175.92 \pm 0.41 \text{ kcal mol}^{-1} \\ &+ 736.05 \pm 1.72 \text{ kJ mol}^{-1} \end{aligned}$$

Similarly for (31) and (32), the enthalpy change for the reaction:



will be given by:

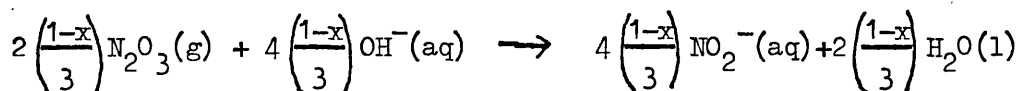
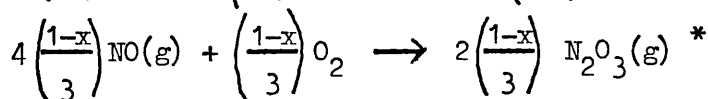
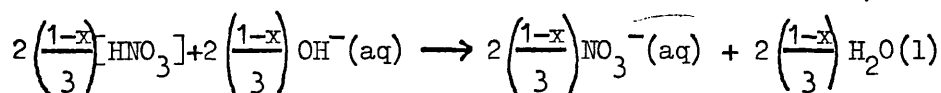
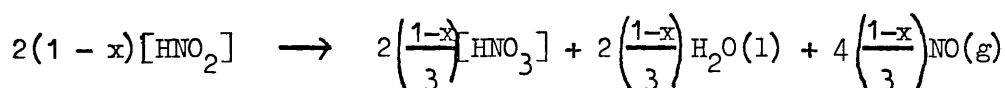
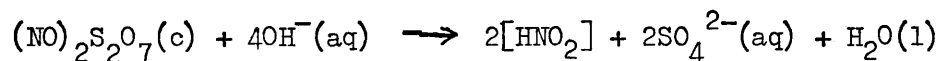
$$\Delta H_{\text{R}}^{35} = \Delta H_{\text{R}}^{31} - \Delta H_{\text{R}}^{32} \quad (36)$$

and substitution of standard thermochemical data from table 2.9 into (35) gives that:

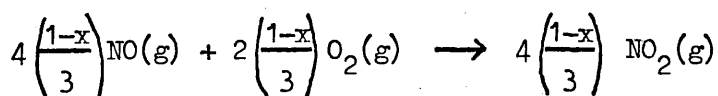
$$\begin{aligned} [2\Delta H_{\text{f}}^{\circ} \text{NOClO}_4(\text{c}) - \Delta H_{\text{f}}^{\circ} (\text{NO})_2\text{S}_2\text{O}_7] &= +277.88 \pm 1.09 \text{ kcal mol}^{-1} \\ &+ 1162.65 \pm 4.56 \text{ kJ mol}^{-1} \end{aligned}$$

If the absolute value for the enthalpy of formation for any one of these nitrosonium compounds is known, then it follows that the enthalpies of formation for the other two may be deduced.

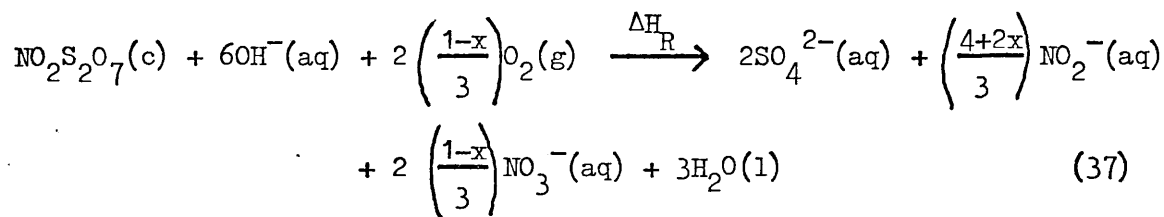
At present, the values derived by substituting the experimentally-determined values for x into (27) (28) and (29) are certainly the most reliable. Consider the decomposition of $(\text{NO})_2\text{S}_2\text{O}_7(\text{c})$ in base according to Vaughan.¹² The experimental details are not available, but the reported enthalpy of reaction of $-107 \text{ kcal mol}^{-1}$ is in good agreement with the value of $-105.7 \text{ kcal mol}^{-1}$ from this study. This value could be derived from (26) by substituting a different value for x assuming that both compounds are equally pure. Alternatively, a slightly lower value can be shown to result from the presence of oxygen in the system. Since the original study did not consider any disproportionation of nitrous acid, it is unlikely that the reaction was carried out under nitrogen. The decomposition of the compound in the presence of oxygen can be considered thus:



*This assumes a limited amount of oxygen; undoubtedly the oxidation could also proceed:



The overall decomposition may therefore be represented by:



Substitution of thermochemical data into (40) gives:

$$\Delta H_{\text{R}} = -376.07 + 16.35x - \Delta H_{\text{f}}^{\circ}(\text{NO})_2\text{S}_2\text{O}_7(\text{c}) \quad (38)$$

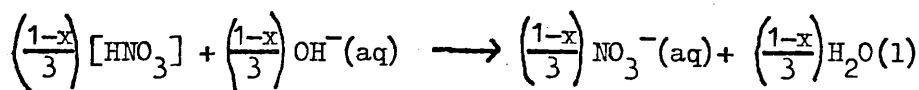
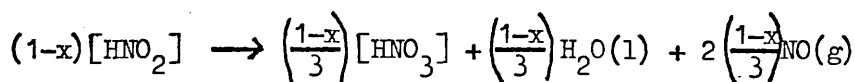
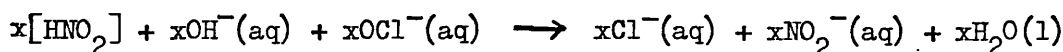
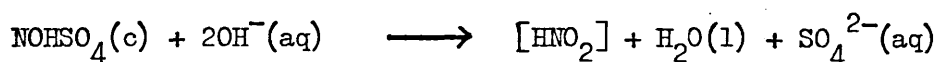
By substituting $\Delta H_{\text{f}}^{\circ}(\text{NO})_2\text{S}_2\text{O}_7 = -248.8 \text{ kcal mol}^{-1}$, $x = 0.71$ into (38)

it is found that:

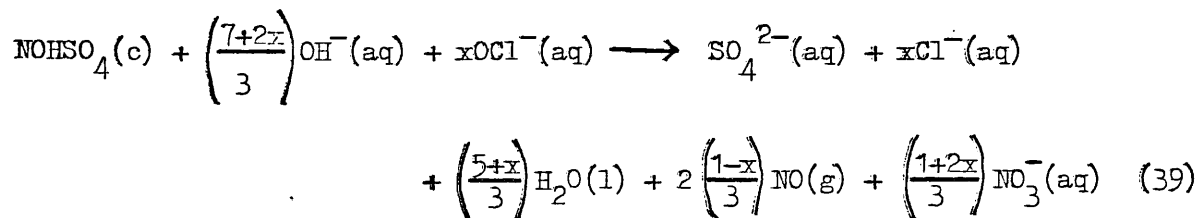
$$\Delta H_{\text{R}} = -115.67 \text{ kcal mol}^{-1}$$

Thus one effect of oxygen in the system is to decrease the value for the enthalpy of reaction, and this could explain the slightly lower value reported by Vaughan, although numerous experimental errors could also be involved. Inspection of (38) indicates an even smaller dependence of ΔH_{R} on x , but the difficulty of determining x under these conditions renders the reaction less favourable calorimetrically.

A similar reasoning may be applied to the oxidative degradation of nitrosonium salts by alkaline hypochlorite solution. Consider the reaction to be carried out in an oxygen-free system; under these conditions the reaction can be broken down into the following steps:



The overall reaction may then be represented by:



and substitution of standard thermochemical data from table 2.9 into (39)

gives that:

$$\Delta H_{\text{R}} = -205.0 - 47.28x - \Delta H_{\text{f}}^{\circ}\text{NOHSO}_4(\text{c}) \quad (40)$$

Inspection of (43) shows that ΔH_{R} is more seriously affected by small changes in x which is reflected in the low precision of the data presented in table 2.3.

If the extent of disproportionation is considered to be approximately the same as in the absence of OCl^- , then substituting $\Delta H_{\text{R}} = -76.22 \text{ kcal mol}^{-1}$ and $x = 0.84$ into (40) gives that:

$$\Delta H_{\text{f}}^{\circ}\text{NOHSO}_4(\text{c}) \approx -168 \text{ kcal mol}^{-1}$$

The degradation of NOClO_4 similarly leads to

$$\Delta H_{\text{R}} = -5.26 - 47.28x - \Delta H_{\text{f}}^{\circ}\text{NOClO}_4(\text{c}) \quad (41)$$

and substituting $\Delta H_{\text{R}} = -55.7$ and $x = 0.76$ into (41) gives that:

$$\Delta H_{\text{f}}^{\circ}\text{NOClO}_4(\text{c}) \approx +15 \text{ kcal mol}^{-1}$$

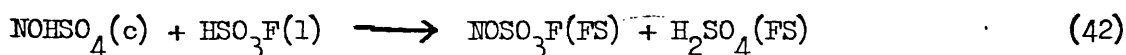
These standard enthalpy of formation values are of the same order of magnitude as the values derived from (27) and (28) of +14.1 and -162.6 kcal mol^{-1} respectively and clearly illustrate the errors involved in the reactions proposed by Woolf and Richards.¹¹ Since the experimental data presented in table 2.3 were obtained under experimental

conditions such that x was unlikely to have remained constant, owing to a different rate of stirring being employed for each individual run, it is not possible to interpret these data further.

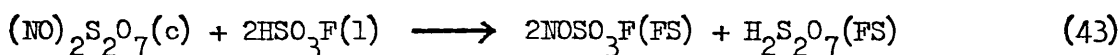
2.6 CONCLUSIONS

This study has emphasised the numerous difficulties associated with the determination of thermochemical data for nitrosonium compounds and has pointed out several errors in the literature arising from the failure of various studies to recognise the disproportionation of nitrous acid. The experimentally determined values from this study are compared with literature values in table 2.10.

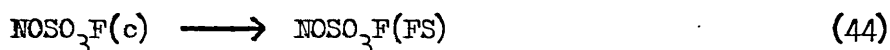
The apparent consistency of the value for $\Delta H_{\text{f}}^{\circ} \text{NOSO}_3\text{F}(\text{c})$ derived by Woolf and Richards from a consideration of the heats of solution of $\text{NOHSO}_4(\text{c})$ and $(\text{NO})_2\text{S}_2\text{O}_7(\text{c})$ in fluorosulphonic acid is fortuitous. Consider the correction applied to these data using $\Delta H_{\text{f}}^{\circ} \text{NOHSO}_4(\text{c})$ and $\Delta H_{\text{f}}^{\circ} (\text{NO})_2\text{S}_2\text{O}_7(\text{c})$ values from this study:



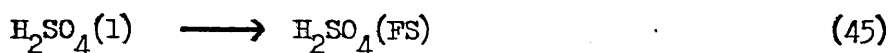
$$\Delta H_{\text{R}} = -10.17 \pm 0.32 \text{ kcal mol}^{-1}$$



$$\Delta H_{\text{R}} = -29.7 \pm 1.0 \text{ kcal mol}^{-1}$$



$$\Delta H_{\text{R}} = -7.35 \pm 0.11 \text{ kcal mol}^{-1}$$



$$\Delta H_{\text{R}} = -0.23 \pm 0.01 \text{ kcal mol}^{-1}$$



$$\Delta H_{\text{R}} = -1.63 \pm 0.01 \text{ kcal mol}^{-1}$$

From (45) it follows that

$$\Delta H_{f,2}^{\circ} \text{H}_2\text{SO}_4(\text{FS}) = -194.14 \text{ kcal mol}^{-1} \quad (47)$$

and substituting (47) and standard data into (42) gives that:

$$\Delta H_{f,3}^{\circ} \text{NOSO}_3\text{F}(\text{FS}) = -168.03 \text{ kcal mol}^{-1}$$

Assuming that the dissolution of $\text{NOSO}_3\text{F}(\text{c})$ in fluorosulphonic acid produces the same state as the dissolution of NOHSO_4 :

$$\Delta H_{f,3}^{\circ} \text{NOSO}_3\text{F}(\text{c}) = -160.7 \text{ kcal mol}^{-1}$$

Inspection of (43) shows that a value for $\Delta H_{f,2}^{\circ}(\text{NO})_2\text{S}_2\text{O}_7(\text{FS})$ is required. Their assumption that this is equal to the sum of the heats of solution of SO_3 and H_2SO_4 appears doubtful. Consider the following thermodynamic cycle (fig. 2.3).

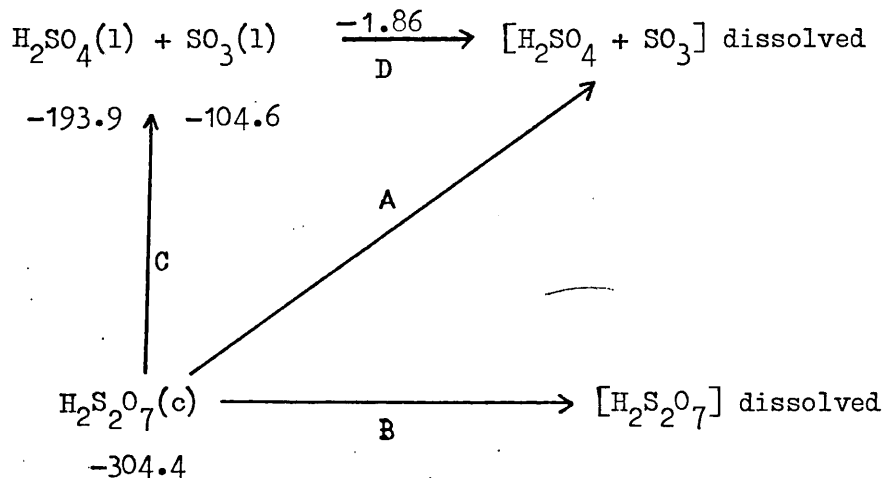


fig. 2.3

The final state after dissolving oleum in fluorosulphonic acid is not specified, but the thermodynamic cycle is not quantitatively consistent with this being identical to dissolving an equimolar mixture of H_2SO_4 and SO_3 . That the enthalpy change for process B is $-1.86 \text{ kcal mol}^{-1}$

is not apparently justifiable. Woolf and Richards apparently assumed that the final state of $\text{H}_2\text{S}_2\text{O}_7(\text{FS})$ was identical with $[\text{H}_2\text{SO}_4 + \text{SO}_3]\text{FS}$ and calculated $\Delta\text{H}_f^\circ\text{H}_2\text{S}_2\text{O}_7(\text{FS}) = -306.2 \text{ kcal mol}^{-1}$ from process A. If these states were identical, then $\Delta\text{H}_f^\circ\text{H}_2\text{S}_2\text{O}_7(\text{FS}) = -300.44 \text{ kcal mol}^{-1}$ should be calculated from process D. This would significantly alter the value derived from (43) for $\Delta\text{H}_f^\circ\text{NOSO}_3\text{F}(\text{c})$ using their data for $\Delta\text{H}_f^\circ(\text{NO})_2\text{S}_2\text{O}_7$. However, it is clearly not possible to derive $\Delta\text{H}_f^\circ\text{NOSO}_3\text{F}(\text{c})$ from (43) in the absence of the correct ancillary data and the apparent consistency of thermochemical data obtained by Woolf and Richards from (42) and (43) is coincidental.

TABLE 2.10

Thermochemical data for nitrosonium salts

Compound	$-\Delta H_f^\circ/\text{kcal mol}^{-1}$	$-\Delta H_f^\circ/\text{kJ mol}^{-1}$	Ref.
$\text{NOClO}_4(\text{c})$	-14.10	-59.0	This work
	-15.58	-65.2	3 corrected
	39.6	165.7	3
$\text{NOHSO}_4(\text{c})$	162.6	680.3	This work
	164.4	687.8	6
	182.7	764.4	11
$(\text{NO})_2\text{S}_2\text{O}_7(\text{c})$	248.8	1041.0	This work
	253.0	1058.6	13
	284.8	1191.6	2
	275.4	1152.3	11

REFERENCES

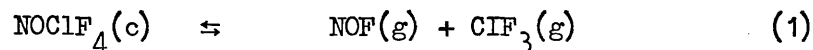
1. R. Belcher, A.J. Nutten, Quantitative Inorganic Analysis, Butterworths (1966).
2. E. Briner, G.H. Lunge, A. van der Wiik, *Helv. Chim. Acta*, 11, (1928), 1125-44.
3. K. Cruse, G. Huck, H. Möller, *Zeit. anorg. allgem. Chem.*, (1949), 259, 173-82.
4. H. Gerding, W.F. Haak, *Chem. Weekblad*, (1956), 52 282-3.
5. J.P. King, J.W. Cobble, *J.A.C.S.*, (1960), 52, 2111-3.
6. T.I. Kunin, *J. Appl. Chem. U.S.S.R.*, (1954), 27, 237-45.
7. T.I. Kunin, *J. Appl. Chem. U.S.S.R.*, (1954), 27, 237-45, ref. (11) and (12) therein.
8. J.E. McDonald, J.P. King, J.W. Cobble, *J. Phys. Chem.*, (1960), 64, 1345-6.
9. S.J. Peake, Ph.D. thesis, Royal Holloway College, (1976).
10. A. Perret, R. Perrot, *Compt. rend.*, (1931), 193, 937-9.
11. G.W. Richards, A.A. Woolf, *J.C.S. A*, (1968), 470-6.
12. R. Vaughan, Ph.D. thesis, John Hopkins University, (1928).
13. D.D. Wagman et al., *N.B.S. Tech. Note*, 270-1, (1969).
14. G. Wilkinson, F.A. Cotton, *Advanced Inorganic Chemistry*, 2nd Edition, Wiley (1968).

CHAPTER 3

A THERMODYNAMIC AND SPECTROSCOPIC INVESTIGATION OF NOBCl_4

3.1 INTRODUCTION

In the previous chapter, a critical discussion of the determination of thermodynamic data for nitrosonium compounds via solution calorimetric procedures was given. An alternative approach will now be considered. For volatile compounds, thermodynamic data may be derived from the temperature dependence of the vapour pressure provided that the nature of the solid-gas equilibrium and the chemical identity of each component in the system can be established. This method⁵⁸ was used to determine $\Delta H_f^\circ \text{NOClF}_4(c)$ assuming the equilibrium to be:



This equilibrium was studied in a stainless steel apparatus, using stainless steel pressure gauges for measuring pressures. NOCl forms volatile nitrosonium salts with both metallic and non-metallic chlorides.^{41,57} It exhibits negligible dissociation⁵³ into NO and Cl_2 at ambient or slightly elevated temperatures, and the compounds may be handled in glass apparatus. This method was extended to the volatile 1:1 compound of NOCl with BCl_3 thus permitting the evaluation of $\Delta H_f^\circ \text{NOBCl}_4(c)$.

3.2 NOBCl_4 , PREPARATION AND RAMAN SPECTROSCOPY

This compound was originally obtained by Geuther¹⁹ in 1874 as a yellow sublimate by reaction of N_2O_4 with an excess of BCl_3 . In 1949, Partington and Whynes³⁷ prepared yellow crystals of the compound by slowly cooling an equimolar mixture of BCl_3 and NOCl from 303 K to below ambient temperature. Olah³⁶ has also described the precipitation of the compound by mixing homogeneous solutions of NOCl

and BCl_3 in CF_2Cl_2 at 223 K. After volatilisation of the solvent and gentle pumping of the solid residue at low temperatures, colourless crystals remained. Since two NO stretching bands at 2123 and 1800 cm^{-1} were observed in the infra-red spectrum, Olah postulated a solid state structure consisting of $\text{NO}^+\text{BCl}_4^-$ in equilibrium with the oxygen-coordinated NOCl polarised species. This inference appeared to be based upon incomplete vibrational data and so before carrying out any pressure measurements, an attempt was made to characterise the solid state species using Raman spectroscopy.

Considerable preparative and manipulative difficulties were experienced since the compound exists as a solid below 297 K only under its own vapour pressure. Melting occurs in a sealed tube at ca. 297 K with the separation of two layers, an upper brown layer and a lower red layer. The lower red layer disappears completely on heating to 333 K. Two apparent modifications of the solid were isolated:

(i) A white flocculent form resembling the product described by Olah and prepared at low temperatures.

(ii) A lemon-yellow crystalline form resembling the product described by Partington and prepared at room temperature. The low-temperature form reverted to the room-temperature form on melting and slowly cooling. Raman spectra were measured for all phases of the system at both ambient and liquid nitrogen temperatures, and also for pure NOCl .

3.3 INTERPRETATION OF RAMAN SPECTRA FOR THE SYSTEM

The vibrational spectrum of NOCl has not been fully reported. All three fundamental frequencies have been observed in the infra-red^{27,23} spectra of the solid and gaseous phases. However, only the gaseous phase Raman spectrum has been investigated,²⁴ and one fundamental frequency ν_3 was observed using 488.0 nm Ar⁺ excitation. Early Raman studies³ were unsuccessful using a Toronto arc owing to the red colour of NOCl. In this study, using 647.1 nm Kr⁺ excitation, Raman shifts were observed for ν_2 and ν_3 from solid, liquid and gaseous samples (Table 3.1). No reason for the apparent absence of ν_1 , which is essentially an N = O stretching mode can be afforded. The Raman shifts observed in the gaseous phase coincide with the published infra-red²⁷ absorption frequencies. In the solid phase, however, there is considerable disagreement. In particular a difference of 34 cm⁻¹ between the Raman and infra-red frequency values for ν_2 strongly suggests that one set of data is incorrect if both refer to the same band. Infra-red data for the liquid phase have not been reported, but both ν_2 and ν_3 in the Raman spectrum are broad, and ν_3 is asymmetric. This possibly reflects considerable association and partial ionisation.⁹



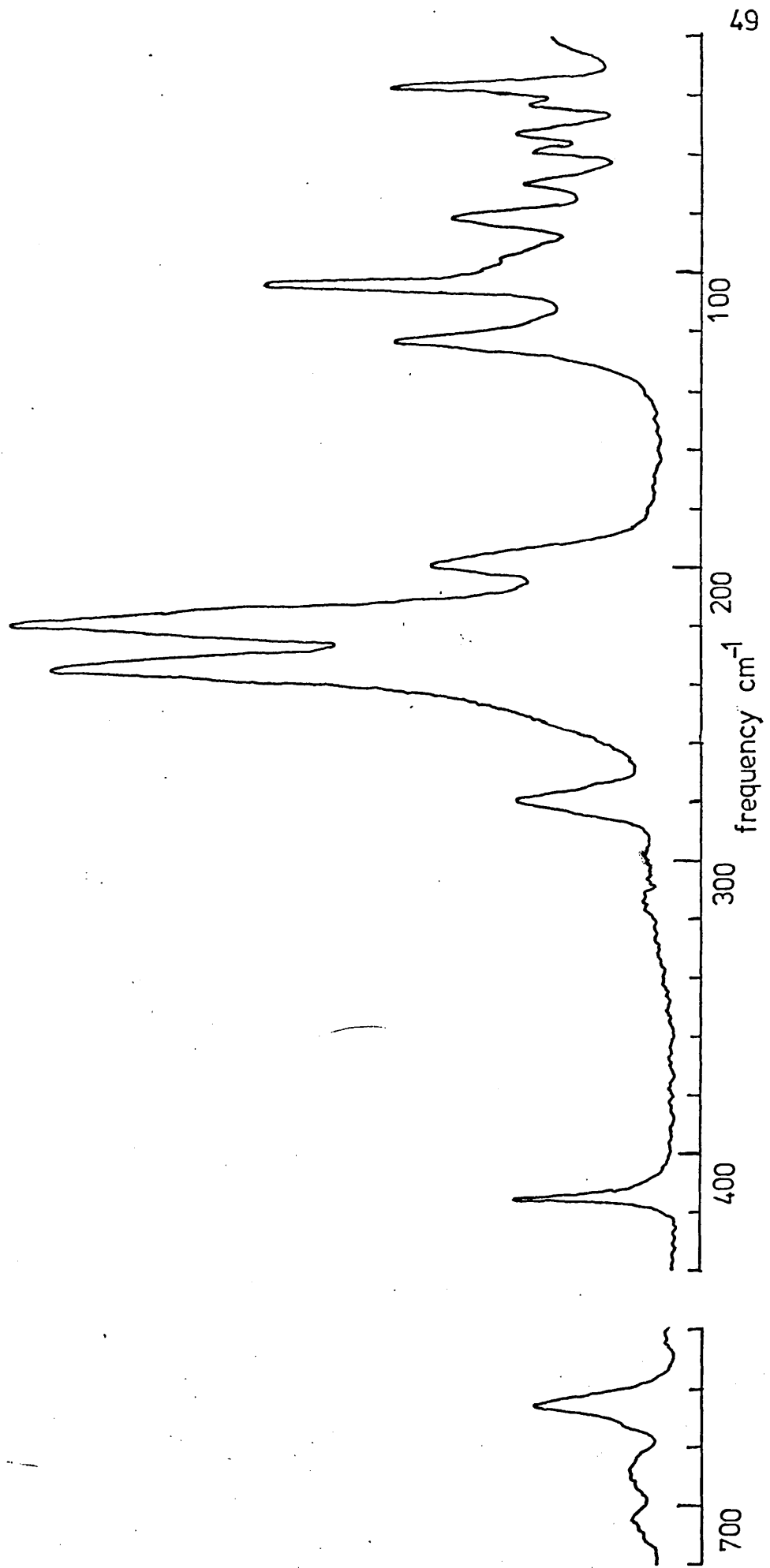
The Raman spectrum of the vapour above solid NOCl.BCl₃ at ambient temperatures exhibits shifts due to the ν_2 and ν_3 modes of NOCl. These are located at the same frequencies as in the pure gas but no bands arising from BCl₃ are observed. This is consistent with BCl₃ being a weaker scatterer, and a spectrum was not observed from gaseous BCl₃ under the same conditions. These observations are consistent

with non-interacting NOCl and BCl₃ in the vapour above solid NOCl·BCl₃.

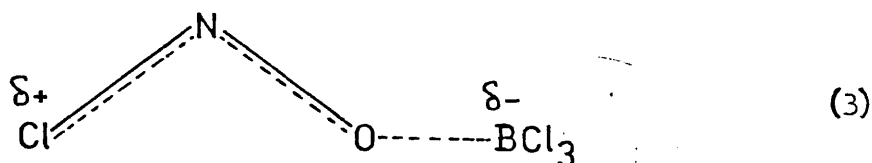
The Raman spectrum of each solid adduct may not be interpreted in terms of the point group symmetries of free NO⁺ and BCl₄⁻ ions. The spectrum of the low-temperature modification at 77 K is reproduced in fig. 3.1. BCl₄⁻ with T_d symmetry would be expected to exhibit four Raman active fundamentals.¹⁶ Shifts of 200, 279 and 416 cm⁻¹ (fig. 3.1) may be ascribed to ν_2 , ν_4 and ν_1 respectively by comparison with standard spectra,¹⁴ but an assignment for ν_3 is more difficult. Raman studies on CsBCl₄ carried out in these laboratories¹⁸ failed to observe ν_3 , while in MePCl₂·BCl₃ two weak broad bands at 724 and 694 cm⁻¹ have been assigned,⁸ (split by ¹⁰B and ¹¹B isotopes respectively). Similar weak bands at 707 and 670 cm⁻¹ were observed in the Raman spectrum of KBCl₄ dissolved in SO₂ and these have been assigned to the ($\nu_1 + \nu_4$) and ν_3 moles of BCl₄⁻ respectively. By analogy, in fig. 3.1, shifts of 695 and 705 cm⁻¹ might be attributed to ν_3 BCl₄⁻. However, it was noted that decreasing the sample temperature resulted in a proportional increase in the intensity of the Raman shifts at 218, 236, 664, 695 and 705 cm⁻¹. It could be argued, therefore, that these shifts arise from a second solid state species and that ν_3 BCl₄⁻ is absent. The nature of a second species, which must possess the empirical formula NOBCl₄ to be consistent with the chemical analyses, is open to speculation.

One possibility is the oxygen-coordinated NOCl·BCl₃ species postulated by Olah.³⁶ If such a compound existed, it would be the only example reported in which NOCl coordinates in this manner. The Raman shifts at 236 and 664 cm⁻¹ are noted to resemble free NOCl in both frequency and relative intensity. However since rapid cooling

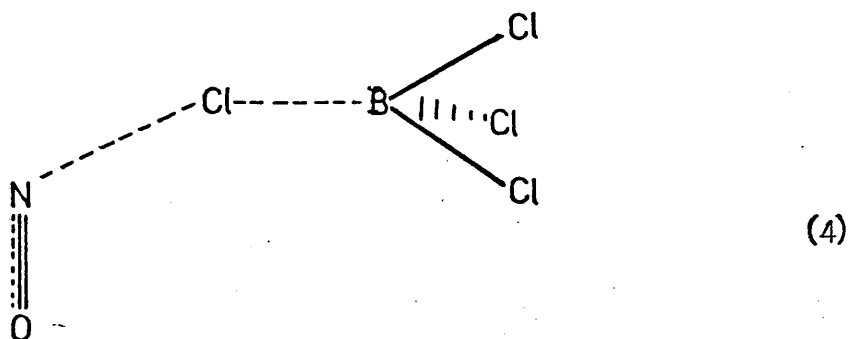
Fig 3-1 The Raman spectrum of NOBCl_4 low temperature modification



of a dilute solution of NOCl in BCl_3 to 77 K produced an identical spectrum to that shown in fig. 3.1 with additional bands due to BCl_3 (see later), the presence of free NOCl is unlikely. These shifts could arise from coordinated NOCl however, and the N-Cl stretching mode at 664 cm^{-1} , which is higher than in gaseous NOCl (596 cm^{-1}), could be explained in terms of double bond character:

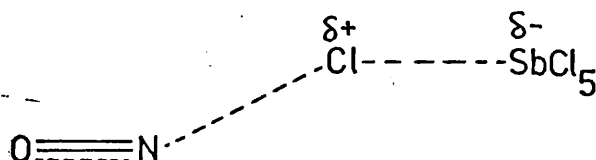


However, bands arising from coordinated BCl_3 are not readily identified. These are observed at 416, 309, 735, 745, 256, 265, and 220 cm^{-1} in the Raman spectrum⁴⁸ of $\text{MeCN} \rightarrow \text{BCl}_3$, and the absence of similar bands in this spectrum, where bands which might be assigned to coordinated NOCl are very intense, strongly suggests that species (3) is absent. Clearly a structure in which all boron is essentially present as BCl_4^- coexisting with both NOCl and NO^+ is required, and the chlorine coordinated NOClBCl_3 species might be considered:

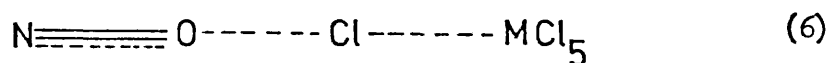


In this case, a high N-Cl stretching frequency is not readily explained and since perturbation of BCl_4^- has occurred, splittings of BCl_4^- degenerate modes would be expected.

This latter example leads to an interpretation of the Raman spectrum of $\text{NOCl} \cdot \text{BCl}_3$ in terms of anion-cation association. Examples involving other nitrosonium salts have been reported^{1,5,6,52} and are identified by a low NO^+ stretching frequency - lower than usually found in simple ionic nitrosonium salts (2309 cm^{-1} in NOClO_4). The NO^+ stretching frequency in the low temperature modification of $\text{NOCl} \cdot \text{BCl}_3$ occurs at 2207 cm^{-1} in the Raman which is considerably higher than reported in the infra-red spectrum³⁶ (2123 cm^{-1}). It seems unlikely that Olah had prepared another form, but considering the volatility, it is almost inconceivable that this adduct could be milled and mounted between NaCl windows, as stated, without undergoing extensive decomposition. This point will be discussed later. Considering only the Raman spectrum, the NO^+ stretching frequency is $\approx 100 \text{ cm}^{-1}$ below that observed in NOClO_4 , and in other nitrosonium compounds exhibiting this phenomenon, anomalous effects have been observed in the vibrational spectra at low temperatures. For example, Gerding⁵² noted that cooling NOSbCl_6 to below 143 K resulted in the appearance of an additional weak broad band in the Raman spectrum at 236 cm^{-1} which he considered to resemble ν_3 of NOCl in various matrices.²³ In order to explain this phenomenon, he proposed that at low temperatures NO^+ became associated with one chlorine atom of the anion:



Consistent with this proposal, splittings of degenerate anion modes were also noted. Adams¹ has reported the low frequency infra-red and Raman spectra of $(\text{NO})_2\text{SnCl}_6$, $(\text{NO})_2\text{TiCl}_6$ and NOSbCl_6 at low temperatures. The appearance of an additional band at ca. 235 cm^{-1} was found to coincide with changes in the external modes which is indicative of a change in the unit cell. From group theoretical considerations based upon a somewhat arbitrary assignment of the new space group, the additional band was attributed to an external mode arising from the restricted rotation of NO^+ as a result of interaction with one chlorine atom of the anion:

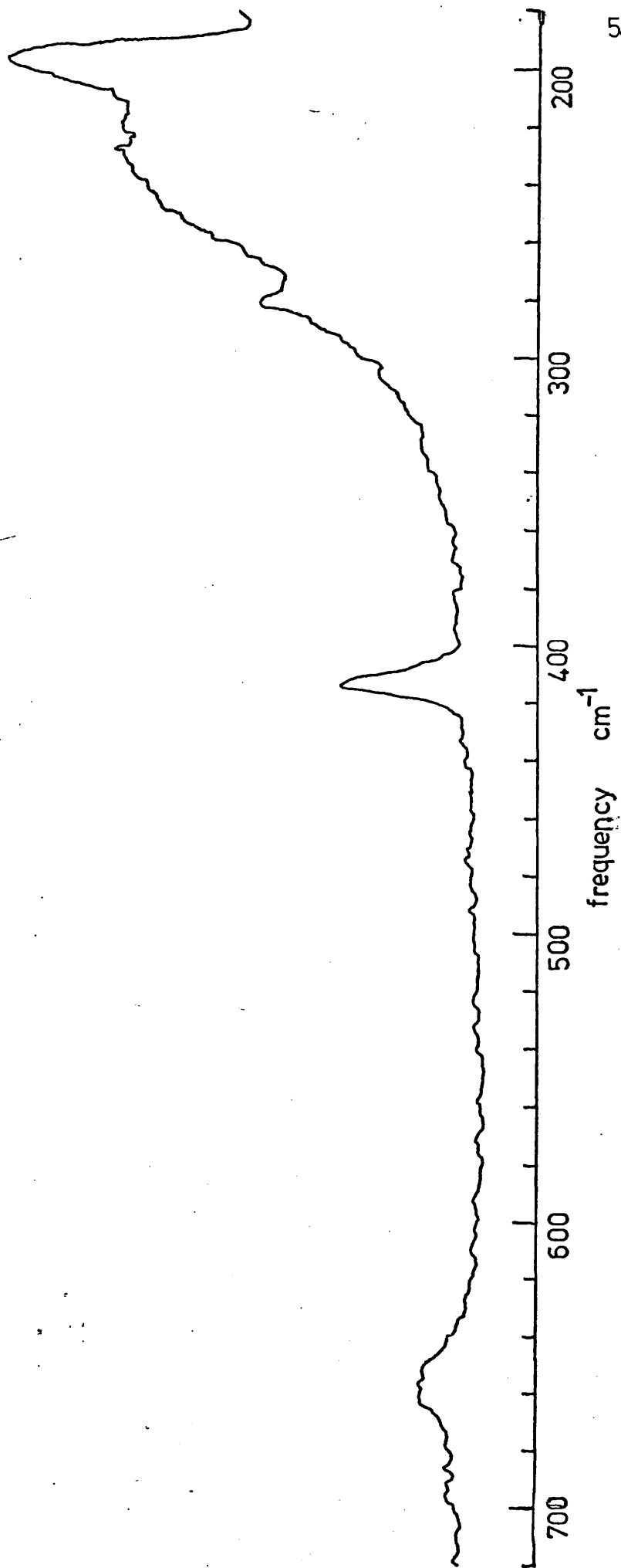


The direction of this interaction was based upon electronegativity values and is in the opposite sense to that proposed by Gerding.⁵² More relevant to $\text{NOCl} \cdot \text{BCl}_3$ however, Barbier et al. have undertaken a single crystal solid state vibrational analysis for NOAlCl_4 ⁵ and NOGaCl_4 ,⁶ and the additional band appearing at ca. 260 cm^{-1} at low temperatures was attributed to a libratory mode of the anion in distinction from the assignment proposed by Adams.¹ This vibrational analysis was possible because the space group for NOAlCl_4 had been determined from some preliminary X-ray data.⁴ NOGaCl_4 was assigned an identical structure by comparison of the external modes.⁶ It is informative to compare the external modes of NOAlCl_4 and NOGaCl_4 with those of $\text{NOCl} \cdot \text{BCl}_3$ (Table 3.2). In common with NOGaCl_4 and NOAlCl_4 eleven Raman active external modes are located if shifts at 218 and 236 cm^{-1} are attributed to $\text{T}(\text{BCl}_4^-)$ and $\text{R}(\text{BCl}_4^-)$ respectively. The site group analysis of the external modes is presented and discussed

in chapter 4. The shift to higher frequency of the translatory mode at 218 cm^{-1} on going from Al to B is consistent with the decrease in mass of the central metal atom. These similarities strongly suggest, therefore, that $\text{NOCl} \cdot \text{BCl}_3$ is isostructural and should be formulated NOBCl_4 . It should be emphasised, however, that the bands at 218 and 236 cm^{-1} in NOBCl_4 are very much more intense than any other external mode. In addition, these bands increase in intensity with decreasing temperature whereas all other lattice modes remain unchanged. At this stage, however, if it is assumed that these are lattice modes, then the bands at 664, 695 and 705 cm^{-1} must be ascribed to $\sqrt{3} (\text{F}_2) \text{BCl}_4^-$, which occurs at a lower frequency and is more intense than reported in other BCl_4^- salts.⁸ The splitting of $\sqrt{3}$ is easily explained in terms of site group splittings (see chapter 4). Similar splittings of $\sqrt{3}$ AlCl_4^- in NOAlCl_4 were also observed, but it is not clear whether the intensity changes relative to $\sqrt{1}$, $\sqrt{2}$ and $\sqrt{4}$ as the temperature is lowered.

The Raman spectrum from the room-temperature modification (fig. 3.2) proved much more difficult to record because the crystals melted upon laser irradiation. It differs from the low-temperature modification in that strong sharp bands at 218 and 236 cm^{-1} are replaced by a shoulder at 240 cm^{-1} , and the sharp BCl_4^- band at 664 cm^{-1} is replaced by a weak broad band at 655 cm^{-1} . In addition, $\sqrt{\text{N}\equiv\text{O}^+}$ has considerably broadened and shifted to 2217 cm^{-1} , which resembles the behaviour of $\sqrt{\text{N}\equiv\text{O}^+}$ in NOSbCl_6 .⁵² If the intensities of the bands at ca. 230 cm^{-1} and the $\sqrt{3}$ mode for BCl_4^- may be regarded as an indication of the degree of anion-cation association, then this effect is very much weaker at room temperature as expected. The yellow colour of the

Fig 3-2 The Raman spectrum of NOBCl_4 - the room temperature modification

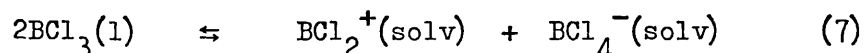


compound was considered by Partington³⁷ to arise from free NOCl, but the latter is not readily detected in the Raman spectrum unless bands at 240 and 655 cm^{-1} are so ascribed.

Additional evidence supporting anion-cation association is obtained from the Raman spectra of the liquid layers formed when the compound melts. The upper brown layer is shown to consist of a weak solution of NOCl in BCl_3 . At ambient temperatures it exhibits bands due to BCl_3 , at the same frequencies as in the pure liquid,³⁴ and bands due to NOCl which have shifted to higher frequency, ν_3 having lost the asymmetry which is observed in the pure liquid. (Table 3.3). Upon rapid cooling to 77 K, a spectrum closely resembling that of the low-temperature modification is obtained together with bands due to BCl_3 .³⁴ Clearly BCl_3 , being non-polar is most unlikely to promote ionisation of NOCl at ambient temperatures, accounting for the loss of asymmetry of ν_3 . At low temperatures, the interaction of NOCl with BCl_3 results in Cl^- transfer with the formation of ion pairs, since the low dielectric medium is unlikely to solvate the ions. Consistent with this BCl_3 has been used as a solvent in the preparation⁵⁴ of BCl_4^- salts, and being a strong Lewis acid is unlikely to promote the formation of an oxygen-coordinated NOCl- BCl_3 species under these conditions. Clearly anion-cation interaction is very much stronger than ion- BCl_3 interaction and hence bands at 218 and 236 cm^{-1} are also observed together with the enhanced intensity of the $\text{BCl}_4^- \nu_3$ mode.

The lower red layer is shown to consist of a solution of BCl_3 in excess NOCl, which being relatively polar, is likely to promote ion formation and possibly enhance the auto-ionisation of BCl_3 , an effect

which has been postulated in certain systems^{21,44,45}:



Since NOCl has also been postulated to solvate NO^+ ,⁹ there is the possibility that at low temperatures NO^+ may interact with either BCl_4^- or NOCl. The Raman spectrum of the lower layer at room temperature was very diffuse because bubble formation resulted upon laser irradiation. A spectrum was obtained, however, by cooling to 278 K, (fig. 3.3). The bands at 200, 280 and 416 cm^{-1} are readily ascribed to BCl_4^- with the ν_3 mode at ca. 660 cm^{-1} now very weak. The broad bands at ca. 250 and 440 cm^{-1} arise from NOCl, $\nu_{\text{N-Cl}}$ at 440 cm^{-1} being very much lower than in the pure liquid (cf. 549 cm^{-1}). A weak broad band asymmetric to the low frequency side was also observed in the $\text{N} \equiv \text{O}^+$ stretching region. These data are consistent with NO^+ being strongly solvated by NOCl, and an identical band in the $\text{N} \equiv \text{O}^+$ stretching region was reproduced by a solution of HNO_3 and N_2O_4 (1:1 v/v) in excess NOCl. In this system, nitric acid enhances the ionisation of N_2O_4 ²⁰:



NO^+ can therefore be solvated by NOCl. Freezing the lower red layer produced a species which did not scatter very well. A resolved Raman spectrum was obtained, however, by heating the complex to 60°C, so that the two liquid layers initially formed coalesced, and then rapidly cooling the tip of the tube in liquid nitrogen, which initiated rapid separation of two layers. This spectrum (fig. 3.4) exhibited bands

Fig 3-3 The Raman spectrum of NOCl_4 melted crystals, lower-layer at 278 K

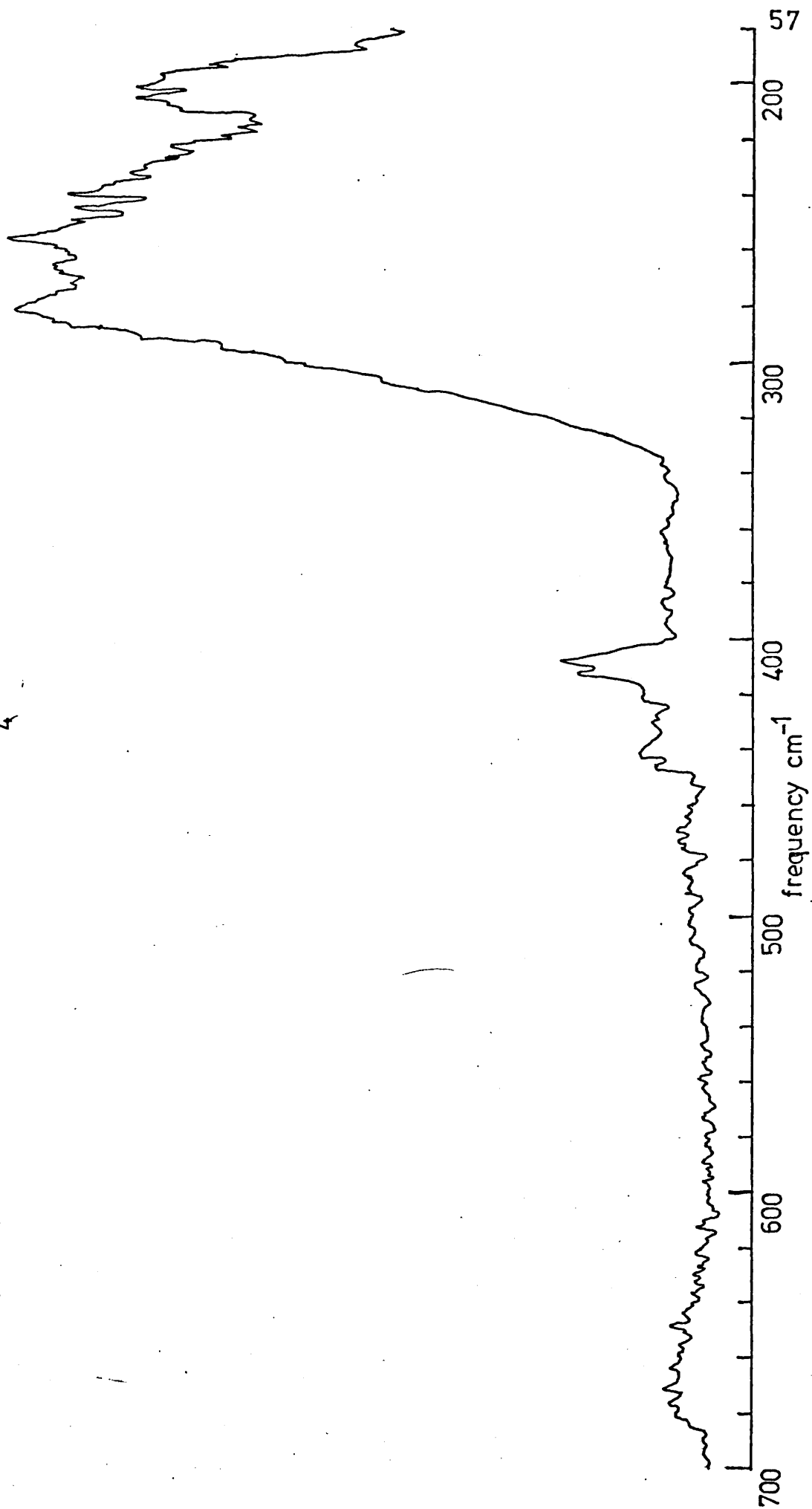


Fig 3 -3 continued

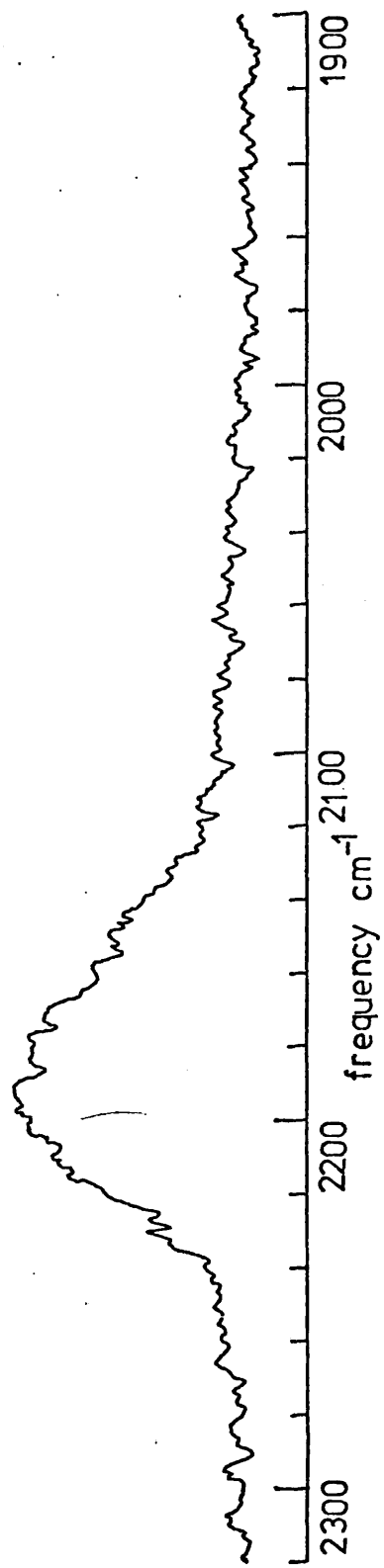


Fig 3-4 The Raman spectrum of NOBCl_4 — melted crystals, lower layer at 77K

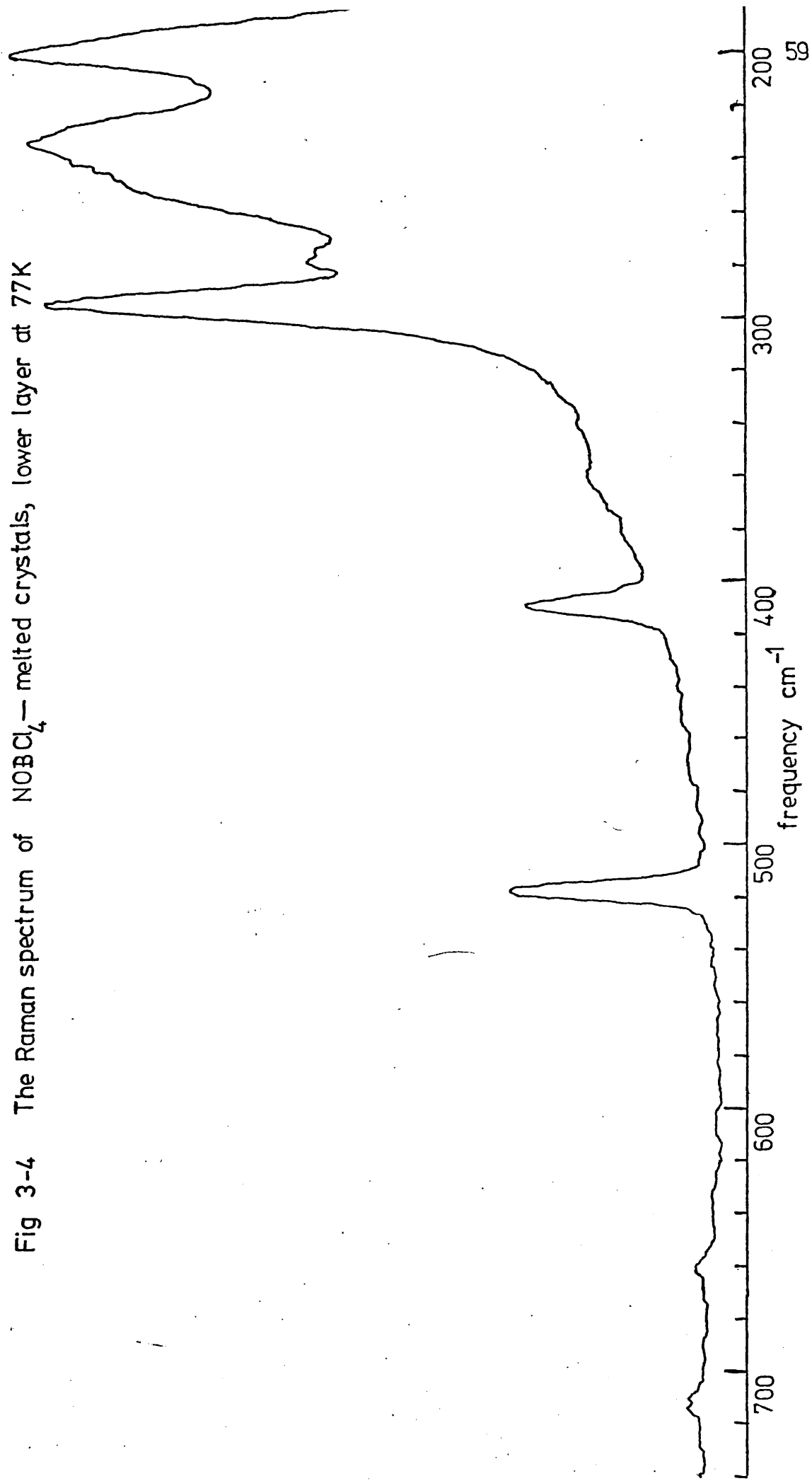
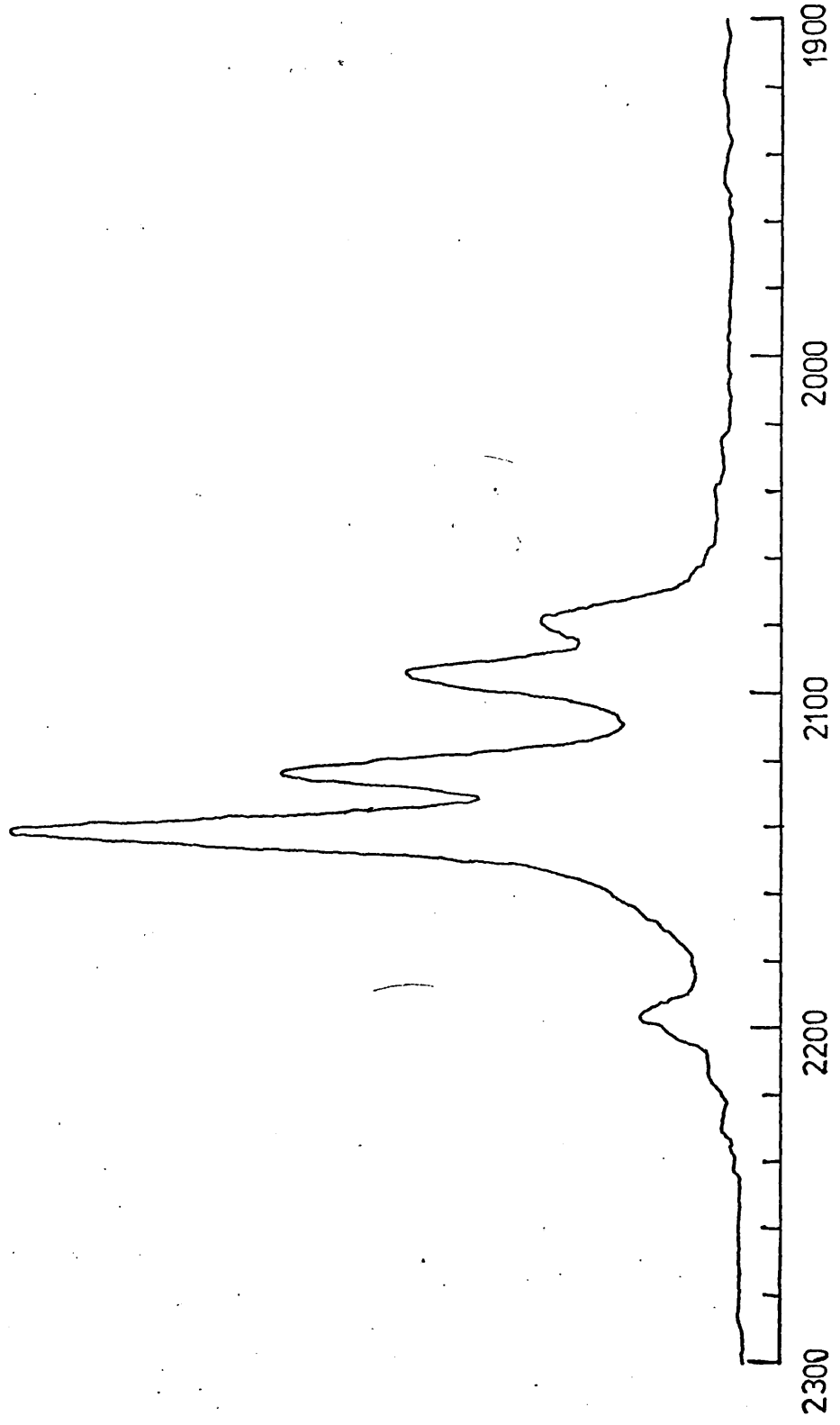
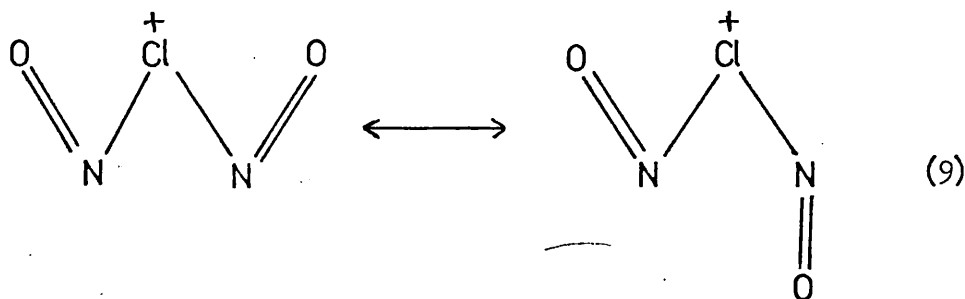


Fig 3 - 4 continued



at 200, 280 and 410 cm^{-1} which may be assigned to BCl_4^- . The ν_3 mode in the region 660-740 cm^{-1} was very weak and varied in intensity on cooling with a broad band centred at ca. 230 cm^{-1} . This clearly indicates that $\text{NO}^+ \text{BCl}_4^-$ interaction is now very much weaker and consequently the interaction of NO^+ with NOCl , as identified by bands at 295 and 518 cm^{-1} , is very much stronger. Large shifts in these bands on going from the liquid to the solid phase are not unusual for NOCl systems.²³ The NO^+ stretching region was very complex, and while a weak band was still observed at 2207 cm^{-1} , four strong bands were observed to the low frequency side at 2140, 2123, 2095 and 2075 cm^{-1} . It is tentatively suggested that in excess NOCl the cation is $[\text{NOClNO}]^+$, for which various rotational isomers are possible, e.g.



The four bands in this region, could arise from solid state coupling of $\text{N}=\text{O}$ vibrations or from the presence of several rotamers frozen out in the lattice. It is impossible to speculate further in the absence of additional spectroscopic or crystal data. A similar band pattern was not resolved from the frozen $\text{HNO}_3/\text{N}_2\text{O}_4/\text{NOCl}$ sample, as might be expected, since a glass was formed upon freezing. 1:2 adducts of metal chlorides with NOCl have been reported in the literature (e.g. $\text{NOCl} \cdot \text{NOFeCl}_4$,²² $\text{NOCl} \cdot \text{NOAlCl}_4$ ²⁵) but no vibrational spectra have been measured.

It is now relatively easy to explain the large difference between the frequencies of the $\text{N}\equiv\text{O}^+$ stretching mode of NOBCl_4 observed at 2207 cm^{-1} in the Raman and apparently at 2123 cm^{-1} in the infra-red.³⁶ Decomposition of the compound results in the formation of NOCl , which would give rise to a band in the infra-red at 1800 cm^{-1} . On cooling, NO^+ can readily interact with NOCl so producing a shift of $\nu_{\text{N}\equiv\text{O}^+}$ to lower frequency. The appearance of a band at 2123 cm^{-1} is consistent with this argument. Thus, it follows that the incomplete infra-red data may be readily explained in terms of an ionic species $\text{NO}^+\text{BCl}_4^-$ without introducing a novel oxygen-coordinated $\text{NOCl}\cdot\text{BCl}_3$ species. Further work might be carried out in order to characterise the $[\text{ONClNO}]^+$ cation in BCl_4^- and other compounds.

TABLE 3.1
VIBRATIONAL DATA FOR NOCl . (cm^{-1})

SOLID (77 K)		LIQUID		GAS		ASSIGNMENT
RAMAN	I.R. ²³	RAMAN	I.R.	RAMAN	I.R. ²⁷	
233(s)	243 (calc)	292(s br) -	-	332(s)	332	ν_3
457(w)	491	549(w br) -	-	598(w)	596	ν_2
-	1948	-	-	-	1800	ν_1

TABLE 3.2

LOW FREQUENCY VIBRATIONAL ASSIGNMENTS FOR $\text{NO}^+\text{MCl}_4^-$ (M = B, Al Ga) cm^{-1}

NOBCl_4	NOAlCl_4	NOGaCl_4	ASSIGNMENT
36	37-41	40	T_A
43	48-52	49-52	R_C
53	58-62	61	R_A
59	64-48	64-71	R_A
69	76	77	T_C
80	81-85	85	T_A
92	98	97	R_C
102	104-108	102-107	T_A
122	118-122	120-126	T_C
218	179	186	T_C
236	264	275	R_C

A = NO^+ C = MCl_4^-

TABLE 3.3
 RAMAN SPECTRA OF NOBCl_4
 MELTED CRYSTALS UPPER LAYER AT R.T.

BAND cm^{-1}	ASSIGNMENT	
257 (m)	BCl_3	
319 (s)	ν_3 NOCl	
468 (should)	}	
471 (s)		BCl_3
475 (s)		
578 (w)	ν_2 NOCl	

3.4 $\Delta H_f^\circ \text{NOBCl}_4(\text{c})$ FROM THE TEMPERATURE DEPENDENCE OF THE DISSOCIATION PRESSURE

The vibrational data for the 1:1 $\text{NOCl} \cdot \text{BCl}_3$ adduct are consistent with the structure $\text{NO}^+\text{BCl}_4^-$ in the solid phase and unassociated NOCl and BCl_3 in the vapour. The solid-gas equilibrium may therefore be represented as:



and the associated enthalpy change ΔH_R may then be evaluated from a pressure-temperature study using the integrated form of the Clausius-Clapeyron equation:

$$\frac{\partial}{\partial t} \log_e P = \frac{\Delta H}{RT^2} \quad (11)$$

Pressures were measured using a Texas quartz gauge and trial experiments showed that the practical temperature range was from 210 K to 257 K. Selected temperatures in this range were maintained using well-stirred slush baths. Although the measured pressures over NOBCl_4 in this temperature range were well below the maximum pressure limit for the gauge (250 Torr), the upper temperature limit was not exceeded because of rapid decomposition of the compound on contact with the glass walls of the vacuum system. This decomposition was not eliminated by preliminary baking of the glassware, although it was substantially reduced at low pressures by allowing the glass walls to become coated with a thin layer of decomposition product. The origin and products of the decomposition remain unknown, but possibilities include (a) the presence of moisture traces in the vacuum system or (b) decomposition of BCl_3 by NOCl . Consistent with the latter possibility, it was noted that a white residue always remained in the reaction flask after preparation and volatilisation of NOBCl_4 under stringently anhydrous conditions. No residue was found after storing a sample of BCl_3 under identical conditions.

The pressure gauge readings are related to absolute pressures by the gauge factor. This varies non-linearly with increasing gauge reading, but is found to be constant over a narrow pressure range. The gauge factor was determined by calibrating the spiral with water(1) over the temperature range 291.2 K to 306.2 K, acetone(1) over the temperature range 210 K to 250 K and benzene(c) over the temperature range 210 K to 255 K. The results are presented in tables 3.4, 3.5 and 3.6 respectively. The gauge factor derived from the water calibration experiment does not vary over the pressure range studied,

TABLE 3.4
TEXAS QUARTZ GAUGE CALIBRATION USING WATER

TEMPERATURE/K	GAUGE READING G	WATER V.P. ⁴³ /Torr	GAUGE FACTOR = $\frac{VP}{G}$
291.7	18.507 ± 0.010	15.971	0.863
292.5	19.507 ± 0.010	16.790	0.861
293.4	20.710 ± 0.010	17.753	0.857
296.7	25.240 ± 0.020	21.714	0.860
298.5	28.026 ± 0.020	24.183	0.863
302.4	35.050 ± 0.010	30.392	0.867
306.2	43.100 ± 0.070	37.729	0.875

TABLE 3.5

TEXAS QUARTZ GAUGE CALIBRATION USING ACETONE

SLUSH BATH	TEMPERATURE/K	GAUGE READING G	ACETONE V.P. ² /Torr	GAUGE FACTOR = $\frac{VP}{G}$
CHLOROFORM	210.2	0.770 ± 0.02	0.722	[0.938]
CHLOROBENZENE	228.2	4.15 ± 0.03	3.670	0.884
ANISOLE	235.7	7.82 ± 0.10	6.608	0.845
BROMO BENZENE	241.5	12.06 ± 0.20	10.100	0.837
CARBON TETRACHLORIDE	250.4	21.35 ± 0.30	18.493	0.866
				$\langle GF \rangle = 0.86$

TABLE 3.6
TEXAS QUARTZ GAUGE CALIBRATION USING BENZENE

SLUSH BATH	TEMPERATURE/K	GAUGE READING G	BENZENE/V.P. ²⁶ /Torr	GAUGE FACTOR = $\frac{VP}{G}$
CHLOROFORM	210.2	0.400 ± 0.01	0.070	0.174
CHLOROBENZENE	228.2	1.350 ± 0.01	0.498	0.370
ANISOLE	235.7	1.930 ± 0.04	1.044	0.246
BROMOBENZENE	241.5	2.730 ± 0.01	1.799	0.659
CARBON TETRACHLORIDE	25.04	5.200 ± 0.10	3.963	0.762
BENZYL ALCOHOL	255.2	7.200 ± 0.10	5.944	0.825

and the high precision of the pressure readings reflects the temperature stability of the lagged water bath. The bath temperatures were measured using a calibrated mercury-in-glass thermometer, and a platinum resistance thermometer showed that the maximum temperature fluctuation was $\pm 0.05^{\circ}\text{C}$. In the case of the acetone calibration experiment, the derived gauge factor is in satisfactory agreement with that from the previous calibration. The lower precision is attributed to temperature fluctuations in the low temperature slush baths employed. Temperatures in the range 255 K to 243 K were measured using a calibrated mercury-in-glass thermometer, whereas those below 243 K could only be estimated using an alcohol thermometer. In these cases, the literature values for the freezing points of the pure solvents were employed. The temperature stability of the low temperature baths is unlikely to be better than $\pm 0.1^{\circ}\text{C}$, and the absolute bath temperatures will be significantly affected by any contamination of the solvents employed. The apparently anomalous gauge reading at 210.2 K may be attributed to the presence of ethanol in the chloroform slush bath. Vapour pressure data for acetone were calculated from the Antoine equation:²

$$\log_{10} (p/\text{kPa}) = 6.2548 - \frac{1216.69}{(T/\text{K} - 42.88)} \quad (12)$$

Table 3.7 illustrates the variation in the gauge factor arising from a possible uncertainty of ± 1 K in the temperature of the chloroform slush bath during the acetone calibration.

TABLE 3.7

TEMP/K	VAPOUR PRESSURE/TORR	G.F. = VP/0.770
209.2	0.673	0.848
210.2	0.722	0.938
211.2	0.797	1.036

The gauge factor fluctuation is therefore within experimental error.

In the case of benzene, however, fluctuations in the bath temperature cannot explain the large variation in the gauge factor over the same temperature range. Benzene vapour pressures were calculated from the Antoine equation.²⁶

$$\log_{10}(p/\text{Torr}) = 10.8842 - \frac{2836.0}{(T/K + 25.31)} \quad (13)$$

One explanation is the presence of impurities in the benzene sample employed, but a more likely reason is malfunction of the gauge. In chronological order, pressure measurements were recorded for water, NOBCl_4 , acetone and then benzene. Subsequently a leak was discovered across the quartz spiral necessitating commercial repair and precluding further experiments. Hence only one set of data for NOBCl_4 was recorded, but since the calibrations for both acetone and water lead to the same gauge factor within experimental error, it is unlikely that the spiral was fractured when measurements for NOBCl_4 were made. The situation is nevertheless unsatisfactory and further measurements over the same temperature range are clearly needed.

The pressure data for NOBCl_4 are presented in table 3.8. A gauge factor of 0.86 was used to convert pressure gauge readings to absolute pressures and the plot of $\log_{10}(p/\text{Torr})$ vs $1/T$ is presented in fig. 3.5. The plot is of the form:

$$\log_{10} p = \frac{-\Delta H}{2.303 RT} + C \quad (14)$$

where ΔH is the molar enthalpy change for process (10). The scatter of the experimentally measured points, through which several straight lines may be drawn, is attributed to the slight decomposition of the sample discussed earlier. Since decomposition occurs to a lesser extent at low temperatures, it seems reasonable to give more weight to these points - minimum slope line (11). However, since uncertainty in the bath temperature increases as the temperature decreases, the best straight line through all the experimental points was also drawn - maximum slope line (1). In the absence of further data, the mean value $\langle \Delta H \rangle = 37.8 \pm 1.9 \text{ kJ mol}^{-1}$ derived from the two slopes will be used in subsequent calculations without prejudice to the possibility of a significant systematic error.

Since the pressure study for NOBCl_4 was carried out over the temperature range 210 K to 250 K, ΔH for (10) refers to an average temperature of 230.2 K. It follows that to calculate $\Delta H_f^\circ \text{NOBCl}_4(c)$, 298.2 K, heat capacity data are required for each component over the temperature range 230.2 K to 298.2 K. No such data are available for $\text{NOBCl}_4(c)$, nor are measurements practical. Extrapolation of the pressure data at an average temperature of 230.2 K to 298.2 K is likely to introduce a significant though indeterminate error, because the degree

TABLE 3.8
PRESSURE MEASUREMENTS FOR NOBCl₄(c)

SLUSH BATH	TEMP T/K	$\frac{10^3}{T}$	GAUGE READING G	PRESSURE P/*Torr	$\log_{10} P$
CHLOROFORM	210.2	4.757	1.25 ± 0.05	1.08 ± 0.04	0.017 - 0.049
CHLOROBENZENE	228.2	4.382	5.75 ± 0.25	4.65 ± 0.22	0.675 - 0.713
ANISOLE	235.7	4.243	13.50 ± 0.50	11.61 ± 0.43	1.048 - 1.081
BROMOBENZENE	241.5	4.141	23.50 ± 1.25	20.21 ± 1.08	1.282 - 1.328
CARBON TETRA- CHLORIDE	250.4	3.994	42.0 ± 2.5	36.12 ± 2.15	1.531 - 1.583

* Gauge Factor = 0.86

$\text{Log}_{10} p$ vs $1/T$ plot for NOBCl_4

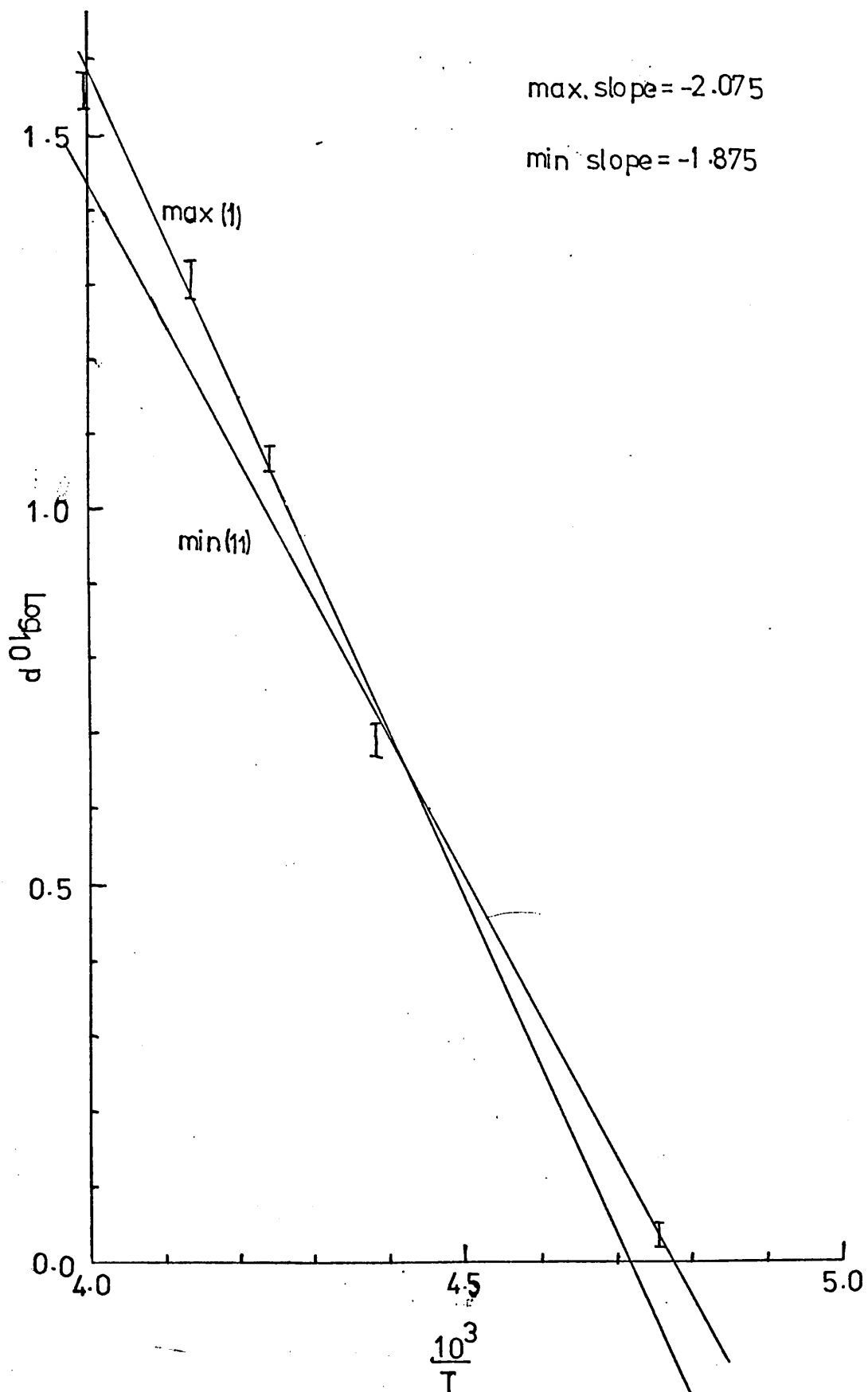


Fig 3-5

of anion-cation association decreases with increasing temperature.

Nevertheless, the value of $\Delta H_f^{\circ} \text{NOBCl}_4(\text{c})$ derived by extrapolation is unlikely to differ grossly from the value at 298.2 K.

Thus from (10)

$$\begin{aligned} \Delta H_f^{\circ} \text{NOBCl}_4(\text{c}) &= \Delta H_f^{\circ} \text{NOCl}(\text{g}) + \Delta H_f^{\circ} \text{BCl}_3(\text{g}) - \langle \Delta H \rangle \\ &\approx [(51.7 \pm 0.3) + (-404.6 \pm 2.5) - (37.8 \pm 1.9)] \\ &\quad (-390.7 \pm 3.2) \text{ kJ mol}^{-1} \end{aligned}$$

Therefore $\Delta H_f^{\circ} \text{NOBCl}_4(\text{c}) \approx -93. \text{kcal mol}^{-1}$.

3.5 THE THERMOCHEMICAL RADIUS FOR NO^+

After measuring ΔH_f° values for a series of compounds MX' , MX'' , MX''' the Kapustinskii Born-Mayer equation in the form^{56,28}

$$U = \frac{120.2 \gamma |Z_+| |Z_-|}{(r_+ + r_-)} \left[1 - \frac{0.0345}{(r_+ + r_-)} \right] \text{ kJ mol}^{-1}$$

where Z_+ = charge on cation

Z_- = charge on anion

γ = number of ions in simplest formula

r_+ = radius of cation (nm)

r_- = radius of anion (nm)

permits the calculation of a thermochemical radius r_{th} for M^+ provided that radii for X' , X'' and $\Delta H_f^{\circ} \text{X}'^-(\text{g})$, $\Delta H_f^{\circ} \text{X}''^-(\text{g})$ are known.

This method is usually applied to complex anions, and the evaluation of r_{th} then permits an estimation of ΔH_f° values for certain hypothetical compounds MY' , MY'' etc. This procedure, however, must encounter

several problems in cases where varying degrees of association between M^+ and X^- are found - e.g. in nitrosonium salts. Since the radius of NO^+ in $NOBCl_4(c)$ is likely to be greater than in $NOCIO_4(c)$, then combination of thermochemical data from these two compounds will generate an average thermochemical radius. Clearly data for compounds such as $NOCIO_4$, $NOHSO_4$, $(NO)_2S_2O_7$, which were classified as nitrosonium salts of simple inorganic ions in chapter 1 should be used to generate one thermochemical radius for NO^+ . Data for compounds derived from $NOCl$ - e.g. $NOBCl_4$, $(NO)_2SnCl_6$, $NOAlCl_4$, on the other hand, should be combined to generate a separate thermochemical radius for NO^+ . Unfortunately, anion radii and ΔH_f^0 values of the gaseous anions are not available for $NOHSO_4$ and $(NO)_2S_2O_7$ and hence there is at present no compound whose data may be combined with $NOCIO_4$. However, unlike cases involving complex anions, $\Delta H_f^0 NO^+(g)$ is well-known⁴⁰ and hence it is theoretically possible to evaluate a thermochemical radius for NO^+ from the experimental data for both $NOBCl_4$ and $NOCIO_4$. This may be carried out as follows using existing anion data.

Two sets of data for the radius of ClO_4^- and $\Delta H_f^0 ClO_4^-(g)$ are available (table 3.9):

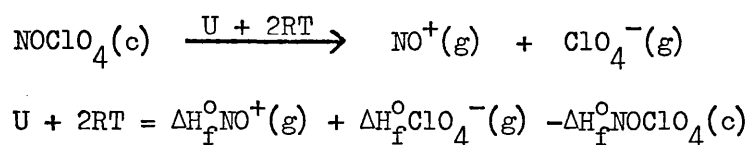
TABLE 3.9

RADIUS/nm	REFERENCE	$-\Delta H_f^0 X^-(g)/kJ\ mol^{-1}$	REFERENCE
(a) ClO_4^-			
0.236	Waddington 56	348.1	calculated
0.185	Solomon 49	235.6	Solomon 49
(b) BCl_4^-			
0.300	Finch et al. 17	924	Finch et al. 17
0.305	Rosolovskii 54	929	Rosolovskii 54

Waddington⁵⁶ calculated a thermochemical radius by application of the Yatsimirskii method to the alkali metal perchlorate salts.

$\Delta H_f^\circ \text{ClO}_4^-(g)$ was calculated using r_{th} and literature data¹⁵ for $\text{KClO}_4(c)$. Solomon's⁴⁹ values were derived from solvation energy calculations based upon enthalpies and free energies of solution of alkali-metal perchlorates.

The radius of 0.185 nm was found empirically to fit the experimental data for $\text{M}^+\text{ClO}_4^-(c)$ ($\text{M} = \text{K, Rb, Cs}$). Since ΔH_{LATT}° was also derived in the calculations, a thermodynamic cycle permitted the evaluation of $\Delta H_f^\circ \text{ClO}_4^-(g) = 235.6 \text{ kJ mol}^{-1}$. Therefore:



(1) Using Waddington's data

$$U = (989.9 - 348.1 - 59.0 - 5.0)$$

$$= 577.8 \text{ kJ mol}^{-1}$$

and substitution in the Kapustinskii equation:

$$\frac{120.2 \cdot 2}{(r_+ + 0.236)} \left[1 - \frac{0.0345}{(r_+ + 0.236)} \right] = 577.8$$

$$\therefore \frac{120.2 \cdot 2}{577.8} (r_+ + 0.236 - 0.0345) = (r_+ + 0.236)^2$$

$$0.416 (r_+ + 0.2015) = (r_+ + 0.236)^2$$

$$r_+^2 + 0.056 r_+ - 0.0281 = 0$$

$$r_+ = 0.14 \text{ nm.}$$

(2) Using Solomon's data:

$$U = (989.9 - 235.6 - 59.0 - 5.0) \\ = 690.3$$

and substitution in the Kapustinskii equation:

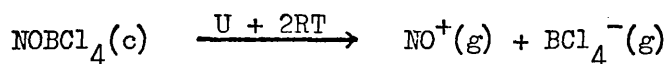
$$\frac{120.2.2}{(r_+ + 0.185)} \left[1 - \frac{0.0345}{(r_+ + 0.185)} \right] = 690.3$$

$$\therefore 0.348 (r_+ + 0.1505) = (r_+ + 0.185)^2$$

$$\therefore r_+^2 + 0.0219 r_+ - 0.0182 = 0$$

$$\therefore r_+ = 0.13 \text{ nm.}$$

Two sets of data^{17,54} for BCl_4^- were independently derived by application of the Yatsimirskii method to measured thermochemical data for CsBCl_4 and RbBCl_4 . In both of these salts, there is no evidence for significant perturbation of BCl_4^- and it may therefore be argued that it is incorrect to use these data in calculations involving NOBCl_4 . While this point should be recognised it is felt that any secondary interaction between NO^+ and BCl_4^- would more seriously perturb NO^+ because it follows that only one quarter of the chlorine atoms in BCl_4^- are involved. Therefore proceeding as above:



$$\therefore U + 2RT = \Delta H_f^\circ \text{NO}^+(g) + \Delta H_f^\circ \text{BCl}_4^-(g) - \Delta H_f^\circ \text{NOBCl}_4(c)$$

$$\therefore U \approx (989.9 - 929 + 391 - 5)$$

$$\approx 447 \text{ kJ mol}^{-1}.$$

Using the Kapustinskii equation

$$U = \frac{120.2.2}{(r_+ + 0.306)} \left[1 - \frac{0.0345}{(r_+ + 0.306)} \right] = 447$$

$$0.539 (r_+ + 0.2715) = (r_+ + 0.306)^2$$

$$r_+^2 + 0.0733r_+ - 0.0526 = 0$$

$$\therefore r_+ \approx 0.20 \text{ nm.}$$

The two values for $r_{\text{th}} \text{NO}^+$ derived from the NOClO_4 calculations are in excellent agreement and demonstrate the importance of using a radius and its associated $\Delta H_f^\circ \text{X}^-(g)$ in thermochemical calculations. The values are also in good, though possibly fortuitous, agreement with the interatomic distance⁴² in NO^+ of 0.11 nm but are clearly lower than $r_{\text{th}} \text{NO}^+ = 0.20$ nm derived from NOBCl_4 calculations as expected. Further comment is not possible, however, owing to the possible experimental uncertainties in measurement of $\Delta H_f^\circ \text{NOBCl}_4(c)$.

3.5 INVESTIGATION OF THE $\text{NO}_2\text{Cl}-\text{BCl}_3$ REACTION

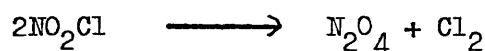
In view of the dissociative nature of NOBCl_4 , it was surprising that NO_2BCl_4 , prepared by reaction of NO_2Cl and BCl_3 in $\text{SO}_2(l)$, was recently claimed³⁸ as a white solid decomposing at $+86^\circ\text{C}$. Although nitronium salts of complex fluoro anions e.g. NO_2SbF_6 and NO_2PF_6 are well characterised,^{13,31} and compounds with simple inorganic anions e.g. NO_2ClO_4 ,³⁵ $\text{NO}_2\text{SO}_3\text{F}$ ⁵⁵ are also known, salts with complex chloro-anions e.g. NO_2BCl_4 which are essentially derived from NO_2Cl , are comparatively rare. It was further surprising that the analogous

preparation of NO_2SbCl_6 apparently yielded a white solid, decomposing at $+112^\circ\text{C}$, when an earlier preparation⁴⁶ in liquid chlorine yielded an unstable adduct readily decomposing at 0°C .

That NO_2Cl might donate Cl^- to a suitable Lewis acid must be related to the donor properties of NO_2Cl . NOCl shows negligible dissociation in the gaseous phase into NO and Cl_2 , and the long N-Cl bond is said to indicate²⁹ some degree of ionic character:



NO_2Cl , however, dissociates in the gaseous phase:⁴⁶



and Seel⁴⁶ believed the equilibrium to lie slightly to the right in the liquid phase. At low temperatures, NO_2Cl reacts with ammonia⁴⁶ giving chloramine and ammonium nitrite, which suggests that NO_2^- and Cl^+ ions are formed. However, a solution of NO_2Cl in $\text{H}_2\text{S}_2\text{O}_7$ shows a band in the Raman spectrum at 1400 cm^{-1} indicative of NO_2^+ and it is clear that under these conditions ionisation giving NO_2^+ and Cl^- occurs. It is tentatively suggested that Cl^- ion transfer resulting in the formation of an ionic nitronium chlorometallate requires a very strong Lewis acid. In the case of BCl_3 , there also exists the possibility of solvolysis by N_2O_4 , first reported as a synthesis of NOBCl_4 in 1874.¹⁹ If the reaction is carried out in $\text{SO}_2(1)$, as described by Paul, then reaction with N_2O_4 giving $(\text{NO})_2\text{S}_2\text{O}_7$ may also occur.⁵² The gaseous phase reaction between NO_2Cl and SO_2 giving $(\text{NO})_2\text{S}_2\text{O}_7$ has been reported to take several days to reach completion.⁵¹

SO₂(l) as a solvent in BCl₄⁻ salt synthesis has been employed previously,^{33,11} although Burg¹⁰ has reported that the chloride ion solvolysis of BCl₄⁻ by SO₂ attains completion in several days. A series of attempted preparations of NO₂BCl₄ in these laboratories indicated that SO₂(l) undoubtedly undergoes reaction in this system producing a white solid which does not correspond to NO₂BCl₄ as described by Paul. As far as possible, the reactions discussed below were monitored by Raman spectroscopy although in several cases, the products could not be identified.

The measured Raman spectrum for NO₂Cl is presented in table 3.10 and fundamentals were located in agreement with the literature^{7,12} in terms of a C_{2v} planar structure. In addition, a weak band at ca. 530 cm⁻¹ was also observed, indicative of chlorine, but no bands at ca. 265, 500, 811, 1325, 1382 and 1724 cm⁻¹ indicative of N₂O₄.²⁰ The presence of a small amount of chlorine is not serious and will tend to suppress any dissociation. The Raman spectrum for a solution of BCl₃ in excess NO₂Cl at -100°C is a superposition of the liquid phase spectra of NO₂Cl and BCl₃. Warming the solution to ca. -50°C results in broadening of NO₂Cl modes with splitting of the bands at 370 and 414 cm⁻¹. BCl₃ modes were unaffected and there was no indication of characteristic BCl₄⁻ modes¹⁴ at 200, 280, 415 and 700 cm⁻¹. On heating to +40°C for five minutes, then cooling, a white deposit formed and the Raman spectrum of the supernatant liquid showed bands at 285 and 540 cm⁻¹, indicative of NOCl.

NO₂Cl and BCl₃ in HCl(l) appeared to undergo no reaction, but upon introducing SO₂(l) at -95°C a colour change from pale green to bright red took place, presumably due to the formation of NOCl.

Upon removal of HCl at -95°C a viscous red liquid remained, which completely solidified on warming to -45°C . An identical solid was obtained in the absence of HCl indicating that, either by virtue of the solvent polarity or interaction with one of the precursors, SO_2 was responsible for these observations. The red solid showed Raman bands at $273(\text{s})$ and $500(\text{m})\text{cm}^{-1}$ indicative of free NOCl , and a weak band at ca. 380cm^{-1} indicative of unreacted NO_2Cl . Since the solid did not scatter very well upon laser irradiation the bulk product is likely to be B_2O_3 .

Interaction of SbCl_5 with an excess of NO_2Cl in a sealed tube produced, upon rapid cooling, a Raman spectrum exhibiting bands at 180 , 290 and 340cm^{-1} indicative¹⁶ of SbCl_6^- and a weak band at ca. 1382cm^{-1} indicative of NO_2^+ . On warming to 0°C decomposition took place with precipitation of a yellow-white solid and the Sb-Cl stretching region ($280 - 350\text{cm}^{-1}$) became very complex. These observations agree very well with the conclusions of Seel et al.⁴⁶ but in no way substantiate the findings of Paul et al.³⁸ His reported infra-red spectrum of NO_2BCl_4 (table 3.9) is in many respects incomplete. Although $\nu_3\text{NO}_2^+$ was observed at 2360cm^{-1} , $\nu_2\text{NO}_2^+$ at ca. 580cm^{-1} was outside the range of the spectrometer. The anion data are not really convincing and BCl_4^- could be more readily identified from the complementary Raman data, which were apparently not measured.

This study therefore casts considerable doubt upon the existence of NO_2BCl_4 and the validity of the experimental work cited.

TABLE 3.10
VIBRATIONAL SPECTRA FOR NO₂Cl (C_{2v})

I.r. GAS ⁷ /CM ⁻¹	I.r. SOLID ⁷ /CM ⁻¹	RAMAN LIQUID ¹² /CM ⁻¹	RAMAN LIQUID/CM ⁻¹ THIS WORK	
1267) 1318) vs	1257) 1321)	1260) 1318) w	1262) 1315) w	ν_1 A ₁
793 vs	804	787 w	789 w, br	ν_2 A ₁
370 vs	399	370 vs	370 vs	ν_3 A ₁
1685 vs	1654	1670 vw	1670 wv, br	ν_4 B ₁
408 vw	426	411 m	414 m	ν_5 B ₁
652 m	653	652 vw	not observed	ν_6 B ₂

TABLE 3.11
INFRA-RED DATA FOR NO₂BCl₄ (R.C. PAUL et al.³⁸)

BAND CM ⁻¹	ASSIGNMENT
3760	$\nu_1 + \nu_3$ NO ₂ ⁺
2360	ν_3 NO ₂ ⁺
1460	$2\nu_3$ BCl ₄ ⁻
1380	$(\nu_1 + \nu_4 + \nu_3)$ BCl ₄ ⁻
1275	$(2\nu_1 + 2\nu_4)$ BCl ₄ ⁻
690	ν_3 BCl ₄ ⁻

REFERENCES

1. D.M. Adams, R. Appleby, J.I.N.C. (1976) 38 1601-3.
2. D. Ambrose, C.H.S. Sprake, R. Townsend, J. Chem. Therm. (1974) 6 693-700
3. W.R. Angus, A.H. Leckie, Proc. Roy. Soc. (London) (1935) A150 615-8.
4. P. Barbier, G. Mairesse, J.P. Wignacourt, C.R. Acad. Sci. Ser. C. (1972) 275 403-4.
5. P. Barbier, G. Mairesse, F. Wallart, J.P. Wignacourt, C.R. Acad. Sci. Ser. C. (1972) 275 475-8.
6. P. Barbier, G. Mairesse, F. Wallart, J.P. Wignacourt, C.R. Acad. Sci. Ser. C. (1973) 277 841-4.
7. D.L. Bernitt, R.H. Miller, I.C. Hisatsune, Spectrochim. Acta. (1967) 23A 237-48.
8. J.I. Bullock, N.J. Taylor, F.W. Parrett, J.C.S. Dalton (1972) 1843-6.
9. A.B. Burg, G.W. Campbell jnr. J.A.C.S. (1948) 70 1964-5.
10. A.B. Burg, E.R. Birnbaum, J.I.N.C. (1958) 7 146-7.
11. D.E. Burge, H. Freund, T.H. Norris, J. Phys. Chem. (1959) 63 1969-71.
12. K.O. Christe, C.J. Schack, R.D. Wilson, Inorg. Chem. (1974) 13 2811-15.
13. P. Cook, S.J. Kuhn, G.A. Olah, J. Chem. Phys. (1960) 33 1669-71.
14. J.A. Creighton, J.C.S. (1965) 6589-91.
15. M.E. Efimov, V.A. Medvedev, J. Chem. Therm. (1975) 7 719-23.
16. J.R. Ferraro, Low frequency vibrations of inorganic and coordination compounds, Plenum Press New York, 1971.

17. A. Finch, P.J. Gardner, N. Hill, N. Roberts, J.C.S. Dalton (1975) 357-9.
18. P.N. Gates, Royal Holloway College (private communication).
19. Geuther, J. Prakt. Chem. (1874) 7 354.
20. J.D.S. Goulden, D.J. Millen, J.C.S. (1950) 2620-27.
21. N.N. Greenwood, K. Wade, J.C.S. (1960) 1130-41.
22. V. Gutmann, J. Phys. Chem. (1959) 63 378-83.
23. I.C. Hisatsune, P. Miller, J. Chem. Phys. (1963) 38 49-54.
24. J.M. Hoell, W.R. Wade, Appl. Phys. Lett. (1974) 25 202-3.
25. H. Houtgraaf, A.M. De Roos, Rec. Trav. Chim. (1953) 72 963-77.
26. A.W. Jackowski, J. Chem. Therm. (1974) 6 49-52.
27. L.H. Jones, R.R. Ryan, L.B. Asprey, J. Chem. Phys. (1968) 49 581-5.
28. A.F. Kapustinskii, Quart. Rev. (London) (1956) 10 283-94.
29. J.A.A. Ketelaar, K.J. Palmer, J.A.C.S. (1937) 59 2629-33.
30. N. Krivtsov, K.V. Titova, V. Ya. Rosolovskii, Zh. Neorg. Khim. (1973) 18 347-52 (Russ).
31. S.J. Kuhn, Can. J. Chem. (1967) 45 3207-9.
32. J. Lewis, R.G. Wilkins, J.C.S. (1955) 56-9.
33. M. Migeon, M.C. Dhamelincourt, C.R. Acad. Sci. Ser. C. (1975) 281 79-81.
34. K. Nakomoto, Infra-red spectra of inorganic and coordination compounds, Wiley (1969).
35. J.W. Nebgen, A.D. McElroy, H.F. Klodowski, Inorg. Chem. 4 1796-9.
36. G.A. Olah, W.S. Tolgyesi, J. Org. Chem. (1961) 26 2319-23.

37. J.R. Partington, A.L. Whynes, J.C.S. (1949) 3135-41.
38. R.C. Paul, D. Singh, K.C. Malhotra, J.C.S.A. (1969) 1396-1400.
39. R.C. Paul, V.P. Kapila, K.C. Malhotra, J.C.S.A. (1970) 2267-73.
40. G. Pilcher, Computer Analysis of ThermoChemical data (Nitrogen Compounds).
41. H. Rheinboldt, R. Wasserfuhr, Ber. (1927) 60B 732-7.
42. G.W. Richards, A.A. Woolf, J.C.S.A. (1968) 470-6.
43. Handbook of Chemistry and Physics 56th Edition 1975-6, C.R.C. Press.
44. C.D. Schmulbach, I.Y. Ahmed, J.C.S.A (1968) 3008-12.
45. C.D. Schmulbach, I.Y. Ahmed, Inorg. Chem. (1969) 8 1414-8.
46. F. Seel, J. Nogradi, R. Posse, Zeit. anorg. allgem. Chem. (1952) 269 197-206.
47. D.W.A. Sharp, J. Thorley, J.C.S. (1963) 3557-60.
48. D.F. Shriver, B. Swanson, Inorg. Chem. (1971) 10 1354-65.
49. M. Solomon, J. Electrochem. Soc. (1971) 118 1614-16.
50. K. Stopperka, V. Grove, Zeit. anorg. allgem. Chem. (1966) 347 19-23.
51. K. Stopperka, F. Wolf, G. Suess, Zeit. anorg. allgem. Chem. (1968) 359 14-29.
52. D.J. Stufkens, H. Gerding, Rec. Trav. Chim. (1970) 89 1267-70.
53. H.A. Taylor, R.R. Denslow, J. Phys. Chem. (1927) 31 374-82.
54. K.V. Titova, I.P. Vavilov, V. Ya. Rosolovskii, Zh. Neorg. Khim. (1973) 18 1131-2.
55. P. Vast, M. Deporcq-Stratmains, C.R. Acad. Sci. Ser. C. (1968) 267 487-9.

56. T.C. Waddington, *Advances in Inorganic and Radiochemistry*,
1 (1959) 158-223.
57. T.C. Waddington, F. Klanberg, *Zeit. anorg. allgem. Chem.* (1960)
304 185-90.
58. E. Dow. Witney, R.O. MacLaren, T.J. Hurley, C.E. Fogle,
J.A.C.S. (1964) 86 4340-2.

CHAPTER 4

VIBRATIONAL SPECTROSCOPY AND CHEMICAL STRUCTURE

4.1 INTRODUCTION

Vibrational spectroscopy has found numerous applications in molecular structure determinations.¹⁸ The extent of the interpretation of a given spectrum, however, depends very much upon the symmetry and complexity of the species concerned. The number of normal modes for a non-linear species with N atoms is $(3N-6)$ but, for highly symmetric species, some of these modes may be doubly or triply degenerate thus reducing the number of observable vibrational bands. In addition, the selection rules which govern spectral activity may also preclude the observation of certain of these modes. The vast majority of chemical substances, however, are of low symmetry and a complete vibrational assignment in terms of normal modes is usually impossible. Nevertheless, in complex molecules certain normal modes of vibration can often be approximately described as stretchings or deformations of particular functional groups. These have characteristic vibrational frequencies which permit certain structural inferences to be drawn from the spectrum of a particular compound. The unequivocal identification of a molecular species from its vibrational spectrum, however, requires the identification of all the normal modes of vibration which is only possible for small symmetric species. In this discussion vibrational data derived only from infra-red absorption and the normal Raman effect will be considered.

Although the Raman effect^{6,23} dates from 1928, it has not attained as wide an application as infra-red absorption. Prior to the introduction of lasers as strong coherent monochromatic sources, the technique could

rarely be routinely applied. One of the chief advantages over infra-red absorption is the convenient measurement of low-frequency vibrations. This, however, is of limited application to complex organic compounds for which laser irradiation may induce photochemical decomposition. The widest application of Raman spectroscopy is in inorganic chemistry where a much larger range of small symmetric species with normal modes at low frequency ($< 600 \text{ cm}^{-1}$) occur. The study of volatile, moisture-sensitive compounds is particularly easy since all samples can be mounted in sealed glass tubes. However, for a complete vibrational assignment, the complementary infra-red data are often essential because the molecular symmetry defines the spectral activity of the normal modes of vibration. Low-frequency infra-red data are comparatively very much more difficult to measure. For volatile moisture-sensitive compounds considerable ingenuity may be called for unless specialised equipment to mount the samples is available. In chapter 5, vibrational analyses of various ICl_4^- and AuCl_4^- salts are attempted, so that certain structural inferences may be drawn. For the purpose of describing the methods used, complex chloroanions generally will be used as examples in the following discussion.

4.2 POINT GROUP SYMMETRY AND VIBRATIONAL ANALYSIS

The preferred regular molecular geometries for a given coordination number may be assigned to particular point groups. The number and spectral activities of the normal modes of vibration for free ions and molecules may be derived using point group analysis. This fundamental technique may be illustrated by considering a simple example. For coordination number four, two regular geometries are tetrahedral (T_d) and square planar (D_{4h}) and the point group analyses^{16,21} for BCl_4^-

and AuCl_4^- ions having these respective geometries are presented in table 4.1. The number of normal modes observed and their spectral activity can be used to determine whether another species MCl_4^- is tetrahedral or square planar. The normal modes may be classified as stretchings or deformations which are observed in characteristic frequency ranges. Thus the region $320 - 360 \text{ cm}^{-1}$ might be classified as the Au-Cl stretching region, and three of the seven AuCl_4^- modes, A_{1g} , B_{2g} and E_u are therefore stretching modes. For BCl_4^- , the B-Cl stretching region covers the range $400 - 700 \text{ cm}^{-1}$ and two modes ($A_1 + F_2$) are therefore stretching modes.

However, the spectra summarised in table 4.1 refer only to the free ions. This situation is realised in the gaseous, and, with few exceptions, the liquid phases. Very often particular compounds exist only in the solid state, or a structure change may occur on going from the solid to the liquid phase. An ion vibrating in a crystal lattice site will experience an electric field created by all the other neighbouring ions. This can have pronounced effects upon the vibrations of the species occupying the site. In addition, solid state infra-red and Raman spectra are characterised by numerous additional low frequency vibrations (below 100 cm^{-1}). These cannot be explained in terms of point group analysis of the free ions. The normal modes of vibration of ions in the solid state are often located at frequencies close to the free ion values observed in solution. However, splittings of degenerate modes are often noted and occasionally, depending upon the resolution of the spectrometer, splittings of non-degenerate modes may also be apparent. Two different methods of solid state vibrational

TABLE 4.1

POINT GROUP ANALYSIS FOR BCl_4^- AND ICl_4^- IONS

POINT GROUP SYMMETRY	EXAMPLE	SYMMETRIES OF THE NORMAL MODES	SPECIAL ACTIVITY	FREQUENCY cm^{-1}	
T_d	BCl_4^-	ν_1	A_1	R	405 *
		ν_2	E	R	193
		ν_3	F_2	R + i.r.	670
		ν_4	F_2	R + i.r.	276
D_{4h}	AuCl_4^-	ν_1	A_{1g}	R	347 **
		ν_2	B_{1g}	R	171
		ν_3	A_{2u}	i.r.	150
		ν_4	B_{2g}	R	324
		ν_5	B_{2u}	inactive	-
		ν_6	E_u	i.r.	356
		ν_7	E_u	i.r.	173

* KBCl_4 in SO_2 (l) M.C. Dhamelincourt, M.M. Migeon, C.R. Acad. Sci Ser. G (1975) 281 79-81.

** KAuCl_4 (soln) J.R. Ferraro, Low frequency Vibrations of Inorganic and Coordination Compounds (Plenum Press, New York 1971).

analysis are available, and have been described in numerous reviews:^{1,11,14,19,25}

(i) Site Group Analysis (S.G.A.).

(ii) Factor Group Analysis (F.G.A.).

Before presenting a brief description of each method, the understanding of certain basic terminology used in crystallography is required. For the vibrational spectroscopist, this has been very clearly presented in a book by Sherwood,²⁵ and may be briefly summarised as follows. Every crystal lattice must have the symmetry of one of the 230 space groups. These are composed of the usual point group symmetry elements plus the unique elements of translation, screw axis and glide plane. When discussing the vibrations of a molecular or ionic solid, the simplest (primitive) unit cell or Bravais space cell should be considered rather than simply the isolated ion or molecule. This may be defined as the smallest unit in which no atoms are equivalent under translations although they may be equivalent under any other symmetry operation. Unless the crystallographic space group is primitive it will contain 2, 3 or 4 times as many atoms as the simplest unit cell. This multiplicity factor may be readily deduced from the first character of the Hermann-Mauguin symbols describing the space group. The multiplicity factors for the various types of crystal structure are presented in table 4.2.

Every atom in the unit cell occupies a specific position or site and since one or more symmetry elements (including identity) pass through each site, the symmetry of the site is described by a site group. The site group is always one of the 32 crystallographic point groups

TABLE 4.2

DERIVATION OF THE NUMBER OF MOLECULES IN THE SIMPLEST
UNIT CELL FROM THE SPACE GROUP¹⁵

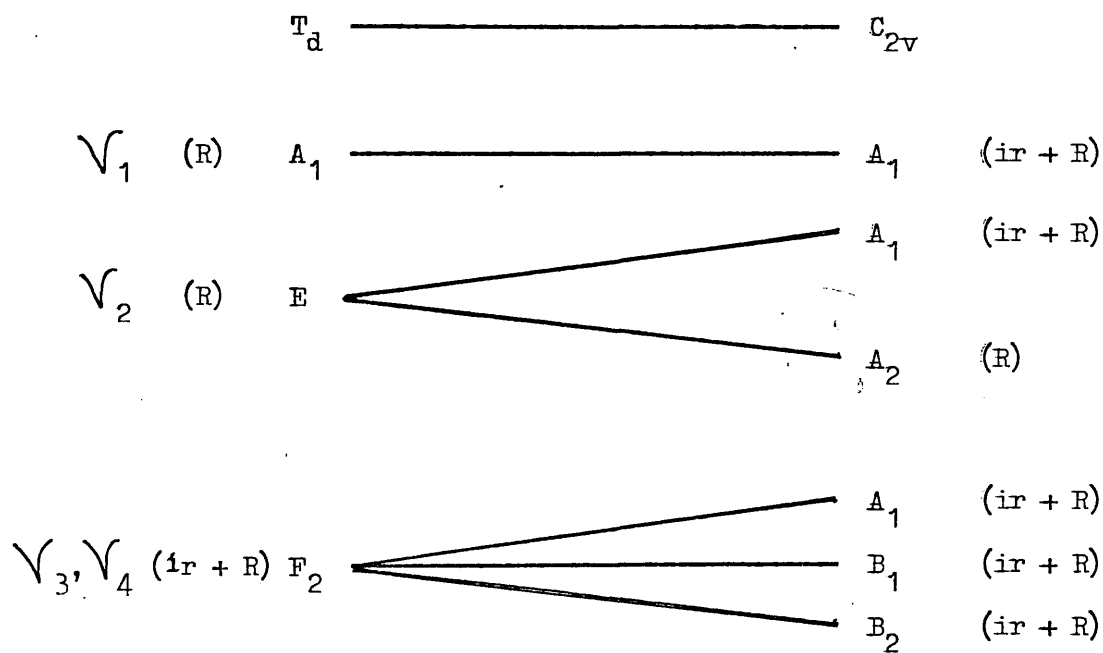
TYPE OF CRYSTAL STRUCTURE	MULTIPLICITY FACTOR
A	2
B	2
C	2
F	4
I	2
P	1
R	3 or 1

and must be a sub-group of the space group. Since any point in a unit cell is related to one or more other points by at least one element of symmetry, sites of a particular site group symmetry will occur in sets. The possible site group symmetries for each of the 230 space groups have been tabulated.^{15,16} The group describing the symmetry of the simplest unit cell is termed the unit cell group and is readily derived by removing the superscript from the Schoenflies symbols describing the space group. It has also been termed the factor group.

4.3 SITE GROUP ANALYSIS (S.G.A.)

Site group analysis may be used to interpret solid state vibrational spectra when there is virtually no interaction between the vibrations of like ions in the unit cell. The method can only account, therefore, for a maximum of $(3n-6)$ internal vibrations from each ion, and the derivation of the internal vibrations may be considered as a simple extension of point group analysis. Consider, as an illustration of the method, a symmetric ionic species - e.g. BCl_4^- with T_d symmetry, vibrating in a lattice site of lower symmetry - e.g. C_{2v} . All the surrounding ions will create an electric field at each BCl_4^- site of lower symmetry than T_d . If the magnitude of this field is sufficient to perturb the BCl_4^- ion, it is then appropriate to discuss the internal vibrations in terms of C_{2v} symmetry. This is very easily carried out using correlation tables,¹⁵ and the C_{2v} site effect upon the BCl_4^- vibrations is presented in table 4.3. The overall effect upon the spectrum will be splitting of degenerate modes and the appearance of formally inactive modes in the infra-red absorption spectrum.

TABLE 4.3

SITE GROUP ANALYSIS FOR BCl_4^- OCCUPYING A C_{2v} CRYSTAL SITE

The site symmetry method can also predict the number of external (lattice) modes which are considered to result from the oscillations of the ions. Since no interaction between like ions is assumed, non-linear polyatomic ions give rise to 3 translatory ($T_x T_y T_z$) and 3 rotatory ($R_x R_y R_z$) oscillations, linear polyatomic ions give rise to 3 translatory and 2 rotatory oscillations, whilst monatomic ions give rise to only 3 translatory oscillations. The number of frequencies and their spectral activity can be determined from the character table of the site group. Thus as an example consider NOAlCl_4 , which was discussed in chapter 3: NO^+ and AlCl_4^- ions were stated to occupy C_S sites.^{7,8} A total of 11 external modes are predicted, 6 (3T + 3R) derived from AlCl_4^- and 5 (3T + 2R) derived from NO^+ , which are all both infra-red and Raman active.

As a point of interest, consideration of the proposed crystal structure reveals a possible fallacy in this particular case. The crystallographic space group was identified as D_{2h}^{16} with 4 molecules per unit cell. Consultation of site symmetry tables^{15,16} shows that the possible site symmetries for this space group are:

$$D_{2h}^{16} : 2C_i(4), C_S(4), nC_1(8)$$

Thus since there is only one set of four equivalent symmetry-related C_S sites, then either 4 NO^+ or 4 AlCl_4^- ions can be accommodated in them. The counter ions must therefore occupy C_i or C_1 sites. Since the site group must be a sub-group of both the point group of the free ion and the unit cell group, AlCl_4^- cannot occupy C_i sites. The following possibilities exist:

Site	C_i	C_S	C_1	No. of lattice modes
	NO^+	$AlCl_4^-$		$6(ir+R)+3(ir)+2(R)$
		NO^+	$AlCl_4^-$	11 (ir + R)
		$AlCl_4^-$	NO^+	11 (ir + R)
			$NO^+, AlCl_4^-$	11 (ir + R)

Further investigation of the crystal structure is required so that the site symmetries of NO^+ and $AlCl_4^-$ can be assigned.

4.4 FACTOR GROUP ANALYSIS (F.G.A.)

Factor group analysis may be used to interpret vibrational spectra when there is more than one molecule in the primitive unit cell and substantial interaction between the vibrations of like ions. Coupling of vibrations can only occur in those combinations permitted by the unit cell group symmetry. This is often referred to as correlation coupling,²⁵ and may be illustrated by the following simple example. Consider two hydroxyl groups in a primitive unit cell aligned along the crystallographic z axis. The OH stretching modes may be coupled in phase and out of phase yielding crystal modes of different symmetries:



If the site group is of lower symmetry than the molecular group, correlation coupling is considered to take place between vibrations labelled according to the site group symmetry. The free ion vibrations

must firstly be correlated to the site group to give an irreducible representation which is then correlated to the factor group. Consider an extension of the example discussed in the previous section - two BCl_4^- ions of T_d symmetry occupying C_{2v} sites in a unit cell of for example D_{2h} symmetry. The correlation is presented in table 4.4. Using this method it is possible to account for a maximum of $m(3n-6)$ modes, where n is equal to the number of atoms in the ion and m is equal to the number of ions in the simplest unit cell. The analysis presented in table 4.4 is observed to be mathematically rigorous. Thus there is at least one space group D_{2h}^r , where r is an integer $1 \leq r \leq 16$, with at least one set of two symmetry-related C_{2v} sites. This is a direct consequence of the correct assignment of a space group to the crystal structure. Inspection of table 4.4 shows that the analysis breaks down if for example three ions had been considered to occupy C_{2v} sites.

The external (lattice) modes are similarly derived by relating the rotational and translational unit vectors of the site group to the factor group (table 4.5). Again this procedure is noted to be mathematically rigorous. If the counter ion is considered to be a mono-atomic cation M^+ occupying C_{2v} sites, then only three translational modes need to be considered. The overall irreducible representation for the external lattice modes is therefore given by:

$$\begin{aligned} \Gamma_{\text{ext}} &= \Gamma_{\text{ext } \text{BCl}_4^-} + \Gamma_{\text{ext } M^+} & (i) \\ &= (A_g + B_{1g} + 2B_{2g} + 2B_{3g} + A_u + B_{1u} + 2B_{2u} + 2B_{3u}) \\ &\quad + (A_g + B_{2g} + B_{3g} + B_{1u} + B_{2u} + B_{3u}) \\ &= (2A_g + B_{1g} + 3B_{2g} + 3B_{3g} + A_u + 2B_{1u} + 3B_{2u} + 3B_{3u}) & (ii) \end{aligned}$$

TABLE 4.4

FACTOR GROUP ANALYSIS FOR BCl_4^- OCCUPYING A C_{2v} SITE IN A PRIMITIVE SPACE GROUP D_{2h}^r WITH TWO MOLECULES PER UNIT CELL

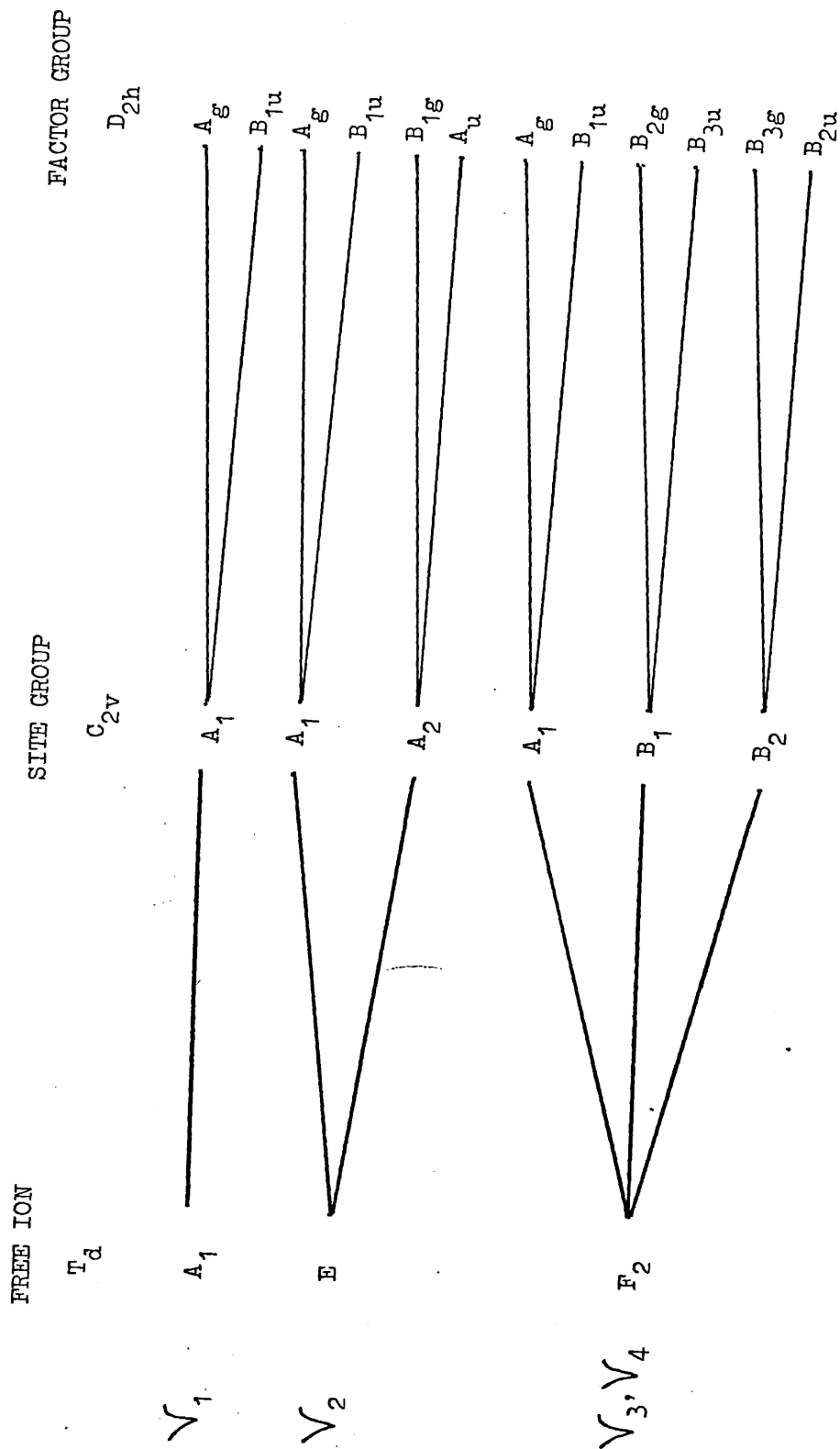
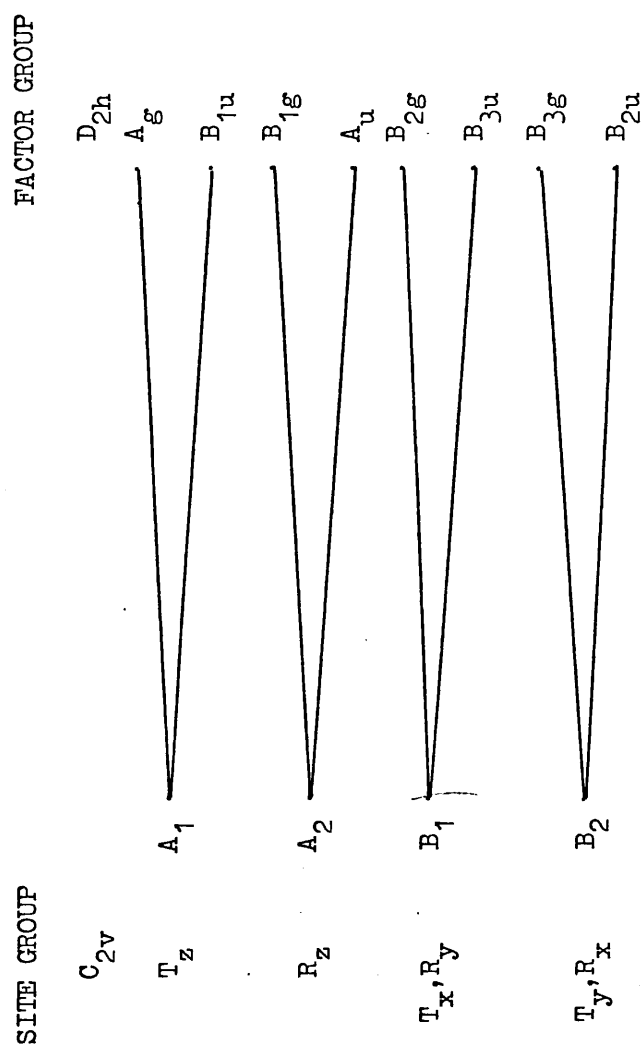


TABLE 4.5

FACTOR GROUP ANALYSIS FOR EXTERNAL MODES



This total representation also contains the acoustic modes of the crystal lattice. These can be easily recognised since they possess the same symmetry as the translational unit vectors of the factor group - D_{2h} . Thus:

$$\Gamma_{\text{acoust.}} = B_{1u} + B_{2u} + B_{3u} \quad (\text{iii})$$

Therefore the optical branch is given by:

$$\Gamma_{\text{ext, optical}} = (2A_g + B_{1g} + 3B_{2g} + 3B_{3g} + A_u + B_{1u} + 2B_{2u} + 2B_{3u}) \quad (\text{iv})$$

This example is an illustration of the correlation method of applying factor group analysis. This method is fully explained in an excellent book by Fateley et al.¹⁵ Adams and Newton,^{3,4} however, have prepared a set of tables which very much simplifies the procedure in certain cases. Thus the derivation of the irreducible representation of the lattice modes in the previous example may be reduced to the addition of three rows in a suitable D_{2h}^r space group table. Thus table 4.6 is a reproduction of the translational and rotational sections of table 2 for the space group D_{2h}^5 . The rows 2E-F, in Wyckoff notation, represent two sets of two symmetry-related C_{2v} sites, which in the example cited both BCl_4^- and M^+ were considered to occupy. As before:

$$\Gamma_{\text{ext}} = \Gamma_{\text{trans } BCl_4^-} + \Gamma_{\text{rot } BCl_4^-} + \Gamma_{\text{trans } M^+}$$

	A_g	B_{1g}	B_{2g}	B_{3g}	A_u	B_{1u}	B_{2u}	B_{3u}
2 E-F TRANS	1	0	1	1	0	1	1	1
2 E-F ROT	0	1	1	1	1	0	1	1
2 E-F TRANS	1	0	1	1	0	1	1	1
	2	1	3	3	1	2	3	3

This representation is identical with equation (ii). The subtraction of the acoustic modes then produces the irreducible representation for the optical branch as before. It is the author's belief, however, that although these tables provide an excellent check in complicated examples, all physical significance of the problem is lost. Further, unless the site symmetries of all the atoms in the ions are known, no information concerning the internal modes can be obtained from these tables.

The correlation method largely replaces an earlier method due to Bhagavantam and Venkatarayadu.^{10,15} The application of this method predicts the same result as the correlation method, but the procedure is much more complicated since a detailed description of the locations and orientations of all the ions in the unit cell is required. Since the correlation method does not require this additional crystallographic information, the Bhagavantam and Venkatarayadu method need not be considered further.

4.5 THE APPLICATIONS OF S.G.A. AND F.G.A. TO SOLID STATE VIBRATIONAL SPECTRA

Individual discussion of F.G.A. and S.G.A. was given in the previous sections, and the basic similarities and differences between the two methods can be appreciated. Clearly both methods can be regarded as extreme cases - in S.G.A. all interaction constants are zero, in F.G.A. all interaction constants are non-zero. Undoubtedly, the intermediate case will often arise in which some interaction constants are zero whilst others are non-zero. In addition, although both methods

predict the number and symmetries of the internal and external modes, whether all of these will in fact be observed largely depends upon (i) the resolution of the spectrometer, (ii) the possibility of accidental coincidences, and (iii) the intensities of the normal modes. The theory of infra-red and Raman band intensities is clearly beyond the scope of this work, but the problem was encountered with $\sqrt{3}\text{BCl}_4^-$ in chapter 3. It therefore follows that in certain cases a complete vibrational assignment may still be impossible. Kettle¹⁹ has considered the intermediate case in some detail and concludes that it is correct to treat certain aspects of the vibrational spectra of complex molecules by S.G.A. and other aspects, where necessary by F. G.A. A further complication should also be recognised. Splittings of non-degenerate modes also arise from isotope effects. Isotopic splittings are large for the lighter elements, but the splitting is not always observed for all the modes. The complexity caused by both factor group and isotopic splittings, which has been observed for $\text{NMe}_4^+ \text{BrCl}_2^-$,¹⁷ can be appreciated.

The discussion so far has considered solid state vibrational analysis in terms of a known crystal structure. The important considerations as far as the work in chapter 5 is concerned is to what extent the reverse procedure is possible - i.e. what information about the crystal structure of a compound can be derived from its vibrational spectra. Considering all the problems described in the previous paragraph, the short answer must be very little. That is, the assignment of space groups and numbers of molecules per unit cell would be impossible in many cases and very unreliable in most others.

Nevertheless, the following structural information can be inferred from solid state vibrational spectra:

(i) Species identification.

In spite of numerous solid state effects, a given ionic species can still often be identified by locating the bands predicted by point group analysis. When solid splittings are observed, these can be regarded as perturbations to the solution spectrum without involving the crystal site symmetry of the species. The dangers of drawing structural inferences from say only the Raman spectrum without substantiation from any other spectroscopic technique in doubtful cases cannot be overemphasised at this stage.

(ii) Identification of similar unit cells.

In related compounds, e.g. NOAlCl_4 ,⁸ NoGaCl_4 ,⁹ the crystal structures might be considered to be identical. This can occasionally be inferred if the vibrational spectra show an identical pattern of lattice modes. The method, however, should consider both the infra-red and Raman spectra, especially in the case of centrosymmetric factor groups.

(iii) Identification of low symmetry sites occupied by ions in the crystal lattice.

When a strong low symmetry electric field is created at a given crystal site, site group analysis can often be used to explain the splittings of degenerate modes. Certain information regarding the site symmetry can be derived from the infra-red and Raman spectra:

(a) Splitting of all degenerate modes and the appearance of formally inactive modes usually implies that the site is of C_{2v} or lower symmetry (not C_i).

(b) For free ions which are centrosymmetric, splitting of degenerate Raman modes without the appearance of formally inactive modes implies that the site group is also centrosymmetric but of lower symmetry.

(c) For free ions which are centrosymmetric, splitting of degenerate Raman modes accompanied by the appearance of formally inactive modes implies that the site is of C_{2v} or lower symmetry (not C_i).

It is usually impossible to specify the exact symmetry of the site.

(iv) Detection of phase changes.

Phase changes are conveniently detected by differential scanning calorimetry (D.S.C.). They can also be recognised by changes in the lattice modes of the vibrational spectrum, but it is not possible to derive an accurate transition temperature. The assignment of the new factor group and site groups resulting from the phase change is usually very difficult, although these have been proposed in certain cases.²

The discussion so far has considered the effect of a low symmetry electric field on the vibrational spectrum of a symmetric ion. This field is created by all the other surrounding ions and can produce a distortion of the ion. If there is a strong secondary interaction between ions of opposite charge, the distortion of the free ion may be considerable. Secondary interactions have been postulated in numerous systems and are the subject of an excellent review by Alcock.⁵

In $NO^+BCl_4^-$, discussed in chapter 3, a strong secondary interaction may be considered to account for the anomalous effects in the Raman spectra

at low temperatures. X-ray crystal data are usually required to identify a secondary interaction, certain interatomic distances being shorter than the sum of the van der Waals' radii. Secondary interactions often result in considerable distortion of the ionic species so that a crystallographic description in terms of free ions is no longer possible. For example, $\text{TeCl}_3^+\text{AlCl}_4^-$ is described crystallographically^{22,20} as consisting of strongly distorted TeCl_6 octahedra sharing three neighbouring chlorine atoms with three different AlCl_4^- tetrahedra. No solid state vibrational data are available for this compound, but an interpretation in terms of TeCl_3^+ ions would probably be very difficult.

The presence of secondary interactions should be recognised, although as far as interpretation of solid state vibrational spectra is concerned, it is the author's belief that these may often be regarded as contributing factors to a strong low symmetry electric field created at crystal sites. This is the approach adopted in chapter 5. It is fully recognised however, that while weak secondary interactions may produce no more than a splitting of degenerate modes and the appearance of formally inactive modes at frequencies close to the free ion values, very strong secondary interactions may produce anomalous effects which may only be resolved if the X-ray crystal structure of the compound is known.

4.6 N.Q.R. SPECTROSCOPY

In order to verify any conclusions drawn from vibrational spectroscopy, confirmatory data from a second spectroscopic technique

are required. For complex chloroanions and chlorocations, N.Q.R. spectroscopy is a suitable technique and N.Q.R. frequency measurements may be carried out on samples sealed in glass ampoules. The detailed theory of the N.Q.R. method is not necessary for a consideration of the arguments in chapter 5, which are purely qualitative. The following simple description is adequate for correlation of the conclusions with those from vibrational spectroscopy.

N.Q.R. signals are observed from nuclei having a nuclear quadrupole moment (i.e. the spin quantum number I is greater than $\frac{1}{2}$). For both ^{35}Cl and ^{37}Cl , $I = 3/2$ and interaction of the nuclear quadrupole moment with an electric field gradient at the nucleus produces a single resonance line from a single bound chlorine nucleus. This is explained as follows. The energies of the various quadrupole states in an axially symmetric field are given by the following equation.

$$E_m = \frac{eQq[3m^2 - I(I+1)]}{4I(2I-1)}$$

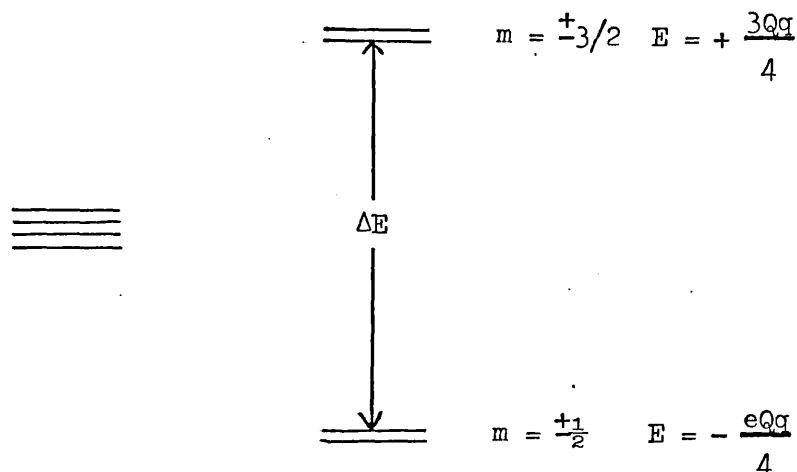
where I = nuclear spin quantum number

m = nuclear magnetic quantum number

q = field gradient at the nucleus produced by the electronic distribution in the molecule

Q = quadrupole moment of the nucleus

For $I = 3/2$, m can have the values $+3/2$, $+1/2$, $-1/2$, $-3/2$. Since in the energy expression, m is squared, the value for $m = -3/2$ will be identical to the value for $m = +3/2$, and a doubly degenerate set of quadrupole energy states results. Similarly, the state from $m = +1/2$ will be doubly degenerate.



The transition energy, ΔE , corresponds to $\frac{eQq}{2}$. Thus for a nucleus with spin $I = 3/2$ in an axially symmetric field, a single transition is expected, and the NQR frequency is related to ΔE by:

$$\Delta E = \frac{eQq}{2} = 2h\nu$$

In $KICl_4$, a single ^{35}Cl resonance line at ambient temperature is observed¹² at 22.3 MHz. This indicates equivalence of all four I-Cl bonds. N.Q.R. spectra are only observed in the solid state and from 'covalently' bonded nuclei - i.e. the electric field gradient arises from the electronic distribution in the chemical bond and no resonance would be observed from a free Cl^- ion. N.Q.R. spectrometry is often an unreliable technique in that resonances are not always observed from compounds in which they would be expected. The reasons for this are not always clear and in some cases an impure compound will give signals whereas the pure compound will not. N.Q.R. signals are usually stronger at low temperatures, and hence it is usual to record spectra at 77 K. The following information may be derived from N.Q.R. spectra:

(i) Species identification.

Characteristic frequencies, which may be measured very precisely if the signal-to-noise ratio is high, are observed from nuclei bound in complex ions - e.g. ICl_4^- , PCl_6^- , SCl_3^+ etc. The technique may be used to distinguish between two species in cases of dispute,¹² e.g. ICl_2^- (≈ 19 MHz) and ICl_4^- (≈ 22 MHz). In KICl_4 , one ^{35}Cl resonance at 22.3 MHz is observed at 295 K. In ICl_4^- salts in which all four I-Cl bonds are inequivalent due to different electric field gradients at each nucleus - e.g. in $\text{KICl}_4 \cdot \text{H}_2\text{O}$, four separate lines are observed.¹³ Large frequency splittings are usually indicative of large distortions. The mean ^{35}Cl resonance frequency, however, will lie in a narrow range characteristic of the ion. Thus in $\text{KICl}_4 \cdot \text{H}_2\text{O}$, four lines at 295 K are observed at 28.17, 24.86, 20.14 and 16.85 MHz. The mean frequency of 22.5 MHz is nevertheless characteristic of ICl_4^- .

(ii) Detection of phase changes.

In normal circumstances, cooling a solid down will produce an increase in resonance frequency. A plot of resonance frequency versus temperature for each resonance line from a given ion will consist of a series of smooth curves. Any sharp changes in the curvature for some or all of the resonances at a temperature T is considered indicative of a phase change. The technique, therefore, can give similar information as DSC. The latter technique may not always be used to determine transition points if the samples are corrosive and attack the sample containers. Transition temperatures derived from N.Q.R., however, may be rather imprecise.

(iii) Detection of secondary interactions.

Anomalous positive temperature coefficients of NQR frequencies may be attributed to secondary interactions between a chlorine atom in the ion and other species in the lattice. The phenomenon usually involves the longest M-Cl bond whose ^{35}Cl resonance frequency occurs at lowest frequency. Thus in $\text{NaICl}_4 \cdot 2\text{H}_2\text{O}$ the lowest ^{35}Cl frequency ranges from 20.008 MHz at 77 K to 20.574 MHz at 293 K. This is considered²⁴ to arise from hydrogen bonding of one chlorine to a water molecule.

These points, which by no means exploit all the information available from N.Q.R. spectra, will be used, where appropriate, to discuss N.Q.R. spectra of the ICl_4^- and AuCl_4^- compounds studied in chapter 5.

REFERENCES

1. D.M. Adams, *Coordination Chem. Rev.*, (1973), 10, 183-93.
2. D.M. Adams, R. Appleby, *J.I.N.C.* (1976) 38 1601-3.
3. D.M. Adams, D.C. Newton, *Tables for factor group and point group analysis*, Beckman R.I.I.C. Ltd. (1970).
4. D.M. Adams, D.C. Newton, *J.C.S. A* (1970) 2822-7.
5. N.W. Alcock, *Advances in Inorganic Chemistry and Radiochemistry* 15 (1972).
6. A. Anderson (Ed.) *The Raman Effect Vol. 1* (Dekker 1971).
7. P. Barbier, G. Mairesse, J.P. Wignacourt, *C.R. Acad. Sci Ser. C*, (1972) 275 403-4.
8. P. Barbier, G. Mairesse, F. Wallart, J.P. Wignacourt, *C.R. Acad. Sci. Ser. C*, (1972) 275 475-8.
9. P. Barbier, G. Mairesse, F. Wallart, J.P. Wignacourt, *C.R. Acad. Sci. Ser. C*, (1973) 277 841-4.
10. S. Bhagavantam, T. Venkatarayudu, *Theory of groups and its application to physical problems*, (Bangalore Press 2nd Edn. 1951).
11. R.L. Carter, *J. Chem. Ed.*, (1971), 48, 297-303.
12. C.D. Cornwell, R.S. Yamasaki, *J. Chem. Phys.* (1957) 27 1060-7.
13. B.O. Cozzini, *Diss. Abstr. B* (1966) 27 1850-1.
14. B.A. De Angelis, R.E. Newnham, W.B. White, *Amer. Miner.* (1972) 57 255-68.
15. W.G. Fateley, F.R. Dollish, N.T. McDevitt, F.F. Bentley. *Infra-red and Raman Selection Rules for molecular and lattice vibrations - The Correlation Method* (Wiley-Interscience 1972).

16. J.R. Ferraro, Low frequency vibrations of Inorganic and Coordination Compounds (Plenum Press, New York (1971)).
17. W. Gabes, H. Gerding, J. Mol. Struct. (1972) 14 267-79.
18. H.A.O. Hill, P. Day (Eds). Physical Methods in Advanced Inorganic Chemistry, (Wiley-Interscience 1968).
19. S.F.A. Kettle, Pure Appl. Chem. (1971) 27 113-25.
20. B. Knebs, B. Buss, D. Altena, Zeit. anorg. allgem. Chem. (1971) 396 257-69.
21. K. Nakamoto, Infra-red spectra of Inorganic and Coordination Compounds (Wiley 1968).
22. T. Okuda et. al. Bull. Chem. Soc. Japan (1975) 48 392-5.
23. C.V. Raman, K.S. Krishnan, Indian J. Phys. (1928) 2, 387.
24. A. Sasane, D. Nakamura, M. Kubo, J. Mag. Res. (1972) 8 179-82.
25. P.M.A. Sherwood, Vibrational Spectroscopy of Solids (C.U.P. 1972).

CHAPTER 5

A STRUCTURAL INVESTIGATION OF ICl_4^- AND AuCl_4^- COMPOUNDS USING
VIBRATIONAL SPECTROSCOPY AND N.Q.R.

5.1 JAILLARD'S COMPOUND - INTRODUCTION

In 1860, M. Jaillard^{36,37} described the preparation of an orange crystalline compound by chlorination of a finely-ground mixture of iodine and sulphur. The analysis of the product, not explicitly reported, was stated to be consistent with the stoichiometry SICl_4 . In 1866 this empirical formula was challenged by R. Weber⁵⁷ who showed the product to be identical, analytically, with that obtained by chlorinating a solution of iodine in carbon disulphide. Weber's analysis was consistent with the stoichiometry $(\text{SCl}_2)_2\text{ICl}_3$, based upon $S = 16$, or in modern terms $\text{SCl}_4 \cdot \text{ICl}_3$ based upon $S = 32$. In 1904, O. Ruff⁴⁷ reported the analysis of the orange material obtained by crystallising ICl_3 from a large excess of SCl_2 to be consistent with the stoichiometry $(\text{ICl}_3)_2\text{SCl}_4$, as distinct from the earlier compounds. No further experimental investigations were apparently reported until 1975, when Forneris and Tavares-Forneris²³ repeated Jaillard's original preparation and interpreted the Raman spectrum of the product, assuming the original analysis, in terms of a mixed crystal containing both $\text{SCl}_3^+\text{ICl}_2^-$ and a novel species SICl_3 (Table 5.1).

Some considerable interest during recent years in ICl_4^- salts⁴⁴ and sulphur-chlorine compounds²⁶ in this department prompted a detailed examination of this spectral analysis. A careful critical consideration of the spectroscopic evidence for SICl_3 together with a literature survey revealed several fallacies which required further experimental investigation.

TABLE 5.1

RAMAN SPECTRUM OF JAILLARD'S COMPOUND IN TERMS OF $\text{SCl}_3^+ \text{ICl}_2^-$ AND $\text{Cl}_3\text{SI} \cdot (\text{cm}^{-1})^{23}$

JAILLARD'S COMPLEX	Cl_3SI (C_{3v})	$\text{SCl}_3^+ \text{ICl}_2^-$	RbICl_2 (solid)	SCl_3^+ in AlSCl_7 melt	SCl_3^+ in AlSCl_7 solid
34					
41					
46					
63					
76					
97					
104					
123					
			96		
140		ClSCl angle def. $\sqrt{4} \text{E SCl}_3^+$		210	206
209		ClSCl angle def.			
242		SCl_3 rock			
255		} ICl_2^- stretch $\sqrt{3} \text{A}_1 \text{ SCl}_3^+$			
274			278	271	
293		SI stretch			
482		SCl sym. stretch			
493		SCl antisym. stretch		504	494
		$\sqrt{2} \text{E SCl}_3^+$			
508			522	516	530

The chief criticisms are as follows:

(i) The novel species SICl_3 was assigned C_{3v} symmetry. However, if such a species existed, the valence shell electron pair repulsion (VSEPR) theory^{10,29} would clearly preclude a regular tetrahedral configuration of three chlorine atoms and one iodine atom about sulphur. If the species were not ionic, then it would be expected to possess the geometry found in SF_4 (fig. 5.1)¹⁰:

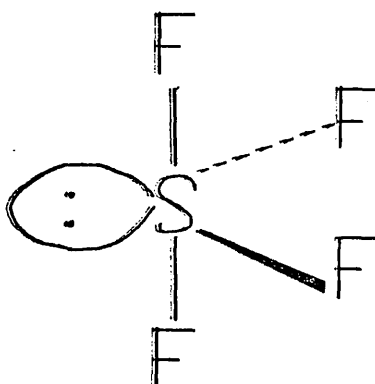


Fig. 5.1

(ii) A solid-state Raman spectrum was interpreted in terms of the point group symmetries of the proposed free ionic and molecular species. The limitations of such an approach were discussed in chapter 4. In particular, SICl_3^+ modes were assigned by comparison with the Raman spectrum¹⁴ of molten $\text{SICl}_3\text{AlCl}_4^-$. The point group analysis approach is clearly feasible in the molten state and four normal modes at 210, 278, 504 and 522 cm^{-1} are observed as expected for C_{3v} symmetry. Upon solidification, in common with other SICl_3^+ salts, the E modes at 210 and 522 cm^{-1} split and the S-Cl stretching region (480-530 cm^{-1}) exhibits three bands of similar relative intensities to those found at 482, 493 and 508 cm^{-1} in Jaillard's compound.

(iii) The vibrational analysis was carried out assuming that the product analysed as $(\text{SICl}_4)_2$, an analysis reported³⁷ in 1860. This is the most serious criticism. The co-existence of an ionic species $\text{SCl}_3^+ \text{ICl}_2^-$ and a molecular species SICl_3 in the same crystal lattice in exactly 1:1 stoichiometry is an ambitious claim. Careful, reproducible elemental analyses are essential especially as a sulphur to iodine mole ratio of 4:1 was used in the preparation.

(iv) Jaillard's original empirical formula, SICl_4 , is inexact in modern terms. The correct assignment of atomic weight values was a historical landmark in the development of modern chemistry. Sulphur assays published last century are likely to be based upon $S = 16$. The correct empirical formula derived from Jaillard's analysis is therefore SI_2Cl_8 , which renders totally invalid the structural interpretation of the Raman spectrum proposed by Forneris and Tavares-Forneris.²³

5.2 THE CONSTITUTION OF JAILLARD'S COMPOUND

Jaillard's original preparation was repeated in these laboratories and two products, as distinguished by Raman spectroscopy, were isolated (fig. 5.2). The analysis of each product is consistent with the stoichiometry SICl_7 in complete agreement with the subsequent analytical work reported by Weber in 1866. The product usually obtained, form 1, is spectroscopically identical with that described by Forneris. Form 2 was occasionally obtained using Jaillard's method but was the exclusive product precipitated when a solution of ICl_3 in SCl_2 was saturated with chlorine. In effect, form 2 may be regarded as a metastable modification in that complete conversion to form 1 takes place over a period of time ranging from several hours to several days at ambient temperature.

Fig 5 - 2 (a) The Raman spectrum of Form 1 $\text{SCl}_3 \cdot \text{ICl}_4^-$

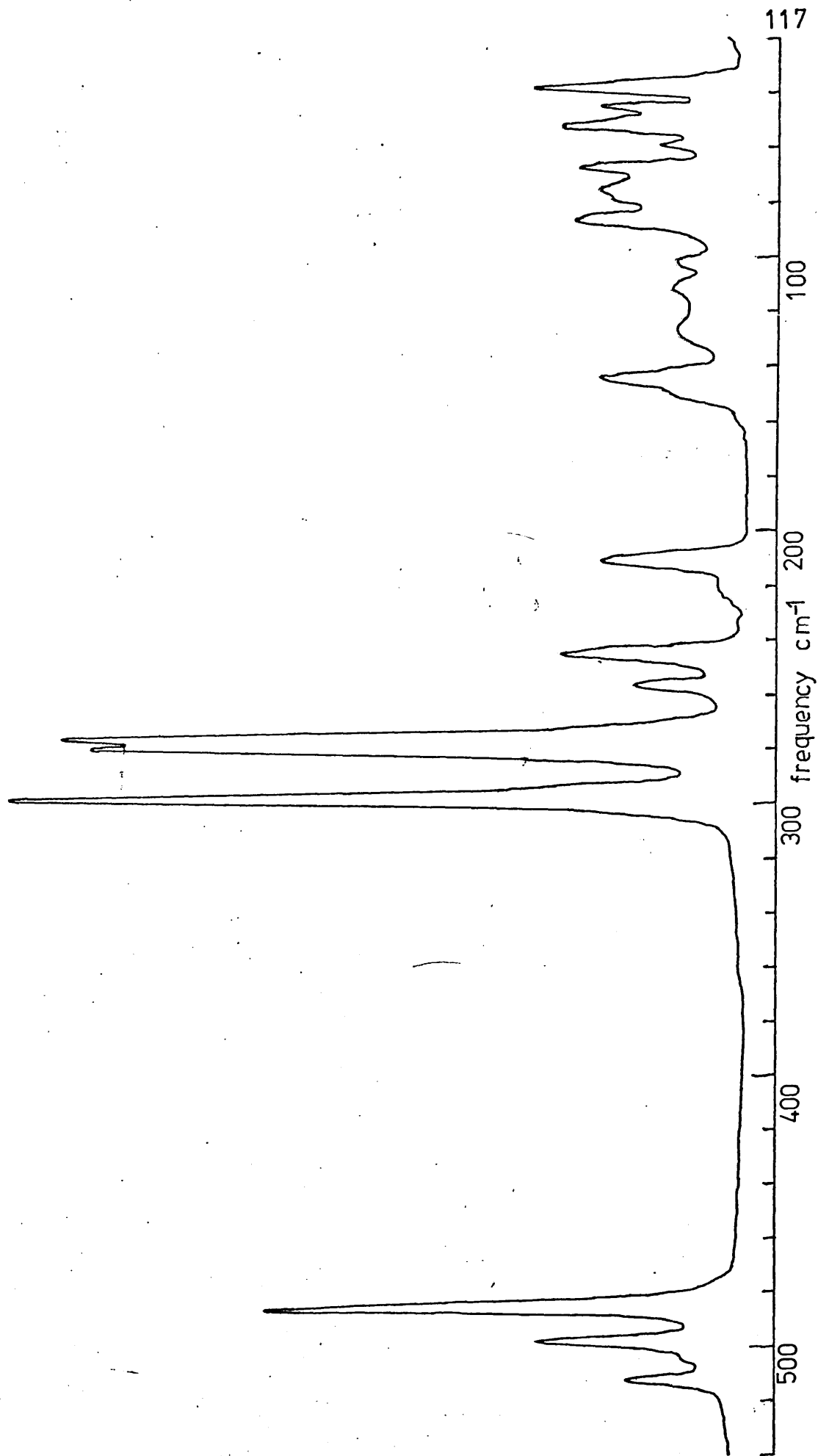
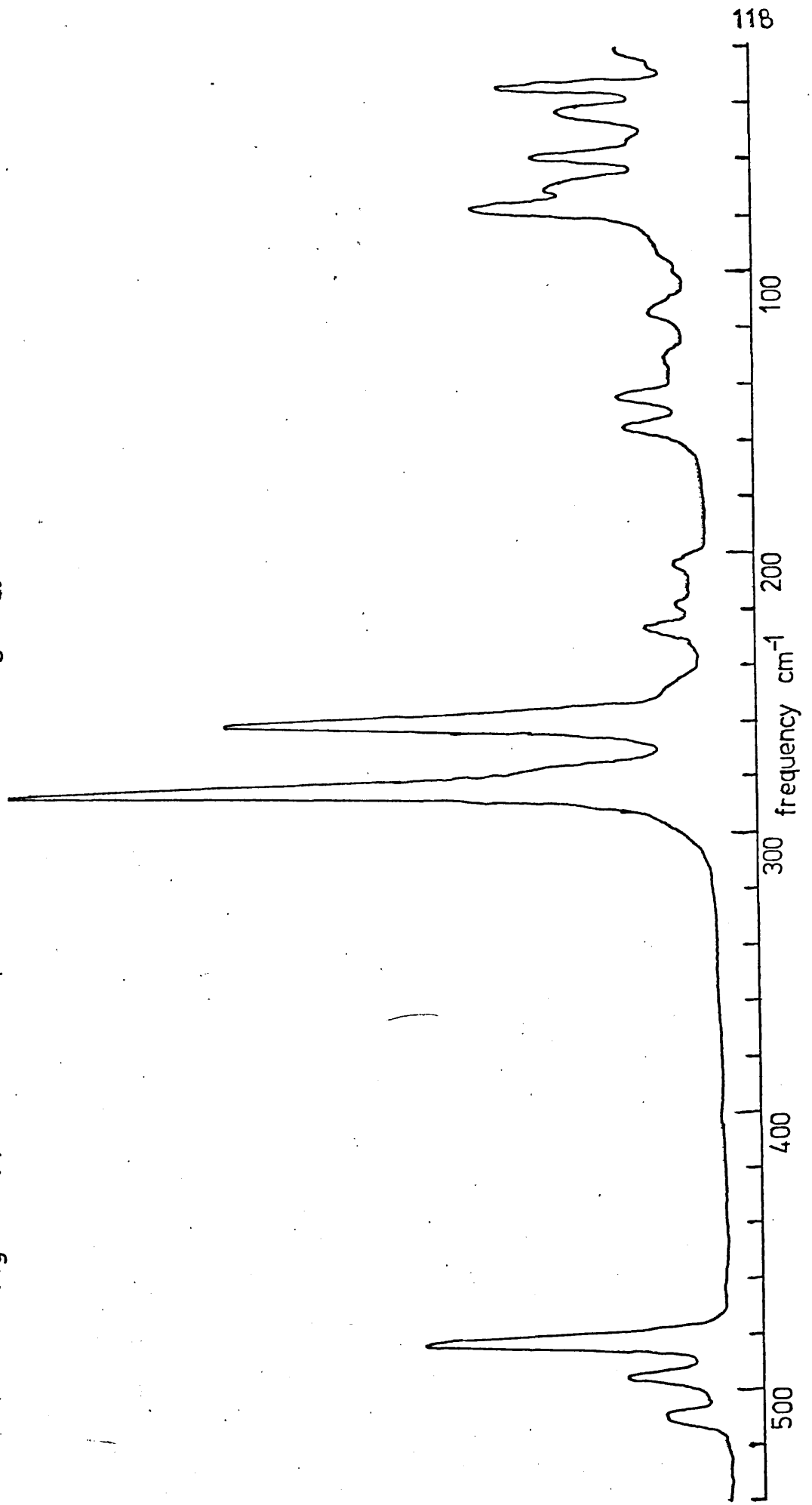


Fig 5 - 2 (b) The Raman spectrum of Form 2 $\text{SCl}_3 \cdot \text{ICl}_4$.



Form 2 may be prepared from form 1 by precipitation with chlorine following complete dissolution in SCl_2 . Undoubtedly this is a reformation process involving an $\text{ICl}_3 - \text{SCl}_2$ intermediate, and saturation with chlorine rapidly precipitates form 2, the kinetic-controlled product, whose crystal structure changes over to form 1, the thermodynamically-stable product. Both modifications of Jaillard's compound are exceedingly volatile at ambient temperature, existing as solids only under their own vapour pressure or in a chlorine atmosphere.

The empirical formula SiCl_7 may be considered in terms of $\text{SCl}_3^+ \text{ICl}_4^-$. Raman shifts arising from SCl_3^+ with approximately C_{3v} symmetry in both forms may be readily identified by comparison with standard spectra (Table 5.3). The S-Cl stretching modes (ν_1 and ν_3) occur at lower frequencies than observed in solid $\text{SCl}_3^+ \text{AlCl}_4^-$,¹⁴ $\text{SCl}_3^+ \text{SbCl}_6^-$ ²⁷ and $\text{SCl}_3^+ \text{SO}_3\text{Cl}^-$,²⁸ but are higher than the shifts of 449 and 471 cm^{-1} reported in solid SCl_4 ^{21,41} (Table 5.2). The latter compound is believed to contain C_{3v} SCl_3^+ units with Cl^- counter ions which may be involved in some secondary bonding.²¹ Bridging chlorine linkages are found in the related⁸ compounds SeCl_4 and TeCl_4 , although in these compounds distinct tetramers of SeCl_3^+ and TeCl_3^+ units occur. Lowering of fundamental frequencies when halide ions are present in a crystal lattice has been observed in certain phosphorus halide systems⁴⁸ - e.g. $\text{PBr}_4^+ \text{Br}^-$. This may possibly arise because PBr_4^+ units are linked by Br^- ions. In $\text{SCl}_3^+ \text{ICl}_4^-$, the S-Cl stretching modes may occur at lower frequencies because of a secondary interaction between SCl_3^+ and ICl_4^- ions. The splitting of both E modes can be explained in terms of SCl_3^+ ions occupying low symmetry sites with negligible correlation coupling taking place.

TABLE 5.2

RAMAN SHIFTS OF SCL_3^+ IN SOLID COMPOUNDS (cm^{-1})

ASSIGNMENT	$\text{SCL}_3^+ \text{AlCl}_4^-$ 14	$\text{SCL}_3^+ \text{SbCl}_6^-$ 41	$\text{SCL}_3^+ \text{SO}_3 \text{Cl}^-$ 28	SCL_4 41	JAILLARD'S 23 COMPOUND
	SOLID	MELT			
$\nu_1 \text{ A}_1$	494	504	509	449	482
$\nu_3 \text{ E}$	516 530	522	519 526	471	493 508
$\nu_2 \text{ A}_1$	271	278	282	281	274
$\nu_4 \text{ E}$	206	210	221 228	?	209

TABLE 5.3

SCl_3^+ RAMAN SHIFTS IN FORM 1 AND FORM 2 $\text{SCL}_3^+\text{ICl}_4^-$ (cm^{-1})

C_{3v} modes	ν_1 A ₁	ν_3 A ₁	ν_2^E	ν_4^E
FORM 1 295 K	485	279*	498, 512	212, 220
77 K	486	278	499, 515	212, 223
FORM 2 295 K	482	282*	496, 510	205, 218
77 K	483	283*	495, 511	204, 218

* modes here are accidentally coincident with I-Cl stretching modes.

The remaining Raman shifts must therefore originate from ICl_4^- . The effect of a strong low symmetry electric field at ICl_4^- sites will have a much more pronounced effect since the rule of mutual exclusion may be relaxed. Thus instead of observing three Raman fundamentals from a D_{4h} ICl_4^- ion,¹⁹ in the limiting case, with no correlation coupling, a maximum of nine normal modes can be accounted for. Four of these may be approximately described as stretching modes and the remaining five as deformations. Raman shifts ascribed to ICl_4^- in both forms are presented in table 5.4. These are the first reported examples of vibrational spectra for ICl_4^- for which removal of the centre of symmetry must be considered. The limited vibrational data reported for other ICl_4^- compounds^{53,33} are consistent with retention of the inversion centre. The most detailed investigation³⁴ of solid Cs ICl_4 detected factor group splittings at high resolution, but because both the site symmetry of ICl_4^- , C_{2h} , and the unit cell group, D_{2h} , are centrosymmetric, the Raman spectrum at low resolution might otherwise be interpreted in terms of D_{4h} point group symmetry. The two Raman active I-Cl stretching modes in this and other salts are observed at ca. 260 and 280 cm^{-1} . In form 2 $\text{SCl}_3^+ \text{ICl}_4^-$, two strong I-Cl stretching modes are similarly observed at these frequencies, but in form 1 $\text{SCl}_3^+ \text{ICl}_4^-$ the two strongest I-Cl stretching modes are shifted to 282 and 296 cm^{-1} . Hiraishi and Shimanouchi³¹ demonstrated mathematically that in complexes where considerable cation-anion interaction is to be expected e.g. K_2PtCl_4 and K_2PtCl_6 , several of the normal modes of vibration of the anion would be drastically raised above the free ion values. They considered that stretching modes would not be significantly affected but that deformation modes could well shift by as much as 50 cm^{-1} . In both form 1 and form 2 $\text{SCl}_3^+ \text{ICl}_4^-$ the strongest deformation mode is located at a

TABLE 5.4

ICl_4^- RAMAN SHIFTS IN FORM 1 AND FORM 2 $\text{SCl}_3^+\text{ICl}_4^-$, $\text{KICl}_4\cdot\text{H}_2\text{O}$, $\text{NaICl}_4\cdot 2\text{H}_2\text{O}$ (cm^{-1})

FORM 1 $\text{SCl}_3^+\text{ICl}_4^-$		$\text{KICl}_4\cdot\text{H}_2\text{O}$		FORM 2 $\text{SCl}_3^+\text{ICl}_4^-$		$\text{NaICl}_4\cdot 2\text{H}_2\text{O}$		ASSIGNMENT
295 K	130 K	295 K	130 K	295 K	130 K	295 K	130 K	
100	106							
110	113		114	112	114		120	}
130	128	120	122	125	130		138	
142	146	142	135	143	144		142	}
150	152	151	146(sh)	154	155		153	
			152					
244	247	219	212	228	228		235	}
256	258	247	248		ca. 250		248	
279	282	271	271	260	260		268	
298	300	291	291	282	284		289	

I-Cl deformation

I-Cl stretching

higher frequency than observed in anhydrous KICl_4 , (at room temperature three Raman bands are observed at 286 (A_{1g}), 260 (B_{2g}) and 128 (B_{1g}) cm^{-1}). Since in form 1 $\text{SCl}_3^+ \text{ICl}_4^-$, the I-Cl stretching frequencies have also shifted to higher frequencies, it is possible that the anion-cation interaction is very much stronger than that considered in the model proposed by Hiraishi and Shimanouchi.

In order to confirm these inferences, ^{35}Cl NQR spectra were measured for both form 1 and form 2 $\text{SCl}_3^+ \text{ICl}_4^-$, and the observed frequencies are presented in table 5.5. Frequencies characteristic of both SCl_3^+ ¹³ and ICl_4^- ^{9,11} ions were observed in each case. A sample of form 2 for which the Raman spectrum showed partial conversion to form 1 also showed ^{35}Cl frequencies from the two different ICl_4^- ions. In form 1, the four ^{35}Cl NQR frequencies from ICl_4^- are spread over a wide range and resemble those reported ¹¹ for $\text{KICl}_4 \cdot \text{H}_2\text{O}$. In the latter compound, X-ray diffraction ¹⁶ has shown considerable distortion of the ICl_4^- ion. Of additional interest, the lowest ^{35}Cl resonance frequency from ICl_4^- in form 1 $\text{SCl}_3^+ \text{ICl}_4^-$ is found to have a positive temperature coefficient. Unlike other reported examples, no hydrogen bonding can be considered to account for this phenomenon but it is tentatively suggested that this arises because of a strong secondary interaction between the ions:

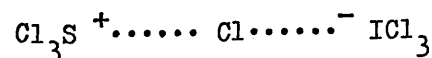


Fig. 5.3

Both NQR and Raman data are therefore consistent with distortion of ICl_4^- . In form 2 $\text{SCl}_3^+ \text{ICl}_4^-$, four ^{35}Cl frequencies from ICl_4^- are spread over a very much narrower range and to a certain extent resemble

TABLE 5.5

^{35}Cl NQR FREQUENCIES FOR FORMS 1 AND 2 $\text{SCL}_3^+\text{ICl}_4^-$, $\text{KICl}_4\cdot\text{H}_2\text{O}$ AND $\text{NaICl}_4\cdot 2\text{H}_2\text{O}$ (MHz)

	$\text{SCL}_3^+\text{ICl}_4^-$ FORM 1		$\text{KICl}_4\cdot\text{H}_2\text{O}$ 11		$\text{SCL}_3^+\text{ICl}_4^-$ FORM 2		$\text{NaICl}_4\cdot 2\text{H}_2\text{O}$ 49	
	296 K	77 K	296 K	77 K	296 K	77 K	296 K	77 K
ICl_4^-	15.30	14.86	16.85	16.95	19.80	20.07	20.574	20.010
	20.54	20.78	20.15	20.25	21.65	21.58	22.184	22.656
	25.57	25.90	24.85	24.90	22.90	23.53	22.896	23.251
mean	27.47	28.12	28.18	28.28	24.95	25.25	23.281	23.827
	22.22	22.42	22.51	22.60	22.33	22.58	22.234	
SCL_3^+	31.818	42.637			41.80	42.90		
	41.367	42.091			41.35	42.45		
	40.753	41.726			40.75	41.80		
mean	41.313							

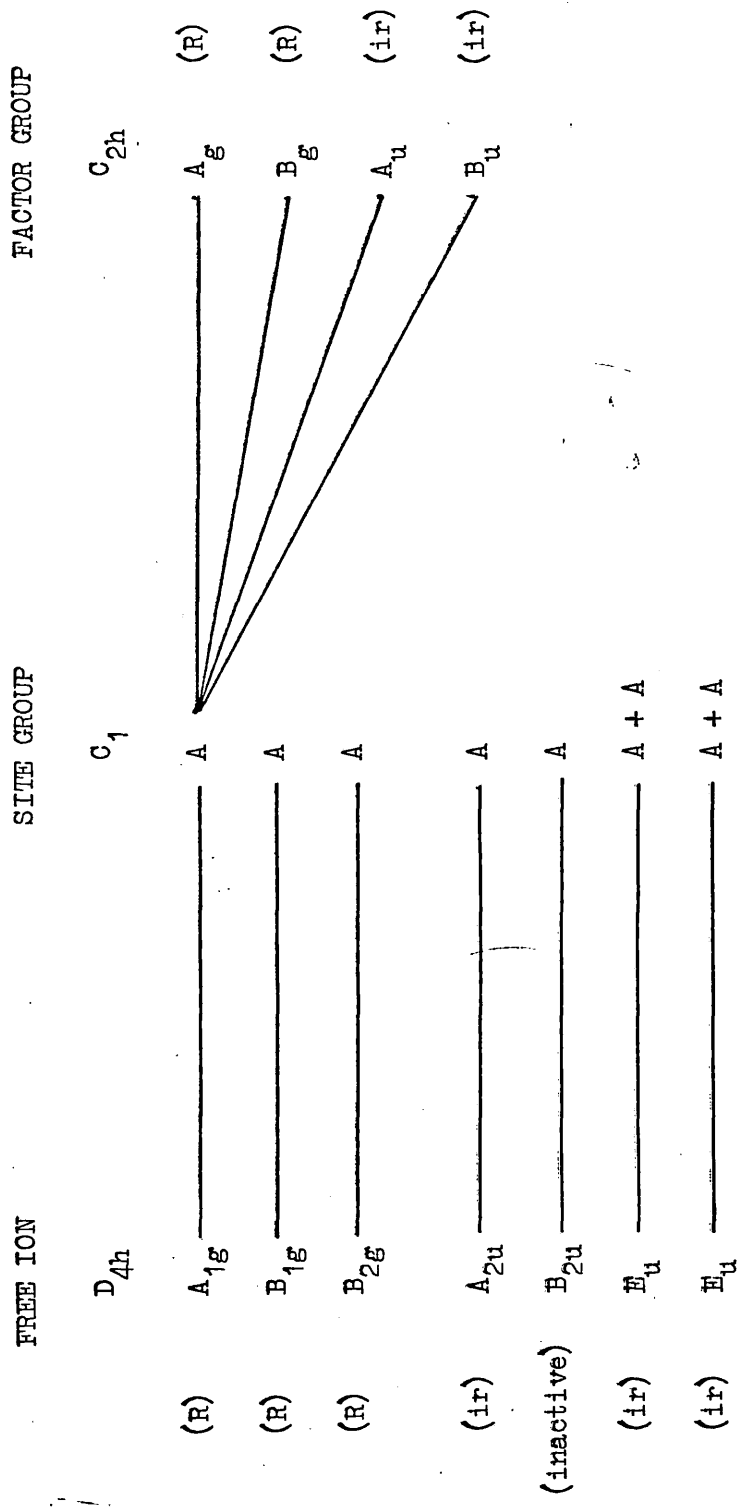
the frequencies observed⁵¹ in $\text{NaICl}_4 \cdot 2\text{H}_2\text{O}$. This resemblance, however, is much less marked than in the previous example of form 1 and $\text{KICl}_4 \cdot \text{H}_2\text{O}$. The frequency at 21 MHz also appears to have a positive temperature coefficient, but this is subject to further investigation because malfunction of the frequency markers did not permit accurate frequency measurements at 77 K.

Although crystal data^{16,4} and NQR frequencies^{11,51} have been reported for both $\text{NaICl}_4 \cdot 2\text{H}_2\text{O}$ and $\text{KICl}_4 \cdot \text{H}_2\text{O}$, no solid-state vibrational data are available. In view of the marked similarities between the ^{35}Cl NQR frequencies observed for these compounds and forms 2 and 1 respectively, Raman spectra were measured and are summarised in table 5.4. Using the published crystal data, a complete vibrational analysis may be attempted. $\text{KICl}_4 \cdot \text{H}_2\text{O}$ crystallises¹⁶ in a monoclinic space group, $\text{P}2_1/m$ (C_{2h}^2), with four molecules per unit cell. Consultation of tables¹⁸ shows that the possible site symmetries for this space group are:

$$\text{C}_{2h}^2 : 4\text{C}_i(2), \text{C}_s(2), n\text{C}_1(4).$$

H_2O , ICl_4^- and K^+ may be all assumed to occupy C_1 sites - these being the only sets of four symmetry-related sites. The complete analysis for ICl_4^- is presented in table 5.6. It follows that site group analysis predicts 9 modes, all of which are both i.r. and Raman active. Each mode may further split into two Raman active modes via correlation coupling. Consistent with the site symmetry approach nine Raman active ICl_4^- modes are observed at low resolution. In terms of site group analysis, fifteen lattice modes are predicted:- both ICl_4^- and H_2O give rise to three translatory and three rotatory modes while K^+

TABLE 5.6
 SOLID STATE VIBRATIONAL ANALYSIS FOR ICl_4^- IN $\text{KICl}_4 \cdot \text{H}_2\text{O}$



gives rise to only three translatory modes. These could not all be resolved in the measured spectrum however.

$\text{NaICl}_4 \cdot 2\text{H}_2\text{O}$ crystallises⁴ in an orthorhombic space group, Pnam (D_{2h}^{26}), with four molecules per unit cell. Consultation of tables¹⁸ shows that the possible site symmetries are

$$D_{2h}^{16} : 2C_i(4), C_s(4), nC_1(8)$$

H_2O molecules will occupy C_1 sites whereas ICl_4^- could occupy either C_s or C_i sites. The predicted vibrational spectrum for each possible case is summarised in table 5.7. At low temperature, two strong I-Cl stretching modes are observed in the Raman spectrum at 268 and 289 cm^{-1} , with two weak bands at 235 and 248 cm^{-1} . In addition, two or possibly three modes are resolved in the I-Cl deformation region. This is an indication, but not conclusive evidence for assigning ICl_4^- ions to C_s lattice sites. Clearly under high resolution, bands from impurities might also be detected. The Raman spectrum from a commercial sample of $\text{NaAuCl}_4 \cdot 2\text{H}_2\text{O}$ which is considered to be isomorphous⁵⁰ with $\text{NaICl}_4 \cdot 2\text{H}_2\text{O}$ shows four Au-Cl stretching modes and possibly five Au-Cl deformation modes at low temperature. This confirms that AuCl_4^- ions occupy C_s sites, and gives credence to the conclusions drawn from the Raman spectrum of $\text{NaICl}_4 \cdot 2\text{H}_2\text{O}$. Similarities with form 2 $\text{SCl}_3^+ \text{ICl}_4^-$ are apparent, but whether the two compounds are isostructural remains unknown.

The complementary infra-red data for these compounds were not easily obtained. Forms 1 and 2 $\text{SCl}_3^+ \text{ICl}_4^-$ could not be mounted into the interferometer sample compartment without undergoing extensive decomposition. An infra-red spectrum for form 1 was eventually obtained over the region 220-350 cm^{-1} using a conventional grating

TABLE 5.7

SOLID STATE VIBRATIONAL ANALYSIS FOR ICl_4^- IN $\text{NaICl}_4 \cdot 2\text{H}_2\text{O}$

FREE ION	SITE GROUP	FACTOR GROUP
D_{4h}	C_i	D_{2h}
(R) A_{1g}	A_g	A_g (R)
(R) B_{1g}	A_g	B_{1g} (R)
(R) B_{2g}	A_g	B_{2g} (R)
		B_{3g} (R)
(ir) A_{2u}	A_u	A_u (inactive)
(inactive) B_{2u}	A_u	B_{1u} (ir)
(ir) E_u	$A_u + A_u$	B_{2u} (ir)
(ir) E_u	$A_u + A_u$	B_{3u} (ir)

Hence 3 Raman modes which may split into 4 via correlation coupling.

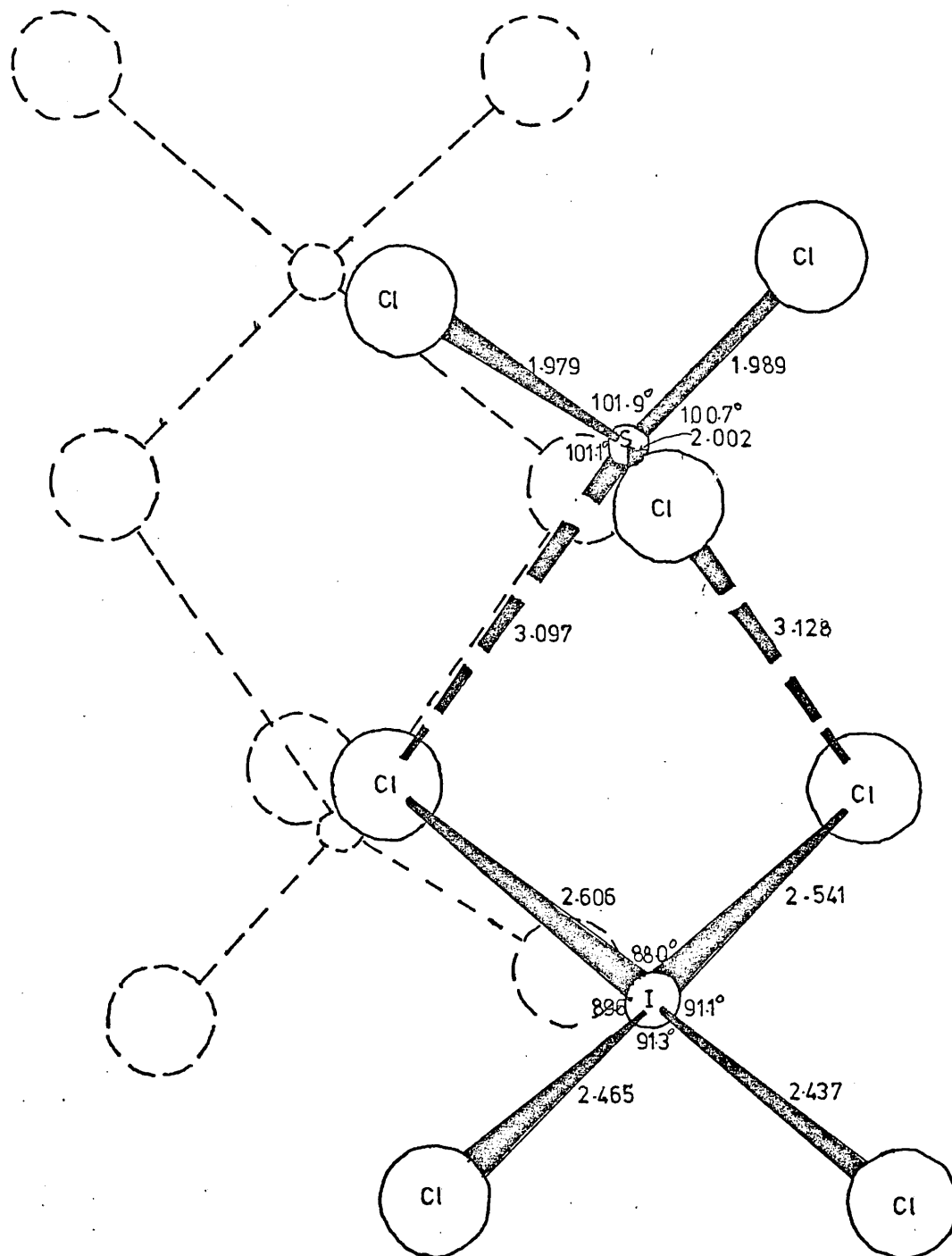
FREE ION	SITE GROUP	FACTOR GROUP
D_{4h}	C_s	D_{2h}
A_{1g}	A'	A_g
B_{1g}	A'	B_{1g}
B_{2g}	A''	B_{2g}
		B_{3g}
A_{2u}	A'	A_u
B_{2u}	A'	B_{1u}
E_u	$A' + A''$	B_{2u}
E_u	$A' + A''$	B_{3u}

Hence 9 Raman modes which may each split into 2 via correlation coupling.

spectrometer, with the crushed crystals mounted between RIGIDEX plates. Manipulation of the compound proved very cumbersome, but a reproducible, though very inferior spectrum was obtained showing coincident infra-red absorption frequencies for all the Raman shifts observed in the region 220-350 cm^{-1} . In addition weak broad bands at ca. 330 and 340 cm^{-1} arising from I_2Cl_6 ²² were observed. It proved impossible to obtain infra-red spectra from $\text{KICl}_4 \cdot \text{H}_2\text{O}$ or $\text{NaICl}_4 \cdot 2\text{H}_2\text{O}$. This may be attributed to the considerable energy absorption by the bound water molecules.

In order to establish whether distortion of ICl_4^- and the often isomorphous⁴⁸ AuCl_4^- could be observed in related compounds, an NQR and vibrational spectroscopic investigation of selected compounds was undertaken. Before describing the results obtained, it is relevant to present here the X-ray crystal structure for Form 1 $\text{SCl}_3^+\text{ICl}_4^-$ carried out at Birmingham University¹⁵ after the spectroscopic investigations described in the subsequent sections had been carried out. The conclusions derived from NQR and vibrational spectroscopy were unequivocally confirmed. The similarity between ICl_4^- ions in form I $\text{SCl}_3^+\text{ICl}_4^-$ and $\text{KICl}_4 \cdot \text{H}_2\text{O}$ is apparent (fig. 5.4 and fig. 5.5). Both crystals have the same unit cell group, C_{2h} , with ICl_4^- ions located in C_1 sites. The similarities between the Raman shifts and ³⁵Cl NQR frequencies are therefore not unexpected. A complete vibrational analysis for form 1 $\text{SCl}_3^+\text{ICl}_4^-$, which crystallises¹⁵ with the $\text{P2}_1/\text{C}$ (C_{2h}^5) space group with four molecules per unit cell, is presented in table 5.8. Both S and I are located in C_1 sites. At the low resolution employed, the Raman spectrum (fig. 5.2) is adequately explained in terms of site group analysis - six SCl_3^+ and nine ICl_4^- modes are observed with nearly coincident SCl_3^+ and ICl_4^- modes at 282 cm^{-1} being

Fig 5-4 The crystal structure of Form 1 $\text{SCl}_3^+ \text{ICl}_4^-$



all bond distances in Å

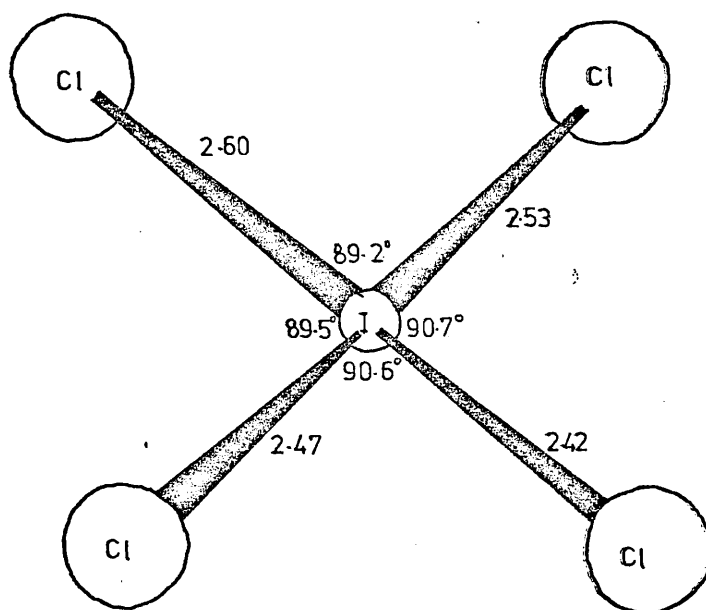
Fig 5-5 The structure of ICl_4^- in $\text{KICl}_4 \cdot \text{H}_2\text{O}$ 

TABLE 5.8

SOLID STATE VIBRATIONAL ANALYSIS FOR FORM 1 $\text{SCl}_3^+ \text{ICl}_4^-$ (i) SCl_3^+

FREE ION	SITE GROUP	FACTOR GROUP
C_{3v}	C_1	C_{2h}
A_1	A	A_g
A_1	A	B_g
E	A + A	A_u
E	A + A	B_u

(ii) ICl_4^-

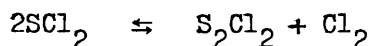
FREE ION	SITE GROUP	FACTOR GROUP
D_{4h}	C_1	C_{2h}
A_{1g}	A	A_g
B_{1g}	A	B_g
B_{2g}	A	A_u
A_{2u}	A	B_u
B_{2u}	A	
E_u	A + A	
E_u	A + A	

(iii) EXTERNAL MODES

SITE GROUP	FACTOR GROUP
C_1	C_{2h}
4SCl_3^+ $R_x R_y R_z$ A	A_g
$T_x T_y T_z$ A	B_g
4ICl_4^- $R_x R_y R_z$ A	A_u
$T_x T_y T_z$ A	B_u

resolved at low temperature. Twelve Raman active external modes are predicted, but considerable overlap at this resolution precludes a complete identification.

This work disproves a claim for the novel species SICl_3 and presents the first vibrational spectroscopic data for a distorted ICl_4^- ion. All investigations have failed to identify the compound of stoichiometry $\text{SICl}_4(\text{ICl}_3)_2$ described by Ruff.⁴⁷ Using the reported method of preparation, the only solid isolated was form $2 \text{SICl}_3^+ \text{ICl}_4^-$. It seems somewhat strange that a stoichiometry of 1:2 for S:I should be derived under conditions employing a large excess of SICl_2 . It is conceivable, however, that Ruff's compound consisted of form $2 \text{SICl}_3^+ \text{ICl}_4^-$ mixed with an equimolar amount of unreacted ICl_3 . No complex anion such as I_2Cl_7^- has ever been reported, and even if such a species existed, treatment with an excess of SICl_2 would undoubtedly result in conversion to form $2 \text{SICl}_3^+ \text{ICl}_4^-$. Nevertheless, analytical data consistent with this coprecipitating with an equimolar amount of ICl_3 are difficult to explain. One possible explanation is as follows. The slight dissociation of SICl_2 ¹⁰ viz:



will result in conversion of ICl_3 to $\text{SICl}_3^+ \text{ICl}_4^-$ with concomitant formation of S_2Cl_2 . Beyond a critical point, no more chlorine is available for reaction and excess ICl_3 remains in solution. Since $\text{KICl}_4 \cdot \text{H}_2\text{O}$ is a known stable hydrate, then it is possible that $\text{SICl}_3^+ \text{ICl}_4^- \cdot \text{ICl}_3$ is also a definite compound existing under certain conditions. Thus ICl_3 may be trapped in the crystal lattice weakly interacting with either ICl_4^- or SICl_3^+ . Undoubtedly such a compound

would be fairly unstable but further preparative work would be clearly of interest to ascertain whether this and other compounds could be isolated.

The origin of this distortion in ICl_4^- compounds is worthy of further comment. In $\text{KICl}_4 \cdot \text{H}_2\text{O}$, a force field calculation¹¹ has indicated that the distortion arises from the strong low symmetry field created at ICl_4^- sites by all the surrounding ions and molecules. The contribution of water molecules to the field was estimated to be significant though not the predominating influence. Consistent with this argument, the lowest ^{35}Cl NQR frequency exhibits a normal negative temperature coefficient. Thus, the crystal structure arising when KICl_4 forms a monohydrate must be significantly different from anhydrous KICl_4 for which NQR⁹ and vibrational spectroscopy indicate an unperturbed D_{4h} ion. In form 1 $\text{SCl}_3^+ \text{ICl}_4^-$, the low symmetry field created at ICl_4^- sites may again be considered to account for the distortion. However, the positive temperature coefficient of the lowest ^{35}Cl NQR frequency for ICl_4^- is indicative of a strong secondary interaction between ICl_4^- and SCl_3^+ . The two longer I-Cl bond lengths closest to SCl_3^+ (fig. 5.5) are consistent with this argument. In form 2 $\text{SCl}_3^+ \text{ICl}_4^-$, a weaker interaction is predicted since the NQR frequencies are spread over a narrower range and no apparent positive temperature coefficient of the lowest NQR line is observed. Thus in metastable $\text{SCl}_3^+ \text{ICl}_4^-$ the orientations and positions of ICl_4^- and SCl_3^+ ions in the crystal lattice are not favourable for a strong secondary interaction. The crystal lattice, therefore, slowly reverts to form 1 $\text{SCl}_3^+ \text{ICl}_4^-$ where SCl_3^+ and ICl_4^- ions are in closer proximity. In distinction from form 2 $\text{SCl}_3^+ \text{ICl}_4^-$, the lowest ^{35}Cl NQR resonance

frequency in $\text{NaICl}_4 \cdot 2\text{H}_2\text{O}$ does exhibit an anomalous positive temperature coefficient which has been attributed to strong hydrogen bonding. All attempts to prepare the anhydrous salt were unsuccessful. It may be, therefore, that if form $2 \text{SCl}_3^+ \text{ICl}_4^-$ possesses a related structure, the compound may be stabilised by trapping a species capable of strong interaction with ICl_4^- ions in the C_1 lattice sites. It is purely speculation that ICl_3 could achieve this by formation of $\text{SCl}_3^+ \text{ICl}_4^-$. ICl_3 (Ruff's compound).

Discussion so far has attempted to correlate the NQR spectroscopic data with conclusions reached from vibrational spectroscopy. With reference to the distortion of square planar ions, numerous points may be raised at this stage:

- (i) To what extent are the ^{35}Cl NQR frequencies related to the strength and the symmetry of a strong low symmetry field at a lattice site?
- (ii) For a given species ICl_4^- , is it possible to predict whether formally inactive Raman bands will be observed from the interval between the highest and lowest ^{35}Cl NQR frequencies?
- (iii) What is the overall effect of secondary interactions upon the NQR spectrum?

Discussion of these points will be reserved until further data for analogous ICl_4^- and AuCl_4^- compounds, in which distortions might arise, have been presented. All ICl_4^- compounds discussed so far may be considered essentially in terms of free ions. Secondary bonding interactions have therefore resulted in only small covalent contributions to the overall electrostatic attraction between the ions. In the following sections, the effects of changing the cation upon the

vibrational and NQR spectra of ICl_4^- and AuCl_4^- ions are presented and discussed.

5.3 ICl_4^- SALTS OF $[\text{SMe}_n\text{Cl}_{3-n}]^+$ CATIONS

Two modifications of $\text{SCl}_3^+\text{ICl}_4^-$ have already been described. The effect of methyl substitution in the cation was investigated with the intention of ascertaining to what extent distortion is dependent upon secondary bonding. Clearly replacing chlorine atoms by methyl groups will result in a larger cation which will not necessarily adopt the same crystal structure as $\text{SCl}_3^+\text{ICl}_4^-$. Thus, it is not possible to specify whether methyl substitution is solely responsible for the observed effects, in the absence of X-ray crystal data.

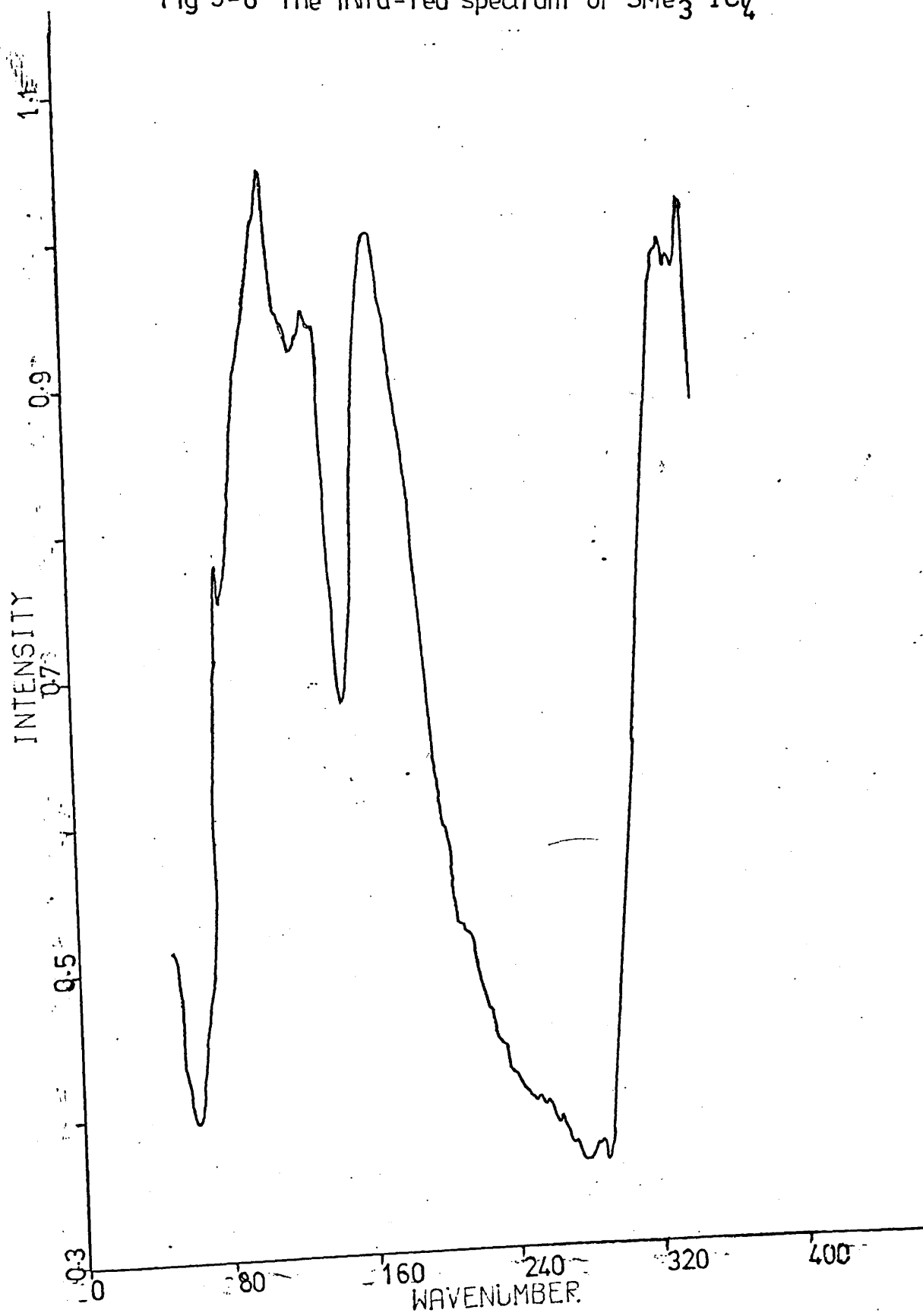
$\text{SMe}_3^+\text{ICl}_4^-$ has been reported,⁴⁶ but no vibrational data are available. The Raman and far infra-red spectra are presented in Table 5.9 and fig. 5.6 respectively, and clearly an interpretation in terms of D_{4h} point group symmetry for ICl_4^- is possible. The absence of a secondary interaction and a strong low symmetry electric field at ICl_4^- crystal sites can therefore be inferred. This is as might be expected since methyl groups, being less electronegative than chlorine atoms, will tend to push negative charge on to sulphur (inductive effect) which will tend to reduce any interaction with ICl_4^- . Unfortunately, NQR signals could not be observed from this compound at ambient or liquid nitrogen temperatures thus precluding confirmation of a D_{4h} ion.

MeSCl_2^+ and Me_2SCl^+ salts of SbCl_6^- have been reported⁵⁶ and the solid state Raman spectrum⁵² for $\text{SMeCl}_2^+\text{SbCl}_6^-$ has been measured. Although solid state splittings of formally active Raman modes were apparent, there was no evidence to suggest that the rule of mutual

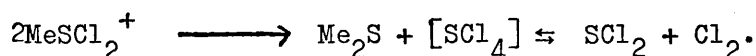
TABLE 5.9

RAMAN SHIFTS FOR $\text{SMeCl}_2^+\text{ICl}_4^-$ AND $\text{SMe}_3^+\text{ICl}_4^-$ (cm^{-1})

$\text{SMeCl}_2^+\text{ICl}_4^-$ T = 130 K	SMeCl_2^+ in $\text{SMeCl}_2^+\text{SbCl}_6^-$ 52	ASSIGNMENT	$\text{SMe}_3^+\text{ICl}_4^-$
110 (w)		?	
125 (w)		ICl_4^- def.	
132 (w)		ICl_4^- def.	135 (w) $\sqrt{2}^B_1g^-\text{ICl}_4^-$
145 (w)		ICl_4^- def.	
150 (w)		ICl_4^- def.	
215 (w, br)	213 (w)	SbCl_2^+ bend A'	
230 (w)		ICl_4^- stretch	
258 (w-m)		ICl_4^- stretch	262 (s) $\sqrt{4}^B_2g^-\text{ICl}_4^-$
270 (should)		ICl_4^- stretch	
275 (s)		ICl_4^- stretch	
295 (should)		ICl_4^- stretch	285 (vs) $\sqrt{1}^A_1g^-\text{ICl}_4^-$
302 (vs)			
482 (w)	462 (w)	CS Cl bend?	
499 (m-s)	513 (m-s)	SbCl_2^+ sym. stretch	
518 (m-w)	535 (m-w)	SbCl_2^+ asym. stretch	
676 (vw)	666 (w)	S-C stretch	

Fig 5-6 The infra-red spectrum of $\text{SMe}_3^+ \text{ICl}_4^-$ 

exclusion had been lifted. This can be regarded as an indication that the site group is also centrosymmetric. $\text{MeSCl}_2^+\text{ICl}_4^-$, a novel compound, was analogously prepared and the Raman spectrum recorded (table 5.9). Although the I-Cl stretching modes are noticeably broader, certain similarities with $\text{SCl}_3^+\text{ICl}_4^-$ are nevertheless apparent. In particular, at low temperature, formally inactive Raman modes at 250 and 260 cm^{-1} are observed. This strongly suggests that ICl_4^- ions occupy low symmetry sites and that there is a secondary interaction between anion and cation. However, $\text{MeSCl}_2^+\text{ICl}_4^-$ is a very unstable compound by comparison with $\text{SCl}_3^+\text{ICl}_4^-$. It readily liquefies even in a sealed tube under chlorine soon after preparation, and crystals are not reformed upon cooling. Decomposition may be considered to occur disproportionately



One of the products of decomposition is SCl_2 , but identification of the other products was not undertaken. Partial decomposition may account for the broad I-Cl stretching modes, but the absence of SCl_3^+ bands precludes contamination from this species. For these reasons, infra-red and NQR spectra were not obtained, which necessarily restricts further discussion. However, it may be tentatively suggested that replacing one chlorine of SCl_3^+ by methyl in $\text{SCl}_3^+\text{ICl}_4^-$ does not significantly reduce the secondary interaction, which may assist in the breakdown of SMCl_2^+ .

5.4 TRICHLOROCHALCOGEN CATIONS WITH AuCl_4^-

Both SeCl_4 and TeCl_4 have been reported to form complexes with metallic and non-metallic species^{27,28} - eg SO_3 , SbCl_5 , PCl_5 .

Vibrational data have been reported for several compounds which have been

characterised as ionic involving TeCl_3^+ and SeCl_3^+ cations. Thus characteristic vibrational frequencies for SeCl_3^+ and TeCl_3^+ may be used to distinguish these species from the SeCl_6^{2-} and TeCl_6^{2-} anions^{1,19} which are also known. It was originally believed¹⁰ that both TeCl_4 and SeCl_4 consisted of $\text{MCl}_3^+\text{Cl}^-$ ions in the solid state, but recent X-ray diffraction⁸ studies for TeCl_4 have indicated this to be incorrect. In fact the solid state structures consist of distinct tetramers of MCl_3^+ units linked by bridging chlorines. Solid state Raman data⁴⁵ have recently been interpreted using this model and factor group analysis.

$\text{MCl}_3^+\text{ICl}_4^-$ (M = Se, Te) have not been reported, but an interesting situation arises as to whether interaction of MCl_4^+ with I_2Cl_6 would produce this species or a cationic iodochloro species $[\text{ICl}_2^+]_2\text{MCl}_6^{2-}$. ICl_2^+ salts have been reported⁵⁵ and the cation has been characterised by both NQR¹⁷ and vibrational spectroscopy.⁵⁸ The former technique readily distinguishes this species from ICl_4^- because the cation resonances are observed at higher frequency (≈ 39 MHz). Since no sulphur analogue SCl_6^{2-} has been reported, this situation did not arise when considering Jaillard's compound. Nevertheless, inspection of the X-ray crystal structure (fig. 5.4) shows that the two longest I-Cl bonds are closest to SCl_3^+ . This may be indicative of a very small contribution from $\text{ICl}_2^+\text{SCl}_5^-$. The anion SCl_5^- has not been isolated although there is some evidence⁵ for SeCl_5^- and TeCl_5^- anions. Thus a third possibility for reaction product of MCl_4 (M = Se, Te) with I_2Cl_6 is $\text{ICl}_2^+\text{MCl}_5^-$, which should also be considered.

In fact, identification of reaction products proved to be very simple because all attempts to react I_2Cl_6 with MCl_4 were unsuccessful. A variation on Jaillard's preparation was not possible because both SeCl_4

and TeCl_4 melt above 100°C , and chlorination of a finely ground mixture of Se/I_2 or Te/I_2 merely resulted in a mixture of the solid chlorides. Interaction between I_2Cl_6 and MCl_4 in solution was also unsuccessful, the only solid product isolated being MCl_4 . SeCl_4 is a very insoluble⁶ compound and could not be retained in solution in AsCl_3 or POCl_3 after addition of I_2Cl_6 . Heating a solution of I_2Cl_6 in AsCl_3 with a suspension of SeCl_4 while passing a current of chlorine was equally unsuccessful. This method has been employed in the preparation of other SeCl_3^+ salts and has succeeded when the slight solubility of SeCl_4 is greater than that of the ionic compound formed.⁵ Thus SeCl_4 is slowly dissolved and precipitated as an ionic SeCl_3^+ salt. In the case of SeCl_4 and I_2Cl_6 , it is possible that a weak ICl_3 complex may be formed with AsCl_3 and POCl_3 thereby precluding reaction with dissolved SeCl_4 . TeCl_4 is markedly more soluble than SeCl_4 , but the only product again precipitated from solution was TeCl_4 . The subsequent work carried out with AuCl_4^- salts strongly indicates that the synthesis of $\text{TeCl}_3^+\text{ICl}_4^-$ is required in order to assist with the NQR frequency assignments for $\text{TeCl}_3^+\text{AuCl}_4^-$. As a suggestion for further work, the solid state high temperature reaction between I_2Cl_6 and TeCl_4 in a sealed tube under pressure might be attempted.

Since all attempts to investigate ICl_4^- salts of other chlorochalcogen cations proved unsuccessful, attention was given to AuCl_4^- salts, which are often found to be isomorphous⁴⁹ with the corresponding ICl_4^- salts. Both species are square planar ions and linear AuCl_2^- and ICl_2^- are similarly known. The preparations of $\text{SCl}_4\cdot\text{AuCl}_3$ and $\text{SeCl}_4\cdot\text{AuCl}_3$ have been reported,⁴⁰ but surprisingly no structural investigations have been carried out. The initial preparative work was concerned with $\text{SCl}_4\cdot\text{AuCl}_3$, in order to ascertain whether two crystal modifications, corresponding to forms 1 and 2 $\text{SCl}_3^+\text{ICl}_4^-$ could be isolated.

$\text{SCl}_4 \cdot \text{AuCl}_3$ was originally prepared⁴⁰ in 1886 by heating metallic gold with SCl_2 . A modified procedure was used starting with SCl_2 and Au_2Cl_6 and a bright yellow powder was isolated. Unlike the ICl_4^- analogue, the gold compound is non-volatile showing no tendency to lose SCl_2 or chlorine at ambient temperature. It may therefore be manipulated in a dry box under nitrogen and infra-red spectra were very much easier to obtain. The measured Raman and infra-red spectra are presented in table 5.10, fig. 5.7 and fig. 5.8. Only one modification could be isolated which indicates that no analogue for the metastable modification of $\text{SCl}_3^+ \text{ICl}_4^-$ exists. Inspection of fig. 5.7 shows that six Raman shifts arising from SCl_3^+ are observed at similar frequencies to those in form 1 $\text{SCl}_3^+ \text{ICl}_4^-$. As was discussed previously, the lowering of S-Cl stretching modes may be indicative of anion-cation secondary interaction, and the three modes at 482, 498 and 512 cm^{-1} in the gold complex compared with modes⁴¹ at 501, 524 and 535 cm^{-1} in $\text{SCl}_3^+ \text{SbCl}_6^-$ are again indicative of this. In the gold compound, the $\nu_3 \text{SCl}_3^+$ mode at 270 cm^{-1} is not masked by anion stretching modes as in form 1 $\text{SCl}_3^+ \text{ICl}_4^-$. The remaining bands in the spectrum can be assigned to lattice modes and AuCl_4^- . Eight Raman bands are observed above 100 cm^{-1} which may be ascribed to AuCl_4^- . Comparison of table 5.10 with table 4.1, which gives the infra-red and Raman modes for KAuCl_4 in aqueous solution shows marked similarities. In this compound, formally active Raman Au-Cl stretching modes have not shifted to higher frequency and formally inactive Au-Cl stretching modes have not shifted to lower frequency, which is observed for the corresponding I-Cl modes in form 1 $\text{SCl}_3^+ \text{ICl}_4^-$. In fact, for a D_{4h} AuCl_4^- species (table 4.1), the infra-red active Au-Cl stretching mode occurs at higher frequency

TABLE 5.10
 VIBRATIONAL SPECTRA FOR $MCl_3^+AuCl_4^-$ (M = S, Se, Te)

$SCl_3^+AuCl_4^-$			$SeCl_3^+AuCl_4^-$			$TeCl_3^+AuCl_4^-$		
RAMAN 130 K	ASSIGNMENT	i.r. 77 K	RAMAN 130 K	ASSIGNMENT	i.r. 77 K	RAMAN 130 K	ASSIGNMENT	i.r. 77 K
95	$AuCl_4^-$ def. ?	97	96	$AuCl_4^-$ def. ?	92			120
120	$AuCl_4^-$ def.	124	110? 128	$AuCl_4^-$ def.	126?			138
146	$AuCl_4^-$ def.	144	147	$AuCl_4^-$ def.	146			144
174	$AuCl_4^-$ def.	173	164	$AuCl_4^-$ def.	165	152 } 158 }	$\nu_4^E TeCl_3^+$	160
186	$AuCl_4^-$ def.	188	172	$AuCl_4^-$ def.	176	176	$\nu_2^{A_1} TeCl_3^+$	180
206 } 218 }	$\nu_4^E SCl_3^+$	{ 206 219	186 } 194 } 205 }	$SeCl_3^+ A_1 + E$	186 197	189	$\nu_2^{B_{1g}} AuCl_4^-$	188
270	$\nu_2^{A_1} SCl_3^+$	269						204?
322	$AuCl_4^-$ stretch	320	314 } 318 }	$AuCl_4^-$ stretch		332	$\nu_4^{B_{2g}} AuCl_4^-$	
343	$AuCl_4^-$ stretch	340	388 } 341 }	$AuCl_4^-$ stretch		357	$\nu_1^{A_{1g}} AuCl_4^-$	
354	$AuCl_4^-$ stretch	352 (br)	352 }	$AuCl_4^-$ stretch		368	$\nu_3^E TeCl_3^+$	-
360	$AuCl_4^-$ stretch		367 } 360 }	$AuCl_4^-$ stretch F.G. splitting of split E				
483 } 497 } 512 }	$\nu_1^{A_1} SCl_3^+$ $\nu_3^E SCl_3^+$	- - -	384 } 390 } 400 }	$SeCl_3^+ A_1 + E$		286	$\nu_1^{A_1} TeCl_3^+$	-

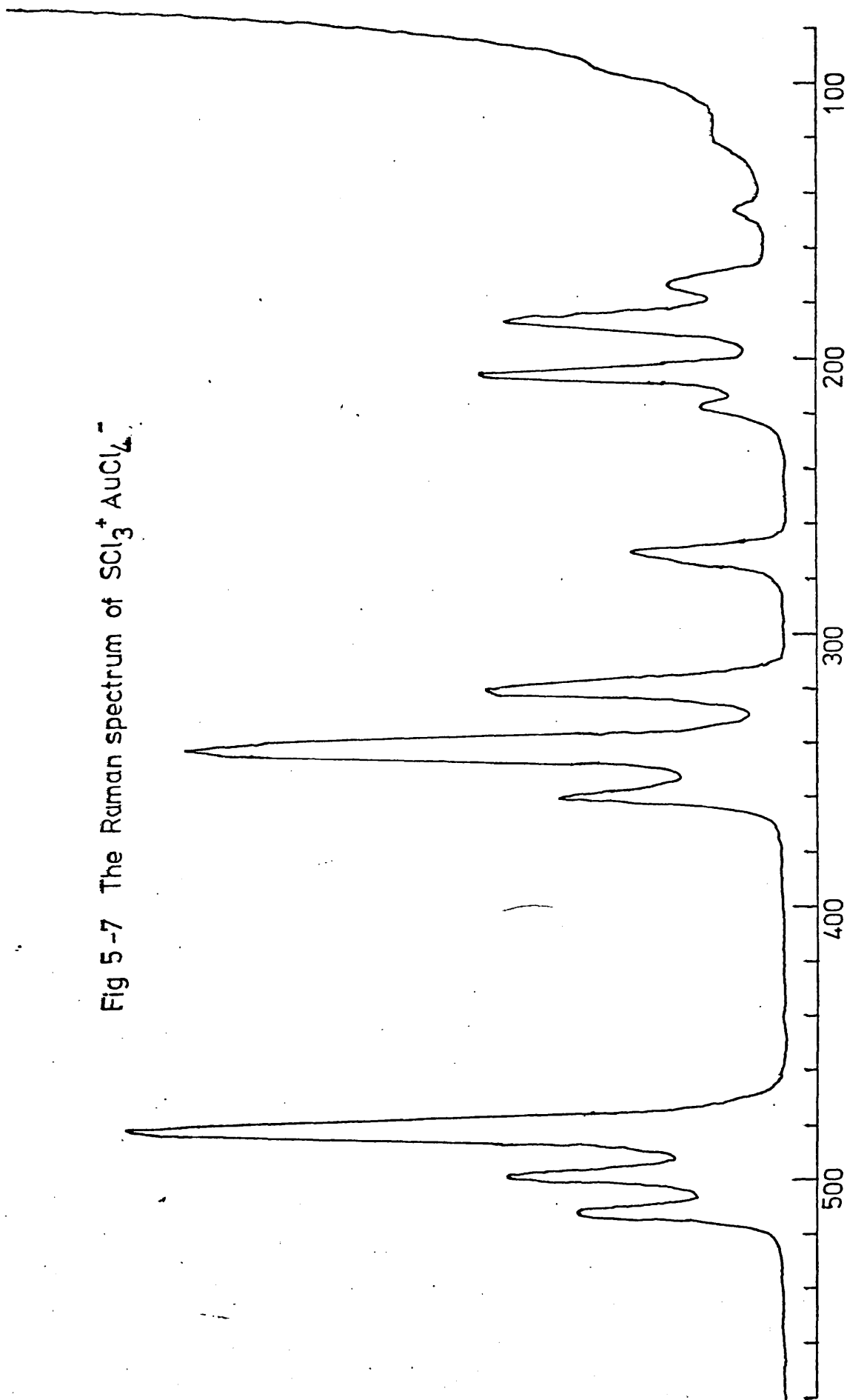
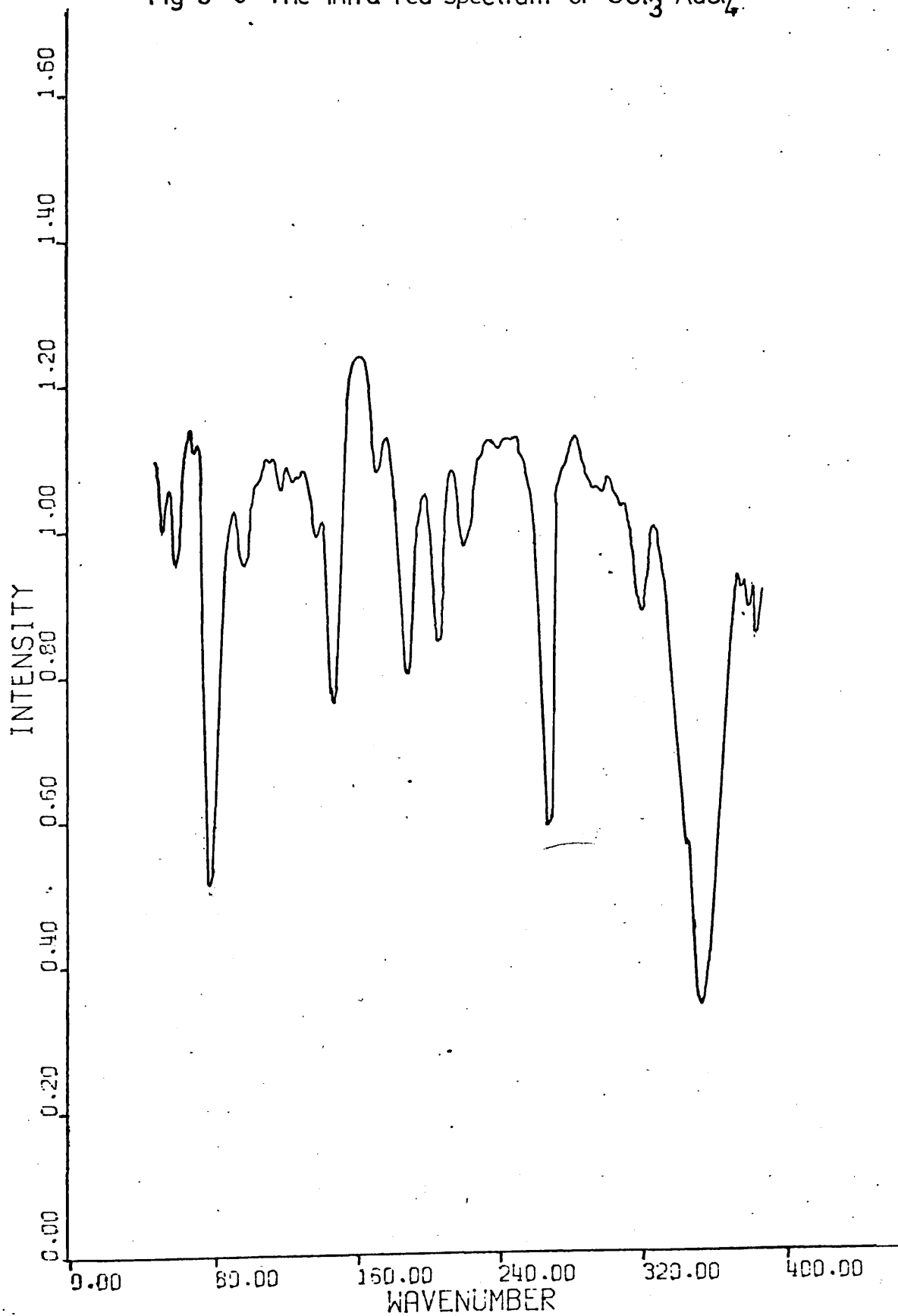
Fig 5 -7 The Raman spectrum of $\text{SCl}_3^+ \text{AuCl}_4^-$ 

Fig 5-8 The infra-red spectrum of $\text{SCl}_3^+ \text{AuCl}_4^-$ 

than the two Raman active modes, whereas for a D_{4h} ICl_4^- species the infra-red active I-Cl stretching mode is at lower frequency than both Raman active modes. From these observations, two points may be considered:

(i) Distortion of $AuCl_4^-$ in $SbCl_3^+AuCl_4^-$ is apparently less than the distortion of ICl_4^- in form 1 $SbCl_3^+ICl_4^-$, so that $AuCl_4^-$ modes are not significantly perturbed.

(ii) The comparatively heavier central metal atom in $AuCl_4^-$ is probably the dominating influence upon the stretching frequencies and a comparable distortion to that observed in $SbCl_3^+ICl_4^-$ may require a very much stronger secondary interaction.

The infra-red and Raman spectra for $SbCl_3^+AuCl_4^-$ show numerous broad bands below 100 cm^{-1} . A weak band is observed at 97 cm^{-1} in the infra-red and at 95 cm^{-1} in the Raman spectrum. This may be attributed to the $\sqrt{5} B_{2u}$ (formally inactive in both i.r. and Raman) modes based upon D_{4h} symmetry, which would be expected to occur at ca. 100 cm^{-1} . The remaining bands below 100 cm^{-1} must be attributed to lattice modes. If the compound is isostructural with form 1 $SbCl_3^+ICl_4^-$, then 12 lattice modes would be expected. The resolution is very poor even at low temperatures, and unlike the examples of $NOAlCl_4^2$ and $NOGaCl_4^3$ mentioned in chapter 4, it is not possible to infer whether the two compounds are isostructural.

The ^{35}Cl NQR spectrum is presented in table 5.11 and four lines arising from $AuCl_4^-$ are observed spread over 5 MHz. This frequency interval is significantly smaller than that observed for form 1 $SbCl_3^+ICl_4^-$ (≈ 13 MHz) but is significantly wider than observed in other $AuCl_4^-$ salts (table 5.12). In addition, the lowest frequency shows a normal negative temperature coefficient which would again seem

TABLE 5.11
 (a) ^{35}Cl NQR FREQUENCIES FOR $\text{MCl}_3^+\text{AuCl}_4^-$ (M = S, Se)

	$\text{MCl}_3^+\text{AuCl}_4^-$		$\text{SeCl}_3^+\text{AuCl}_4^-$	
	295 K	193 K	295 K	77 K
MCl_3^+				
^{35}Cl	not observed	not observed	37.230	37.500
mean			42.76 (42.743)	37.700
^{37}Cl	"	"	42.335 (42.321)	37.475
mean			41.305 (41.295)	37.020
			41.80 (42.120)	37.398
			32.53 ?	29.725
			29.34	39.55
			28.99	29.303
			28.56	29.19
			28.96	29.488
AuCl_4^-				
^{35}Cl	29.87 (29.752)	20.225	31.825	32.250
mean	27.577 (27.578)	27.775	26.770	26.860
	27.36 (27.370)	27.64	26.480	26.750
	25.217 (25.185)	25.217	23.825	24.030
	27.493 (27.471)	27.714	27.225	27.643
			27.921 (27.933)	
			30.60 (30.613)	
			27.955 (27.957)	
			27.912 (27.917)	
			25.214 (25.247)	

Values in parentheses from ref. 20.

TABLE 5.11 (continued)

(b) NQR FREQUENCIES FOR $\text{TeCl}_3^+\text{AuCl}_4^-$

$\nu^{35}\text{Cl}$	$\nu^{37}\text{Cl}$	$\frac{\nu^{35}\text{Cl}}{\nu^{37}\text{Cl}}$ (theoretical 1.2688)
T = 295 K		
30.987	24.42	1.2689
29.255	23.045	1.2694
28.902	22.782	1.2686
28.79	22.685	1.2691
27.473	21.64	1.2695
26.65	21.01	1.2684
25.445	20.07	1.2678
T = 193 K		
31.36	24.726	1.2683
29.545	23.29	1.2686
29.226	23.04	1.2685
29.073	22.912	1.2688
27.66	21.79	1.2694
26.873	21.178	1.2689
25.675	20.235	1.2688
T = 77 K		
31.675	24.97	1.2685
29.80	23.499	1.2681
28.508	23.265	1.2683
29.322	23.12	1.2683
27.808	21.94	1.2675
27.04	21.335	1.2674
25.878	not investigated	-

TABLE 5.12

 ^{35}Cl NQR FREQUENCIES FOR AuCl_4^- SALTS (MHz) 50

	$\text{NaAuCl}_4 \cdot 2\text{H}_2\text{O}$	KAuCl_4	$\text{KAuCl}_4 \cdot 2\text{H}_2\text{O}$	CsAuCl_4	NH_4AuCl_4	$\text{NH}_4\text{AuCl}_4 \cdot 2/3 \text{H}_2\text{O}$
T = 298 K	28.770	17.573	27.686	27.885	27.809	27.627
	28.368	27.545	26.967	27.098	26.993	27.431
	27.400	27.231				26.977
	25.685	27.088				26.617
MEAN	27.556	27.359	27.327	27.492	27.401	27.309
T = 77 K	29.466	27.214	28.183	28.419	28.130	-
	28.867	27.907	27.137	27.800	27.300	
	27.998	27.598				
	25.356	27.320				
MEAN	27.922	27.760	27.660	28.110	27.715	

to indicate that any secondary bonding between SCl_3^+ and AuCl_4^- is very much weaker than the secondary bonding between SCl_3^+ and ICl_4^- in form $1 \text{ SCl}_3^+ \text{ ICl}_4^-$. Unlike the ICl_4^- complexes, cation frequencies were only observed at low temperatures. Subsequent to obtaining these measurements, Russian workers²⁰ published details of the ^{35}Cl NQR spectrum of $\text{SCl}_3^+ \text{ AuCl}_4^-$. Their results (table 5.11) agree very well with those from this study. However, the interpretation given was made in the absence of any vibrational data. Briefly, they considered the large spread of anion resonances to be indicative of a bridged species (fig. 5.9)

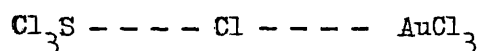


Fig. 5.9

Presumably, the lowest ^{35}Cl resonance frequency arising from the bridged chlorine. This is clearly the extreme limit of secondary bonding viz. discrete three-centre bond formation. The Raman data from this work are clearly not consistent with this explanation. There is an apparent contradiction in that the non-appearance of cation lines at room temperature was attributed to free rotation of SCl_3^+ . This results in the ^{35}Cl resonances being shifted to ca. 0.5 MHz which is outside the frequency range of many commercial spectrometers. It is considered that this explanation is plausible¹² and has been postulated in other systems. However, if there is free rotation of SCl_3^+ at room temperature, then a discrete three-centre bond does not account for the large frequency range over which chlorine resonances from AuCl_4^- are spread. In fact, free rotation of SCl_3^+ is consistent with the Raman

spectrum from which it was concluded that the secondary interaction between SCl_3^+ and AuCl_4^- was weaker than the corresponding interaction in form 1 $\text{SCl}_3^+\text{ICl}_4^-$.

The corresponding SeCl_3^+ and TeCl_3^+ compounds were synthesised from MCl_4 ($\text{M} = \text{Se}, \text{Te}$) and Au_2Cl_6 in AsCl_3 as a solvent. The selenium compound was originally reported in 1887, whereas the tellurium compound is apparently novel. Both salts were obtained as orange crystalline solids for which only one crystal modification exists and vibrational data are presented in table 5.10, fig. 5.10, fig. 5.11, fig. 5.12 and fig. 5.13. Comparison of the Raman spectra from the two compounds shows that they are not isostructural and this was confirmed by X-ray powder studies. The SeCl_3^+ salt contains a distorted AuCl_4^- ion and X-ray powder studies have shown it to be isomorphous with $\text{SCl}_3^+\text{AuCl}_4^-$. The TeCl_3^+ salt, on the other hand, shows only three Raman bands which may be attributed to AuCl_4^- , which is consistent with a centrosymmetric ion. The Raman spectrum for $\text{SeCl}_3^+\text{AuCl}_4^-$ is complicated in that there is overlap between Se-Cl and Au-Cl stretching modes, and at low temperatures non-degenerate Au-Cl stretching modes are apparently split. The relative intensities of the two bands from each mode are consistent with isotope effects but could also be interpreted in terms of correlation coupling between AuCl_4^- ions. If the compound is isostructural with form 1 $\text{SCl}_3^+\text{ICl}_4^-$, then reference to the vibrational analysis (table 5.8) shows that nine AuCl_4^- modes predicted by site-group analysis would each split into four modes under correlation coupling. Since the unit cell group is centrosymmetric, two modes are Raman active and two are infra-red active. This is clearly a feasible explanation for splittings of the Au-Cl stretching modes. The vibrational

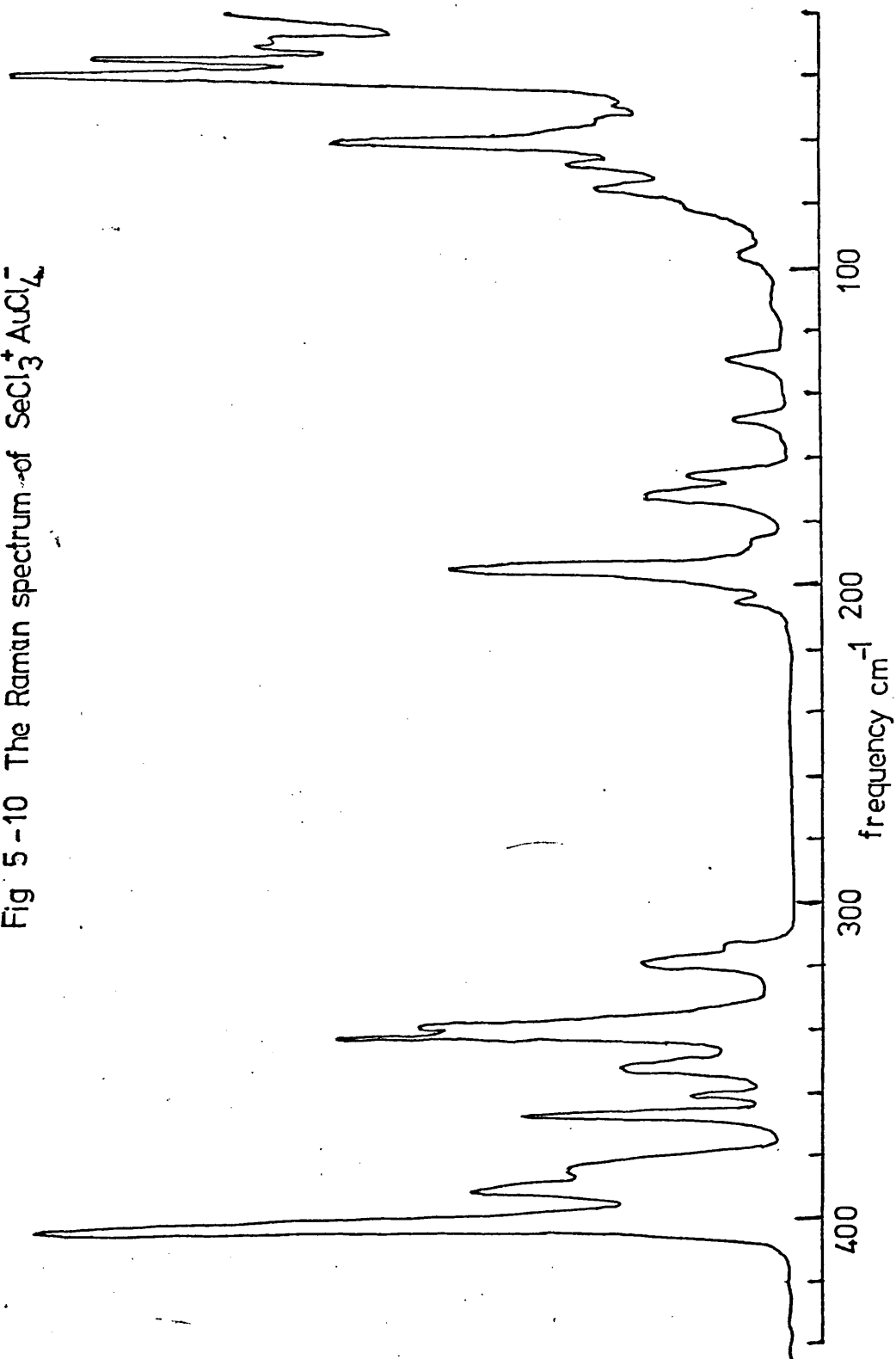
Fig 5-10 The Raman spectrum of $\text{SeCl}_3^+ \text{AuCl}_4^-$ 

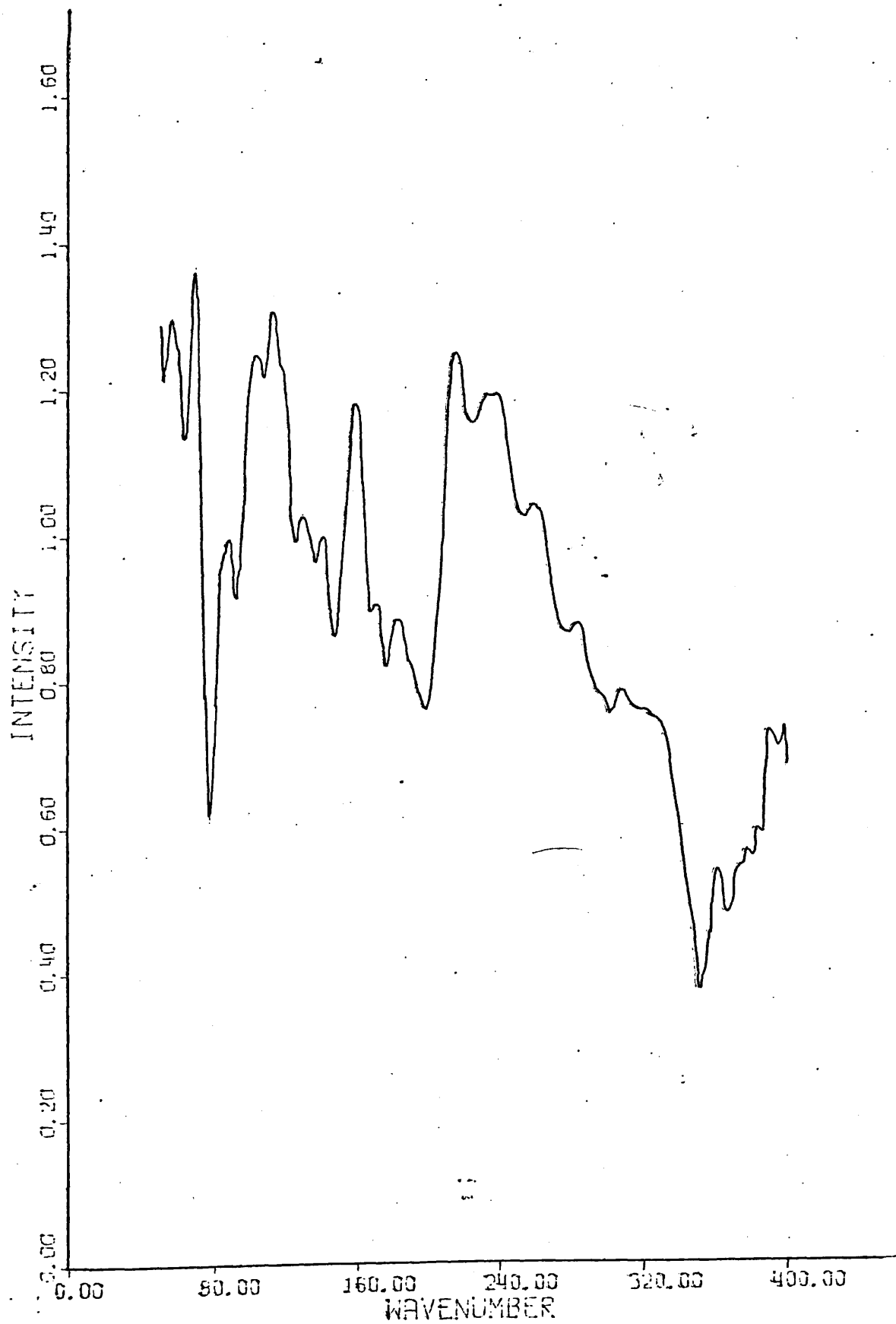
Fig 5-11 The infra-red spectrum of $\text{SeCl}_3^+ \text{AuCl}_4^-$ 

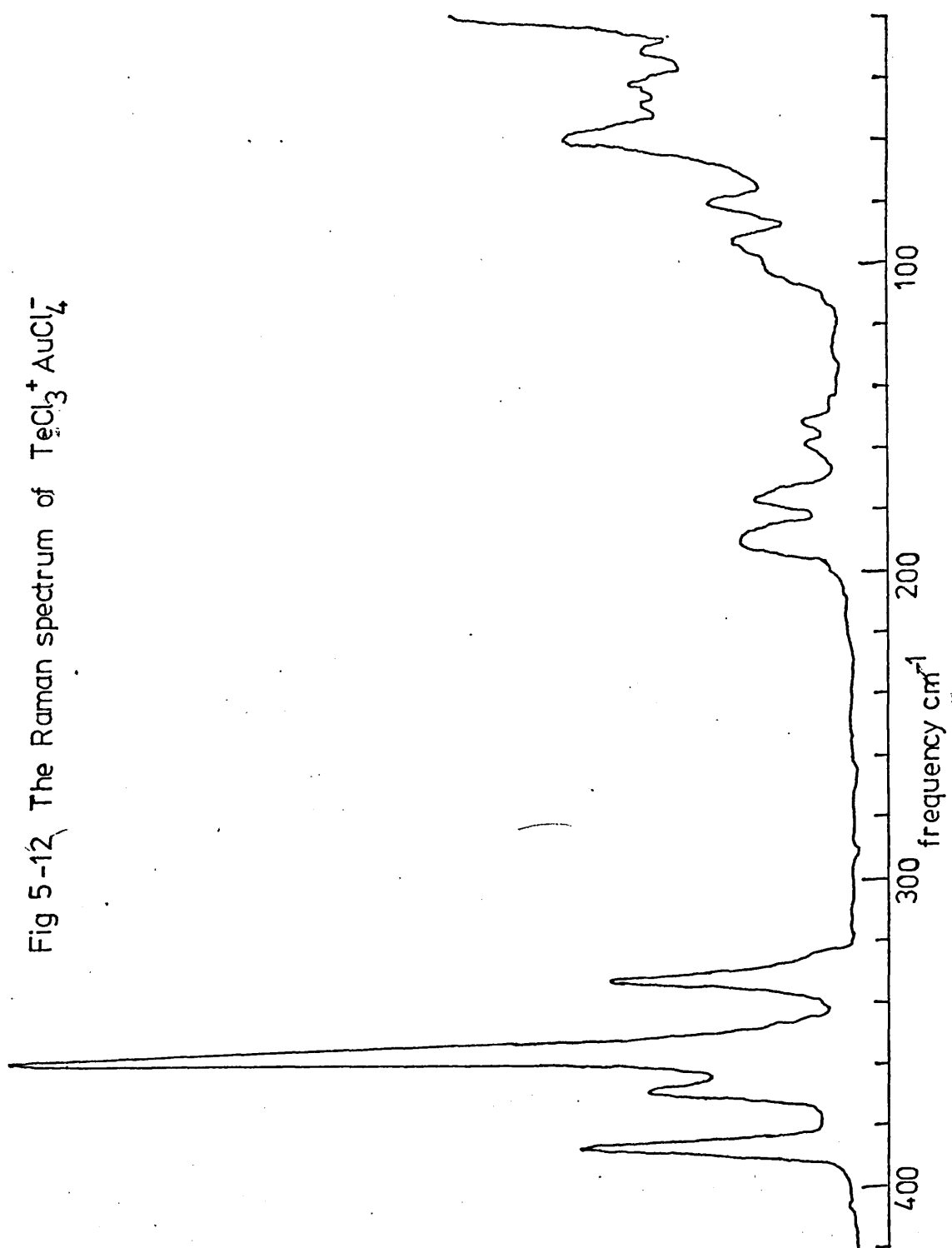
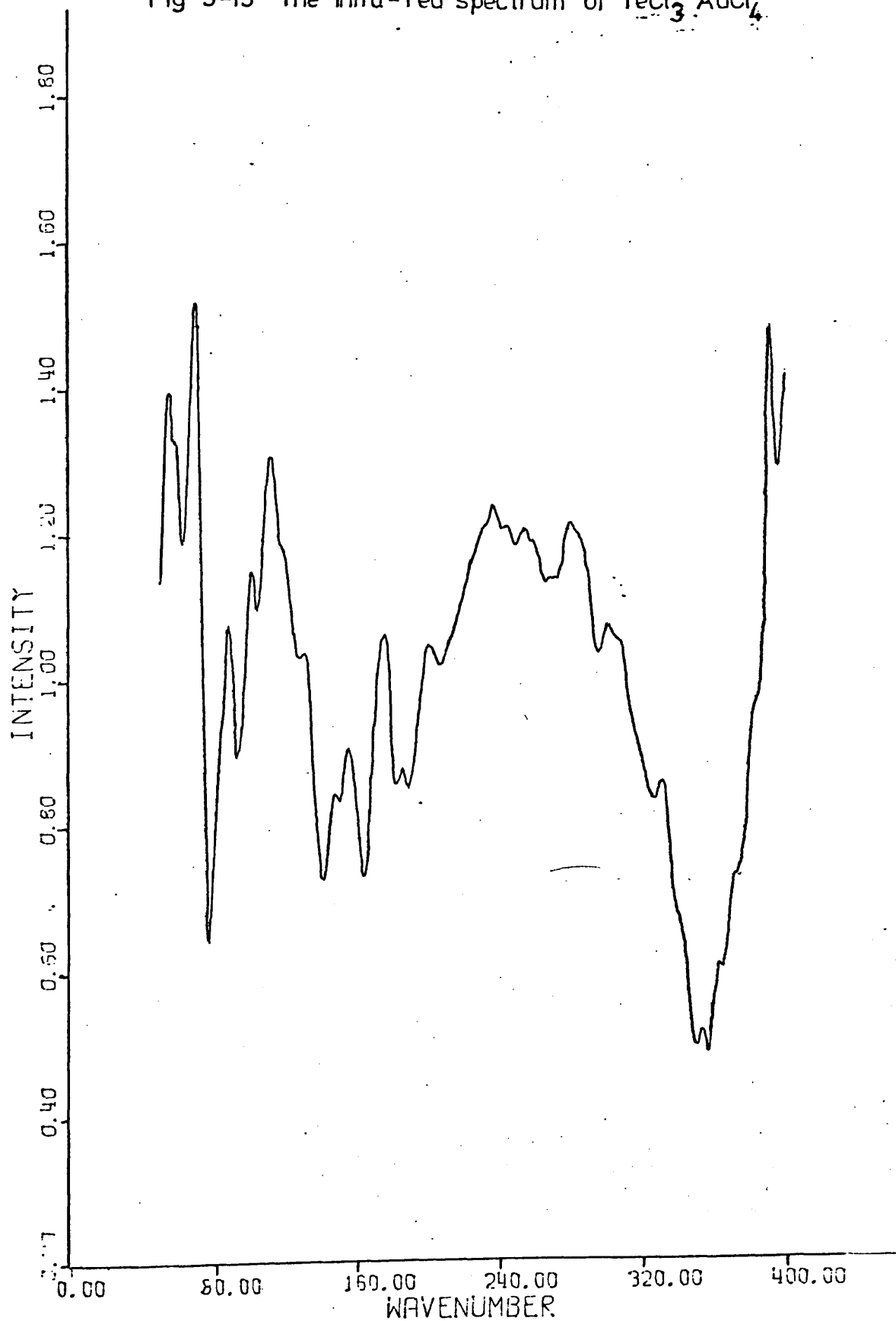
Fig 5-12 The Raman spectrum of $\text{TeCl}_3^+ \text{AuCl}_4^-$ 

Fig 5-13 The infra-red spectrum of $\text{TeCl}_3^+ \text{AuCl}_4^-$ 

assignment presented in table 5.10 was made by comparison with the AuCl_4^- modes in $\text{SCl}_3^+\text{AuCl}_4^-$. There are, however, significant differences:

(i) The strongest Au-Cl deformation in the Raman spectrum of $\text{SCl}_3^+\text{AuCl}_4^-$ is located at 186 cm^{-1} ; in $\text{SeCl}_3^+\text{AuCl}_4^-$, this is apparently shifted to 172 cm^{-1} . The weak band observed at 186 cm^{-1} in $\text{SeCl}_3^+\text{AuCl}_4^-$ is considered more likely to arise from SeCl_3^+ (cf. similar bands in the spectra of other compounds, table 5.13).

(ii) The formally Raman-inactive Au-Cl stretching mode (E_u) in $\text{SCl}_3^+\text{AuCl}_4^-$ is located at 354 and 360 cm^{-1} . In $\text{SeCl}_3^+\text{AuCl}_4^-$, the situation is complicated by the presence of three bands in this region at 352 , 360 and 367 cm^{-1} , which could be attributed to factor group splittings of this Au-Cl stretching mode. Alternatively, the bands at 360 , 367 and 384 , 390 cm^{-1} could be attributed to factor group splittings of the already-split $\sqrt{2}$ (E) SeCl_3^+ mode. This explanation seems plausible, although unlike in other examples where factor group splittings have been postulated, the stronger bands are located at higher frequency. The intensities of the bands at 384 , 390 and 400 cm^{-1} are not consistent with isotopic splittings of the $\sqrt{1}(A_1)$ SeCl_3^+ mode (see Appendix 2). Further, it is considered that the sample is not contaminated with SeCl_4 which would show Se-Cl stretching modes⁴⁵ at 399 and 366 cm^{-1} .

Four ^{35}Cl NQR frequencies arising from AuCl_4^- are observed (table 5.11) and the interval between the highest and lowest frequency is even wider than in $\text{SCl}_3^+\text{AuCl}_4^-$. The lowest frequency again exhibits a normal negative temperature coefficient which is an indication that any secondary bonding between SeCl_3^+ and AuCl_4^- is very weak.

TABLE 5.13

RAMAN DATA FOR SeCl_3^+ AND TeCl_3^+ CATIONS (cm^{-1})

$\text{MCl}_3^+ \text{C}_{3v}$	$\text{SeCl}_4 \cdot \text{AlCl}_3$	$\text{SeCl}_4 \cdot \text{GaCl}_3$	$\text{SeCl}_4 \cdot \text{SO}_3$	$\text{SeCl}_4 \cdot \text{SbCl}_5$	$\text{TeCl}_4 \cdot \text{AlCl}_3$	$\text{TeCl}_4 \cdot \text{SO}_3$	$\text{TeCl}_4 \cdot \text{GaCl}_3$	$\text{TeCl}_4 \cdot \text{SbCl}_5$
$\nu_1 \text{ A}_1$	416	418	416	408	390(p)	391	389	397
$\nu_2 \text{ E}$	395	394	392	353	367 (dp)	373 356	375	385 357
$\nu_3 \text{ A}_1$	234?	204	207	?	169	180	-	180
$\nu_4 \text{ E}$	186?	169	181	?	146 (dp)	154	-	148

)

The ^{35}Cl resonance lines from SeCl_3^+ merit very little comment because comparable data from other SeCl_3^+ salts are not currently available. Although frequencies for SeCl_4 have been reported⁷ these add little to the discussion since distinct tetramers of SeCl_3^+ ions are present. $\text{SeCl}_3^+\text{SbCl}_6^-$ was apparently studied by Japanese workers,⁴¹ but in the absence of a translation the observed resonance frequencies cannot be distinguished. It is significant, however, that unlike $\text{SbCl}_3^+\text{AuCl}_4^-$, cation signals are observed at room temperature. This may be taken as an indication that rotation of SeCl_3^+ is restricted and the secondary bonding with AuCl_4^- is stronger than in the SbCl_3^+ salt.

The Raman spectrum from $\text{TeCl}_3^+\text{AuCl}_4^-$ is comparatively simple. Three modes due to AuCl_4^- and five from TeCl_3^+ are observed - the splitting of $\sqrt{3}(\text{E}) \text{TeCl}_3^+$ not being observed. Two explanations may be considered to account for these observations:

(i) The electric field created at AuCl_4^- sites is sufficiently weak not to perturb the AuCl_4^- ions which may be considered in terms of D_{4h} symmetry.

(ii) The electric field created at AuCl_4^- sites is strong but the sites are centrosymmetric.

Table 5.14 demonstrates that any lower centrosymmetric point group still only predicts three Raman active modes for AuCl_4^- . This explanation is plausible because TeCl_3^+ Raman modes are split and the complementary low-frequency infra-red data show splittings of degenerate AuCl_4^- deformations. Thus the different crystal lattice accommodating TeCl_3^+ and AuCl_4^- ions does not permit a strong secondary interaction between anion and cation. This might be considered analogous to SbCl_3^+ and ICl_4^- ions in the metastable modification.

TABLE 5.14

CORRELATION OF D_{4h} TO LOWER CENTROSYMMETRIC POINT GROUPS FOR $AuCl_4^-$

	D_{4h}	C_{2v}	C_{2h}	C_i
A_{1g}	A_g	A_g	A_g	A_g
B_{1g}	B_{1g}	B_g	B_g	A_g
B_{2g}	A_g	A_g	A_g	A_g
A_{2u}	B_{1u}	B_u	A_u	A_u
B_{2u}	A_u	A_u	A_u	A_u
E_u	$B_{2u} + B_{3u}$	$A_u + B_u$	$A_u + B_u$	$A_u + A_u$
E_u	$B_{2u} + B_{3u}$	$A_u + B_u$	$A_u + B_u$	$A_u + A_u$

There is no obvious reason otherwise, why secondary bonding between AuCl_4^- and TeCl_3^+ should not be important. It is clearly present in $\text{TeCl}_3^+\text{AlCl}_4^-$ upon inspection of the X-ray crystal structure.³⁹

The ^{35}Cl NQR frequencies were also measured (table 5.11) and four lines arising from AuCl_4^- were observed, spread over a very narrow frequency range. This is consistent with only a small distortion of AuCl_4^- . Complete assignment of the resonances is somewhat difficult because resonances from AuCl_4^- and TeCl_3^+ overlap. In addition, the spectrum is unusual in that ^{37}Cl resonances were observed from anion and cation at both ambient and liquid nitrogen temperatures. In all the previous compounds discussed, ^{37}Cl resonances could only be observed weakly from the chlorocations at low temperatures. These difficulties of assignment are unlikely to be resolved in the absence of further data from related compounds. As in the case of SeCl_3^+ compounds, NQR data for TeCl_3^+ compounds are somewhat limited. Frequencies for TeCl_4 are available⁴² and also for $\text{TeCl}_3^+\text{AlCl}_4^-$ where three ^{35}Cl resonances at 29.420, 29.574 and 30.570 MHz are observed at ambient temperatures.⁴² However, this does not assist with the assignment of $\text{TeCl}_3^+\text{AuCl}_4^-$ because the crystal structure indicates a strong anion-cation interaction. The compound, in fact, is described crystallographically³⁹ as consisting of strongly distorted TeCl_6 octahedra sharing three neighbouring chlorine atoms with three different AlCl_4^- tetrahedra. A solid state vibrational spectroscopic analysis has not apparently been undertaken, but it follows that this could not be carried out in terms of TeCl_3^+ cations. Thus assignment of three ^{35}Cl NQR frequencies in $\text{TeCl}_3^+\text{AuCl}_4^-$ to TeCl_3^+ is impossible. Since the frequencies are close together, the average value obtained from four lines assigned to AuCl_4^- does not permit an unequivocal

assignment. Clearly any three of the four highest resonances could be assigned to TeCl_3^+ and further attempts to prepare $\text{TeCl}_3^+\text{ICl}_4^-$, which may possess a related structure, are required.

5.5 ICl_4^- AND AuCl_4^- COMPOUNDS OF SUBSTITUTED CHLOROPHOSPHORUS CATIONS

In the previous sections, ICl_4^- and AuCl_4^- ions were shown to be distorted in chlorochalcogen salts. Further investigations were carried out with different chlorocations to ascertain whether this phenomenon was peculiar only to sulphur, selenium and tellurium. Raman data for various substituted chlorophosphorus cationic derivatives, PCl_4ICl_4 , $\phi\text{PCl}_3\text{ICl}_4$, $\phi_3\text{PClICl}_4$ and $\text{PCl}_4\text{AuCl}_4$ are presented in table 5.15. The assignment of cation frequencies was made by reference to the literature^{38,48} for PCl_4^+ and to the measured spectra for PCl_6^- derivatives of ϕPCl_3^+ and $\phi_3\text{PCl}^+$. The latter samples were kindly loaned by Dr. K.B. Dillon of Durham University, and the measured spectra showed cation bands of comparable relative intensities to those observed in the ICl_4^- salts. The remaining bands in the spectra of all four compounds may be attributed to AuCl_4^- and ICl_4^- ions and these may be considered in terms of centrosymmetric point groups. In the ICl_4^- salts, the two I-Cl stretching modes are located at ca. 260 and 280 cm^{-1} which is expected for an undistorted square planar ion. On the basis of vibrational spectroscopy, therefore, it may be inferred that either a very weak low symmetry electric field is created at ICl_4^- sites or that the field created is strong but centrosymmetric. The cation vibrations do not yield any additional information. In the PCl_4^+ salts, vibrational assignments are consistent with T_d symmetry. The F_2 mode at ca. 660 cm^{-1} and the A_1 mode at ca. 460 cm^{-1} are split in both compounds.

TABLE 5.15

RAMAN SHIFTS FOR SUBSTITUTED CHLOROPHOSPHORUS CATIONS WITH AuCl_4^- , ICl_4^- (below 700 cm^{-1})

$\text{PCl}_4 \text{ ICl}_4$	$\phi \text{ PCl}_3 \text{ ICl}_4$	$\phi_3 \text{ PCl ICl}_4$	$\text{PCl}_4 \text{ AuCl}_4$	ASSIGNMENT	
295 K	295 K	295 K	295 K	130 K	130 K
136 (w-m)	138 (m-w, br)	134 (w)	140 (w, br)	140 (w, br)	$\nu_2 \text{ ICl}_4^-$
	140 (m-w)				$\phi \text{ PCl}_3^+$
183 (vw)			148 (should)		$\phi_3 \text{ PCl}^+$
				174 (m)	$\nu_2 \text{ AuCl}_4^-$
				183 (w)	PCl_4^+
					$\phi \text{ PCl}_3^+$
	200 (w, br)	200 (w, br)			$\phi \text{ PCl}_3^+$
	220 (w)	222 (w)			$\phi_3 \text{ PCl}^+$
246 (should)			200 (vw)		$\phi_3 \text{ PCl}^+$
246 (should)			238 (vw)		PCl_4^+
264 (m)	256 (s)	257 (s)	258 (s)	258 (s)	$\nu_4 \text{ ICl}_4^-$
			268 (should)	263 (m)	$\phi_3 \text{ PCl}^+$
				272 (w)	$\phi_3 \text{ PCl}^+$
288 (vs)	279 (vs)	282 (vs)	284 (vs)	287 (vs)	$\nu_1 \text{ ICl}_4^-$
					$\nu_1 \text{ AuCl}_4^-$
				326 (s)	$\nu_4 \text{ AuCl}_4^-$
				350 (vs)	PCl_4^+
456 (w)			456 (m)	454 (m)	PCl_4^+
660 (vw, br)			646 (vw)	646 (vw)	PCl_4^+
			658 (vw)	655 (vw)	PCl_4^+

The splittings of the A_1 mode are of the correct relative intensities to arise from isotope effects and similar splittings have been observed in other salts.⁴⁸ The F_2 splittings are not consistent with isotope effects and therefore arise from site group effects. This may be an indication that solid state effects in these compounds are important, but for the ICl_4^- modes, the complementary infra-red data are required.

³⁵Cl NQR frequencies could not be observed from ICl_4^- in $PCl_4^+ICl_4^-$ or $\phi_3 PCl^+ICl_4^-$. The NQR frequencies observed from $\phi PCl_3^+ICl_4^-$ and $PCl_4^+AuCl_4^-$ are presented in table 5.16 together with cation data from the other two compounds. These data support the conclusions reached from vibrational spectroscopy but the following individual comments are worth mentioning:

(i) In $\phi PCl_3^+ICl_4^-$, two anion frequencies are observed at 295 K and four at 77 K. This could indicate that a phase change occurs but variable temperature Raman studies failed to detect this. The two frequencies at 295 K are comparable with those observed⁹ from $CsICl_4$ in which ICl_4^- ions occupy C_{2h} (centrosymmetric) sites. As was discussed previously, the Raman spectrum of the latter compound at low resolution can be interpreted in terms of D_{4h} point group symmetry.

(ii) In $\phi PCl_3^+ICl_4^-$, four cation resonances are observed at 77 K. This is somewhat unusual since there are only three chlorine atoms present in each individual cation.

(iii) In $PCl_4^+AuCl_4^-$, four anion frequencies are observed at both 295 K and 77 K spread over ≈ 2 MHz. This undoubtedly arises from some distortion of $AuCl_4^-$, but since the Raman spectrum did not apparently indicate this it is tentatively suggested that distortion is produced by a strong electric field at $AuCl_4^-$ sites of C_i symmetry. This explanation is consistent with only three bands from $AuCl_4^-$ being observed in the Raman spectrum.

TABLE 5.16

NQR SPECTRA FOR $\text{PCl}_4^+\text{ICl}_4^-$, $\phi \text{PCl}_3\text{ICl}_4^-$, $\phi_3\text{PClICl}_4^-$ AND $\text{PCl}_4\text{AuCl}_4^-$ (MHz)

	$\text{PCl}_4^+\text{AuCl}_4^-$	$\phi_3\text{PCl}^+\text{ICl}_4^-$	$\phi \text{PCl}_3^+\text{ICl}_4^-$	$\text{PCl}_4^+\text{ICl}_4^-$
	T = 295 K	T = 77 K	T = 295 K	T = 77 K
CATION	NOT OBSERVED	32.41	29.425	29.860
		32.335		NOT INVESTIGATED
		32.27		30.55
		32.14		30.45
MEAN		32.29		30.375
				30.25
				30.406
ANION	28.99	29.90	NOT OBSERVED	22.925
	27.96	28.27	OBSERVED	22.825
	27.14	27.59		22.700
	27.04	27.45		22.613
MEAN	27.78	28.30	22.287	22.766
				NOT OBSERVED
				OBSERVED
				32.325
				32.225
				32.135

These investigations have failed to identify strong secondary bonding effects in substituted chlorophosphorus systems. The effect of phenyl ϕ substitution on PCl_4^+ is somewhat different from substituting methyl groups on SCl_3^+ . The indications are that upon phenyl substitution, the electric field strength at ICl_4^- sites is increased. Two points, however, must again be emphasised as with the chlorosulphonium systems. Firstly, phenyl substitution considerably increases the cation size, so that a change in crystal structure undoubtedly occurs on going from PCl_4^+ to ϕPCl_3^+ to $\phi_3\text{PCl}^+$. Secondly, there is the possibility that phenyl groups will shift the positive charge from the phosphorus atom. Contributions from such canonical forms may enhance the secondary bonding to ICl_4^- and so increase the strength of the electric field created at ICl_4^- sites. In this respect, the effect of phenyl substitution on SCl_3^+ in $\text{SCl}_3^+\text{ICl}_4^-$ merits experimental and spectroscopic investigation.

5.6 AuCl_4^- AND ICl_4^- WITH NITROGENOUS BASES

A recent publication concerning triatomic polyhalide anions^{24,25} reported Raman spectra for the NMe_4^+ salts and both factor group and isotopic splittings of the anion modes were observed. Investigation of the corresponding ICl_4^- and AuCl_4^- salts was therefore undertaken in order to ascertain whether similar splittings could be observed and, more importantly, to establish the effect upon the NQR frequencies. A commercial sample of $\text{NBu}_4^+\text{ICl}_4^-$ and also $\text{NMe}_3\text{H}^+\text{ICl}_4^-$ were similarly investigated as examples in which the cation size has been increased and decreased respectively. In the latter compound, there is also the possibility of strong hydrogen bonding. Other ICl_4^- salts investigated

were pyridinium pyH^+ , deuteropyridinium pyD^+ and 3-chloropyridinium 3-ClpyH^+ .

The Raman spectra for $\text{NMe}_4^+\text{ICl}_4^-$, $\text{NBu}_4^+\text{ICl}_4^-$ and $\text{NMe}_3\text{H}^+\text{ICl}_4^-$ are presented in table 5.17. Bands arising from the cations were not observed at this resolution, and consequently splittings of I-Cl stretching modes are apparent in $\text{NMe}_4^+\text{ICl}_4^-$ and $\text{NBu}_4^+\text{ICl}_4^-$. In each case these may be attributed to a combination of both isotope and factor group effects upon an otherwise centrosymmetric ICl_4^- ion. However, to be consistent with this argument, it is not the same I-Cl stretching mode which is affected in each case. Thus consider $\text{NMe}_4^+\text{ICl}_4^-$ at 130 K when the broad bands observed at room temperature are fully resolved. The shifts at 280, 288 cm^{-1} and 302, 208 cm^{-1} may be ascribed to factor group splittings of the $\sqrt{1}$ I-Cl stretching mode. It may be envisaged that two or possibly four ICl_4^- ions per unit cell are coupled so that each degenerate Raman active mode is split into two. Each mode is then further split by chlorine isotopes. The expected intensities of bands arising from all possible $^{35}\text{Cl}/^{37}\text{Cl}$ isotopic substitution at natural abundance in ICl_4^- are 81: 104: 27: 27: 12: 1 (see appendix 2 for the derivation). In this case only the two strongest bands arising from $[\text{I}^{35}\text{Cl}_4]^-$ and $[\text{I}^{37}\text{Cl}^{35}\text{Cl}_3]^-$ are fully resolved. Factor group splittings of the deformation mode at 140 cm^{-1} are also apparent but the $\sqrt{4}$ I-Cl stretching mode is apparently unaffected. Unfortunately, ^{35}Cl NQR frequencies could not be observed, but the infra-red spectrum showed an intense absorption consisting of two bands at ca. 210 and 250 cm^{-1} , other bands in the spectrum being unresolved. These bands may arise from either

- (i) Factor group splittings of the infra-red active E_u I-Cl stretching mode
- or (ii) Site group splittings of the infra-red active E_u I-Cl stretching mode.

TABLE 5.17

 ICl_4^- VIBRATIONS IN SALTS WITH NITROGENOUS BASES

$\text{Me}_4\text{N}^+\text{ICl}_4^-$	$\text{nBu}_4\text{N}^+\text{ICl}_4^-$	$\text{Me}_3\text{NH}^+\text{ICl}_4^-$	ASSIGNMENT
T=ambient T = 130 K	T=ambient T=130 K	T=ambient T=130 K	
137 (w,br) 137 (w) 148(should)	133(w)	136 (w)	$\sqrt{2} B_{1g} \text{ICl}_4^-$
	255 (should) 264(s)	257 (m) 263 (s) 270 (m)	$\sqrt{4} B_{2g} \text{ICl}_4^-$
256 (vs) 259 (s)	286(m-s)	289 (vs) 276 (vs)	$\sqrt{1} A_{1g} \text{ICl}_4^-$
277 (s) 279 (s) 288 (m)		283 (vs)	
294 (s,br) 302 (m) 308(should)		300 (m) 307 (m)	?

The infra-red spectrum is therefore consistent with correlation coupling of D_{4h} ICl_4^- modes. The observed spectra may also be explained in terms of two crystallographically different ICl_4^- ions, giving rise to Raman shifts at:

(i) 140, 260, ca. 280 cm^{-1}

(ii) 150, ca. 280, ca. 300 cm^{-1}

However, on the basis of the crystal data²⁵ for the related ICl_2^- salts, the former explanation is preferred.

The Raman spectrum for $NBu_4^+ICl_4^-$ may be explained in terms of isotopic splittings. At 77 K, three bands indicative of a centrosymmetric ion are observed but in distinction from the previous example, the ν_4 I-Cl stretching mode at ca. 260 cm^{-1} is split. The bands at 270, 264 and 256 cm^{-1} are of the correct relative intensities (see Appendix 2) for isotope splittings. Unfortunately, NQR frequencies could not be observed from this compound, and further discussion is therefore not possible.

A sample of $NMe_3H^+ICl_4^-$ was kindly loaned by Dr. K.B. Dillon of Durham University for vibrational spectroscopic measurements. The NQR spectrum was considered to be consistent with an undistorted ICl_4^- ion. The Raman spectrum, however, table 5.17, showed four bands which precludes a simple interpretation in terms of D_{4h} point group symmetry - the characteristic bands of D_{4h} ICl_4^- at 142, 260 and 282 cm^{-1} are accompanied by a weak band at 305 cm^{-1} which may not be attributed to the cation. Subsequent attempted preparations recently carried out in these laboratories however, failed to produce a pure compound. The Raman spectrum for each impure product showed a band at ca. 307 cm^{-1} , for which the intensity relative to the other three was different for each preparation.

It is possible, therefore, that this band arises from an impurity and that the original sample underwent decomposition during transit. Further discussion of these alkyl ammonium ICl_4^- salts will not be attempted.

Pyridinium tetrachloroiodate was similarly received from Durham University for vibrational spectroscopic measurements. The NQR spectrum, table 5.19, showed one resonance at 22.375 MHz at 295 K and two resonances at 25.364 and 19.924 MHz at 77 K. The transition temperature was believed to be close to 223 K. These data are consistent with a $\text{D}_{4h} \text{ICl}_4^-$ ion at ambient temperature and a trans (D_{2h} or C_{2h}) or cis (C_{2v}) ICl_4^- species at 77 K. Differential scanning calorimetry (D.S.C.) identified a phase transition at $(215.2 \pm 0.5)\text{K}$. Raman spectra, table 5.18, were recorded over a wide temperature range in an attempt to see if the temperature of the phase change could be confirmed. At ambient temperature, (fig. 5.14), three bands at 140, 268 and 288 cm^{-1} were observed indicative of a $\text{D}_{4h} \text{ICl}_4^-$ species. Cation frequencies were not observed at low resolution. Cooling the sample resulted in sharpening of these three bands and at ca. 213 K a weak band appeared at 302 cm^{-1} . At ca. 203 K, splitting of the lattice modes was apparent. However, it was impossible to establish the transition temperature by vibrational spectroscopy because:

(i) It is impossible to measure exactly the temperature of the sample using the low temperature sample holder (see chapter 6 for further details).

(ii) There is some confusion as to the precise change in the vibrational spectrum corresponding to the transition. This could be taken as either the temperature at which the additional band appears (213 K) or the temperature at which changes in the lattice modes occur

TABLE 5.18

VARIABLE TEMPERATURE RAMAN SPECTRUM FOR PyH^+ICl_4

295 K	273 K	223 K	213 K	193 K	163 K	133 K	ASSIGNMENT
38(s)	40(m)	42(m)	40(m)	40(m)	42(m)	42(m)	} LATTICE MODES
48(s)	52(m)	57(m)	51(m)	50(m)	52(m)	52(m)	
				56 (should)	58 (should)	58 (should)	
			58(m)	60(m)	62(m)	62(m)	
	80(vw)	82(vw)	86(w)	88(w)	89(w)	89(w)	
	100(vw)	102(vw)	112(w)	114(vw)	116(w)	116(w)	
			130(vw)	128(vw)	128(vw)	128(vw)	
140(w)	140(w)	140(w)	142(w)	143(w)	144(w)	144(w)	
266(s)	266(s)	266(s)	267(s)	267(s)	268(s)	268(s)	
286(vs)	286(vs)	288(vs)	282(m-s)	282(m-s)	283(m-s)	283(m-s)	
			301(m-s)	301(m-s)	302(m-s)	302(m-s)	
			308 (should)	308 (should)	308 (should)	308 (should)	

Fig 5-14 The Raman spectrum of pyridinium tetrachloroiodate 295 K

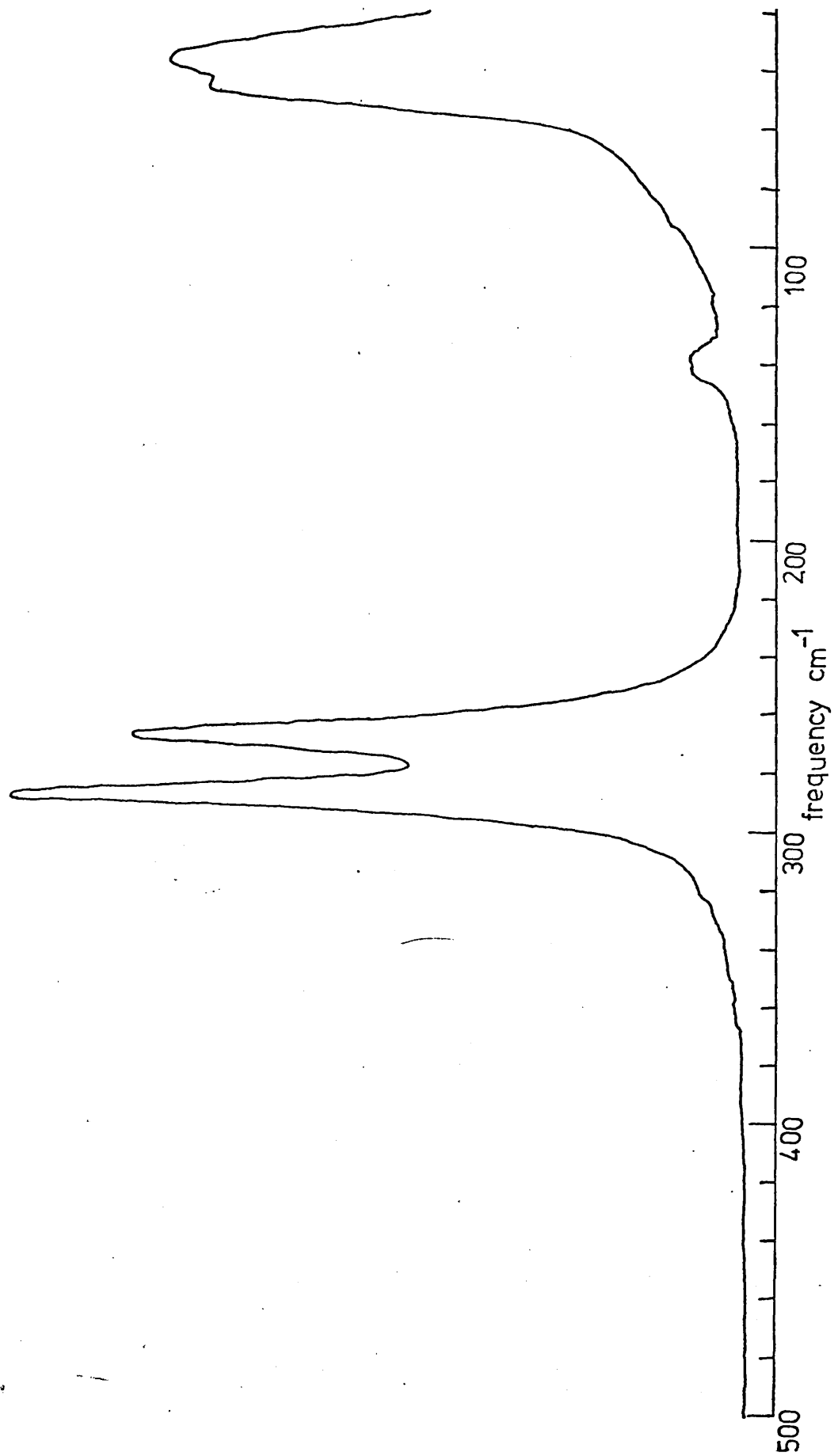
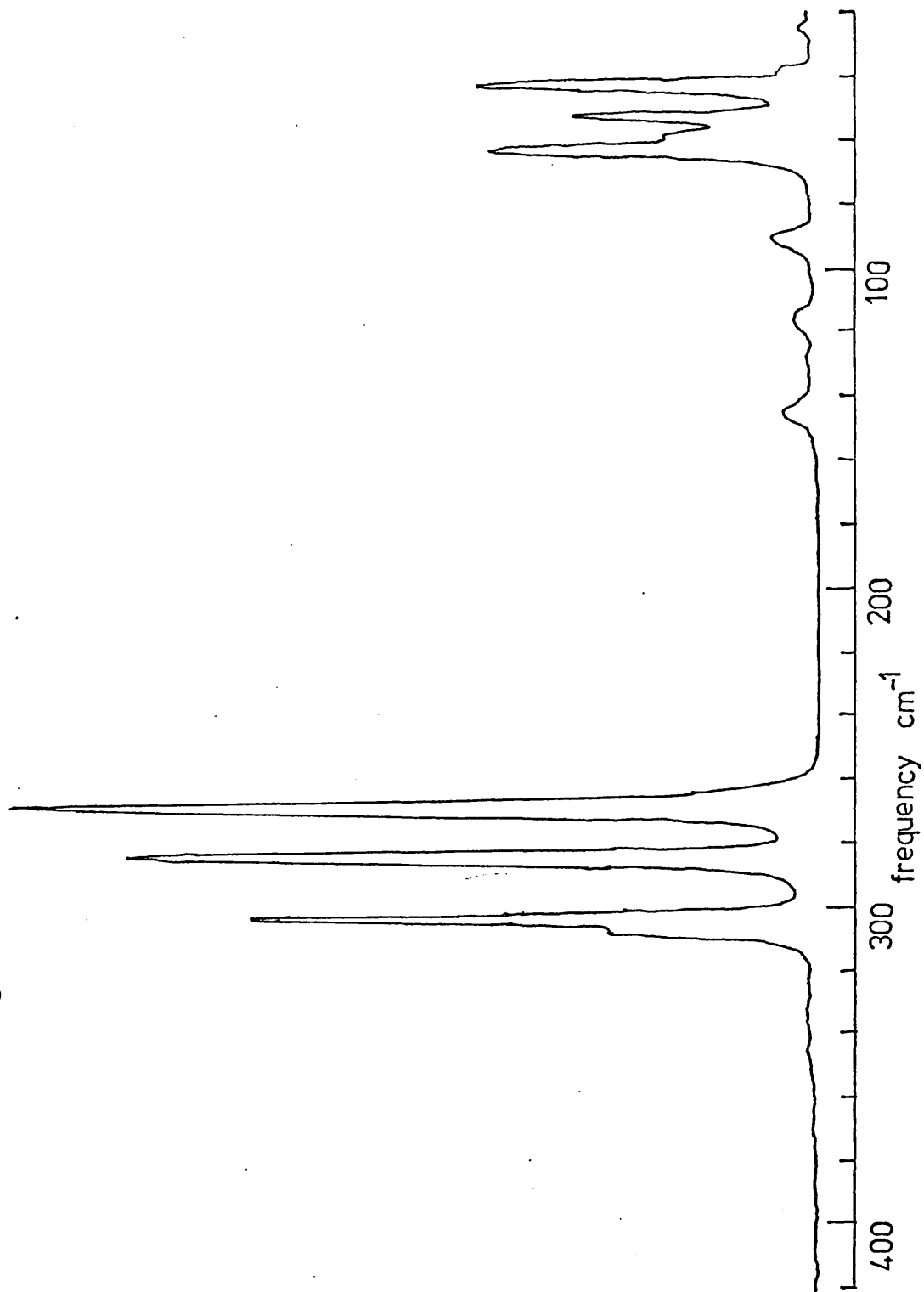


Fig 5-15 The Raman spectrum of pyridinium tetrachloroiodate 129 K



(203 K). Although the former point is closer to the D.S.C. transition temperature, the latter point theoretically seems the more reasonable choice. However, since there is undoubtedly an error in the temperature recorded on the cold cell controller unit especially as a yellow sample is being irradiated by a red source, further discussion is not justified.

Cooling the sample below 200 K produced an increase in the intensity of the new band at 302 cm^{-1} with concomitant decrease in intensity of the band originally observed at 288 cm^{-1} . At 130 K, the three bands observed in the I-Cl stretching region resembled those in $\text{NMe}_4^+\text{ICl}_4^-$ although isotopic splittings were absent. The I-Cl deformation at 144 cm^{-1} was markedly decreased in intensity and accompanied by the appearance of a new band at 128 cm^{-1} . To be consistent with the NQR data, the following explanation is tentatively put forward. At ambient temperatures, pyH^+ and ICl_4^- occupy lattice sites such that there is only a weak secondary interaction between Cl and H^+ . As the temperature is lowered, two chlorines of the anion trans to each other become strongly associated with the H^+ of the pyridinium cation. At the transition temperature, distortion of the lattice results in formally $\text{D}_{2h}\text{ICl}_4^-$ ions being strongly coupled via the cation:

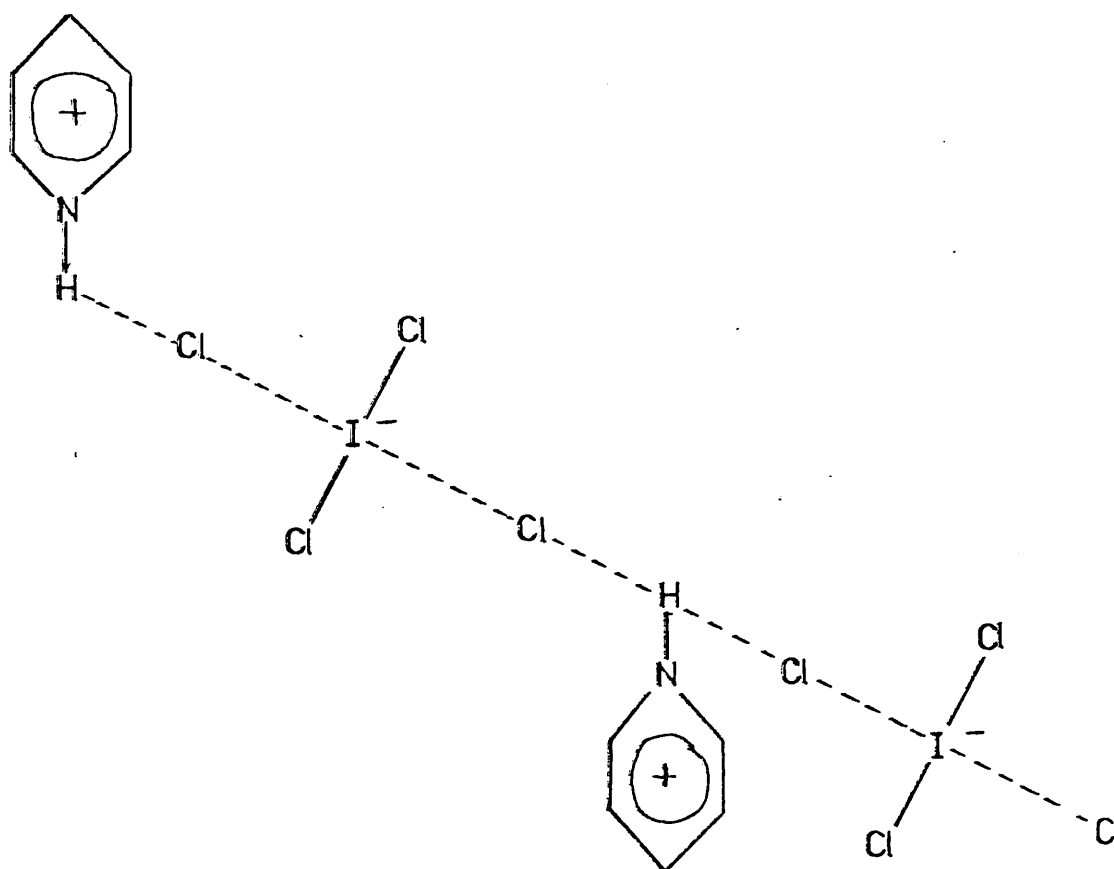


Fig. 5.16

Coupling of formally centrosymmetric ICl_4^- ions takes place producing splittings of degenerate modes. A similar situation has been postulated²⁵ in $\text{pyH}^+\text{ICl}_2^-$ to account for factor group splittings. An alternative explanation in terms of a C_{2v} ion is also possible. Correlation of D_{4h} to C_{2v} shows that 9 Raman active ICl_4^- modes would be expected. Four I-Cl stretching modes are observed in the low temperature spectrum (130 K). However, unlike the band pattern observed for ICl_4^- in form 1 $\text{SCl}_3^+\text{ICl}_4^-$, the additional stretching mode is observed at a higher frequency than the two formally Raman active D_{4h} I-Cl stretching modes. For this reason, the former explanation in terms of a centrosymmetric ion

is preferred. Nevertheless, it should be pointed out that in I_2Cl_6 , which has a D_{2h} planar structure with two bridging chlorines, the terminal I-Cl stretching modes are located at 314 and 344 cm^{-1} in the Raman. If cis I-Cl stretchings occur at higher frequency then the C_{2v} structure cannot be entirely eliminated and investigation of the infra-red spectrum would provide some additional evidence.

Similar effects were observed in the spectra of $PyD^+ ICl_4^-$. This sample was received from Durham University but since the transition temperature by DSC was identical with that for $pyH^+ ICl_4^-$, it is plausible that some deuterium scrambling had occurred. The ^{35}Cl NQR resonances (table 5.19) are slightly different from those observed in $pyH^+ ICl_4^-$ however. In 3-chloropyridinium tetrachloroiodate, $3-ClpyH^+ ICl_4^-$ similar coupling of vibrations could not be observed. The NQR spectrum at both ambient and liquid nitrogen temperatures was consistent with an undistorted ICl_4^- ion, and no transition point could be detected. The Raman spectrum is in accord with this - three bands only at 142, 258 and 280 cm^{-1} are observed at ambient temperature, but at 130 K, however, the two bands corresponding to the I-Cl stretching modes are asymmetric on the high frequency side. This can be attributed to isotopic splittings. Substitution of chlorine in the 3-position on the pyridinium ring is sufficient to eliminate coupling of ICl_4^- modes. Whether this is a steric or electronic effect remains unknown. The electron withdrawing properties of chlorine, however, substituted at the three position in the pyridinium ring tend to increase the basicity of the nitrogen,³⁰ resulting in reduced attraction of the proton to the ICl_4^- ions.

TABLE 5.19

³⁵Cl NQR FREQUENCIES FOR pyH⁺ICl₄⁻, pyD⁺ICl₄⁻

	pyH ⁺ ICl ₄ ⁻	pyD ⁺ ICl ₄ ⁻
T = 295 K	22.375	22.375
T = 77 K	25.364	25.277
	19.924	19.872
mean	22.644	22.574

TABLE 5.20

VARIABLE TEMPERATURE RAMAN SPECTRA FOR 3-ClpyH⁺ICl₄⁻

295 K	250 K	230 K	200 K	170 K	130 K
110(br,w)	116(w)				
		123(w)	122(w)	123(w)	124(w)
144(w)	143(w)	145(m)	145(m)	145(m)	144(w)
256(s)	256(s)	257(s)	258(s)	258(s)	257(s)
266(should)	264(should)	265(should)	265(should)	265(should)	265(m-s)
278(vs)	278(vs)	278(vs)	280(vs)	281(vs)	280(vs)
			288(should)	287(should)	286(should)

$\text{NMe}_4\text{AuCl}_4^-$ does not resemble the corresponding ICl_4^- salt and so it is considered separately. At ambient temperature, three Raman shifts due to AuCl_4^- were observed at 172, 324 and 353 cm^{-1} indicative of a centrosymmetric ion. At 223 K, splitting of the Au-Cl stretching mode at 324 cm^{-1} was apparent and further cooling to 130 K resulted in splitting of the other Au-Cl stretching mode. These splittings are not consistent with isotope effects (see Appendix 2). NQR signals could not be observed at ambient temperatures, but at 193 K and 77 K, five ^{35}Cl resonances were apparent. At both temperatures, one line was very much weaker than the other four. The average of the four similar frequencies at 77 K was 28.34 MHz which is indicative of AuCl_4^- . The remaining line at 28.74 MHz is at a considerably higher frequency than would be expected for a symmetrical AuCl_4^- species. At 193 K, however, the weaker line is located at 28.01 MHz which is close to the average of the other four frequencies, 28.036 MHz, indicative of AuCl_4^- . The NQR spectra could be interpreted in terms of two crystallographically different types of centrosymmetric AuCl_4^- ions. A similar explanation was given to account for the ^{81}Br NQR frequencies⁴³ in KIBr_2 . The splitting of the Raman modes at low temperature is consistent with this argument, but the explanation requires further spectroscopic investigations.

5.7 NOAuCl_4^-

NOAuCl_4^- was investigated by vibrational spectroscopy and NQR in order to ascertain whether anion-cation association producing anomalous effects in the Raman spectrum at low temperature could be observed. The corresponding ICl_4^- salt has already been investigated

TABLE 5.21

(a) RAMAN SHIFTS FOR $\text{NMe}_4^+\text{AuCl}_4^-$

T = 295 K	T = 220 K	T = 170 K	T = 130 K
36(s)	41(s) 60(should)	32(m) 42(m-s) 60(should)	31(m) 42(m-s) 60(should)
172(m)	175(m)	175(m)	174(m)
324(m-s)	324(should) 327(m-s)	325(m) 328(m-s) 353(should)	324(m) 328(m-s) 351(should)
353(s)	355(s)	357(s)	356(s)

(b) ^{35}Cl NQR FREQUENCIES FOR $\text{NMe}_4^+\text{AuCl}_4^-$

	T = 295 K	T = 77 K	T = 193 K
$^{35}\text{Cl AuCl}_4^-$	NOT OBSERVED	29.521 28.574 27.657 28.623	29.045 28.275 27.430 27.395
mean		28.344	28.036
odd line		28.740	28.010

by French workers,³² and was found to be dissociated into NOICl_2 and chlorine at temperatures above 250 K. The Raman spectrum at low temperature was interpreted in terms of D_{4h} symmetry. NOAuCl_4 , however, is a stable compound showing no dissociation into NOCl and Au_2Cl_6 at ambient temperature. The three bands in the Raman spectrum at 295 K, at 181, 322 and 346 cm^{-1} , are indicative of a centrosymmetric AuCl_4^- ion and a weak broad band at ca. 2200 cm^{-1} is indicative of NO^+ . The latter band is located at lower frequency than observed for simple NO^+ salts, typically $\nu_{\text{N=O}^+}$ at 2309 cm^{-1} in NOClO_4 , and as discussed in chapter 3, this is consistent with anion-cation interaction. At 130 K, ν_{NO^+} had gained intensity and was shifted to 2180 cm^{-1} . The AuCl_4^- modes were considerably sharper and the deformation at ca. 180 cm^{-1} was apparently split. Consistent with similar effects observed in NOBCl_4 , NOSbCl_6 ,⁵⁴ NOAlCl_4^2 etc., a weak broad band was also observed at ca. 275 cm^{-1} which may be attributed to an external mode as discussed in chapter 3.

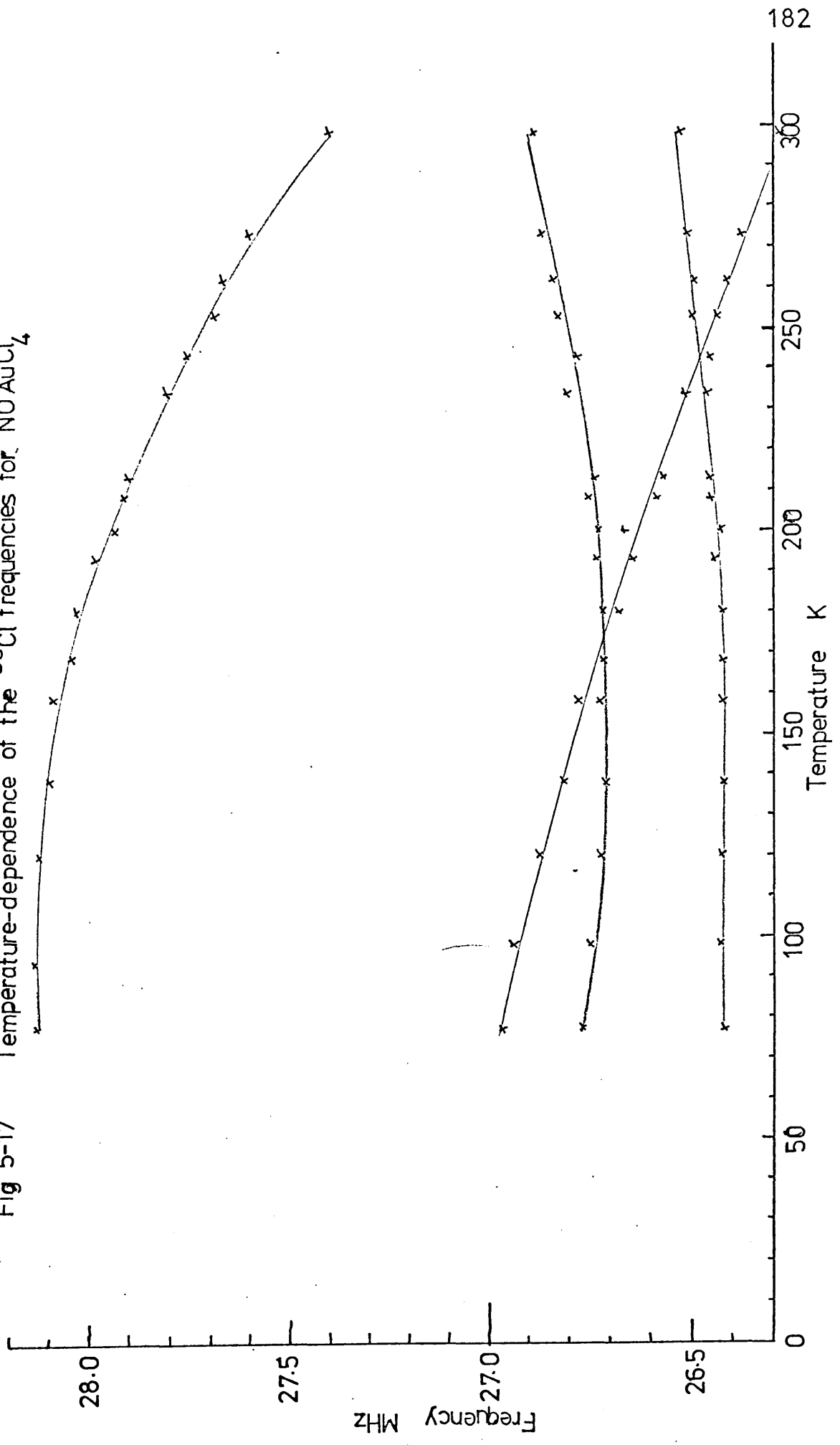
Initial investigation of ^{35}Cl NQR frequencies at 77 K, 193 K, 273 K and 293 K indicated anomalous positive temperature coefficients of certain frequencies. In order to establish the cross-over of lines, a full frequency-temperature study was carried out over the temperature range 77-300 K and results are presented graphically in fig. 5.17. The most interesting feature of this plot is that the two lowest frequencies at 77 K both show anomalous positive temperature coefficients. This is indicative of two chlorine atoms in AuCl_4^- strongly interacting with NO^+ , and possible distorted AuCl_4^- ions are shown in fig. 5.18(a) and (b).

TABLE 5.22

RAMAN SHIFTS FOR $\text{NO}^+\text{AuCl}_4^-$

T = 295 K	ASSIGNMENT	T = 77 K
54 (should)		35 (m) 40 (m) 55 (m) 63 (w) 74 (w) 93 (w)
	LATTICE MODES	
181 (m, br)	$\nu_2 \text{ B}_{1g} \text{ AuCl}_4^-$	181 (m) 190 (should)
	AuCl_4^-	275 (w)
322 (m)	$\nu_4 \text{ B}_{2g} \text{ AuCl}_4^-$	322 (s)
346 (vs)	$\nu_1 \text{ A}_{1g} \text{ AuCl}_4^-$	349 (vs)
2200 (w, br)	$\nu \text{ NO}^+$	2180 (s)

Fig 5-17 Temperature-dependence of the ^{35}Cl frequencies for NO AuCl_4



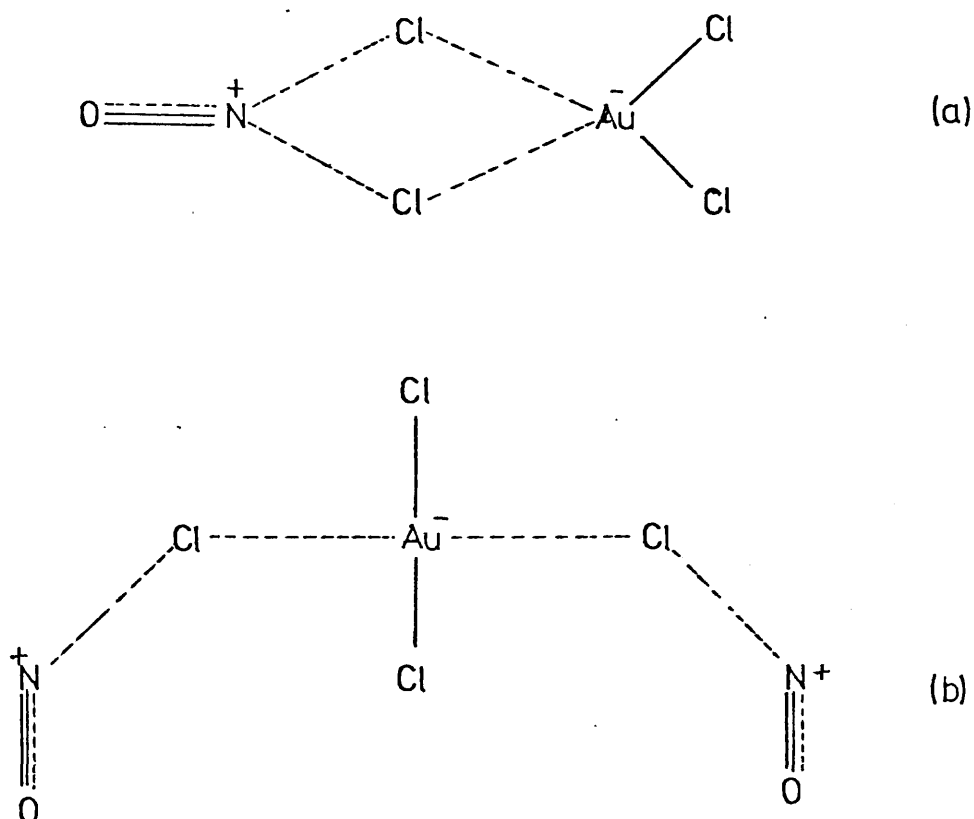


Fig. 5.18

The three shifts observed in the Raman spectrum at low temperatures are more consistent with the centrosymmetric AuCl_4^- species in 5.18(b). It should also be pointed out, however, that the interval between the highest and lowest ^{35}Cl NQR frequencies at both 295 K and 77 K is very much less than in $\text{SbCl}_3^+\text{AuCl}_4^-$ and $\text{SeCl}_3^+\text{AuCl}_4^-$, for which it is concluded that AuCl_4^- is distorted and $\text{TeCl}_3^+\text{AuCl}_4^-$, in which no distortion is evident. NQR data for related NO^+ compounds are again very limited. In NOSbCl_6 , in which similar Raman effects are observed, six ^{35}Cl resonances from SbCl_6^- are observed¹³ at 77 K spread over a narrow range, while only three resonances are apparent at 193 K and 295 K. In this compound therefore there is a definite phase change between 77 K and 193 K. For NOAuCl_4 , this is less obvious from the NQR spectrum.

Study of NOAuCl_4 by DSC is merited and further investigation of NO^+ salts showing strong anion-cation interaction at low temperatures by NQR and X-ray crystallography.

5.8 STRUCTURAL INFORMATION FOR ICl_4^- AND AuCl_4^- SALTS FROM VIBRATIONAL SPECTROSCOPY AND N.Q.R.

In the previous sections, the interpretation of the vibrational spectra of selected ICl_4^- and AuCl_4^- salts was carried out in terms of free ions. In several compounds, a strong anion-cation secondary bonding interaction was postulated, which implies that there is significant covalent character to an otherwise electrostatic interaction.

Absolute confirmation of a secondary bonding interaction is derived from the X-ray crystal structure. However, these are available for only two of the compounds studied, form $1 \text{ SCl}_3^+ \text{ICl}_4^-$ and $\text{KICl}_4 \cdot \text{H}_2\text{O}$, and in both cases substantiate the inferences drawn from spectroscopic studies. In other cases, NQR spectroscopy was used to identify distortion of the ICl_4^- or AuCl_4^- ion, which was considered to arise from a secondary interaction. This was then considered to contribute significantly to a low symmetry electric field created at MCl_4^- ($\text{M}' = \text{Au}, \text{I}$) which was postulated to account for the observed vibrational spectrum. At the end of section 5.2 various questions were raised concerning the extent to which vibrational spectroscopy and NQR might be correlated. An attempt will now be made to discuss these questions in relation to the subsequent results obtained.

The first point for discussion concerns symmetric ions in low symmetry crystal sites. If the associated electric field is very weak, the vibrational spectrum can be adequately interpreted in terms of the

point group symmetry of the free ion. For the compounds studied, crystallographic data substantiating this claim are not available, KICl_4 was considered to be an example within this category since three Raman shifts and one ^{35}Cl NQR frequency are observed. In cases where the interpretation of the vibrational spectrum may be carried out in terms of the site group symmetry - i.e. the associated electric field is strong, then in general two or four ^{35}Cl NQR frequencies from M^+Cl_4^- are observed. Limited examples are available for which the site symmetry is known unequivocally. Thus in CsICl_4 , ICl_4^- ions occupy centrosymmetric (C_{2h}) lattice sites and two ^{35}Cl NQR frequencies are observed - i.e. the electric field imparts centrosymmetric distortion upon ICl_4^- . In $\text{pyH}^+\text{ICl}_4^-$, two ^{35}Cl NQR frequencies from ICl_4^- are observed at low temperature, which are more widely separated than in CsICl_4 . The Raman spectrum could be adequately explained in terms of D_{2h} , C_{2h} or possibly C_{2v} site group symmetry, although in this case there are additional complications from correlation coupling. Nevertheless, subject to crystallographic verification, the electric field had distorted one or both pairs of cis or trans I-Cl bands. In both $\text{KICl}_4 \cdot \text{H}_2\text{O}$ and form 1 $\text{SbCl}_3^+\text{ICl}_4^-$, ICl_4^- ions occupy C_1 lattice sites - the lowest possible site group symmetry. It is significant that by far the largest frequency intervals between the highest and lowest ^{35}Cl NQR lines for ICl_4^- reported are found in these compounds (splitting ≈ 13 MHz at 77 K). In $\text{SbCl}_3^+\text{AuCl}_4^-$ and $\text{SeCl}_3^+\text{AuCl}_4^-$, which may be isostructural with form 1 $\text{SbCl}_3^+\text{ICl}_4^-$, the ^{35}Cl NQR frequency interval for AuCl_4^- is larger than observed for any other AuCl_4^- salt. These limited examples suggest that the ionic distortion is related to the site group symmetry.

The second point for consideration relates to the low symmetry electric field and the frequency interval separating the highest and lowest ^{35}Cl NQR lines. The particular case of interest concerns whether a critical frequency interval for a given ion must be exceeded before changes in the vibrational spectrum are observed. There are insufficient examples with which to discuss this point, but consider as illustrations the two isomorphous compounds $\text{NaICl}_4 \cdot 2\text{H}_2\text{O}$ and $\text{NaAuCl}_4 \cdot 2\text{H}_2\text{O}$. The lowest ^{35}Cl NQR frequency in each salt shows an anomalous positive temperature coefficient, indicative of hydrogen bonding³⁵ so that to a first approximation similar interactive effects are involved. In $\text{NaAuCl}_4 \cdot 2\text{H}_2\text{O}$ the NQR frequency intervals at 77 K and 295 K are 2.1 and 4 MHz respectively. In $\text{NaICl}_4 \cdot 2\text{H}_2\text{O}$ the corresponding values are 2.7 and 3.8 MHz. The Raman spectrum of the former compound is interpreted in terms of C_s symmetry for the anion at both 295 and 77 K. In the latter compound, this only becomes apparent under high resolution at 77 K. That there is a stronger low symmetry field in the case of $\text{NaAuCl}_4 \cdot 2\text{H}_2\text{O}$ may be interpolated from this frequency interval if it is remembered that splittings for ICl_4^- salts tend to be much larger - cf. $\text{SCl}_3^+ \text{AuCl}_4^-$ and form 1 $\text{SCl}_3^+ \text{ICl}_4^-$ with intervals of 5.4 and 13.2 MHz respectively at 77 K. In form 2 $\text{SCl}_3^+ \text{ICl}_4^-$ which is believed to have a related crystal structure - or at least to have ICl_4^- ions in C_s lattice sites, the corresponding frequency interval for ICl_4^- at both 295 K and 77 K is 5.2 MHz. The Raman spectrum can be interpreted in terms of C_s site group symmetry at both temperatures which is not entirely surprising if it is considered that a critical frequency interval for an ion in a specified site exists.

The model used in this study assumes that a secondary interaction distorts the ion by contributing significantly to the low symmetry electric field. From X-ray diffraction, a measure of the strength of a secondary interaction can be derived from the extent to which intermolecular distances are shorter than van der Waal's distances and intramolecular distances are longer than 'normal' bonds (see chapter 4). A rather empirical estimation for a given ion may be derived from NQR frequencies, by considering the following ratios for a given species

- (i) $\frac{\text{highest NQR frequency}}{\text{mean frequency}} \times 100\% = K_H$
- (ii) $\frac{\text{lowest NQR frequency}}{\text{mean frequency}} \times 100\% = K_L$
- (iii) $\frac{\text{frequency interval}}{\text{mean frequency}} \times 100\% = K_{AV}$

These ratios have been calculated for $\text{SCl}_3^+\text{ICl}_4^-$ (forms 1 and 2), $\text{KICl}_4 \cdot \text{H}_2\text{O}$, $\text{NaICl}_4 \cdot 2\text{H}_2\text{O}$, $\text{NaAuCl}_4 \cdot 2\text{H}_2\text{O}$, $\text{SCl}_3^+\text{AuCl}_4^-$, and $\text{SeCl}_3^+\text{AuCl}_4^-$ and the results are presented in table 5.23. In all of these compounds a secondary interaction was postulated, although an anomalous positive temperature coefficient for the lowest ^{35}Cl NQR frequency is not observed in all cases. The extent to which these ratios relate to the strength and symmetry of the electric field created at anion sites, however, remains unknown.

TABLE 5.23

NQR CALCULATIONS FOR ICl_4^- AND AuCl_4^- SALTS

COMPOUND	K_H	K_L	K_{AV}
$\text{SCl}_3^+\text{ICl}_4^-$ (form 1)	123.6	68.9	54.8
	125.2	66.1	59.2
$\text{SCl}_3^+\text{ICl}_4^-$ (form 2)	111.7	88.7	23.1
	111.7	88.8	22.9
$\text{KICl}_4 \cdot \text{H}_2\text{O}$	125.2	74.9	50.3
	125.2	75.0	50.3
$\text{NaICl}_4 \cdot 2\text{H}_2\text{O}$	104.7	92.5	12.3
	106.5	89.0	17.5
$\text{NaAuCl}_4 \cdot 2\text{H}_2\text{O}$	104.4	93.2	11.1
	105.5	90.8	14.7
$\text{SCl}_3^+\text{AuCl}_4^-$	108.6	91.6	16.9
	109.6	90.4	19.3
$\text{SeCl}_3^+\text{AuCl}_4^-$	116.9	87.5	29.4
	118.1	86.9	31.2

* For each example the first value is at 295 K, the second at 77 K.

REFERENCES

1. D.M. Adams, D.M. Morris *J.C.S. A* (1967) 2067-70.
2. P. Barbier, G. Mairesse, F. Wallart, J.P. Wignacourt, *C.R. Acad. Sci. Ser C* (1972) 275 475-8.
3. P. Barbier, G. Mairesse, F. Wallart, J.P. Wignacourt, *C.R. Acad. Sci. Ser C.* (1973) 277 841-4.
4. R.J. Bateman, *Diss Abstr. B* (1969) 30 1616.
5. I.R. Beattie, H. Chudzynska, *JCS A* (1967) 984-90.
6. G. Brauer, *Handbook of preparative inorganic chemistry Vol. 2* Academic Press (1965).
7. P.J. Bray, *J. Chem. Phys.* (1955) 23 703-6.
8. B. Buss, B. Krebs, *Angew. Chem. Internat. Edn.* (1970) 9 463.
9. C.D. Cornwell, R.S. Yamasaki, *J. Chem. Phys.* (1957) 27 1060-7.
10. F.A. Cotton, G. Wilkinson, *Advanced Inorganic Chemistry 2nd Edn.* Wiley (1969).
11. B.O. Cozzini, *Diss Abstr. B* (1966) 27 1850-1.
12. K.B. Dillon, R. Lynch, University of Durham, private communication.
13. J.V. DiLorenzo, R.F. Schneider, *Inorg. Chem.* (1967) 6 766-70.
14. H.E. Doorenbos, J.C. Evans, R.O. Kagel, *J. Phys. Chem.* (1970) 74 3385-8.
15. A.J. Edwards, *J.C.S. Dalton* (in press).
16. R.J. Elema, J.L. de Boer, A. Vos. *Acta. Cryst.* (1963) 16 243-7.
17. J.C. Evans, G.Y.S. Lo, *Inorg. Chem.* (1967) 6 836-7.
18. W.G. Fateley, F.R. Dollish, N.T. McDevitt, F.F. Bentley, *Infra-red and Raman selection rules for molecular and lattice vibrations.* Wiley (1972).
19. J.R. Ferraro, *Low frequency vibrations of inorganic and coordination compounds*, Plenum Press (1971).
20. Z.A. Fokina, S.I. Kuznetsov, E.V. Bryukhova, N.I. Timoshchenko, *Koord. Khim.* (1977) 3 1235-6.
21. M. Feuerhahn, R. Minkwitz, *Zeit. anorg. allgem. Chem.* (1976) 426 247-52.
22. R. Forneris, J. Hiraishi, F.A. Miller, M. Uehara, *Spectrochim Acta.*, (1970) 26A 581-91.

23. R. Forneris, Y. Tavares-Forneris, *J. Mol. Struct.* (1975) 24 205-13.
24. W. Gabes, H. Gerding, *J. Mol. Struct.* (1972) 14 267-79.
25. W. Gabes, Ph.D. Thesis, University of Amsterdam (1973).
26. P.N. Gates, Royal Holloway College, unpublished work.
27. H. Gerding, D.J. Stufkens, *Rev. Chim Miner* (1969) 6 795-815.
- 28.. H. Gerding, D.J. Stufkens, H. Gijben, *Rec. Trav. Chim.* (1970) 89 619-24.
29. R.J. Gillespie, *J. Chem. Ed.* (1970) 47 18-23.
30. I.I. Grandberg, G.K. Faizova, A.N. Kost, *Chem. Abstr.* 66 10453b.
31. J. Hiraishi, T. Shimanouchi, *Spectrochim. Acta.* (1966) 22 1483-91.
32. J.P. Huvenne, P. Legrand, *C.R. Acad. Sci Ser. C* (1972) 274 2073-6.
33. J.P. Huvenne, P. Legrand, *Can. J. Spec.* (1972) 17 105-9.
34. J.P. Huvenne, P. Legrand, B. Boniface, F. Wallart, *Spectrochim. Acta.* (1975) 31A 1937-43.
35. K. Ichida, Y. Kuroda, D. Nakamura, M. Kubo, *Bull. Chem. Soc. Japan* (1971) 44 1996-7.
36. M.P. Jaillard, *Compt. Rend.* (1860) 50 149.
37. M.P. Jaillard, *Ann. Chim. Phys.* (1860) 59 454-6.
38. T.J. Kistenmacher, G.D. Stucky, *Inorg. Chem.* (1968) 7 2150-5.
39. B. Krebs, B. Buss, D. Altena, *Zeit. anorg. allgem. Chem.* (1971) 386 257-69.
40. L. Lindet, *Ann. Chim. Phys* (6) (1887) 11 209-14.
41. H. Morishita, H. Ota, K. Hamada, *Nagasaki Daigaku Kyoikugakubu Shizen Kagaku Kenkyu Kokoku* (1974) 25 61-7.
42. T. Okudu, K. Yamada, Y. Furukawa, H. Negita, *Bull. Chem. Soc. Japan* (1975) 48 392-5.
43. T. Okudu, I. Tomoyasu, K. Yamada, H. Negita, *Bull. Chem. Soc. Japan* (1977) 50 1695-7.
44. S.J. Peake, Ph. D. Thesis, Royal Holloway College, London (1976).
45. R. Ponsioen, D.J. Stufkens, *Rec. Trav. Chim* (1971) 90 521-7.
46. A.I. Popov, J.N. Jessup, *J.A.C.S.* (1952) 74 6127.
47. O. Ruff, *Ber.* (1904) 37 4519.
48. F.J. Ryan, Ph. D. Thesis, Royal Holloway College, London (1972).

49. A. Sasane, T. Matuo, D. Nakamura, M. Kubo, Bull. Chem. Soc. Japan (1970) 43 1908.
50. A. Sasane, D. Nakamura, M. Kubo, J. Mag. Res. (1971) 4 257-73.
51. A. Sasane, D. Nakamura, M. Kubo, J. Mag. Res. (1972) 8 179-82.
52. J. Shamir, J. Raman Spect. (1975) 3 95-9.
53. H. Stammreich, R. Forneris, Spectrochim. Acta. (1960) 16 363-7.
54. D.J. Stufkens, H. Gerding, Rec. Trav. Chim. (1970) 89 1267-70.
55. C.G. Vonk, E.H. Wiebenga, Rec. Trav. Chim. (1959) 78 913-20.
56. W. Warthmann, A. Schmidt, Spectrochim. Acta (1974) 30A 1243-6.
57. R. Weber, Ann. der. Physik und Chem. (1866) 128 459-66.
58. W.W. Wilson, F. Aubke, Inorg. Chem (1974) 13 326-32.

CHAPTER 6

EXPERIMENTAL

6.1 PREPARATIVE

(a) NITRONIUM AND NITROSONIUM SALTS

Volatile and moisture-sensitive reactants used in the synthesis of nitronium and nitrosonium salts proved easier to handle on a vacuum line than in conventional quickfit apparatus. For the purpose of purifying and storing quantities of volatile compounds, the grease-free vacuum system (fig. 6.1) was constructed. Greaseless joints (J. Young Co. Ltd.) and greaseless taps (Jencon Ltd.) were employed to facilitate cleaning, repair and adaptation. The line essentially consisted of two fractionating systems, A and B, and three manifolds, C, D and E, fitted with taps for attaching reaction vessels. Vapour pressure measurements as purity checks were made using the mercury manometer G. The pumping system consisted of a rotary pump (W. Edwards Co. Ltd.) and a mercury diffusion pump.

Nitrosyl chloride (Matheson Co. Ltd.), from a lecture bottle, was fractionated through a trap at -78°C , to remove N_2O_4 , before being condensed and stored in a U-tube at -196°C ; any nitric oxide impurity was pumped away.

Boron trichloride (BDH), supplied in ampoules, was transferred in a glove bag to an ampoule fitted with a greaseless tap, and was degassed several times on the line prior to use; no other purification was attempted.

Dinitrogen tetroxide (Matheson Co. Ltd.), from a lecture bottle, was separated from dinitrogen trioxide (m.pt. -102°C) by slowly drawing the gas through a trap at -78°C and pumping the condensate at

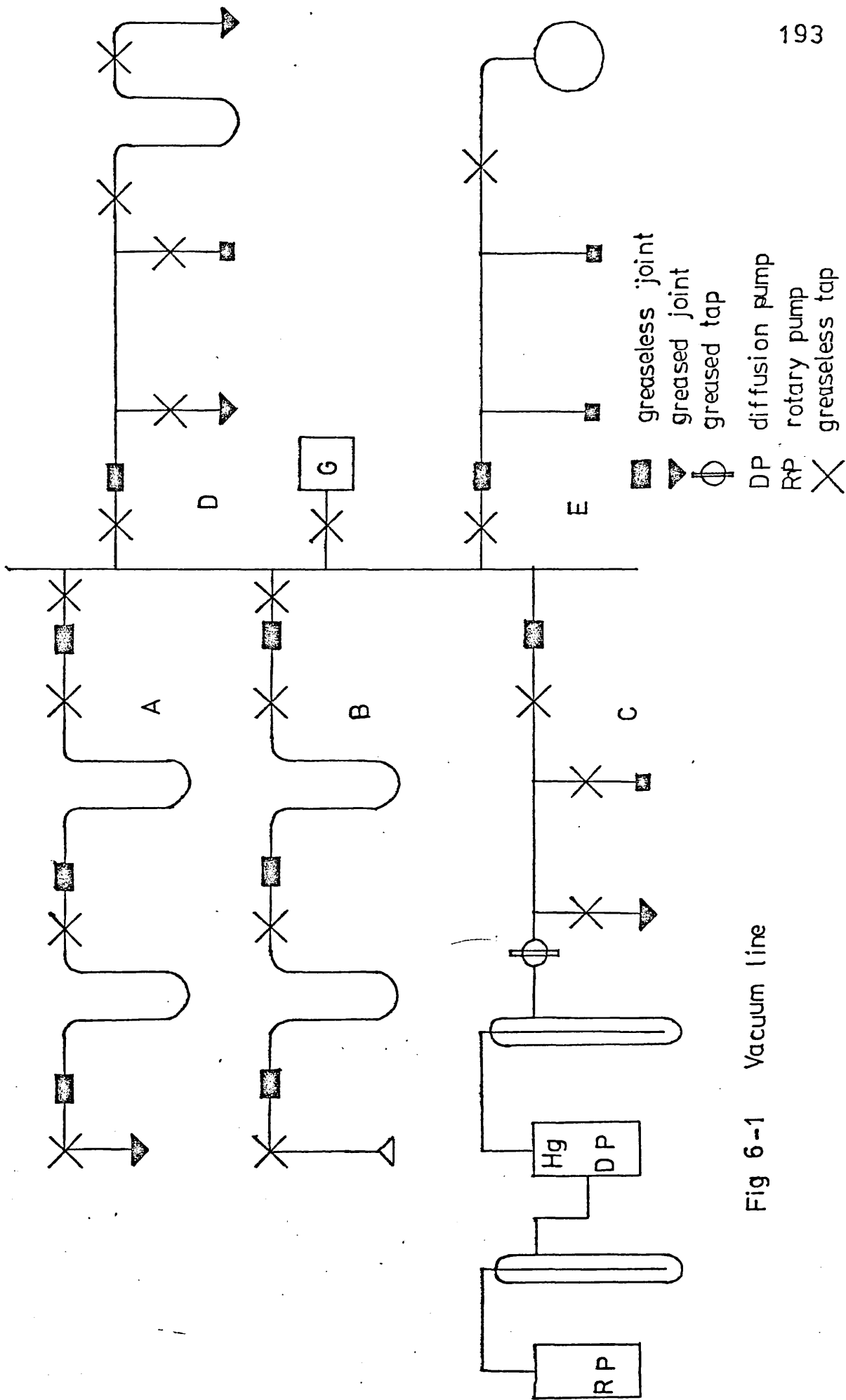


Fig 6--1 Vacuum line

-78° until a colourless glass was obtained on cooling to -196°C.

Nitryl chloride was prepared according to the method of Brauer² from chlorosulphonic acid and freshly-distilled anhydrous nitric acid. The liberated gas was dried over conc. sulphuric acid and collected in the condensation trap (fig. 6-2) at -196° under an atmosphere of dry nitrogen. The product was stored at -78°C on the line.

Hydrogen chloride was generated from conc. hydrochloric acid by dehydration with conc. sulphuric acid using an apparatus previously employed in this laboratory and described elsewhere.¹⁸ The gas was condensed as described in the previous preparation, and stored on the line at -196°C.

Sulphur dioxide (BDH), supplied in a cylinder, was dried with conc. sulphuric acid prior to collection in a U-tube and storage on the line at -196°C.

Chlorine (BDH), supplied in a cylinder, was condensed into a U-tube when required.

NOBCl₄

This was prepared using a modification of the method described by Partington and Whynes.¹¹ BCl₃ (10.6 g, 0.1 mol) was weighed out and transferred to the reaction flask on the line. An equimolar quantity of NOCl (6.1 g) was similarly weighed and condensed into the flask which was then warmed to ca. + 30°C so that two layers separated. Samples for analysis, spectroscopy and thermodynamic measurements were transferred from the cooled reaction flask into the appropriate tubes at -196°C, and pumped at -23°C until a pure white flocculent material remained.

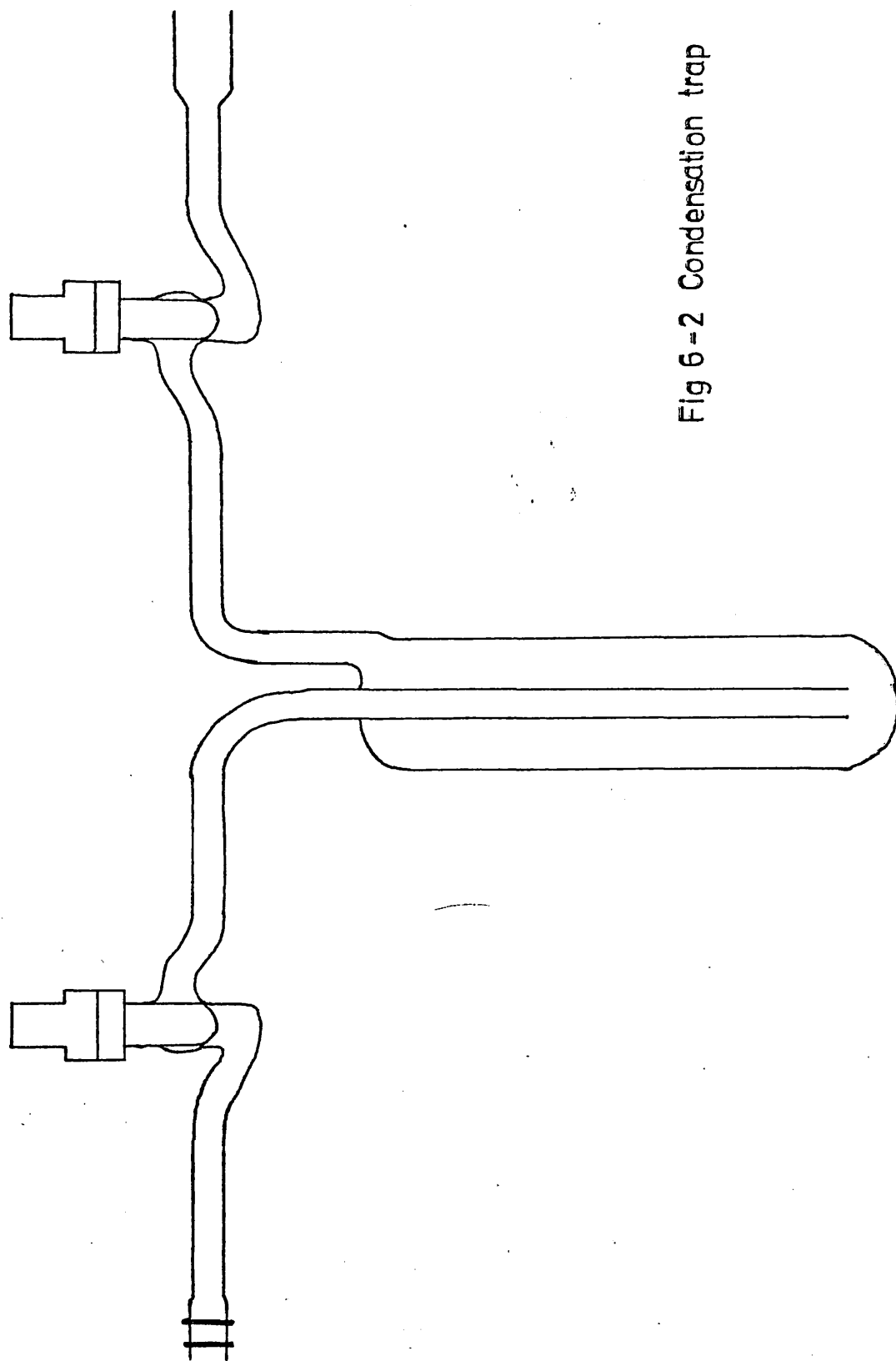


Fig 6 -2 Condensation trap

(Anal.: Found: B = 5.88%, Cl = 77.10%, B:Cl ratio 1:3.99

NOBCl_4 requires: B = 5.92%, Cl = 77.64%, B:Cl ratio 1:4).

NITRYL CHLORIDE-BORON TRICHLORIDE REACTION

Three unsuccessful attempts to prepare this adduct using essentially variations on a method reported by Paul et al.¹² were carried out.

(i) Reaction in $\text{SO}_2(1)$

This preparation followed the method given in ref.12.

BCl_3 (5.3 g, 0.05 mol) was weighed out and transferred at -196°C to a reaction flask together with NO_2Cl in excess of the molar equivalent. SO_2 (50 cm^3) was then condensed into the flask, which was removed from the line and warmed to -45°C . The contents of the flask solidified and the large red lumps deposited did not dissolve in a further quantity of SO_2 (25 cm^3). After 3 hr, the flask was pumped, while slowly raising the temperature from -45°C to ambient. The red colour faded, leaving a white residue which was not readily powdered and for which a Raman spectrum could not be obtained. Dissolution of the residue in water was complete with evolution of SO_2 .

(ii) Reaction in $\text{Cl}_2(1)$

This method is based upon an earlier preparation for $\text{NO}_2\text{Cl}.\text{SbCl}_5$.¹⁹ BCl_3 (5.3 g, 0.05 mol) was weighed out and condensed into the reaction flask containing chlorine (50 cm^3) and an excess of NO_2Cl . The flask was warmed to -78°C and removed from the line, shaken and allowed to stand overnight at -78°C . A green solution was formed which completely volatilised on pumping at -80°C .

(iii) Reaction in HCl (1)

BCl_3 (5.3 g, 0.05 mol) was weighed out and transferred to the reaction flask containing hydrogen chloride (40 cm^3) and an excess of NO_2Cl . The flask was warmed to -96°C , removed from the line and shaken. A straw-coloured solution resulted which completely volatilised on warming to room temperature, indicating that no reaction had taken place.

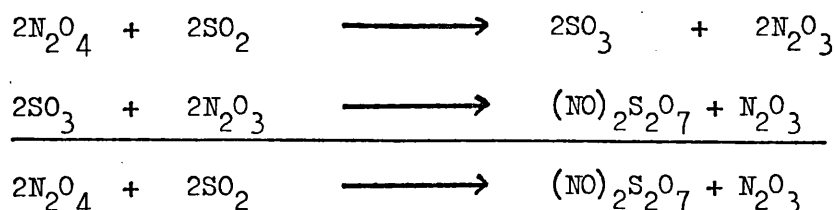
The procedure was repeated using a mixture of HCl (30 cm^3) and SO_2 (20 cm^3) as solvent. On warming to -96°C the liquid slowly changed colour from pale green to bright red, and after one hour, the solvent HCl was gently removed by pumping to leave a viscous red liquid which completely solidified on warming to -45°C . The red solid was rapidly transferred at room temperature to a Raman tube and a spectrum indicating NOCl was recorded. Further pumping of the solid yielded a white powder as in (i).

DINITROSONIUM PYROSULPHATE

The method adopted was essentially that described by Jones et al.⁹ and involved interaction of SO_2 and N_2O_4 (1:1 mole ratio) in a sealed ampoule.

SAFETY NOTE

This reaction does not proceed according to the equation presented⁹ viz:



Reactions carried out in sealed ampoules which were no more than one fifth full resulted in violent explosions. One reaction product is presumably NO, which does not condense under pressure, and the reaction therefore proceeds thus:



A thick-walled (≈ 5 mm) glass ampoule of 50 cm³ capacity was evacuated on the line and carefully cooled to -196°C . Great care was taken to cool the ampoule slowly in order to avoid cracking. N_2O_4 (3 cm³ measured at 0°C) and SO_2 (3 cm³ measured at 0°C) were condensed into the ampoule, which was then carefully sealed and embedded in a bucket of sand. After 24 hr, the ampoule was carefully cooled to -196°C and transferred to a dry box. The tip was fractured in order to release the pressure and the white solid residue was pulverised and transferred to a dry sample tube, which was stored in the glove box [Anal: Found: NO = 25.36%, S = 27.16% $(\text{NO})_2\text{S}_2\text{O}_7$ requires: NO = 27.41%, S = 27.20%].

NITROSONIUM HYDROGENSULPHATE

NOHSO_4 was prepared according to the method of Woolf and Richards,¹⁶ which is essentially a modification of the method of Brauer.² SO_2 gas was slowly passed into a well-stirred solution of nitric acid 98% - glacial acetic acid (3:1 v/v, 100 cm³) at 0°C . The precipitate was filtered through a No. 1 glass sinter with protection from moisture and washed successively with aliquots (20 cm³) of glacial acetic acid and carbon tetrachloride. The product was dried in vacuo over anhydrous magnesium perchlorate for several hours and then transferred to a sample

tube and stored in the dry box. N.B. P_2O_5 is not a suitable desiccant since the compound acquires a pink colouration after several hours. [Anal: Found: NO = 23.66%, S = 25.33% $NOHSO_4$ requires NO = 23.61% S = 25.18%].

NITROSONIUM PERCHLORATE

$NOClO_4$ was prepared by a laboratory scale modification of a patented industrial process.¹⁴ The apparatus employed (fig. 6.3) consists of a reaction flask A and a solvent reservoir B from which reactants can be transferred to A by application of a positive dry nitrogen pressure at C. Fuming nitric acid (15 cm^3) was placed in the flask A which was cooled in an ice-salt bath. N_2O_4 (30 cm^3) was condensed into B and then transferred to C. Perchloric acid (70%, $14.3 \text{ g } 8.4 \text{ cm}^3$) was placed in B and added dropwise to A with vigorous stirring. The precipitated $NOClO_4$ which slowly formed was filtered through a sinter, with protection from moisture, and dried overnight in an evacuated desiccator over anhydrous magnesium perchlorate.

SAFETY NOTE

On no account should $NOClO_4$ be mixed with organic solvents, as violent explosions have been reported. [Anal: Found: NO = 23.15%, Cl = 27.30% $NOClO_4$ requires NO = 23.17%, Cl = 27.39%].

(b) TETRACHLOROIODATE SALTS

(1) JAILLARD'S CRYSTALS - STABLE MODIFICATION

The stable modification of Jaillard's compound,⁸ $SCl_3^+ ICl_4^-$, may be conveniently prepared by chlorinating a mixture of iodine and sulphur using the apparatus shown in diagram 6.4.

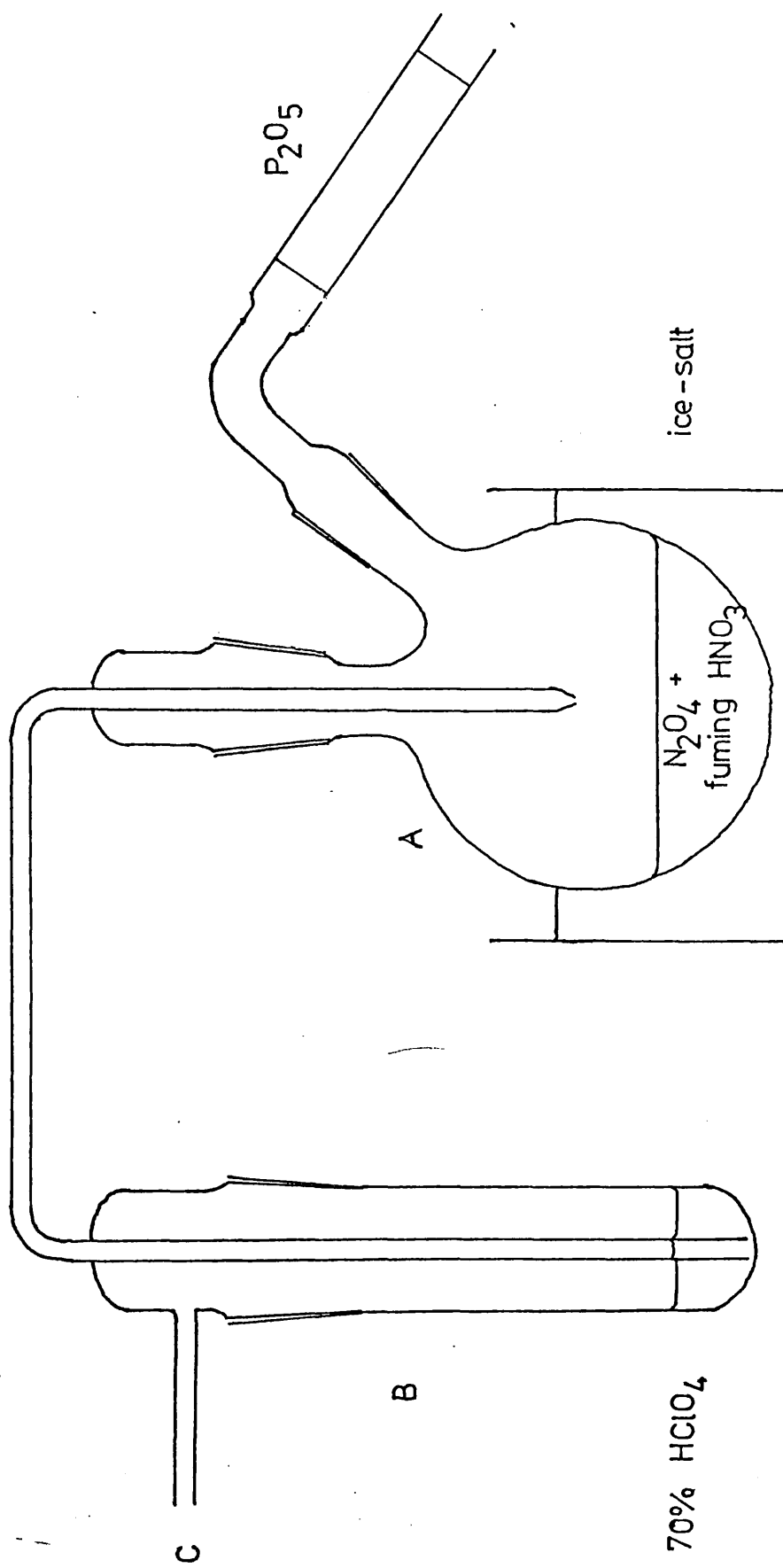


Fig 6-3 Apparatus for the preparation of NOClO_4

Sulphur (1 g) and iodine (1 g) were finely ground together and introduced into the bulb A through the ground glass joint B. The integral Raman tube was fitted to B and a very slow stream of dry chlorine was passed through, initiating immediate reaction with the formation of a viscous red liquid. The flask A was occasionally agitated to ensure complete dissolution of the iodine while the temperature rose to 60°C. After 1 hr., the solution began to deposit orange crystals and the current of chlorine was passed until all excess SCl_2 had been displaced. The orange-yellow crystalline mass was broken up with a glass rod, while passing a current of chlorine, and samples transferred to various tubes fitted to B for analysis and spectroscopic studies [Anal: Found: I = 31.14% Cl = 60.70%, SICl_7 requires I = 31.17% Cl = 60.96%].

N.B. This method has occasionally given the unstable modification, but the latter can be exclusively prepared as follows.

(2) JAILLARD'S CRYSTALS - UNSTABLE MODIFICATION

The metastable form of Jaillard's compound, $\text{SCl}_3^+ \text{ICl}_4^-$, can be prepared from ICl_3 and SCl_2 in either CHCl_3 or excess of SCl_2 as solvent.

Finely powdered iodine (1 g) was transferred to a two-neck round-bottom flask, one inlet being fitted with a gas inlet tube and the other fitted with an upright water-cooled condenser fitted with a P_2O_5 guard tube. Chlorine was condensed into the flask at -80°C and the slurry was stirred for 1 hr. The flask was slowly warmed to room temperature so that excess chlorine vaporised, and SCl_2 (30 cm^3) was added to the flask and the mixture refluxed gently to ensure complete dissolution of ICl_3 . The solution was then cooled to room temperature and the

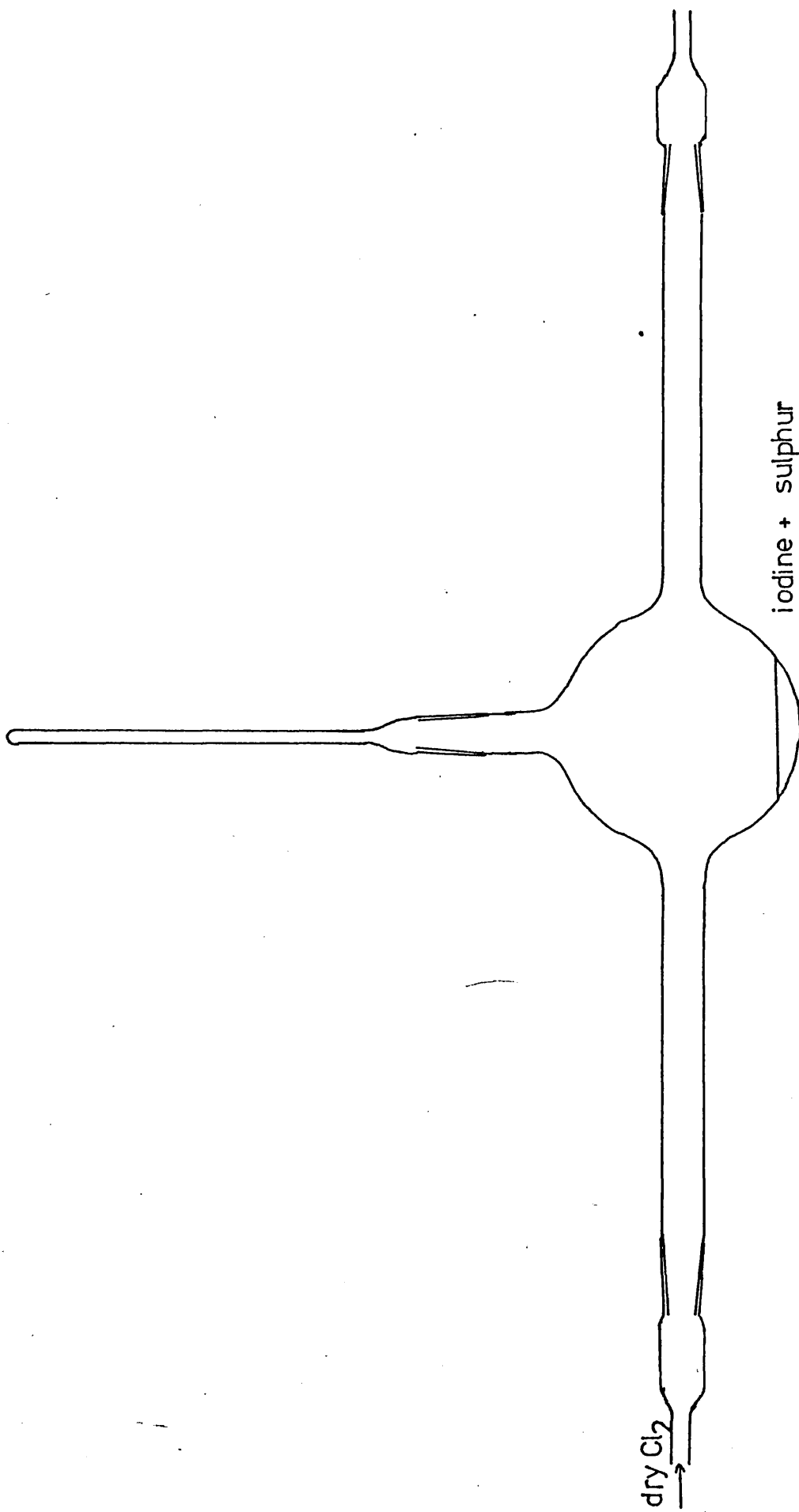
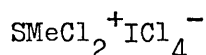
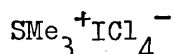


Fig 6 -4 Apparatus for the preparation of Form 1 $\text{SCl}_3^+ \text{ICl}_4^-$

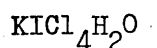
product precipitated by passing a current of dry chlorine. Excess SbCl_2 was separated by decantation, the last traces being removed in a current of chlorine. [Anal: Found: I = 30.99% Cl = 60.97%, SbCl_7 requires I = 31.17% Cl = 60.96%].



The preparation of this novel compound was based upon the method reported²⁰ for $\text{SMeCl}_2^+ \text{SbCl}_6^-$. Finely powdered iodine (2 g, 0.016 mol) was dissolved in CH_2Cl_2 (100 cm^3) contained in a 250 cm^3 three-neck round-bottom flask fitted with a gas inlet tube, a condenser with CaCl_2 guard tube and a pressure-equalising dropping funnel. A current of chlorine was passed through the flask until a brown solution of ICl_3 resulted. Me_2S_2 (0.74 g, 0.008 mol) in CH_2Cl_2 (50 cm^3) was slowly added to the stirred flask to precipitate a yellow flocculent material which was separated from the solvent by decantation, then washed with 3 x 10 cm^3 aliquots of cold CH_2Cl_2 and dried in a current of chlorine. [Anal: Found: I = 33.22% Cl = 54.83%, SCH_3ICl_6 requires I = 32.82% Cl = 55.04%].



This was prepared by chlorinating SMe_3I (2 g) in glacial acetic acid (200 cm^3) containing 1% water according to Popov.¹⁵ The crystals were filtered by suction, washed with dry CCl_4 and dried in an oven overnight at 50°C. [Anal: Found: I = 36.2% Cl = 40.6% SMe_3ICl_4 requires I = 36.7% Cl = 41.0%].



This was prepared by reacting KIO_3 with concentrated hydrochloric acid according to Filhol.⁴ The method used for drying the product

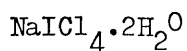
is most important and the crystals should be stored in a stoppered vial.

Finely powdered KIO_3 (15 g) was slowly added, with stirring, to conc. HCl (50 cm^3) contained in a conical flask whereon the temperature rose and chlorine gas was evolved. The solution slowly deposited needle-shaped crystals which were filtered by suction, pressed between filter papers and dried in a desiccator over CaCl_2 for not more than 1 hr. [Anal: Found: I = 38.60% Cl = 44.03%, $\text{KICl}_4 \cdot \text{H}_2\text{O}$ requires I = 38.94% Cl = 43.52%].

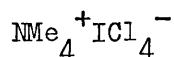
KICl_4

This may be prepared by dehydrating $\text{KICl}_4 \cdot \text{H}_2\text{O}$ with thionyl chloride, but it was found that a purer product resulted from a modification of the method of Brauer² involving the reaction of KIBr_2 with SO_2Cl_2 rather than chlorine.

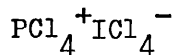
KIBr_2 (10 g), prepared according to the method of Brauer,² was weighed into a 100 cm^3 two-neck flask fitted with a gas inlet tube and CaCl_2 guard tube, and covered with SO_2Cl_2 (50 cm^3). Stirring the mixture resulted in copious evolution of bromine fumes which were periodically displaced from the flask by a current of dry nitrogen. After several hours, the pale yellow powder remaining was separated by decantation and washed with 2 x 10 cm^3 aliquots of SO_2Cl_2 , the last traces of which were removed in a current of chlorine. [Anal: Found: I = 40.86% Cl = 46.01% KICl_4 requires I = 41.23% Cl = 46.07%].



This was prepared according to the method of Gutierrez de Celis⁷ by dissolving NaCl (5 g) in HCl solution (7% w/v, 10 cm³) and adding iodine (10 g). A yellow crystalline material was precipitated from solution by passing a current of chlorine. The crystals were filtered by suction, pressed between filter papers to remove the mother liquor and dried in a desiccator over CaCl₂ for 1 hour. [Anal: Found: I = 38.36% Cl = 42.53%, NaICl₄·2H₂O requires I = 38.71% Cl = 42.92%].



This was prepared by modification of a method reported by Buckles³, NMe₄Cl (2.4 g, 0.022 mol) was dissolved in glacial acetic acid containing 8% CCl₄ (40 cm³) contained in a two-neck round-bottom flask fitted with a CaCl₂ guard tube and a solid addition tube containing ICl₃ (4.7 g, 0.02 mol), which was slowly added to the well-stirred solution. The pale-yellow product separating was filtered by suction, washed with CCl₄ and dried in vacuo. [Anal: Found: I = 36.70% Cl = 41.42% NMe₄ICl₄ requires I = 37.03% Cl = 41.4%].



This was prepared from ICl₃ and PCl₅ in CH₂Cl₂ by analogy with the preparation of SMeCl₂ICl₄ [Anal: Found: I = 28.63% Cl = 64.10%, IPCl₈ requires I = 28.74% Cl = 64.24%].

(c) TETRACHLOROAUROATE SALTS

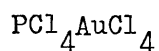
The starting material for the subsequent preparations was auric chloride, Au_2Cl_6 , which was prepared from sodium tetrachloroaurate dihydrate, on loan from Johnson-Matthey Chemicals, by the following method.

$\text{NaAuCl}_4 \cdot 2\text{H}_2\text{O}$ (10 g) was dissolved in water (30 cm^3) and the solution saturated with SO_2 gas. The brown suspension of colloidal gold obtained was heated to boiling, in order to remove excess SO_2 , and coagulate the gold, which was separated by decantation and washed several times with hot distilled water. The pure gold was completely dissolved in aqua-regia (30 cm^3), warming gently to initiate the reaction, and the excess nitric acid removed from solution by boiling with aliquots of concentrated hydrochloric acid (10 cm^3) until evolution of brown fumes ceased. The solution was evaporated to low volume on a water-bath and set aside to crystallise in a desiccator. The crystalline chloroauric acid, $\text{HAuCl}_4 \cdot n\text{H}_2\text{O}$, was dehydrated in a current of dry chlorine at a temperature not exceeding 200°C . The water condensing at the cool ends of the furnace tube was periodically removed with a tissue. When dehydration was complete, (usually after 3 h.) the dark red auric chloride was stored in a desiccator over P_2O_5 .

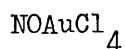
IMPORTANT

It is essential that auric chloride used in subsequent preparations should be completely dry, otherwise impure products are obtained. It is advisable to continue heating in a stream of chlorine for 30 min. after evolution of water has apparently ceased.

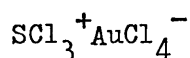
Gold residues recovered from subsequent preparations were converted similarly to auric chloride. Residues contaminated with selenium or tellurium, however, required an intermediate purification step since sulphur dioxide precipitates both of these elements in addition to gold. The contaminated gold was therefore boiled several times with aliquots of distilled water until the decanted liquid contained only traces of chloride. The gold was then separated by boiling the residue with concentrated nitric acid which dissolved the selenium and tellurium.



This was prepared according to the method of Groeneveld⁵ by reacting auric chloride with PCl_5 in phosphorus oxychloride as solvent. [Anal: Found: Cl = 54.7% Au = 38.0% PAuCl_8 requires Cl = 55.4% Au = 38.5%].



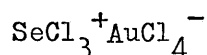
This preparation is a modification of the method of Partington and Whynes.¹¹ An excess of NOCl , which had been dried by passing through a column of type 4A molecular sieve, was condensed at -78°C on to Au_2Cl_6 (3.0 g) contained in a two-neck round-bottom flask fitted with a gas inlet-tube and a CaCl_2 guard tube. The resulting slurry was stirred at -78°C for 60 min. and then warmed to room temperature so that excess NOCl evaporated, the final traces being removed in a current of dry nitrogen, leaving a pale yellow powder [Anal: Found: Cl = 38.8% Au = 52.7% NOAuCl_4 requires Cl = 38.45% Au = 53.4%].



This has been prepared by heating gold with SCl_2 in a sealed tube by Lindet,¹⁰ but a simplification was used starting from auric chloride.

Au_2Cl_6 (3 g) was added to freshly-distilled SCl_2 (50 cm^3) contained in a two-neck round-bottom flask (100 cm^3) fitted with a gas inlet tube and a vertical water-cooled condenser protected by a CaCl_2 guard tube. The flask was gently warmed to 60°C and a slow stream of chlorine was passed through until the yellow precipitate initially formed was free from particles of gold. Excess of SCl_2 was decanted in a stream of chlorine which was passed through the flask until the last traces had vaporised. [Anal: Found: Cl = 52.02% Au = 40.87% AuSCl_7 requires Cl = 52.01% Au = 41.27%].

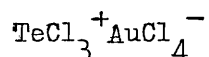
NOTE: Some reduction of Au_2Cl_6 on addition to SCl_2 was always noted even if the latter had been presaturated with chlorine.



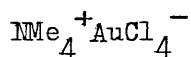
The preparation from gold and selenium with arsenic trichloride has been reported by Lindet,¹⁰ but a modification of the method using SeCl_4 and Au_2Cl_6 was employed.

Selenium (0.94 g 0.012 mol) was suspended in AsCl_3 (50 cm^3) contained in a three-neck round-bottom flask fitted with a gas inlet tube, a vertical water cooled condenser protected by a CaCl_2 guard tube and a solid addition tube. A current of dry chlorine was passed through the suspension, forming a white precipitate of SeCl_4 which was heated under reflux, and small quantities of POCl_3 were added until a homogeneous solution resulted. The dissolution process is very slow and additional AsCl_3 may also be added if necessary. Au_2Cl_6 (3.6 g 0.012 mol) was added to the hot solution and refluxing was continued in a current of dry chlorine for 60 min. An orange crystalline solid precipitated and was separated from the mother liquor by decantation, washed in the flask with $2 \times 10 \text{ cm}^3$ aliquots of SO_2Cl_2 and dried in a

current of chlorine [Anal: Found: Cl = 46.95 Au = *, SeAuCl_7 requires Cl = 47.35% Au = 37.58%].



This compound has not been previously reported. The preparation was analogous to that for $\text{SeCl}_3^+ \text{AuCl}_4^-$ from Te and Au_2Cl_6 but the initial refluxing to dissolve TeCl_4 is not required since it is much more soluble in AsCl_3 . [Anal: Found: Cl = 43.13% Au = *, TeAuCl_7 requires Cl = 43.33% Au = 34.39%].



This was prepared from $\text{NaAuCl}_4 \cdot 2\text{H}_2\text{O}$ and NMe_4Cl in aqueous solution according to Goggin⁶ [Anal: Found: Cl = 34.39% Au = 47.40%, $\text{NMe}_4\text{AuCl}_4$ requires Cl = 34.34% Au = 47.70%].

Samples of $\phi\text{PCl}_3^+ \text{ICl}_4^-$, $\phi_3\text{PCl}^+ \text{ICl}_4^-$, $\text{pyH}^+ \text{ICl}_4^-$, $\text{pyD}^+ \text{ICl}_4^-$, $\text{NMe}_3\text{H}^+ \text{ICl}_4^-$, $3\text{-ClpyH}^+ \text{ICl}_4^-$ and $\phi_2\text{I}^+ \text{ICl}_4^-$ were prepared and analysed at Durham University.

6.2 ELEMENTAL ANALYSIS

Elemental analysis was carried out on all compounds using literature methods suitably modified where necessary.

(a) NO^+

Various methods for the direct analysis of NO^+ by an indirect titration with KMnO_4 in a strong sulphuric acid medium have been reported^{17,21} but were found to give very poor reproducibility. On certain occasions, when Fe(II) was used to estimate the unreacted KMnO_4 , the solution turned cherry-red and a low analysis was obtained. These methods were considered to be very unsatisfactory and Devarda's method,¹ described below, was subsequently used in all cases.

The sample (0.2 g) was reacted with very strong caustic soda, pH > 12, (150 cm³) contained in a stoppered flask, care being taken not to lose gaseous product. After 30 min the flask was fitted with a splash head and water-cooled condenser, with the receiver dipping below the surface of a saturated solution of boric acid (50 cm³). Powdered Devarda's alloy (2 g) was added to the reaction flask which was warmed gently to initiate reaction. When the reaction had subsided the solution was gently boiled and 100 cm³ of distillate collected. The liberated ammonia was titrated directly with 0.1M H₂SO₄ to a potentiometric or methyl orange end point.

(b) Boron

Boron, as boric acid after hydrolysis, was determined directly by potentiometric titration with standard alkali in the presence of mannitol according to the method of Belcher and Nutten.¹

(c) Sulphur

Sulphur was determined gravimetrically as barium sulphate according to the method described by Belcher and Nutten.¹ In the presence of oxides of nitrogen it proved essential to evaporate the solutions to low volume several times with hydrochloric acid prior to starting the analysis in order to avoid high answers.

(d) ClO₄⁻

Although Ti(III)¹ is known to reduce ClO₄⁻ to Cl⁻, which may then be determined potentiometrically (see below), this method was found to give high results when using commercial titanium (III) sulphate since a high impurity level of chloride is invariably present. A large excess of Ti(III) is required since an eight electron reduction

is involved. The reduction was more conveniently carried out by fusing the perchlorate salt (0.25 g) with twenty times its own weight of anhydrous K_2CO_3 at $700 - 800^\circ C$ for several hours,¹⁷ the residue being extracted with N/1 H_2SO_4 (40 cm^3).

(e) Cl^-

Chloride ion was determined by potentiometric titration with 0.1M Ag^+ in a buffered medium (0.2M in acetic acid, 0.2M in sodium acetate)¹ using a commercial silver electrode with internal reference (Metrohm, Switzerland). Great care was taken to protect solutions from light at all times during the titration. Determinations were also carried out using the standard Volhard procedure.¹

(f) ICl_4^-

Tetrachloroiodate salts were reduced with aqueous sulphur dioxide in a stoppered flask, the excess being removed by boiling. The iodide and chloride ions in solution were determined in a buffered medium by potentiometric titration with Ag^+ as for Cl^- . Since the solubility product of AgI is less than that for $AgCl$, the first step in the potentiometric titration graph corresponds to the iodide equivalence point and the second step to the total halide equivalence point¹ (see fig. 6.5).

(g) $AuCl_4^-$

Tetrachloroaurate salts were reduced with aqueous sulphur dioxide as above, and the solution boiled to remove excess sulphur dioxide and to coagulate the gold, which was collected on a No.541 ashless filter paper, washed several times with hot water and ignited

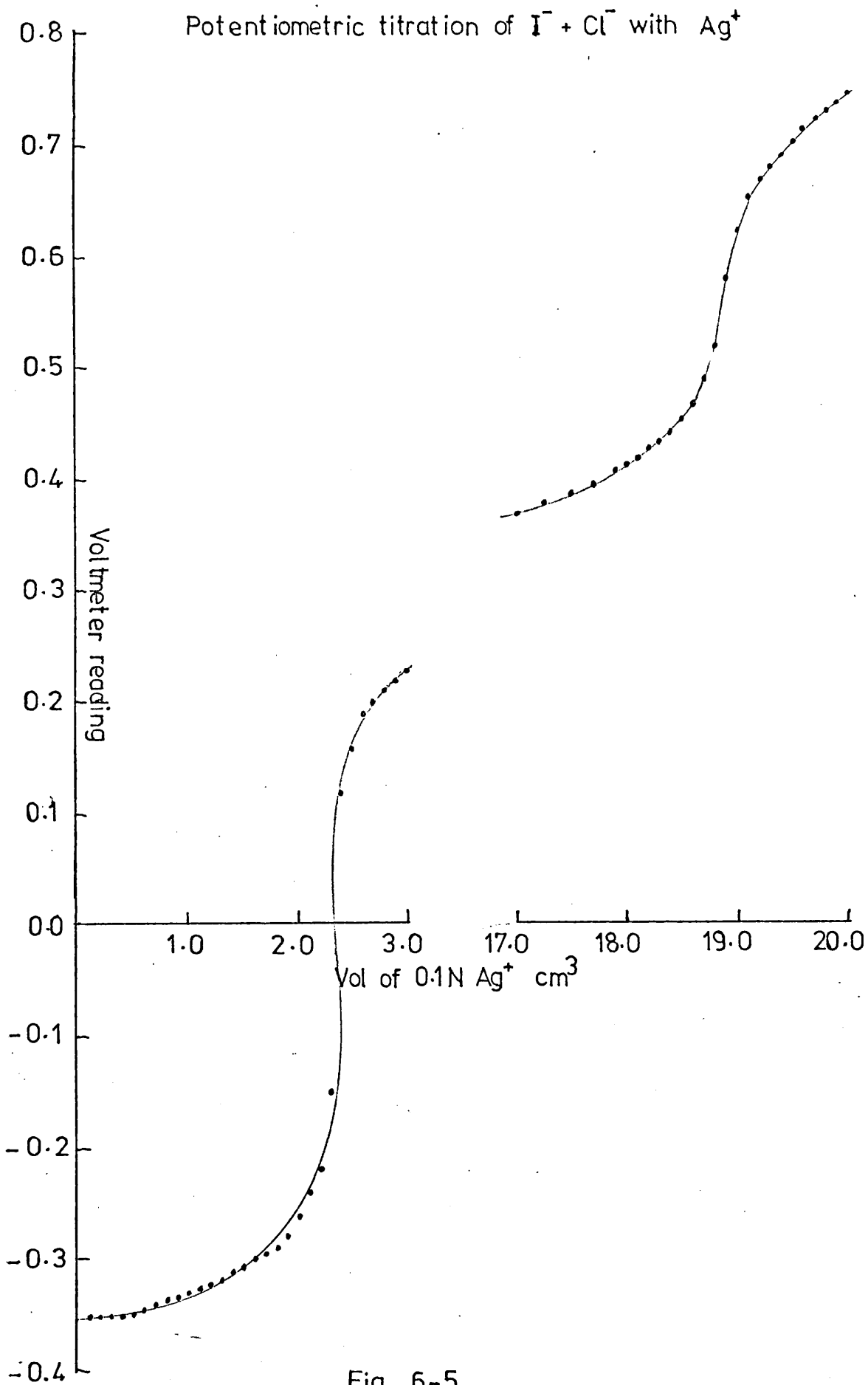


Fig 6-5

at 700°C to constant weight. In general slightly low answers were obtained by this method, the limitation being the small scale employed. In the cases of $\text{SeCl}_3^+\text{AuCl}_4^-$ and $\text{TeCl}_3^+\text{AuCl}_4^-$ a gold analysis was not possible owing to the difficulties associated with separation from selenium and tellurium. The filtrate and washings were combined and analysed for chloride by potentiometric titration with Ag^+ .

6.3 SOLUTION CALORIMETRY

Enthalpies of reaction of nitrosonium salts with 0.1M aqueous sodium hydroxide were measured using a solution reaction calorimeter, operated in a partial differential isoperibol mode and which had been constructed in this laboratory and fully described elsewhere.¹³ In order to protect the underside of the aluminium lid of the reaction vessel from corrosion by oxides of nitrogen, it was periodically coated with a film of teflon from a spray dispenser.

Since reactions were carried out under nitrogen, the fragile ampoules were filled in a dry box as follows in order to avoid touching the delicate bulbs. The fragile ampoule was rested vertically upon a small cotton-wool plug contained inside a small plastic tube and weighed with a B5 test tube fitted with a lightly-greased stopper. The ampoule was fitted into the small clamp (see fig. 6.6) so permitting manipulation in the dry-box. A small quantity of nitrosonium salt was added by means of a small funnel and the greased B5 stopper transferred to the ampoule, avoiding any loss of grease, which was then reweighed together with the open B5 test tube. The B5 stopper was then replaced

Clamp for manipulating solution calorimeter ampoules
in the glove-box

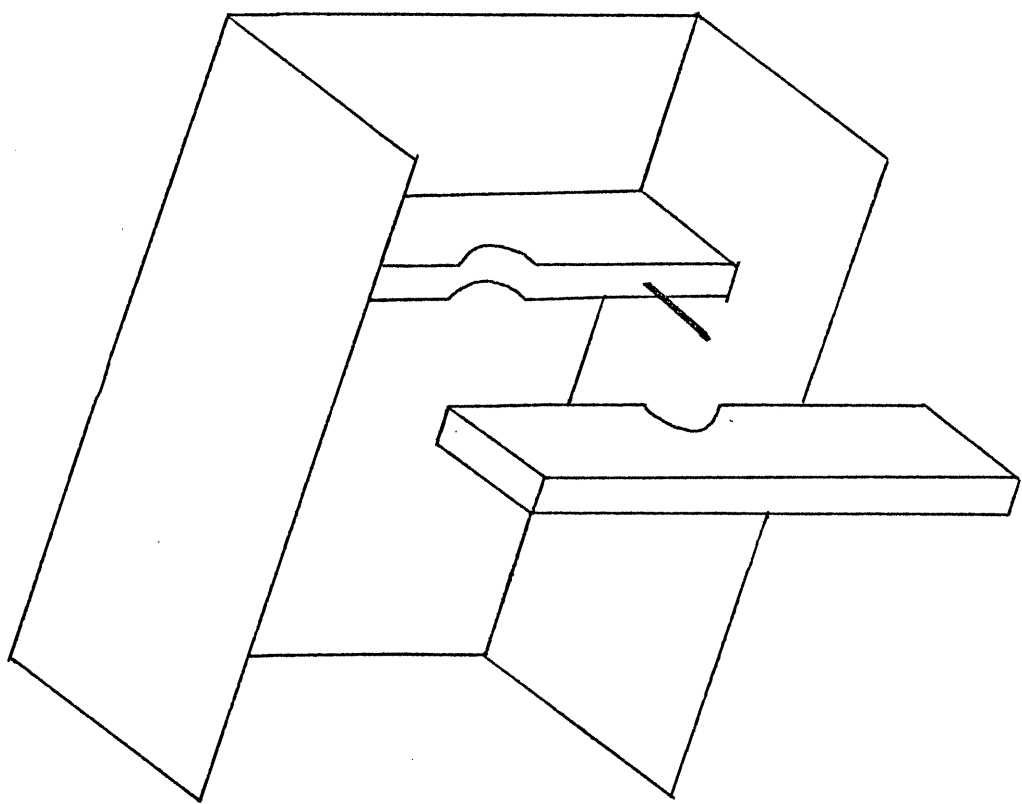


Fig 6-6

by the ampoule holder under nitrogen and mounted into the calorimeter. The cooling fin was removed from the lid and a slow current of nitrogen passed through. The calorimetric fluid prepared in boiled-out deionised water was introduced by a pipette, ensuring at all times that the level of liquid in the calorimeter vessel was not less than one inch below the nitrogen inlet tube. The current of nitrogen was gently blown across the surface of the stirred calorimetric fluid to cool the vessel to 25°C. The nitrogen inlet was then removed and the non-vented vessel sealed with a small rubber bung.

In order to determine the stoichiometry of the thermochemical reaction, post-calorimetric analyses for nitrite and total nitrogen in solution were performed on reactions carried out in a vessel of 200 cm³ capacity. This was of similar design to those of 100 cm³ capacity except that a nylon rather than an aluminium lid was fitted.

PROCEDURE FOR POST-CALORIMETRIC ANALYSIS

A scale of 0.2 - 0.3 g of nitrosonium salt was employed. Before proceeding with the analysis, the air-space and solution were purged with nitrogen gas for 5 min in order to remove all nitric oxide gas.

(i) NITRITE ANALYSIS

0.1N KMnO_4 (25.0 cm³) was transferred to a beaker and diluted to 250 cm³ with distilled water. Concentrated sulphuric acid (5 cm³) was added and the solution heated to 40°C. An aliquot of the test solution (50.0 cm³) was slowly added with the tip of the pipette dipping below the surface of the liquid. The solution was cooled to room temperature and 0.1N Fe(II) solution (25 cm³) was added and the excess back-titrated with 0.1N KMnO_4 .

(ii) NITRITE AND NITRATE ANALYSIS

An aliquot of test solution (100.0 cm³) was made strongly alkaline (pH > 12) and reduced with Devarda's alloy as in the analysis for NO⁺.

(iii) NITRIC OXIDE

It was not possible to measure NO directly using this small scale, and so it was determined by difference using the nitrogen content of the sample initially weighed out and the results of the previous two analyses.

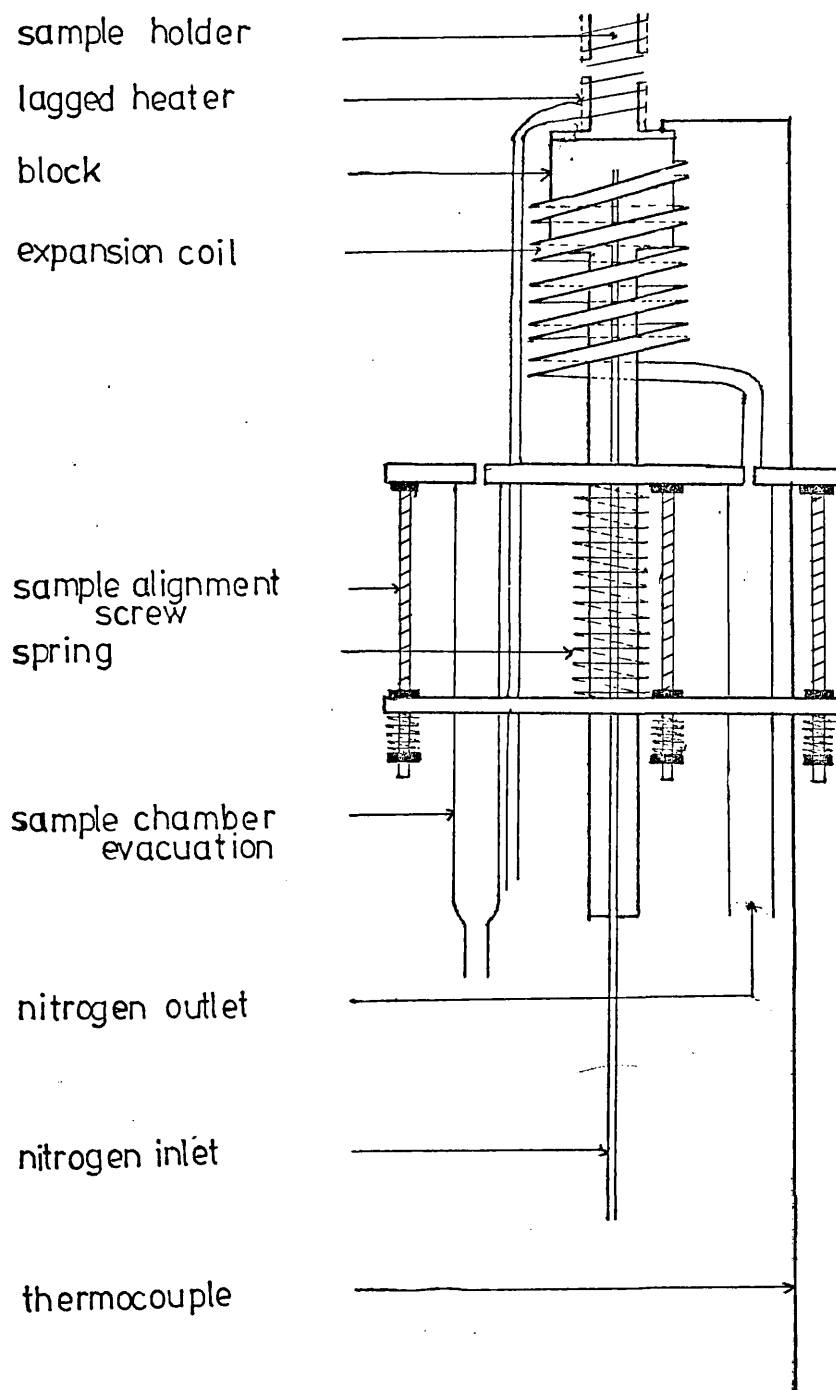
The limitation of this analytical procedure is discussed in Chapter (2) and illustrated in appendix (1).

6.4 VIBRATIONAL SPECTROSCOPY

Raman spectra were recorded using a CODERG PHO RAMAN SPECTROMETER^A with Kr⁺ laser excitation (COHERENT RADIATION). The exciting lines employed were 647.1 nm (red), 568.2 nm (yellow-green) and 530.8 nm (green). Solid samples were sealed in melting point tubes or in discarded n.m.r. tubes of 5 mm diameter. Volatile compounds prepared on a vacuum line were condensed and sealed into tubes made from thin-wall tubing of total diameter 7.5 mm and wall thickness of less than 1 mm. The latter tubes were used when making low temperature measurements.

The cold cell is illustrated in fig. 6.7, the initial work on NOBCl₄ was carried out when no heater control unit was available and so all spectra obtained were at temperatures approaching -196°C. Subsequent work at fixed temperatures employed a proportional temperature control

Fig 6-7 The Raman cold cell



unit (Beckman R.I.I.C. London). The chief disadvantage of the assembly is the uncertainty of the temperature at which spectra are recorded. The thermocouple is fitted to the base of the sample holder and even if good thermal contact between holder and sample tube is achieved, there are still several limiting factors:

- (i) The temperature gradient between the base and top of the sample holder.
- (ii) The temperature gradient across the sample tube.
- (iii) The heating effect of the laser on the sample.

The first two factors can be overcome by allowing the sample to equilibrate in vacuo; the third factor is dependent upon the sample colour and laser line employed. An assessment of the error in the recorded temperature on the proportional controller was attempted by measurement of the transition temperature in $\text{pyD}^+\text{ICl}_4^-$, and comparing this with the value of -58°C obtained from differential scanning calorimetry (DSC). However, numerous problems associated with the change in the Raman spectrum during the phase transition were experienced (see Chapter 5) and the attempt proved unsuccessful.

Far infra-red spectra at low temperatures were measured in the range $200\text{--}400\text{ cm}^{-1}$ using a P.E. 325 double beam spectrophotometer. In the range $50\text{--}400\text{ cm}^{-1}$, infra-red data were derived from the Fourier transform of the interferogram recorded using a Grubb-Parsons Cube interferometer. In all cases the solid samples were mounted between RIGIDEX plates of 2 mm thickness either as a thin layer of the solid or as a thin dispersion in nujol.

6.5 TENSIMETRY

Pressure measurements were obtained using a commercial quartz gauge (Texas Instruments, precision gauge model No.144) which measures the torque exerted on a stretched quartz spiral when a pressure difference is applied across the ends. The gauge factor was determined by measuring the vapour pressure of pure distilled water over the temperature range 290 K to 306 K, analar acetone (BDH, dried over anhydrous calcium sulphate) over the temperature range 210 K to 250 K and analar benzene (BDH) over the temperature range 210 K to 255 K. These compounds were condensed and sealed under vacuum into break-seal ampoules which were blown onto the sample line of the gauge. The system was then evacuated on both sides of the spiral in order to set the meter zero. Above 290 K samples were immersed in a well-stirred water bath whose temperature was maintained using a mercury contact thermometer. Low temperature baths were prepared by mixing liquid nitrogen with pure organic solvents in a dewar vessel until a well-stirred slush was obtained. NOBCl_4 was similarly condensed into a break-seal ampoule. The compounds were immersed in a bath at the lowest temperature to be studied, and exposed to the gauge by fracturing the break-seal with a glass-covered magnetic follower. In the case of NOBCl_4 only, the sample was pumped at 210 K until a white flocculent material resulted. At high temperatures, thermal equilibrium was attained after 15-20 min and the gauge reading was recorded after 30 min. Using the low temperature baths, the gauge reading after 15-20 min was recorded in order to avoid replenishing the bath during a measurement.

6.6 DIFFERENTIAL SCANNING CALORIMETRY (D.S.C.)

Transition points of ICl_4^- salts over the temperature range 173 K to 273 K were determined using a Perkin Elmer model 1B D.S.C. operated in the low temperature mode. The samples were sealed into aluminium pans with exclusion of moisture.

6.7 N.Q.R. SPECTROSCOPY

NQR spectra were recorded on a mid-range Decca spectrometer (5-55 MHz) using Zeeman modulation. The resonances were measured at both -196°C and at room temperature where observable. In studies of phase transitions, intermediate temperatures were attained using appropriate slush baths. Resonant frequencies were determined with an accuracy of ca. ± 10 kHz by interpolation between the spectrometer frequency markers, which were calibrated by means of a frequency counter (Advance Instruments T.C.16).

REFERENCES

1. R. Belcher, A.J. Nutten, Quantitative Inorganic Analysis Butterworths (1969).
2. G. Brauer (ed.), Handbook of Preparative Inorganic Chemistry Vol. 1 Academic Press (1963-5).
3. R.E. Buckles, J.F. Mills, J.A.C.S., (1954), 76, 3716.
4. M. Filhol, J. de Pharm., (1839), 25, 431-47.
5. W.L. Groeneveld, Rec. Trav. Chim., (1952), 71, 1152-6.
6. P.L. Goggin, J. Mink, J.C.S. Dalton, (1974), 1479-83.
7. M. Gutierrez de Celis, Anales. soc. espan. fis quim, (1932), 30, 540.
8. M.P. Jaillard, Ann. Chim. Phys., (1860), 59, 454-6.
9. C. Jones, W. Price, H. Webb, J.C.S., (1929), 312.
10. L. Lindet, Ann. Chim. Phys. (6), (1887), 11, 209-14.
11. J.R. Partington, A.L. Whynes, J.C.S., (1949), 3135-41.
12. R.C. Paul, D. Singh, K.C. Malhotra, J.C.S. A, (1969), 1396-1400.
13. S.J. Peake, Ph.D. Thesis, Royal Holloway College London, (1976).
14. Pierrefitte Societe Generale d'Engrais et Produits Chimiques, Fr. 1,471,198, March 3 1967, C.A. 67 75006y.
15. A.I. Popov, J.N. Jessup, J.A.C.S., (1952), 74, 6127.
16. G.W. Richards, A.A. Woolf, J.C.S. A, (1968), 470-6.
17. V. Ya. Rosolovskii, E.S. Rumyantsev, Russ J. Inorg. Chem., (1963), 8, 689-92.
18. F.J. Ryan, Ph.D. Thesis, Royal Holloway College, (1972).

19. F. Seel, J. Nogradi, R. Posse, *Zeit. anorg. allgem. Chem.*, (1952), 269, 197-206.
20. W. Warthman, A. Schmidt, *Spect. Acta.*, (1974), 30A, 1243-6.
21. E. Wilke-Dorfurt, G. Balz, *Zeit. anorg. allgem. Chem.*, (1927), 159, 219.

Appendix 1

POST-CALORIMETRIC ANALYSES IN NITROSONIUM SALT CALORIMETRY

In Chapter 2 it was stated that small titration errors in the determination of nitrite and nitrate in solution after degradation of a nitrosonium salt led to anomalous values for the $\text{NO}_3^-:\text{NO}$ mole ratio. This statement will now be substantiated by considering the effect of a possible error of $\pm 0.05 \text{ cm}^3$ in each titration. The analytical procedure is presented in Chapter 6, and is briefly summarised below.

The nitrosonium salt was decomposed in aqueous base (200.0 cm^3) under nitrogen and the solution was then purged with oxygen-free nitrogen to displace the nitric oxide.

NITRITE ANALYSIS

0.1N KMnO_4 (25.0 cm^3) was diluted to 250 cm^3 and acidified with sulphuric acid. The temperature was raised to 40°C and an aliquot of the test solution (50.0 cm^3) was added. 0.1N Fe(II) solution (25.0 cm^3) was then added and the excess determined by titration with 0.1N KMnO_4 .

NITRITE AND NITRATE ANALYSIS

An aliquot of the test solution (100.0 cm^3) was made strongly alkaline and then heated with Devarda's alloy. The liberated ammonia was absorbed into boric acid solution and titrated directly with $0.1\text{NH}_2\text{SO}_4$ to a potentiometric end point.

NITRIC OXIDE

This was determined by difference using the result of the previous analysis and the weight of nitrosonium salt decomposed.

Analytical data are presented in table 1 and derived values for the $\text{NO}:\text{NO}_3^-$ mole ratio assuming an error of $\pm 0.05 \text{ cm}^3$ in each titration are presented in table 2. The deviation of this ratio from the expected value of 2:1 is thus explained.

TABLE 1

NOClO_4 decomposed in 200.0 cm^3 of aqueous base	2.100×10^{-3} mol.
Final titre in nitrite assay P	6.75 cm^3
Final titre in nitrite and nitrate assay Q	8.80 cm^3
Strength of KMnO_4 solution	0.1032N
Strength of Fe(II) solution	0.100N
Strength of H_2SO_4 solution	0.100N

TABLE 2

$\text{NO}_2^-/\text{NO}_3^-/\text{NO}$ mole ratios

Species	Titres used in calculation cm^3	P-0.05	P-0.05	P+0.05	P+0.05
		Q-0.05	Q+0.05	Q-0.05	Q+0.05
$\text{NO}_2^-/\text{mol} \times 10^3$		1.548	1.548	1.569	1.569
$\text{NO}_3^-/\text{mol} \times 10^3$		0.202	0.222	0.181	0.201
$\text{NO}/\text{mol} \times 10^3$		0.350	0.330	0.350	0.330
$\text{NO}:\text{NO}_3^-$		1.73:1	1.50:1	1.93:1	1.64:1

Appendix 2

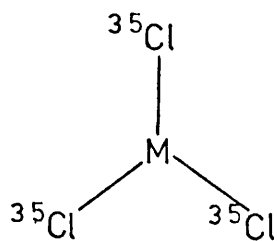
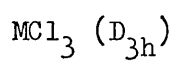
CHLORINE ISOTOPE EFFECTS ON THE VIBRATIONS OF MCl_n

In addition to the site group and factor group effects described in Chapter 4 which produce splittings of the normal modes of vibration of a solid state species, splittings may also arise from isotope effects. In this section the relative intensities of the splittings produced by chlorine isotopes at natural abundance for the singly-degenerate vibrational modes of MCl_2 , MCl_3 and MCl_4 are calculated. These calculations are based upon a ratio of 3:1 for $^{35}Cl: ^{37}Cl$ isotopes and consider the probability of each possible substituted species. Since substitution of ^{37}Cl for ^{35}Cl in effect changes the symmetry of a species, the effects upon doubly or triply degenerate modes may be more complex.

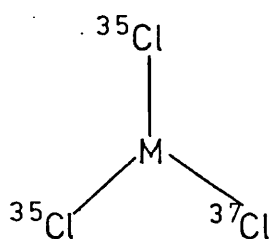
MCl_2 ($D_{\infty h}$)



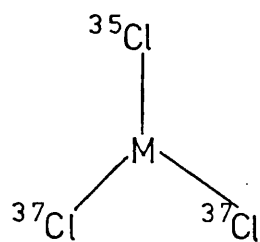
ratio 9:6:1



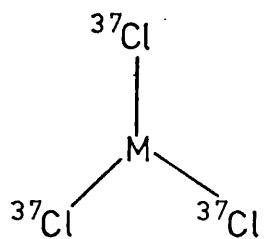
$$P = \frac{3}{4} \cdot \frac{3}{4} \cdot \frac{3}{4} \cdot {}^3C_0 = 27:64$$



$$P = \frac{3}{4} \cdot \frac{3}{4} \cdot \frac{1}{4} \cdot {}^3C_1 = 27:64$$

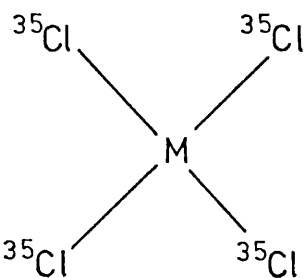
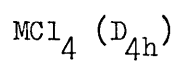


$$P = \frac{3}{4} \cdot \frac{1}{4} \cdot \frac{1}{4} \cdot {}^3C_2 = 9:64$$

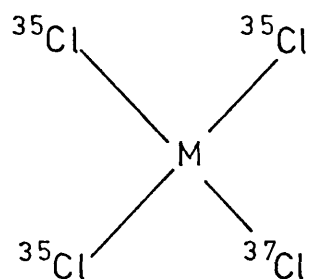


$$P = \frac{1}{4} \cdot \frac{1}{4} \cdot \frac{1}{4} \cdot {}^3C_3 = 1:64$$

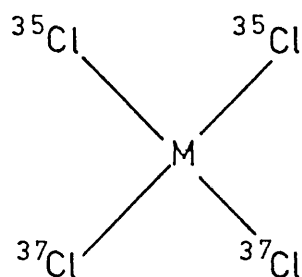
ratio 27:27:9:1



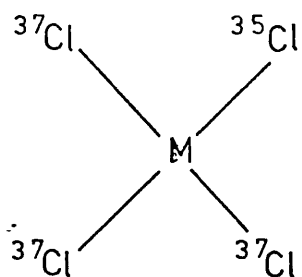
$$P = \frac{3}{4} \cdot \frac{3}{4} \cdot \frac{3}{4} \cdot \frac{3}{4} \cdot {}^4C_0 = 81:256$$



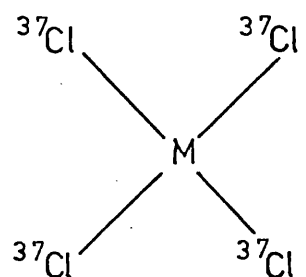
$$P = \frac{3}{4} \cdot \frac{3}{4} \cdot \frac{3}{4} \cdot \frac{1}{4} \cdot {}^4C_1 = 108:256$$



$$* P = \frac{3}{4} \cdot \frac{3}{4} \cdot \frac{1}{4} \cdot \frac{1}{4} \cdot {}^4C_2 = 54:256$$



$$P = \frac{3}{4} \cdot \frac{1}{4} \cdot \frac{1}{4} \cdot \frac{1}{4} \cdot {}^4C_3 = 12:256$$



$$P = \frac{1}{4} \cdot \frac{1}{4} \cdot \frac{1}{4} \cdot \frac{1}{4} \cdot {}^4C_4 = 1:256$$

* may split into cis and trans species

$$\text{ratio} = 81:108:54:12:1$$